Denis N. Gerasimov · Eugeny I. Yurin

Kinetics of Evaporation



Springer Series in Surface Sciences

Volume 68

Series editors

Roberto Car, Princeton University, Princeton, NJ, USA

Gerhard Ertl, Fritz-Haber-Institut der Max-Planck-Gesellschaft, Berlin, Germany Hans-Joachim Freund, Fritz-Haber-Institut der Max-Planck-Gesellschaft, Berlin, Germany

Hans Lüth, Peter Grünberg Institute, Forschungszentrum Jülich GmbH, Jülich, Germany

Mario Agostino Rocca, Dipartimento di Fisica, Università degli Studi di Genova, Genova, Italy

This series covers the whole spectrum of surface sciences, including structure and dynamics of clean and adsorbate-covered surfaces, thin films, basic surface effects, analytical methods and also the physics and chemistry of interfaces. Written by leading researchers in the field, the books are intended primarily for researchers in academia and industry and for graduate students.

More information about this series at http://www.springer.com/series/409

Denis N. Gerasimov · Eugeny I. Yurin

Kinetics of Evaporation



Denis N. Gerasimov Moscow Power Engineering Institute Moscow, Russia Eugeny I. Yurin Moscow Power Engineering Institute Moscow, Russia

ISSN 0931-5195 ISSN 2198-4743 (electronic) Springer Series in Surface Sciences ISBN 978-3-319-96303-7 ISBN 978-3-319-96304-4 (eBook) https://doi.org/10.1007/978-3-319-96304-4

Library of Congress Control Number: 2018948689

© Springer International Publishing AG, part of Springer Nature 2018

This work is subject to copyright. All rights are reserved by the Publisher, whether the whole or part of the material is concerned, specifically the rights of translation, reprinting, reuse of illustrations, recitation, broadcasting, reproduction on microfilms or in any other physical way, and transmission or information storage and retrieval, electronic adaptation, computer software, or by similar or dissimilar methodology now known or hereafter developed.

The use of general descriptive names, registered names, trademarks, service marks, etc. in this publication does not imply, even in the absence of a specific statement, that such names are exempt from the relevant protective laws and regulations and therefore free for general use.

The publisher, the authors and the editors are safe to assume that the advice and information in this book are believed to be true and accurate at the date of publication. Neither the publisher nor the authors or the editors give a warranty, express or implied, with respect to the material contained herein or for any errors or omissions that may have been made. The publisher remains neutral with regard to jurisdictional claims in published maps and institutional affiliations.

This Springer imprint is published by the registered company Springer Nature Switzerland AG The registered company address is: Gewerbestrasse 11, 6330 Cham, Switzerland

Preface

Every writer is surprised anew how, once a book has detached itself from him, it goes on to live a life of its own; it is to him as though a part of an insect had come free and was now going its own way.

Friedrich Nietzsche was an experienced writer and knew a thing or two about the book publishing industry. A book is whatever the reader makes of it, and while for a fiction book this is not a big issue (sometimes, it is quite the opposite), for a scientific work, a skewed perception might be lethal. Of course, there are happy exceptions to this rule, such as when these skewed perceptions are positive, and benevolent readers find in the book something that was not even there to begin with. Perhaps the most graphic example of this can be seen in a Sadi Carnot book, where future generations managed to find a 2nd law of thermodynamics, something about which Carnot himself did not, and could not, have the slightest idea. Even Carnot's statement:

...when a body has experienced any changes, and when after a certain number of transformations it returns to precisely its original state, that is, to that state considered in respect to density, to temperature, to mode of aggregation – let us suppose, I say, that this body is found to contain the same quantities of heat absorbed or set free in these different transformations are exactly compensated.

which is in blatant contradiction to thermodynamics and proves ineffectual $\oint dQ = 0$: most of our contemporaries are confident that the 2nd law originated in Carnot's book and that Clausius only developed it later on. Incidentally, Clausius himself (the actual author of the 2nd law of thermodynamics), explained quite reasonably the perceived priority of his predecessor: Carnot's proponents had simply never read his books. This really can happen, and quite often, too.

However, authors usually cannot rely on a reader's benevolence. Very few people were able to perform a "Sadi Carnot." There are many more of those whose works were unappreciated and/or forgotten. For example, when reading Anatoly Vlasov's neglected books, one can only wonder not at how deeply understood physical kinetics can be, but rather how shallow modern textbooks are on this subject.

vi Preface

What can the author do to prepare their dear child for an independent journey, where the parent can support them in neither word nor deed? Apparently, the only possible way is to equip them with a special travel bag which contains weapons to counter threats and accusations, even if some of these weapons seem just too bizarre (like in the old Australian movie "Around The World in Eighty Days").

The role of the traveling bag is played by this preface. First of all, there is a credential letter, the book's "passport," explaining what it should be, and more importantly, what it should not. Besides this, there is a tuning fork to establish the key for its correct interpretation ... in addition to many other things, of course.

The title might be misinterpreted by those who are used to understanding "kinetics" as a relevant branch of theoretical physics called "physical kinetics," that is, according to the common unofficial classification used in Russia as per Landau and Lifshitz', *Physical Kinetics*, Vol. 10. Although this book discusses the kinetic equation itself, and all its solutions in relation to the evaporation problem, its content is not limited to solving Boltzmann's equation using, say, the momentum method.

The term "kinetics" is used in the title in a broader sense, as a definition of a process that has evolved over time. We could have used the term "dynamics of evaporation" for the title, but that indicates a different scale for the processes described.

We look at the evaporation process at the molecular and atomic level, not on a larger scale. More precisely, macroscopic magnitudes are also defined, but only as a reduction from the previous, microscopic level. The book does not cover at all the empirical correlations required for "engineering" applications and similar purposes. Where necessary, a degree of self-discipline was required in order to remain faithful to, and so not go beyond, the scope of the project: it was essential to keep a focus on detail rather than provide readers with an exhaustive list of all the findings obtained for evaporation.

The key purpose of *Kinetics of Evaporation* is to discuss the essential principles of this phenomenon, which manifest themselves in various forms: from a child's toy called "drinking bird" to amazing thermocouple indicators near evaporating liquid surfaces. The emphasis throughout the book is on the word "discuss," i.e., this is not intended to be a didactic account of the available scientific findings. We go on to posit that overall in the field of evaporation, we have had few findings that have been obtained under sufficiently rigorous controls or which have been wholly unambiguous. For instance, a lot of results were obtained because of the incorrect use of Maxwell's distribution function as a boundary condition at the evaporating surface. We are not sure what to do about such results now.

The hardest part of any endeavor is to find a balance between "everything and everything." This is particularly true for a book. That said, below is a brief list of traps we, like many others, tried to avoid when writing.

Trying to see the wood for the trees: how much detail does one go into? How comprehensively should a formula derivation be described? We have had countless debates on this, the most heated of which were with students at lectures. Our firm

Preface vii

stance is that formula deductions in this book should be comprehensive while also being complex to the extent that they can be followed and understood by your average postgraduate or a good student. Authors are often tempted to demonstrate the depths of their intelligence with phrases like "Now we can easily derive that ..." (which actually should have been followed by 3 pages of calculations). We believe that we successfully avoided that evil.

"Old and new works." We saw not only overviews, but even monographs that contain nothing but references to old works that had already been published. There is nothing wrong with this: someone gathered all the findings into a single volume and insofar as it was published, they did a good job. In this case, the monograph is just an extensive organized digest of known publications and does not contain any new research. We could criticize this style by saying that it is unclear what is to be gained from such works, if readers are already familiar with the original research and the book does not contain any summaries therein. The opposite extreme would be to posit a new great theory without mentioning previous findings at all; although few authors have gone that far in recent times. We strove to achieve a happy medium, however, it should be admitted that we often found ourselves gravitating to the latter scenario, simply because of the specific nature of our subject matter. Hopefully, we avoided doing so to the greatest extent possible, certainly insofar as the Alexander Alekhine aphorism about an Aron Nimzowitsch book:

This book has both new and good ideas, however all good ideas here are old, and all the new ones are bad.

"Straightforward and comprehensive." The "no redundancy" principle is meaningless because it depends on how "necessary" is defined. Can the topic of evaporation be explored without mentioning issues of radiation heat transfer or the structural design of a thermocouple and its operation principle? And what if they determine the interpretation of experimental data, based on which fundamental conclusions are drawn about the physical nature of this phenomenon itself? We were unable to avoid including such matters, amongst others, in *Kinetics of Evaporation*. There you have it. Such sections are marked in side headings titled "sidesteps." These may be skipped by the reader without any risk to the comprehension of matters of evaporation.

"Specialist or student?" It is an obviously challenging goal to write a book that would be equally fascinating to both an expert (who knows pretty much everything about the subject) and student (who has a lot to learn). It is doubtful that an acceptable balance is possible. We aimed to make the material comprehensible for as wide an audience as possible. In fact, the book should be understood by any senior student who is familiar with physics.

"Why did you ignore X, Y, and Z's work?" In conclusion we need to touch upon the most sensitive matter: the completeness of citations. More specifically, the citation system we use. Evaporation and contiguous matters are the subject matter of thousands of valuable scientific publications. We did not aim to create a publication guidebook and, as such, avoided starting every section with "This matter viii Preface

was explored by ..." Some findings are looked into in detail in this book, and many works are cited at the end of each chapter. It goes without saying that we have not been able to mention all the publications that deserve to be cited within the scope of this work. One of us still remembers when, as a postgraduate, he looked through the references section of a newly published book, did not find any reference to his own work, and thus put the book back on the shelf with a sigh. This scenario is inevitable, and we apologize in advance to the authors of all the works we did not mention.

Having dealt with general morphological principles, we can move on to the book's content. The structure of the book is determined by its purposes and objectives and the aforementioned balances.

The first, introductory chapter describes the evaporation process with broad brushstrokes. In a way, this is the only chapter that does not fit into the "no larger than a molecule" principle we proclaimed earlier.

Chapters 2–4 are preparatory, and outline the methods mentioned in the book: methods of statistical physics, physical kinetics, and numerical modeling. Those chapters cannot be left out completely, even though we have a wide range of monographs and even textbooks on each of those subjects. We tried to balance conciseness and oversimplicity with a more detailed elaboration of more or less unconventional issues that are not always covered, at least in textbooks.

Chapters 5 and 6 define the distribution functions of evaporating particles. This path was long and winding, particularly in Chap. 6, but overall, it looks like we were successful.

Chapters 7 and 8 look at the direct application of the outcomes of the previous two chapters. It should be emphasized that absolute exact matching of theory and experiment is not the goal in itself. Theory should be theory, it should aim at defining general physical regularities, albeit in a simplified form, and in no way attempt to translate half-empirical expressions into experimental data. Simply put, in some cases the concordance between the theory and the experiment was too perfect, but we do not make a big deal of it: with such a complex process as evaporation, we are happy to settle for a matching order of magnitude.

Chapter 9 is a step beyond. This chapter is not about boiling! It looks at boiling in relation to its close relative: evaporation. We did not even try to systemize the physics of boiling here, or look into specific matters of boiling. Dear colleagues, save your breath! Some evaporation issues overlap with boiling, which we gladly report in Chap. 9, but certainly without going into too much detail. We did not even mention that there is actually no such thing as the boiling curve (that was a joke).

In essence, this book discusses the physics of evaporation at the microlevel, which already suggests that it is not intended to be in any way a comprehensive overview. To be honest, no approach would succeed in achieving this, simply because of the current state of the issue. In short, to quote Bohr:

The task of this book is not to find out how evaporation is. This book concerns what we say about evaporation.

Preface ix

We would like this to be the point of departure for our reader also.

We are deeply grateful to Svetlana Morgunova for her invaluable help with illustrations, Roman Makseev for the experiments, Maria Lyalina for proofreading, and Oleksandr Dominiuk for editing the English translation.

Moscow, Russia

Denis N. Gerasimov Eugeny I. Yurin

Contents

1	"Liq	quid-Va	npor" Phase Transition	1
	1.1	Evapor	ration and Condensation	1
		1.1.1	Phases and Transitions	1
		1.1.2	Units	2
		1.1.3	Evaporation Perennially	3
		1.1.4	This Book Is Not About Condensation	4
		1.1.5	Evapotranspiration	4
		1.1.6	A Droplet on a Candent Surface	5
	1.2	What (Can We Obtain from Thermodynamics?	6
		1.2.1	Basic Principles of Thermodynamics	6
		1.2.2	Phase Equilibrium	9
		1.2.3	The Nucleation of a New Phase	11
		1.2.4	The Evaporation Temperature	15
		1.2.5	Magic Bird	16
		1.2.6	Thermodynamic Diagrams	19
	1.3		Can We Obtain from Hydrodynamics?	21
		1.3.1	Navier–Stokes Equations	21
		1.3.2	Conditions on an Interfacial Surface	22
		1.3.3	Movement of the Interfacial Boundary	24
		1.3.4	Dynamics Near the Evaporation Surface	25
	1.4		ary Conditions	27
		1.4.1	Boundary Conditions for Hydrodynamics	27
		1.4.2	Boundary Conditions for Kinetics	28
	1.5	Conclu	asion	29
	D of	rancac		20

xii Contents

2	The	Statisti	cal Approach	31
	2.1	From 1	Mechanics to Probability	31
		2.1.1	From Mechanics	31
		2.1.2	Through a Chaos	32
		2.1.3	to Probability	34
		2.1.4	Irreversibility Versus Unidirectionality	38
		2.1.5	"Tomorrow It Will Be Raining	
			with 77% Probability"	39
	2.2	Distrib	oution Function	40
		2.2.1	Probability Density Function	40
		2.2.2	Special Probability Functions	41
		2.2.3	Poisson and Gauss	42
		2.2.4	Spatial Scales	43
		2.2.5	Example: The Debye Radius	44
		2.2.6	Distribution of Potential Energy	46
		2.2.7	The Statistical Approach	47
		2.2.8	The Principle of the Maximal Entropy	49
		2.2.9	The Virial Theorem	50
	2.3		Iaxwell Distribution Function	51
		2.3.1	Physical Models	51
		2.3.2	The Maxwellian of Maxwell	53
		2.3.3	Modern View on Maxwellian	55
		2.3.4	The Maxwellians for 2D and 3D Cases	57
		2.3.5	The Maxwellian Distribution Function	
			of Kinetic Energy	57
		2.3.6	The Meaning of the Maxwellian	
			Distribution Function	58
	2.4	Conclu	ısion	59
	Refe			60
			led Literatures	60
_				
3			e Approach	61
	3.1	-	nics of Probability	61
		3.1.1	Kinetic Equations	61
		3.1.2	The Liouville Theorem	62
	3.2		ogoliubov–Born–Green–Kirkwood–Yvon Chain	64
		3.2.1	Kinetic Equations	64
	3.3		oltzmann Kinetic Equation	65
		3.3.1	Derivation from the BBGKY Chain	65
		3.3.2	The Differentiability	67
		3.3.3	Spatial Scales for the Distribution Function	71
		3.3.4	Temporal Scale for the Distribution Function	71

Contents xiii

	3.4	The Vla	asov Approach: No Collisions	72
		3.4.1	Collisionless	72
		3.4.2	The Hamiltonian of the Macrosystem	75
		3.4.3	Crystallization	76
		3.4.4	Limitations of the Vlasov Approach	78
	3.5	The Ki	netic Equation for Practical Purposes	79
		3.5.1	The Split Decision	79
		3.5.2	Interactions at Intermediate Scales	80
		3.5.3	The Relaxation Approach	81
	3.6	The Ev	rolution of Probability: The Mathematical Approach	81
		3.6.1	The Master Equation	81
		3.6.2	The Kinetic Equation in an External Field	82
		3.6.3	The Kinetic Equation for a Self-consisted Field	83
		3.6.4	The Kinetic Equation for Collisions	84
		3.6.5	The Diffusion Equations	85
		3.6.6	The Stationary Equations	86
	3.7	The Ki	netics of Gas Near the Evaporation Surface	87
		3.7.1	The Liquid	87
		3.7.2	The Region of Vapor-Liquid Interaction	87
		3.7.3	The Knudsen Layer	89
		3.7.4	The Boundary Layer	89
		3.7.5	The Bulk of the Gas	90
	3.8		sion	90
				91
	Reco	ommende	ed Literatures	91
4	Nun	nerical F	Experiments: Molecular Dynamics Simulations	93
	4.1		Statistics to Mechanics: There and Back Again	93
		4.1.1	From Kinetics to Mechanics	93
		4.1.2	The Statistics for the Boltzmann Case	94
		4.1.3	Interaction Potential	96
		4.1.4	The Wrong Method to Solve Equations	96
		4.1.5	The Results of Numerical Simulations	98
		4.1.6	How to Calculate Temperature	98
		4.1.7	How to Calculate Pressure	99
		4.1.8	How to Calculate Heat Flux	99
		4.1.9	From Mechanics to Statistics, Part Two	100
		4.1.10	The Role of Molecular Dynamics Simulations	103
	4.2	Technic	ques of Molecular Dynamics	103
		4.2.1	Motion Equations	103
		4.2.2	Interatomic Potential	106
		4.2.3	Initial and Boundary Conditions	107
		4.2.4	Step-by-Step Guide for Simple Modeling	111

xiv Contents

	4.3	Compu	tte Unified Device Architecture	112
	4.4	Conclu	sion	116
	Refe	erences .		117
	Reco	ommend	ed Literatures	118
5	Velo	city Dis	stribution Function of Evaporated Atoms	121
	5.1		axwellian Distribution Function?	121
		5.1.1	Our Expectations	121
		5.1.2	Experimental Results	122
		5.1.3	Numerical Simulation Results	123
	5.2	Theore	tical Calculation of the Distribution Function	125
		5.2.1	The Simplest Form of Velocity Distribution Function	125
		5.2.2	Probability of Evaporation	129
		5.2.3	Distribution of Tangential Velocities	130
		5.2.4	Some Thoughts Concerning Condensation	131
		5.2.5	Distribution Function on an Irregular Surface	132
		5.2.6	A Generalization	135
		5.2.7	About Fluxes from an Evaporation Surface	136
		5.2.8	The Binding Energy: Preliminary Remarks	136
		5.2.9	Fluxes at the Surface	137
		5.2.10	Atoms or Molecules?	137
	5.3	Molecu	ılar Dynamics Simulations	138
		5.3.1	A Classification	138
		5.3.2	Numerical Simulation of Evaporation	139
		5.3.3	Velocity Distribution Function for Evaporated	
			Particles	141
	5.4	Conclu	sion	144
				145
	Reco	ommend	ed Literatures	146
6	Tota	al Fluxes	s from the Evaporation Surface	147
	6.1	Distrib	ution Function for Potential Energy in Condensed Media	147
		6.1.1	Work Function as a Distribution Function	147
		6.1.2	Potential Energy Distribution Function	148
		6.1.3	Analytical Description of Vaporization	155
		6.1.4	Sidestep: Trouton's Rule	157
		6.1.5	Fluctura	158
		6.1.6	Numerical Simulations	162
		6.1.7	Numerical Simulations (Continued)	166
	6.2	Numbe	er of Evaporated Particles	167
		6.2.1	The Possibility to Escape	167
		6.2.2	The Surface Layer of a Liquid	169
		6.2.3	The Moment of Escape	170
		6.2.4	Deformation of the Distribution Function	172
		6.2.5	Number of Particles at the Surface	174

Contents xv

	6.3	Mass a	and Energy Fluxes from an Evaporation Surface	175
		6.3.1	Evaporation, Condensation and Their Sum	175
		6.3.2	Temperature of the Evaporation Surface	177
		6.3.3	Fluxes from the Evaporation Surface	178
	6.4	Evapo	ration and Condensation: the Balance Equations	181
		6.4.1	Attractors of a Dynamic System	181
		6.4.2	What We May Expect for Phase Transitions	182
		6.4.3	Timescale from the Viewpoint of a Vapor	184
		6.4.4	Timescale from the Viewpoint of a Liquid	185
		6.4.5	The Simple Experiment	186
		6.4.6	Fluctuations with Temperature	188
	6.5		on-linear Effect Within Evaporation: Hyperevaporation	190
	6.6	Conclu	asion	193
				195
	Reco	ommend	led Literatures	195
7	The	Evanor	ration Coefficient	197
•	7.1		vaporation and Condensation Coefficients	197
		7.1.1	Overview	197
		7.1.2	The Hertz–Knudsen Formula	198
		7.1.3	The Condensation Flux	200
		7.1.4	A Sidestep: The Accommodation Coefficient	203
	7.2		xperiment	204
		7.2.1	How to Determine an Evaporation Coefficient	204
		7.2.2	The Experimental Results	211
		7.2.3	Explanations for Discrepancy (A Preliminary Round)	212
	7.3	Calcul	ation of the Evaporation Coefficient	214
		7.3.1	Some Definitions	214
		7.3.2	What Is the Evaporation Coefficient?	214
		7.3.3	Analytical Calculation	215
		7.3.4	Numerical Calculations	218
		7.3.5	The Evaporation Coefficient Is Unnecessary	218
		7.3.6	Condensation Coefficient Versus Stick Coefficient	219
	7.4	About	the Condensation Coefficient	219
		7.4.1	Two Types of Condensation Coefficient	219
		7.4.2	A Sidestep: A Collision Map	220
		7.4.3	Estimation of the Role of an Evaporation Flux	222
		7.4.4	A Sidestep: A Common Consideration	226
		7.4.5	The Sticking Coefficient	227
		7.4.6	Experimental Values for Evaporation and Condensation	
			Coefficients	229
	7.5	Conclu	asion	230
	Refe			231
			led Literatures	232

xvi Contents

8	Tem	peratu	re Jump on the Evaporation Surface	233			
	8.1	Out of	Equilibrium: The Difference Between the Temperature				
		of a L	iquid and of a Vapor	233			
		8.1.1	Non-equilibrium Kinetics	233			
		8.1.2	Some History of the Temperature Jump	237			
		8.1.3	Discontinuity of Parameters: A Brief Overview	238			
	8.2	Confus	sing Experiments	240			
		8.2.1	Experimental Temperature Jump: An Overview	241			
		8.2.2	Some Experiments and Experimental Data	242			
		8.2.3	The Temperature of the Interface	243			
		8.2.4	Correlation with the Mass Flux	245			
		8.2.5	The First Step of a Thousand-Mile Journey	247			
	8.3		red Temperature Jump	247			
		8.3.1	Which Is Stronger: The Equilibrium or Non-equilibrium				
			Distribution Function?	248			
		8.3.2	What Is a Thermocouple	250			
		8.3.3	What Does a Thermocouple Measure?	251			
		8.3.4	Temperature of the Thermocouple	252			
		8.3.5	Additional Fluxes	257			
		8.3.6	A Sidestep: Thermal Radiation	258			
		8.3.7	Comparison with Experimental Results	260			
		8.3.8	What Features Should Be Brought into Account	265 268			
	8.4						
				270			
	Reco	ommend	led Literatures	270			
9	Evaporation in the Processes of Boiling and Cavitation						
	9.1						
		9.1.1	The Boiling Curve	271			
		9.1.2	A Sidestep: The Mathematics of the Boiling Curve	272			
		9.1.3	The Physics of Nucleate Boiling	273			
		9.1.4	A Sidestep: The Heat Transfer Coefficient	275			
		9.1.5	Back to Boiling and Evaporation	279			
	9.2	Film E	Boiling	280			
		9.2.1	Common Description	280			
		9.2.2	The Rayleigh–Taylor Instability	280			
		9.2.3	Evaporation and Instability	282			
	9.3	Transi	ent Boiling	283			
		9.3.1	Common Description	283			
		9.3.2	Maximum Heat Flux on a Solid Surface	284			
		9.3.3	Types of Heat Fluxes	285			
		9.3.4	The Maximum Contact Temperature				
		9.3.5	A Sidestep: "An Infinite Rate of Diffusion"				

Contents xvii

	9.3.6	Stationary Evaporation Versus Explosive Evaporation	289	
	9.3.7	Boiling	290	
	9.3.8	Numerical Simulation of Explosive Evaporation	290	
	9.3.9	Liquid-Wall Interaction	294	
9.4	Cavitati	ion	295	
	9.4.1	Cavitation and Sonoluminescence	295	
	9.4.2	The Rayleigh Equation and Its Boundary Condition	299	
	9.4.3	The Evolution of the Cavitation Bubble	301	
	9.4.4	Evaporation Induced by Condensation	301	
	9.4.5	Numerical Simulations	306	
	9.4.6	A Sidestep: The Boiling Chamber	306	
9.5	Conclus	sion	308	
Refe	erences .		309	
Rec	ommende	ed Literatures	309	
Appendix A: Distribution Functions				
Appendix B: Special Functions				
Index			319	

Chapter 1 "Liquid-Vapor" Phase Transition



1.1 Evaporation and Condensation

1.1.1 Phases and Transitions

Every substance consists of molecules, but these molecules may coexist in various forms, creating many kinds of matter at different aggregate states. In thermodynamics, aggregate states are a particular case of phases: substances with uniform properties.

Almost any substance can be in a solid state at a sufficiently low temperature. In this state, closely arranged molecules (or atoms) form a periodic structure, which can be destroyed at a high temperature (note that we simplify all the processes; e.g., a short-range order may be preserved during melting).

In liquid, molecules can move relatively freely. Despite the permanent interaction with its neighbors, any molecule may travel in the medium, but in heavy traffic: this motion represents the diffusion process—a molecule moves from point A to point B in a very winding way, like a sailor who is drunk.

When the temperature rises, a liquid will turn into a gas.

Molecules move freely in the gas phase—from collision to collision. Usually, gas is a rarefied medium, and molecules rarely interact (i.e., collide) with one another; in a limiting case we may assume that interaction is absent entirely. Such a gas is referred to as the ideal gas, and its properties can be described by simple relations, such as the Clapeyron equation:

$$p = nT, (1.1.1)$$

that connects the pressure p, number density of particles n = N/V (the ratio of the number of particles to the volume) and temperature T.

The most popular theories usually describe a liquid as a dense vapor; this approach is suitable far from the melting point. The higher the pressure, the higher

the density of the vapor, thus, in such a representation, the gas becomes more and more similar to a liquid as the pressure increases. At some point—the critical point—the difference between a liquid and its gas vanishes. At higher pressures, the substance represents a so-called supercritical fluid—neither a liquid, nor gas, but something else: a dense medium with strong fluctuations.

The subject of this book is the "liquid–vapor" phase transition. The first requirement of such transition is the existence of two separate phases: liquid and vapor. As we shall see, these phases may not be distinguishable for all thermodynamic parameters, but only if pressure and temperature are less than critical values: $p < p_c$, $T < T_c$.

The standard description of the phase transition implies heating (or, alternatively, cooling) of the substance and, after the temperature of the phase transition has been achieved, this substance turns into a new phase at the same temperature—the temperature of the phase transition; all the energy transferred to the body at this temperature is spent on the phase transition. This description is suitable for boiling—the volume phase transition from liquid to vapor, but it cannot be applied for evaporation.

The thermodynamic approach given above is based on an important assumption: both liquid and vapor phases must be in equilibrium (we discuss the thermodynamic concept of equilibrium in the next section). In simple terms, equilibrium means that the rate of the "liquid–vapor" phase transition is equal to the "vapor–liquid" phase transition at these conditions, i.e., without additional heat being transferred to the system no phase transition occurs—the observer cannot see any variations in the amount of the two phases.

Evaporation is a surface process: molecules of a liquid detach from the surface and become vapor. The reverse process of evaporation is condensation: molecules of vapor fall onto a liquid surface and attach to it, becoming part of the condensed phase. The rate of the direct process (evaporation) and the reverse process (condensation) are equated in rare cases: the most frequent occurrence being when one of these two processes dominates the other.

Thus, evaporation is only a half of the total process of the interfacial "evaporation-condensation" mass exchange, which is likely to be in non-equilibrium. It is dangerous to apply the conclusions of equilibrium thermodynamics to the evaporation process, i.e., the phase transition going in only one direction.

1.1.2 Units

To some, the Clapeyron equation in the form of (1.1.1) looks strange. One may feel intuitively that something has been lost in this correlation.

The missing factor in (1.1.1) is the Boltzmann constant $k = 1.38 \times 10^{-23}$ J/K. This constant was introduced to physics by Max Plank (simultaneously with "his

own" constant h) as the proportional coefficient between the entropy S and the logarithm of thermodynamic probability W:

$$S = k \ln W, \tag{1.1.2}$$

note that this constant is displayed on the monument of Boltzmann's grave.

Indeed, in physics, k is used only in combination with temperature; e.g., in the differential form TdS, as the mean kinetic energy of a molecule kT/2, or in the factor of the Boltzmann distribution $\exp(-\varepsilon/kT)$. Interestingly, in the Stefan-Boltzmann law $E = \sigma T^4$ the Boltzmann constant (at the forth degree) hides in σ . Thus, the purpose of constant k is to convert temperature into energy units.

Here and almost everywhere in this book we omit the Boltzmann constant. Moreover, we will usually also use kelvin as the unit of energy (except in some sections, where joules are native units—such as in thermodynamics), thus, k has no value for us. If someone wants to reduce any correlation from this book to the "normal view" (e.g., to transform (1.1.1) to its regular form), then one may simply replace $T \to kT$.

Perhaps it looks inconvenient when we state that the interaction energy of two atoms is 112 K, however, because temperature is the measure of all kinds of energy distributed on atoms (kinetic energy as well as potential, etc.), this approach seems logical.

1.1.3 Evaporation Perennially

Evaporation is a surface process: molecules of liquid are torn from their neighbors and fly out as a gas. Why does this happen?

Molecules in liquid are bound to each other—both in the bulk of the liquid and at its surface. Surface molecules can see a way to escape, however, commonly they cannot achieve such an escape: they are bound within their neighborhood. To break such a connection, a molecule must have high kinetic energy—so high that it can overcome the potential energy binding it in place. The probability of evaporation for a given particle is not very high, but is non-zero: after Maxwell, we know that the kinetic energy is distributed as:

$$f \sim \exp(-\varepsilon/T)$$
 (1.1.3)

(see the exact relations in Chaps. 5 and 6), so this probability increases with temperature; thus, there always exist molecules with sufficient kinetic energy at any temperature.

Try to leave a glass of water for the night: you will find it partially empty in the morning. Despite the low chance a particle has to break away from the surface, many molecules do. Alas, not all liquids can repeat this trick: an open bottle of glycerol will not change its liquid level, even after a year.

The persistence of evaporation is the main distinction between evaporation and boiling: with the second process taking place only at high temperatures, while evaporation occurs in any temperature condition, albeit, at a sufficiently different speed.

A more "scientific" issue in terms of evaporation is that it is a non-equilibrium process. Usually, when we observe evaporation, we are dealing with a system that is far from an equilibrium state (note that in an equilibrium state, in very wet air, the level of water in the glass will stay the same all night). Thus, the best recommendation for treating evaporation may be to forget all the principles of equilibrium. We may say that evaporation is a non-equilibrium phase transition.

1.1.4 This Book Is Not About Condensation

This book considers only evaporation. Despite the fact that we will need to turn our attention to condensation from time to time, we will not discuss any special problems associated to condensation.

This one-direction focus of our book is determined by the single special property of condensation: for this phenomenon, gas processes are very important. Our book considers, mainly, the processes at, or near, to a liquid surface. The "kinetics of condensation" would need to consider how a gas attaches itself to a liquid, and a book containing such information would be about double the number of pages of this book.

Thus, the title of our book is very specific: a book of short stories about the detachment of atoms from a liquid surface. Some may wonder how a 300-page book can be written on such a plain subject? Well, this is evaporation. There are many angels on the head of this pin.

1.1.5 Evapotranspiration

Evapotranspiration is one of the main processes supporting life—the life of land-based creatures. Possibly, evapotranspiration takes second or the third spot in terms of importance after sunlight (they say that air is significant too).

It is hard to imagine Earth with non-evaporating water; let us better imagine the planet Glyz. On this planet, all life forms are based on glycerol; typical Glyzenians consist of $\sim 80\%$ glycerol. It all looks rather unusual, but so what? Less than two decades ago there were conceptions about methane-based life forms on Titan (Saturn's moon), so why should we not assume a glycerol-based life form in this subsection? Here consider a life based on super-glycerol (a not yet discovered modification), that cannot evaporate absolutely.

As a freak of nature, there are oceans of glycerol on Glyz, seas of glycerol, rivers of glycerol ... Stop. How would there be rivers on Glyz? Rivers have sources, they

cannot flow from nowhere. Since our glycerol (the future super modification) is non-evaporating, there is no glycerol in the Glyz atmosphere. Thus, there is no fog, no rain, no river sources or rivers (except for possible glycerol volcanic activity, as in the cryovolcano on Triton). Actually, from the point of view of the biology of Glyzenian organisms, our Glyz is a desert surrounded by an ocean of glycerol. Glycerol-based life forms might live in the ocean, but no crossopterygian walks on the dry land of Glyz.

Sad story. Fortunately, the history of Earth followed a different path: we have water cycle.

On our planet, water evaporates from large reservoirs (oceans and seas), and vapor is spread by winds above dry land, where it falls as rain. Rivers collect the water, bring it to the oceans, and so on, until our dear Sun initiates the cycle once more.

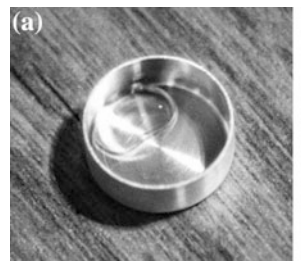
1.1.6 A Droplet on a Candent Surface

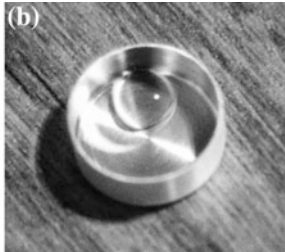
We can put a droplet of water on a table and watch how it evaporates. Actually, this is not a very interesting pastime. However, the same process can look much more impressive when a liquid is placed on a hot surface. In this case, instead of a puddle of water, one sees many droplets moving around the surface.

Who first saw droplets on an overheated surface? In modern literature, this effect is referred to as the "Leidenfrost effect" (named after Johann Gottlob Leidenfrost who observed such an effect in the middle of eighteenth century).

Because the term "overheated" depends on the kind of liquid, we present this effect for liquid nitrogen at room temperature. For nitrogen, with its boiling temperature of 77 K (at atmospheric pressure), a table at 300 K is like a frying pan; we may also observe this phenomenon in domestic conditions (see Fig. 1.1.).

Initially, nitrogen is poured into a cup of diameter ~ 1 cm. Once placed in a cup (i.e., a frying pan), nitrogen began to evaporate and form a droplet (Fig. 1.1a). After that, a spherical droplet formed (Fig. 1.1b), which evaporated gradually (Fig. 1.1c). Perhaps, "gradually" is not the correct word: all process shown in Fig. 1.1 take less than 1 min.





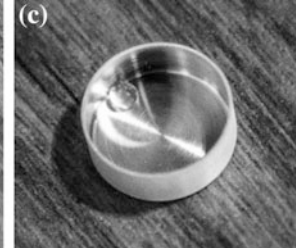


Fig. 1.1 Formation and evaporation of a nitrogen droplet in air

To be more accurate, various effects may lead to the formation of a spherical droplet on a surface, not least wettability. However, the main physical reason that governs the Leidenfrost effect is intensive evaporation of a liquid—a surface being so hot that a liquid simply cannot coexist with it; because of such a high rate of evaporation droplets bounce back from the surface and even roll on it, like solid beads. However, in Fig. 1.1 we see a caught droplet: there is no way it can escape, so we can take pictures of it.

In the last chapter of this book, we will consider a similar effect.

We have used a lot of thermodynamic concepts here. Let us investigate the ability of thermodynamics to describe the evaporation process.

1.2 What Can We Obtain from Thermodynamics?

1.2.1 Basic Principles of Thermodynamics

Many details of this book are concerned with thermodynamic concepts, so we must discuss these basic assertions of science closely. Perhaps, it seems strange to discuss the foundations of thermodynamics in such a place, but we feel that it is necessary in order to consider results obtained and discussed in this book. For example, we will discuss situations where temperature is not temperature, and consider how we can obtain an equilibrium state with a Maxwellian distribution function (MDF) from mechanical equations. So, we spend several pages considering common observation, especially considering the fact that all the thermodynamics can be expounded in a single lection.

Thermodynamics is a comparatively simple science, if you are not in the mood to overload it with epic concepts such as the "heat death of the Universe." The main principle of thermodynamics is the assumption of equilibrium: each isolated system reaches a stationary stable state, with no subsequent changes. Our daily experience acknowledges this assumption, but we have no sufficient proof from a mechanics standpoint (see Chap. 2).

There are only a few basic laws of thermodynamics, and enormous amounts of consequences arising from them.

Zeroth law. There exists a single parameter—temperature T—that describes equilibrium: the stationary state with the absence of fluxes. This means that the condition T = const is enough (at zero total fluxes) to describe the equilibrium state.

First law. All heat δQ conducted to the system is spent changing the inner energy of this system dU and to do work $\delta A = p dV$:

$$\delta Q = dU + \delta A. \tag{1.2.1}$$

For complex systems, there are many kinds of work that can be done; for instance, the surface work σdF (σ is the surface tension and F is the surface area) and the electric field work EdD (E is the electric field strength and D is the magnetic induction).

Second law. The differential form of (1.2.1) has an integrating multiplier, i.e., there exists a function of entropy S with the following differential:

$$dS = \frac{\delta Q}{T}. ag{1.2.2}$$

This integrating multiplayer is the inverted temperature T^{-1} , the existence of which was stated in the 0th law.

The 2nd law from (1.2.2) can be obtained through pure mathematical procedures. Entropy exists in any case of a simple system—a system with a single kind of work. For complex systems, the differential form (1.2.1) can be represented in the form:

$$\delta Q = \sum_{k=1}^{N} X_k dx_k, \quad N > 2,$$
 (1.2.3)

(note that in (1.2.3) $X_1 = 1$ and $X_1 = U$). The form of (1.2.3) is holonomic only if the Frobenius conditions are satisfied:

$$X_1 \left(\frac{\partial X_3}{\partial x_2} - \frac{\partial X_2}{\partial x_3} \right) + X_2 \left(\frac{\partial X_1}{\partial x_3} - \frac{\partial X_3}{\partial x_1} \right) + X_3 \left(\frac{\partial X_2}{\partial x_1} - \frac{\partial X_1}{\partial x_2} \right) = 0 \tag{1.2.4}$$

for any triad of $X_{1,2,3}$; (1.2.4) may also be represented as $\vec{X} \cdot \text{rot} \vec{X} = 0$. We see that, actually, the 2nd law in this formulation is reduced to a mathematical theorem. But historically the 2nd law was established by Clausius with some physical assumptions—the inability of spontaneous heat transfer from a cold body to a hot body. However, this "physical approach" to the 2nd law is not the most debated statement.

In reality, there exist several formulations of the 2nd law with different strengths, as was noted by T.A. Afanasieva-Erenfest. Briefly, these formulations may be expressed as:

- The existence of entropy as a thermodynamic parameter in (1.2.2).
- The directness of entropy to the maximum value $S \to S_{\text{max}}$ in an isolated system.
- The assertion that the state with S_{max} is the only attractor of any isolated (thermo-)dynamic system.

Usually, the spears were broken at the fields of the second and third statements, since the first assertion is clear, at least from the mathematical point of view.

There is also the 3rd law of thermodynamics that can be formulated in various ways. The simplest expression of which is:

$$\lim_{T \to 0} C_{V} = 0, \quad \lim_{T \to 0} C_{p} = 0, \tag{1.2.5}$$

while in a more common form the 3rd law can be expressed as (Bazarov 1991):

$$\lim_{T\to 0} \left(\frac{\partial S}{\partial p}\right)_T = 0, \quad \lim_{T\to 0} \left(\frac{\partial S}{\partial V}\right)_T = 0. \tag{1.2.6}$$

Another formulation of the 3rd law is the statement that T=0 is an unreachable value, because there are no processes that could provide a transition to this point. However, the 3rd law is not as interesting as the first three laws, especially the 0th law

Temperature is a special function, indeed. From the statistical point of view, temperature determines all energy distributions in a system or in any sub-system. For instance, *T* determines velocity distributions of particles, the electron energy of atoms, vibrational and rotational degrees of freedom of molecules, etc. There also exists the temperature of thermal radiation (for instance, a non-adjusted TV set receives radiation of 2.7 K—cosmic background radiation). These many of roles of temperature exist due to the 0th law: temperature defines the equilibrium state.

The reverse side of this is the fact that the term "temperature" can be formulated only for equilibrium media. In non-equilibrium, all distributions mentioned above lose their sense, just like temperature itself loses its sense. Sometimes temperature is defined only through the mean chaotic energy of molecules in a gas, i.e., $T = \overline{mv^2}$, and for some cases we may see that $\overline{v_x^2} \neq \overline{v_y^2} \neq \overline{v_z^2}$ (e.g., at the evaporation surface a normal component of velocity $v_z \neq v_x \sim v_y$). Being consecutive, we have to conclude that there are three temperatures T_x , T_y , T_z in the general case; however, this consistency may cause irritation to an expert of pure thermodynamics.

The famous half-measure to avoid this problem is the assumption of a local thermal equilibrium. Following this concept, we may apply the term "temperature" to an elementary point (a microscopic volume containing many particles) of the medium, despite the fact that temperature in the neighborhood of this elementary point is different. So, total equilibrium does not exist, but we are able to use all the equilibrium correlations at a given point; i.e., all distribution functions determined at this point correspond to equilibrium ones at the relevant (local) temperature.

However, this approach does not work in every case: to apply this idea, we have to be sure that temperature exists at least on a small scale. For many situations, this assumption is wrong, i.e., distributions at any point (in any microscopic volume) do not correspond to the equilibrium distribution. In such a case, the problem is not reduced to the value of temperature: such a term as "temperature" cannot be used. For a third-party example let us consider the Boltzmann distribution of excited energy:

$$w \sim e^{-E/T},\tag{1.2.7}$$

which cannot be applied for non-equilibrium plasma; consequently, attempts to determine its temperature based on the assumption of distribution (1.2.7) gives an error of $\sim 100\%$ for T. This error is not a kind of experimental inaccuracy but is a systematic error, which follows from an incorrect theory.

Another instance is appropriate to the theme of this book. Temperature cannot be defined in the so-called Knudsen layer (the region with the spatial scale of about one mean free path—the average distance between two successive collisions of molecules) in case of different conditions at the boundaries of this layer. Such a situation takes place near the evaporation surface; in simple words, the temperature of vapor near the evaporation surface does not exist.

Note that we will consider the problems of spatial scales in detail in Chaps. 2 and 3; here we return to thermodynamics.

In addition to the inner energy, several thermodynamic functions can be introduced:

- 1. Enthalpy H = U + pV.
- 2. The Helmholtz free energy F = U TS.
- 3. The Gibbs free energy $\Phi = U + pV TS$.

Each potential describes a stable equilibrium at corresponding external conditions in the most frequent case.

Using specific parameters (per unit of mass) [x] = [X]/m, where [x] denotes any quantity given above, we can rewrite (1.2.1) in the form:

$$Tds = du + pdv, (1.2.8)$$

which is correct in any case: as for a closed system with m = const so for an open system where $m \neq \text{const}$. For an open system we can multiply (1.2.8) by m and obtain:

$$TdS = dU + pdV - \varphi dm, \qquad (1.2.9)$$

where the specific Gibbs energy $\varphi = u + pv - Ts$. If our system consists of *n* substances, then we must use the sum $\sum_{i=1}^{n} \varphi_i dm_i$ instead of the last term of (1.2.9).

1.2.2 Phase Equilibrium

For an isolated system with two phases of substance (see Fig. 1.2), we have for each phase:

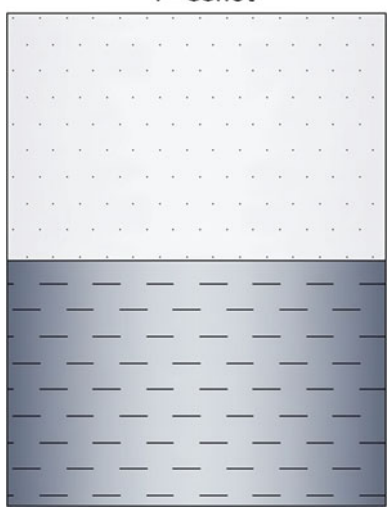
$$dS_1 = \frac{dU_1}{T_1} + \frac{p_1 dV_1}{T_1} - \frac{\varphi_1(p_1, T_1) dm_1}{T_1}, \qquad (1.2.10)$$

$$dS_2 = \frac{dU_2}{T_2} + \frac{p_2 dV_2}{T_2} - \frac{\varphi_2(p_2, T_2) dm_2}{T_2}.$$
 (1.2.11)

As $U = U_1 + U_2 = \text{const}$, $V = V_1 + V_2 = \text{const}$ and $m = m_1 + m_2 = \text{const}$ so $dU_1 = -dU_2$, $dV_1 = -dV_2$, $dm_1 = -dm_2$ and for the total $dS = dS_1 + dS_2$ we get:

Fig. 1.2 The isolated system





$$dS = \left(\frac{1}{T_1} - \frac{1}{T_2}\right) dU_1 + \left(\frac{p_1}{T_1} - \frac{p_2}{T_2}\right) dV_1 - \left(\frac{\varphi_1}{T_1} - \frac{\varphi_2}{T_2}\right) dm_1.$$
 (1.2.12)

The condition of equilibrium for such a system is dS = 0, and for arbitrary deviations dU_1 , dV_1 and dm_1 we obtain that:

$$T_1 = T_2 = T$$
, $p_1 = p_2 = p$, $\varphi_1(p_1, T_1) = \varphi_2(p_2, T_2)$. (1.2.13)

Let us consider small variations of pressure dp and temperature dT in both phases. In a common case we will use different deviations of pressures: $dp_1 \neq dp_2$. This inequation arises, for example, in a system with a gaseous phase consisting of vapor and a buffering (non-condensing) gas. We have:

$$\varphi_1(p_1 + dp_1, T + dT) = \varphi_2(p_2 + dp_2, T + dT),$$
 (1.2.14)

$$\varphi_1(p_1,T) + \frac{\partial \varphi_1}{\partial p_1} dp_1 + \frac{\partial \varphi_1}{\partial T} dT = \varphi_2(p_2,T) + \frac{\partial \varphi_2}{\partial p_2} dp_2 + \frac{\partial \varphi_2}{\partial T} dT.$$
 (1.2.15)

Derivatives of the Gibbs energy are $\frac{\partial \varphi}{\partial p} = v$, $\frac{\partial \varphi}{\partial T} = -s$ (specific volume and specific entropy correspondingly) and $\varphi_1(p_1,T) = \varphi_2(p_2,T)$ because of (1.2.13). The difference of entropies is:

$$s_2 - s_1 = \frac{r}{T},\tag{1.2.16}$$

where r is the specific heat of the phase transition (e.g., the latent heat of vaporization). Thus:

$$v_2 \frac{dp_2}{dT} - v_1 \frac{dp_1}{dT} = \frac{r}{T}.$$
 (1.2.17)

This important equation has two particular forms. The first case is the Clapeyron-Clausius relation for $dp_1 = dp_2 = dp$:

$$\frac{\mathrm{d}p}{\mathrm{d}T} = \frac{r}{T(\nu_2 - \nu_1)}. (1.2.18)$$

This equation establishes the correlation between pressure and temperature along the phase equilibrium curve. As we know, a single-phase substance has two degrees of the freedom; this fact is reflected in the equation of state in form p = f(v, T). In a two-phase system, we have a single freedom degree, i.e., the dependence p = f(T), represented in (1.2.18). In other words, phase transition occurs at p = const and T = const.

The second equation that follows from (1.2.17) describes isothermal variation of pressure—the Poynting equation for dT = 0:

$$\frac{\partial p_2}{\partial p_1} = \frac{v_1}{v_2}.\tag{1.2.19}$$

It follows from (1.2.19) that the increase of pressure in one of equilibrium phases tends to the pressure increase in the second phase. For example, if the pressure of a liquid was increased (e.g., with a noble gas added to the chamber), the pressure of the saturated vapor will increase too.

Note that we may take into account an inequality of temperatures $dT_1 = dT_2$, but this consideration would not contain any physical meaning.

1.2.3 The Nucleation of a New Phase

Nucleation is an important but slightly overestimated aspect of the problem. Thermodynamics predicts some interesting results for nuclei of a new phase in a given media, but it is rare in practical situations for the basic assumptions of this consideration to be correct.

Let us consider a thermodynamic system at constant pressure p and temperature T. Initially there is a homogeneous phase in a chamber, with mass m at the Gibbs energy:

$$\Phi^0 = F^0 + pV^0 = \varphi_1 m = (f_1(v_1, T) + pv_1)m. \tag{1.2.20}$$

After the formation of a nucleus of mass m_2 with radius R (see Fig. 1.3) the Gibbs energy becomes:

$$\Phi = f_1(v_1, T)m_1 + f_2(v_2, T)m_2 + F_\sigma + pv_1m_1 + pv_2m_2.$$
 (1.2.21)

Here the free surface energy is:

$$F_{\sigma} = \sigma S = \sigma \cdot 4\pi R^2, \tag{1.2.22}$$

where σ is the surface tension.

There are three independent parameters in (1.2.21)—let them be v_1 , v_2 and m_2 . Other parameters can be expressed as $m_1 = m - m_2$ and $R = \sqrt[3]{\frac{3m_2v_2}{4\pi}}$. That is, the variation of the Gibbs energy of a two-phase system is:

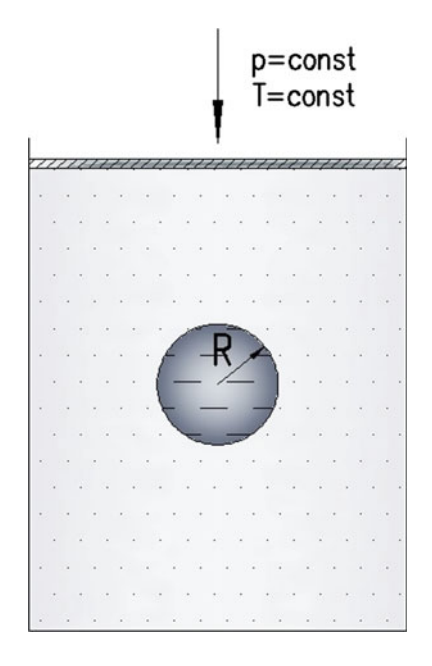
$$\delta\Phi = \frac{\partial\Phi}{\partial v_1}\delta v_1 + \frac{\partial\Phi}{\partial v_2}\delta v_2 + \frac{\partial\Phi}{\partial m_2}\delta m_2. \tag{1.2.23}$$

In equilibrium this variation must be equal to zero, i.e., for independent δv_1 , δv_2 and δm_2 we have:

$$\frac{\partial \Phi}{\partial v_1} = 0, \quad \frac{\partial \Phi}{\partial v_2} = 0, \quad \frac{\partial \Phi}{\partial m_2} = 0,$$
 (1.2.24)

or, with (1.2.21):

Fig. 1.3 Formation of a droplet



$$-\frac{\partial f_1(v_1, T)}{\partial v_1} = p_1 = p, \qquad (1.2.25)$$

$$-\frac{\partial f_2(v_2, T)}{\partial v_2} = p_2 = p + \frac{2\sigma}{R},\tag{1.2.26}$$

$$f_1(v_1, T) + pv_1 = f_2(v_2, T) + \underbrace{\left(p + \frac{2\sigma}{R}\right)}_{p_2} v_2.$$
 (1.2.27)

Equations (1.2.25)–(1.2.27) describe phase equilibrium in a two-phase system with a spherical separation surface. And we see that pressure in the first phase coincides with external pressure, while pressure in the new phase exceeds this value by $\frac{2\sigma}{R}$ (the so-called Laplace jump, see Sect. 1.3.2). Introducing a specific Gibbs energy in the form of (1.2.20), we can rewrite (1.2.27) as a usual condition:

$$\varphi_1(p_1, T) = \varphi_2(p_2, T). \tag{1.2.28}$$

Equation (1.2.28) is similar to (1.2.13), which was obtained for an isolated system.

How expedient is a nucleation in the given thermodynamic system? To answer this question, we must consider the change in the Gibbs energy $\Delta \Phi = \Phi - \Phi^0$:

$$\Delta\Phi = (\varphi_2(p, T) - \varphi_1(p, T))m_2 + 4\pi R^2 \sigma. \tag{1.2.29}$$

When $\Delta\Phi$ <0 the formation of a new phase is more favorable (from the thermodynamic point of view). To establish a function $\Delta\Phi$ of thermodynamic parameters, and of the radius R, we use expansions for φ_1 and φ_2 :

$$\varphi_{2}(p,T) - \varphi_{1}(p,T) = \underbrace{\varphi_{2}(p_{s},T) - \varphi_{1}(p_{s},T)}_{0} + \underbrace{\frac{\partial \varphi_{2}}{\partial p}(p - p_{s}) - \frac{\partial \varphi_{1}}{\partial p}(p - p_{s})}_{P_{s}}$$
(1.2.30)

where p_s is the saturation pressure for a flat interfacial surface. Thus, we have:

$$\Delta\Phi = (v_2 - v_1)(p - p_s) \frac{4\pi R^3}{3v_2} + 4\pi R^2 \sigma. \tag{1.2.31}$$

In the case of $(v_2 - v_1)(p - p_s) < 0$ the variation $\Delta\Phi$ can be negative for sufficiently large R. In this case, function $\Delta\Phi(R)$ has a maximum at:

$$R = R_{\rm m} = \frac{2\sigma v_2}{(v_2 - v_1)(p_{\rm s} - p)}.$$
 (1.2.32)

Usually the radius in (1.2.32) is referred to as the critical radius of nucleation, because when $R > R_{\rm m}$ we have $\frac{\partial \Delta \Phi}{\partial R} < 0$ (see Fig. 1.4), i.e., the growth of the nucleus is thermodynamically favorable. Note that if $v_2 > v_1$ (the new phase is "lighter" than the old phase, such as steam in water) then $p < p_s$, otherwise the actual pressure in a system would exceed the saturation pressure.

The formation of nuclei in an electrical field has special features; this physics is used in the Wilson cloud chamber—the track detector of ionized particles—a vessel filled with saturated (or even oversaturated) vapor.

However, despite the oversaturation, the vapor does not condense. Why? Because for condensation, the critical size of a nucleus (of a droplet) must not be less than the size calculated in (1.2.32). There may be two kinds of nuclei:

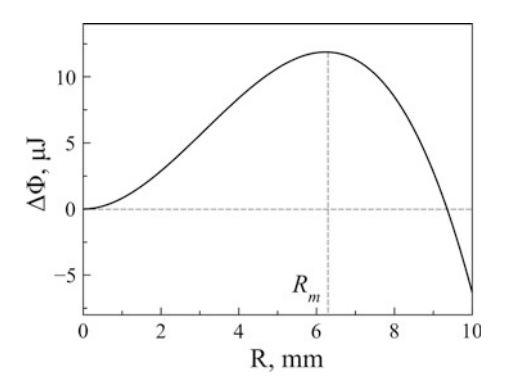
- The spontaneous nucleus: due to fluctuations, a large cluster (or a small droplet) is formed in the vapor.
- The heterogeneous nucleus: in this case, small impurities play a role as the condensation center.

We see that experimental conditions must provide the absence of both types of nuclei: oversaturation must be insignificant, i.e., the probability of the formation of nucleus of radius $R_{\rm m}$ must vanish, and the vapor must be of high purity. Under these conditions, there is no condensation in the Wilson chamber; of course, in addition, we must prevent condensation on the chamber walls.

Condensation begins in a cloud chamber with the presence of ionized particles inside it: ionized radiation produces charged particles inside the chamber, and these charges form droplets around them. Again, why?

To take into account the effect of electricity we must add a term of corresponding free energy into (1.2.20) and (1.2.21). The free energy of an electric field in a media with dielectric permittivity ε is:

Fig. 1.4 Critical radius corresponds to a maximum of $\Delta\Phi$



$$F_{\rm E} = \int \frac{ED}{2} dV = \int \frac{\varepsilon_0 \varepsilon E^2}{2} dV. \tag{1.2.33}$$

Since the electric field around the charge q of radius δ is:

$$E = \frac{q^2}{4\pi\varepsilon\varepsilon_0 r^2},\tag{1.2.34}$$

we have for the initial stage (a pure vapor with $\varepsilon = 1$) energy (1.2.33):

$$F_{\rm E}^{0} = \int_{s}^{\infty} \frac{\varepsilon_0 E_{\rm v}^2 4\pi \, r^2 \mathrm{d}r}{2} = \frac{q^2}{8\pi\varepsilon_0 \delta},\tag{1.2.35}$$

while for the vapor with a droplet around the charge we have:

$$F_{\rm E} = \int_{\delta}^{R} \frac{\varepsilon \varepsilon_0 E_1^2}{2} dV + \int_{R}^{\infty} \frac{\varepsilon_0 E_{\rm v}^2}{2} dV = \frac{q^2}{8\pi \varepsilon_0 R} \left(1 - \frac{1}{\varepsilon} \right) + \frac{q^2}{8\pi \varepsilon \varepsilon_0 \delta}, \qquad (1.2.36)$$

where ε is the permittivity of the liquid. Thus, we see that the difference of the total Gibbs energy now is:

$$\Delta \Phi = \Phi - \Phi^0 + F_E - F_E^0, \tag{1.2.37}$$

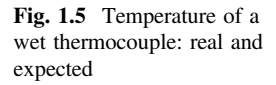
and, because $\varepsilon > 1$ for any liquid, and $\delta \to 0$, we see that $\Delta \Phi < 0$ and the formation of a new phase is thermodynamically favorable.

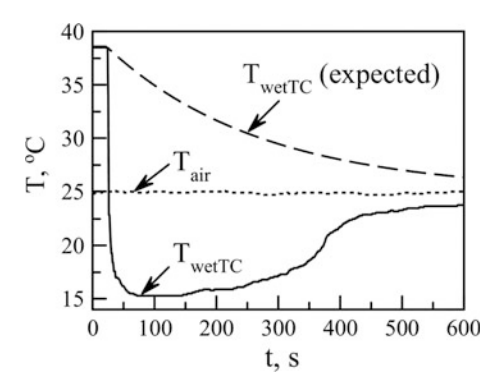
Note that the cloud chamber has a close relative: the boiling chamber, where liquid boils up under the influence of ionizing radiation. The physical basis of the boiling chamber is absolutely different; this subject will be discussed in Sect. 9.4.6 of the last chapter of this book.

1.2.4 The Evaporation Temperature

Now we are ready to apply our knowledge of thermodynamics to a real-life problem. Let us take a thermocouple (for details about the thermocouple, see Sect. 8.3), put it in warm water and get it out in air. Can we predict the temperature-time dependence T(t) for this wet thermocouple?

Why not? It is easy: we know that temperature must converge to the temperature of the surrounding medium, which plays the role of a thermostat in this experiment. Then, we may expect that the temperature of the thermocouple will monotonically decrease with time, tending to room temperature.





Then, let us conduct this experiment. The temperature dependence on time (the so-called thermogram) is presented in Fig. 1.5 (obtained with K-type thermocouples ATA-2008 for recorder ATE-2036).

Well, we have to realize that a mistake has crept into our chain of logic. We see that temperature drops significantly, to values much lower (by several degrees) than room temperature. How can it be possible? When the temperature of the thermocouple becomes equal to the temperature of the surrounding air, how can further heat transfer be feasible—at zero temperature difference between the wet thermocouple and air? Then, on the next cooling stage, when *T* drops below room temperature, is it an infringement of the 2nd law of thermodynamics—heat transferring from the cold body (wet thermocouple) to the hot body (air)?

The answer from a molecular point of view is simple: high-energy molecules leave the liquid shell on the thermocouple, as a result, liquid cools further and further. It is more interesting to answer these questions from a thermodynamic point of view.

Thermodynamics says that evaporation of a droplet from the thermocouple junction is a non-equilibrium process. In our experiment, conducted in an ordinary dry atmosphere, the reverse (condensation) flux is negligible, and the liquid phase is out of equilibrium with the vapor phase. In such conditions, for example, the Clapeyron–Clausius equation makes no sense.

As for breaking the 2nd law of thermodynamics, our formulation given above is only a logical trick, a sophism. Heat transfers from air to a liquid film on the thermocouple, this heat is being spent on evaporation, and the non-equilibrium phase transition, leads to the temperature decrease of the liquid layer, and, consequently, of the thermocouple.

Now, let us discuss an even more interesting trick.

1.2.5 Magic Bird

Magic bird is an old popular toy known in different countries under various names. For instance, in Russia it is called the "Hottabych's bird" (Hottabych is a wizard

from a Russian fairy tale). Sometimes they call it "Chinese duck" or "drinking duck." At the time of writing this book, you can find and buy this toy on Amazon by searching for "drinking bird." This toy is a glass tube (in the shape of a bird) filled with a volatile liquid and a vapor of this liquid; e.g., non-magic methylene chloride (CH₂Cl₂, dichloromethane) can be used.

Magic bird cannot fly but it shows a confusing trick. Initially, you have to position it in front of a glass of water and humidify its sponge-covered head (see Fig. 1.6a). Upon releasing the toy, the bird begins to sway, and the liquid inside the bird's body rises. Its center of mass rises, and, at some moment, the bird falls face down into the glass (see Fig. 1.6b). Liquid transfuses to the lower part of the bird, as shown in the figure, the bird straightens and the cycle repeats.

And the cycle repeats ... and repeats. Actually, magic bird can work for days or weeks, while it has enough fuel (i.e., enough water to drink).

We have met people who seriously consider magic bird to be a perpetual motion machine of the second kind. They do not know much about thermodynamics, of course!

Magic bird possesses two "liquid-vapor" transitions: (1) at its head and (2) within its body. The phase transition at its head is water evaporation from the sponge covering its head into the air. This is a non-equilibrium phase transition: there is no equilibrium between the liquid (water in the sponge) and its vapor (in air) here. The phase transition in the bird's body is the equilibrium vaporization of methylene chloride.

For methylene chloride we have the Clapeyron-Clausius equation:

$$\frac{\mathrm{d}p_{\mathrm{s}}}{\mathrm{d}T} = \frac{r}{T(\nu'' - \nu')},\tag{1.2.38}$$

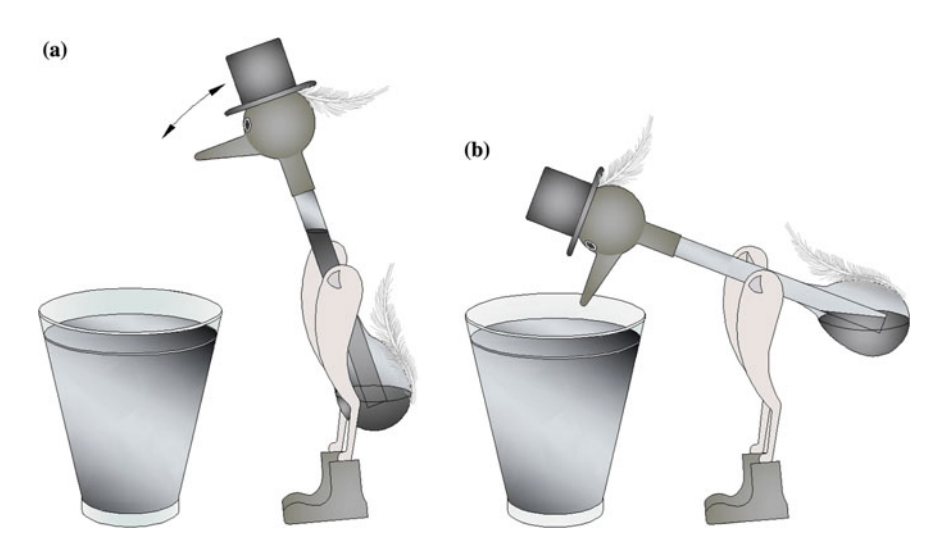


Fig. 1.6 a Magic bird, stage 1 (straightened), b magic bird, stage 2 (inclined)

where p_s is the saturation pressure, T is temperature, r is the enthalpy of vaporization and v' and v'' are specific volumes of liquid and vapor correspondingly. This vaporization occurs far from the critical point (the critical pressure for CH_2Cl_2 is 63.6 bar, taken from the National Institute of Standards and Technology (NIST) database), at low pressure, so we can neglect v' in (1.2.38) and use the Clapeyron equation for vapor:

$$v'' = \frac{RT}{p_s},\tag{1.2.39}$$

with $R = 98 \frac{J}{\text{kg K}}$ for methylene chloride.

Let us estimate the height of the column of the liquid inside the bird's body that can be reached when the bird's head is cooled by 1 K. First, for such low ΔT we can replace the derivative on the left-hand side of (1.2.38) as $\frac{\mathrm{d}_p}{\mathrm{d}T} \to \frac{\Delta p}{\Delta T}$ and put $r=3.4\times 10^5~\mathrm{\frac{J}{kg}}=\mathrm{const}$ (all data is taken from the NIST database). Then, according to (1.2.39), when the temperature of the bird's head falls to ΔT , pressure in the upper part (over the liquid) decreases to $\Delta p=\Delta p_s$, and the column of liquid rises to a height:

$$\Delta h = \frac{\Delta p \cdot v'}{g},\tag{1.2.40}$$

where $g = 9.8 \text{ m/s}^2$ is the acceleration of gravity. Thus, we have from (1.2.40) and (1.2.38) with (1.2.39):

$$\Delta h = \frac{r p_{\rm s} v'}{gRT^2} \Delta T. \tag{1.2.41}$$

Using $p_{\rm s}=63$ kPa for room temperature T=300 K and a specific liquid volume $v'=7.7\times 10^{-4} {{\rm m}^3\over {\rm kg}}$ we obtain $\Delta h\approx 20$ cm.

As we saw in Sect. 1.2.4, the value of ~ 1 K for the temperature difference between the evaporating water and air can be easily achieved; thus, we understand that a bird of ~ 10 cm height works well. Note that the bird cannot work on water: if dichloromethane was replaced by water, the lifting height calculated with (1.2.41) would be very small.

Again, it is all clear from a thermodynamics point of view. Of course, this magic bird is not a perpetual motion machine of the second kind; it does not scoop up energy from an equilibrium environment to produce work. The source of the non-perpetual motion of the drinking bird is the non-equilibrium conditions that are in place: in the absence of evaporation from the bird's head its motion is impossible. We may suggest two ways to prevent evaporation: create a wet atmosphere (the condensation flux equalizes that of evaporation) or cool down the room (rein up the evaporation itself). In both cases, the show would stop.

We may note that, of course, magic bird needs water to perform its magic motion: the evaporation of water from the bird's head is the driving force of this machine. In the absence of a glass of water (but with a wet head) the bird performs many wobbles but will stop sooner or later.

1.2.6 Thermodynamic Diagrams

In the final part of this section, we present thermodynamic diagrams for two main substances that will be treated in this book: water and argon. Water is the ordinary liquid for experimental investigations, while argon is the hero of computational simulations.

The most popular thermodynamic diagrams for phase transitions are P-T, P-V and T-S diagrams. Phase diagrams for water and argon - two liquids that will be often used in this book—are shown in Fig. 1.7 (data taken from the NIST database).

On T–S and P–V diagrams saturation curves have two branches: the left branch from the side of a liquid, and the right branch from the side of a vapor. Inside these curves one can see two-phase regions: an area of the coexistence of both phases.

It is easy to show that on a T–S diagram the saturation curve from the side of the liquid phase almost coincides with the isobars. The incline of the saturation curve is defined by the derivative:

$$\left(\frac{\partial s}{\partial T}\right)_{\text{sat}} = \left(\frac{\partial s}{\partial T}\right)_p + \left(\frac{\partial s}{\partial p}\right)_T \left(\frac{\partial p}{\partial T}\right)_{\text{sat}}.$$
 (1.2.42)

Then, we can transform this derivative with:

$$\left(\frac{\partial s}{\partial p}\right)_{T} = -\left(\frac{\partial v}{\partial T}\right)_{p}, \ \left(\frac{\mathrm{d}p}{\mathrm{d}T}\right)_{\mathrm{sat}} = \frac{r}{T(v'' - v')}, \ \left(\frac{\partial s}{\partial T}\right)_{p} = \frac{c_{p}}{T}.$$
 (1.2.43)

(the first expression follows from Maxwell equations, while the second is the Clapeyron-Clausius correlation), where:

$$\left(\frac{\partial v}{\partial T}\right)_p = \alpha v. \tag{1.2.44}$$

Here α is the volumetric thermal expansion coefficient. Far from the critical point $v'' \gg v'$, and we have for the left saturation curve:

$$\left(\frac{\partial s}{\partial T}\right)_{\text{sat}}^{\text{left}} = \frac{c_{\text{p}}'}{T} - \alpha' \frac{v'}{v''} \frac{r}{T}.$$
(1.2.45)

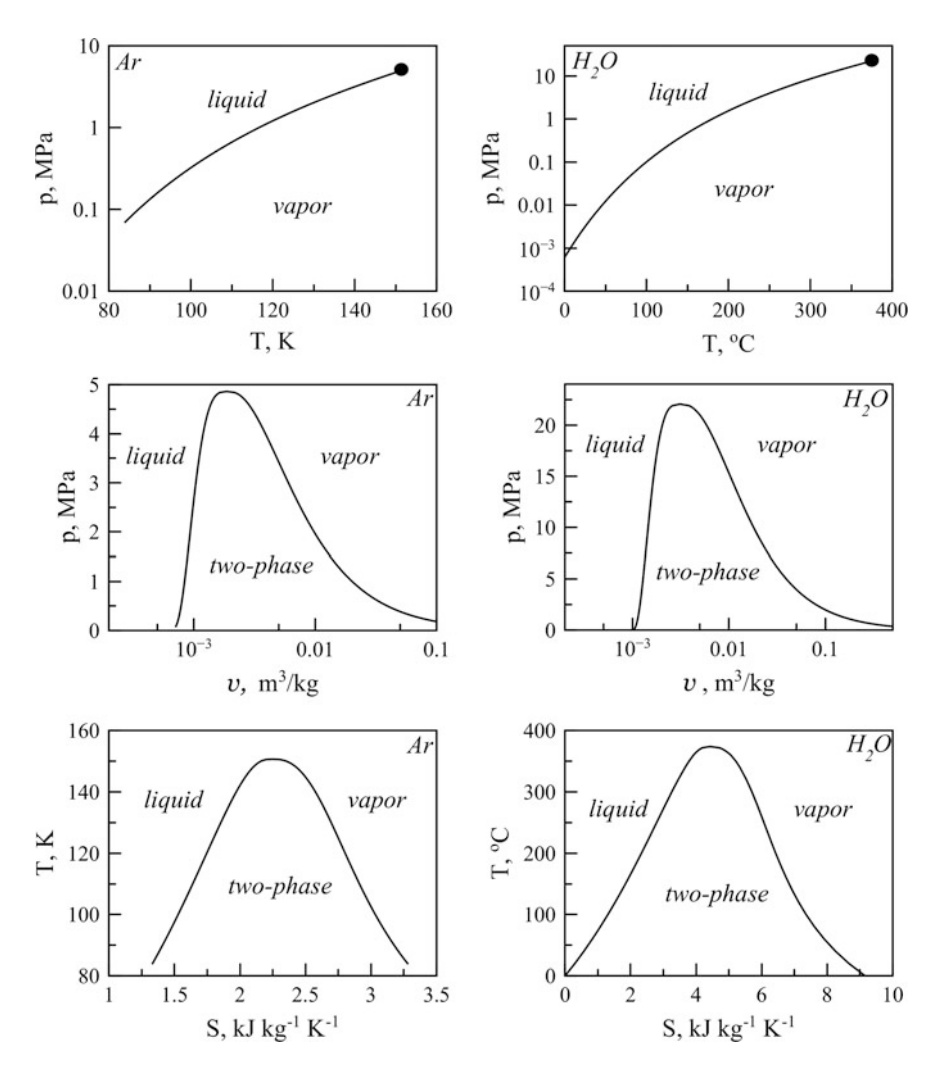


Fig. 1.7 Thermodynamic diagrams for argon and water

For example, for water $c_p' \sim 10^3$ J/(kg K); thus, the first term for $T \sim 10^2$ K is ~ 10 J/(kg K²). As $\alpha' \sim 10^{-4}$ K⁻¹, $\nu'/\nu'' \sim 10^{-3}$ and $r \sim 10^6$ J/Kg, we see that the second term is $\sim 10^{-3}$ J/(kg K²), and, consequently, this term can be neglected. For the right branch of the saturation curve—from the vapor side:

$$\left(\frac{\partial s}{\partial T}\right)_{\text{out}}^{\text{right}} = \frac{c_{\text{p}}^{"}}{T} - \alpha^{"} \frac{r}{T}.$$
 (1.2.46)

Assuming that vapor is an ideal gas, we have $\alpha'' = \frac{1}{T}$, and for water, for example, the first term is still $\sim 10 \text{ J/(kg K}^2)$ while the second term is $\sim 10^2 \text{ J/(kg K}^2)$. That is the reason why the right branch of the saturation curve has a negative incline.

Analogically, it is easy to explain why in the P-V diagram the left branch is almost vertical; however, we are now far away from evaporation—the non-equilibrium phase transition of "liquid-vapor." Let us go back.

1.3 What Can We Obtain from Hydrodynamics?

1.3.1 Navier-Stokes Equations

Hydrodynamics is based on three conservation equations. All three may be written in common form:

$$\frac{\partial A}{\partial t} + \operatorname{div} \vec{J}_A = \dot{A},\tag{1.3.1}$$

where A is the volume quantity, \vec{J}_A is the flux of the quantity A, and \dot{A} is the source of A. So, for the mass we have $A = \rho$ (mass density), $\vec{J}_A = \rho \vec{v}$ and $\dot{A} = 0$:

$$\frac{\partial \rho}{\partial t} + \operatorname{div} \rho \vec{v} = 0. \tag{1.3.2}$$

The equation for momentum conservation is much more complicated. Omitting all preliminary considerations, we may write for the *i*th projection of velocity v_i the Navier–Stokes equation (Landau and Lifshitz 1959):

$$\rho \frac{\partial v_i}{\partial t} + \rho v_k \frac{\partial v_i}{\partial x_k} = -\frac{\partial p}{\partial x_i} + \frac{\partial \varsigma_{ik}}{\partial x_k} + \rho g_i, \qquad (1.3.3)$$

where g_i is the projection of gravity acceleration, and the viscous stress tensor is:

$$\varsigma_{ik} = \mu \left(\frac{\partial v_i}{\partial x_k} + \frac{\partial v_k}{\partial x_i} - \frac{2}{3} \delta_{ik} \frac{\partial v_m}{\partial x_m} \right) + \eta \delta_{ik} \frac{\partial v_m}{\partial x_m}. \tag{1.3.4}$$

We use the regular definition for the mute summation—the convention on the summation of repeated indexes, i.e., $a_ib_i = \sum_i a_ib_i$; for instance, the operator $\partial v_m/\partial x_m$ means the divergence of vector \vec{v} .

In (1.3.4) coefficient μ is the shear viscosity, while η is the bulk (volume, second) viscosity. For an incompressible fluid, $\rho = \text{const}$, $\partial v_m/\partial x_m = 0$ and the quantity η does not play a role in (1.3.4). However, for problems of compressible flows, where $\text{div}\vec{v} \neq 0$, coefficient η becomes significant.

Navier–Stokes equations cannot be solved analytically; moreover, there are serious doubts that these constructions have a solution at all. Until now, there is no certain proof whether (1.3.3) has a solution or not (as far as we can judge, the answer is "no"). However, these problems are absolutely out of the scope of this book.

Because of the complexity of Navier–Stokes equations, other representations of velocity may be used. For instance, from Helmholtz theorem, velocity (specifically, any vector) may be expressed with scalar potential ϕ and vector potential $\vec{\Psi}$:

$$\vec{v} = \nabla \phi + \text{rot}\vec{\Psi}. \tag{1.3.5}$$

For some problems, it is easier to find potentials ϕ or $\vec{\Psi}$. For example, for the 2D flow of an incompressible fluid the velocity $\vec{v}(x,y)$ may be expressed with a potential $\vec{\Psi}$ that has a single z projection $\Psi_z(x,y)$; in this case the function Ψ_z is termed the "stream function."

1.3.2 Conditions on an Interfacial Surface

The Navier–Stokes equation is the second-order differential equation for v_i ; thus, we have to define two boundary conditions for any projection of velocity. Note that for a non-viscous fluid $\mu = \eta = 0$ we have a single-order differential equation that, consequently, demands a single boundary condition.

The simplest boundary condition for a fluid velocity on a solid wall is the zero tangential and normal projections of velocity: $v_{\tau} = v_n = 0$. However, for the liquid surface circumstances are much more complicated: here—on the interfacial surface—we may have the source (for evaporation) or the sink (for condensation) of the vapor mass flux. We will consider the boundary conditions for velocity in Sect. 1.4, but here we want to scrutinize conditions for pressure.

At the interfacial boundary, defined as $\zeta(x, y)$, pressure takes a discontinuity—the Laplace jump of pressure: the difference in pressure of two phases:

$$p_1 - p_2 = \sigma \left(\frac{\zeta_{xx}}{\sqrt{1 + \zeta_x^2}} + \frac{\zeta_{yy}}{\sqrt{1 + \zeta_y^2}} \right),$$
 (1.3.6)

where indexes at ζ denote corresponding derivatives. Pressure is higher in the convex phase. For a smooth curvature of the interface, we may omit derivatives $|\zeta_x|, |\zeta_y| \ll 1$.

Now let us consider the liquid surface; the corresponding coordinate that defines this surface is $z = \zeta(x)$ (for simplicity, we will not consider the second coordinate y).

The velocity in the liquid phase may be described with the scalar potential ϕ , i.e., with $v_x = \frac{\partial \phi}{\partial x}$ and $v_z = \frac{\partial \phi}{\partial z}$, so for an incompressible fluid from condition div $\vec{v} = 0$ we have:

$$\Delta \phi \equiv \frac{\partial^2 \phi}{\partial x^2} + \frac{\partial^2 \phi}{\partial z^2} = 0. \tag{1.3.7}$$

We can write (1.3.6) for the difference between the pressure of the vapor p_1 and of the liquid p_2 . Suppose that $p_1 = \text{const}$ and express p_2 from the Bernoulli law:

$$p_2 = p_1 - \rho g \zeta - \rho \frac{\partial \phi}{\partial t}. \tag{1.3.8}$$

Finally, we have the equation at the surface:

$$\rho g\zeta + \rho \frac{\partial \phi}{\partial t} - \sigma \frac{\partial^2 \zeta}{\partial x^2} = 0. \tag{1.3.9}$$

For the following circumstances, we assume the dependence $\sigma(\zeta)$. Differentiating (1.3.9) for time and taking into account that the normal velocity at the interface is $\frac{\partial \zeta}{\partial t} = v_z = \frac{\partial \phi}{\partial z}$, while also considering correlation (1.3.7), we have:

$$\rho \frac{\partial^2 \phi}{\partial t^2} + (\rho g - \sigma_{\zeta} \zeta_{xx}) \frac{\partial \phi}{\partial z} + \sigma \frac{\partial^3 \phi}{\partial z^3} = 0, \qquad (1.3.10)$$

where $\sigma_{\zeta} = \frac{d\sigma}{d\zeta}$ and $\zeta_{xx} = \frac{\partial^2 \zeta}{\partial x^2}$ are as declared above.

Then, represent the dependence $\phi(z) \to \phi(kz)$, where k is defined as $\frac{\partial \phi}{\partial z} = k\phi$, consequently, $\frac{\partial^3 \phi}{\partial z^3} = c_3 k^3 \phi$, where parameter c_3 depends on the function $\phi(kz)$; if $\phi \sim \exp(kz)$, then $c_3 = 1$. Thereby, (1.3.10) may be expressed as:

$$\frac{1}{\phi} \frac{\partial^2 \phi}{\partial t^2} + \left(g - \frac{\sigma_{\zeta}}{\rho} \zeta_{xx} \right) k + \frac{\sigma c_3 k^3}{\rho} = 0. \tag{1.3.11}$$

In a particular case, for $\sigma_{\zeta} = 0$, we may obtain the solution for the gravitational-capillary wave on the surface as the function:

$$\phi = Ae^{kz}e^{i\omega t - ikx} \tag{1.3.12}$$

with the dispersion equation in the form that follows from (1.3.11):

$$\omega^2 = gk + \frac{\sigma k^3}{\rho}.\tag{1.3.13}$$

Note that the dependence on coordinate x in (1.3.12) arises after the dependence $\sim e^{kz}$ due to (1.3.7).

However, when the surface tension depends on the local level of the liquid surface, i.e., $\sigma_{\zeta} \neq 0$, we cannot describe the problem in such a simple manner; function (1.3.12) is not the solution to (1.3.10). At first, we have to enucleate the realism of dependence $\sigma(\zeta)$: how may the surface tension depend on the coordinate of the surface?

The dependence $\sigma(\zeta)$ exists for binary liquids at their condensation from a vapor on cooled solid surfaces. At these conditions, the temperature at the surface depends on the liquid height ζ ; thus, if the components have different rates of evaporation, the fractions of components will depend on ζ . Thereby, because surface tension strongly depends on concentrations C of components, we finally get the dependence $\sigma(\zeta)$. Specifically, we have:

$$\frac{\mathrm{d}\sigma}{\mathrm{d}\zeta} = \frac{\mathrm{d}\sigma}{\mathrm{d}C} \frac{\mathrm{d}C}{\mathrm{d}T} \frac{\mathrm{d}T}{\mathrm{d}\zeta}.\tag{1.3.14}$$

As a result of this process, a pseudo-dropwise condensation occurs: condensation, in the form of large drops, sits on a very thin liquid film (Ford and Missen 1968; Hijikata et al. 1996). In the belles-lettres version, this effect is named the "tear of wine."

We can see something similar in (1.3.11). Neglecting gravity, i.e., considering pure capillarity, with relation $\zeta_{xx} = \frac{\rho \partial \phi}{\sigma \partial t}$ from (1.3.9) we get:

$$\frac{1}{\phi} \frac{\partial^2 \phi}{\partial t^2} = \frac{\sigma_{\zeta}}{\sigma} \frac{\partial \phi}{\partial t} - \frac{c_3 \sigma k^3}{\rho}.$$
 (1.3.15)

For example, if $\sigma_{\zeta} > 0$ and $\frac{\partial \phi}{\partial t} > 0$ we may see that for a sufficiently large first term on the right-hand side of (1.3.15) that the second derivative (on the left-hand side) would be positive. This means that if the potential ϕ starts to grow at a sufficiently high rate (at $\sigma_{\zeta} > 0$), it will show accelerated growth. We may refer to this behavior as instability, and the process as a whole represents a strong deformation of the liquid surface.

Thus, evaporation may appear by itself even on a foreign object—during the condensation process.

1.3.3 Movement of the Interfacial Boundary

The problem depicted in the title of this section is termed as the Stefan problem. The surface of a phase transition is determined by two conditions:

- The temperature is equal to the temperature of the phase transition T_s .
- The heat flux normal for the interface takes a jump:

$$\underbrace{-\lambda_1 \frac{\partial T_1}{\partial n}}_{q_1} + \lambda_2 \frac{\partial T_2}{\partial n} = \rho \, rv, \qquad (1.3.16)$$

with thermal conductivity λ , mass density ρ , latent heat of phase transition r and velocity of the moving interfacial boundary ν .

Equation (1.3.16) must be solved in combination with the heat conductance equation:

$$\frac{\partial T}{\partial t} = a\Delta T,\tag{1.3.17}$$

 $(a=\frac{\lambda}{\rho\,c_{\rm p}}$ is the thermal diffusivity and $\Delta=\sum_k\frac{\partial^2}{\partial x_k^2})$ and the boundary condition for (1.3.17). In general, it is impossible to solve this problem analytically, except in some special cases. For slow boundary motion, when $v\ll a/l$ (l is the spatial scale; this is certainly not a perfect estimation), we may solve the Stefan problem in two steps: (1) find the temperature distributions in two phases and (2) determine the boundary velocity v from (1.3.16).

Equation (1.3.16) can be applied to find the velocity of the evaporation front: due to mass leakage because of evaporation, the coordinate of the liquid surface moves. Sometimes, this velocity may be found neglecting the heat flux q_2 in (1.3.16), i.e., the velocity $v = \frac{q}{\rho r}$ is determined only by the heat flux conducted from one of the phases (e.g., from the vapor). The rate of mass lost per unit of the surface area $J = \frac{1 \text{d}m}{S \text{d}t}$ can be calculated in this case as J = q/r.

Nevertheless, one key feature distinguishes evaporation from other sorts of phase transitions, such as boiling or melting. Evaporation takes place at any surface temperature, consequently, we cannot assume that the temperature of the evaporation surface is equal to some special temperature T_s . We cannot put the temperature of the evaporation surface, for example, equal to the boiling temperature, especially considering the fact that the surface temperature is lower than the temperature of the bulk of a liquid: because fast molecules leave the surface (evaporate), the mean kinetic energy of surface molecules is always lower than inside the liquid. In simple words, fast molecules always sink at the liquid surface, so the temperature of the surface always decreases. Another question is how big is this temperature difference -0.1 K or 10 K?

1.3.4 Dynamics Near the Evaporation Surface

Far from the interface, we have a common hydrodynamic problem. The mass flux in a vapor consists of two parts: the convective term $\rho \vec{v}$ and the diffusive one $-D\nabla n$, where n is the mass concentration of the vapor.

Usually, for simplicity, only one part of the mass flux is considered: either convective or diffusive. In the case of evaporation in air, the latter approach can be used, so we have the diffusion equation in vapor:

$$\frac{\partial n}{\partial t} = D \frac{\partial^2 n}{\partial x^2} \tag{1.3.18}$$

with a boundary condition at the evaporation surface for the mass flux:

$$\left. \frac{\partial n}{\partial x} \right|_{x=0} = -\frac{J}{D}.\tag{1.3.19}$$

The mass flux can be determined under the assumptions discussed in the previous subsection through the heat flux q from the liquid phase, i.e.:

$$J = \frac{q}{r} = -\frac{\lambda}{r} \frac{\partial T}{\partial x} \bigg|_{x=0}.$$
 (1.3.20)

As for temperature, in our statement—in the absence of convective fluxes—we have the diffusive form of (1.3.17).

Note that we may formulate the problem for a droplet in spherical coordinates; such a solution directs us to J. C. Maxwell and will be considered in Chap. 7.

Here we discuss the non-stationary solution of the system of (1.3.17)–(1.3.18) for liquid at x < 0 and vapor at x > 0 (axis \vec{x} is directed for the liquid surface into the vapor), with initial and boundary conditions:

$$T(t=0,x<0) = T_0, \quad T(t,x\ge0) = T_g, \quad n(t=0,x\ge0) = 0,$$
 (1.3.21)

Further, we will neglect to consider the movement of the interface: strictly, as it was discussed in Sect. 1.3.3, if the position of the interface was x = 0 at t = 0, then this position will be x < 0 for t > 0. The gas temperature is assumed to be constant: $T_g = \text{const.}$

Thus, we obtain a simple solution for temperature inside a liquid, i.e., for x < 0:

$$T(t,x) = T_g - \left(T_0 - T_g\right) \operatorname{erf}\left(\frac{x}{2\sqrt{at}}\right), \tag{1.3.22}$$

where erf(x) is the error function (see Appendix B). Thus, the heat flux on the liquid surface is:

$$q(t) = -\lambda \frac{\partial T}{\partial x}\Big|_{x=0} = \frac{\lambda (T_0 - T_g)}{\sqrt{\pi \, at}}.$$
 (1.3.23)

Consequently, we have for vapor concentration (x > 0):

$$n(t,x) = \frac{1}{\sqrt{\pi}} \int_{0}^{t} \frac{J(\tau)}{\sqrt{t-\tau}} \exp\left(-\frac{x^2}{4D(t-\tau)}\right) d\tau, \qquad (1.3.24)$$

where the mass flux on boundary J(t) is defined by (1.3.20) with (1.3.23).

Correlation (1.3.24) determines the vapor mass in the gaseous phase. We see that we may obtain the solution even for a non-stationary problem. Of course, we make some assumptions here, such as constant temperature in the vapor, so that all the heat flux on the liquid surface is spent on evaporation. However, actually, we have the complete solution to the problem in macroscopic language. We may also introduce the convective flux to the problem, and solve it at least numerically. Do we see any problem with the macroscopic description presented here?

We have a sufficient description, what else?

1.4 Boundary Conditions

1.4.1 Boundary Conditions for Hydrodynamics

As mentioned in Sect. 1.3, hydrodynamic equations (Navier–Stokes equations) require velocities on the interfacial surface: normal projection v_n and tangential projection v_τ . One may hope that by defining these velocities, it becomes possible to find all the physics of evaporation. In reality, hydrodynamic equations are exact, fundamental correlations; for instance, Navier–Stokes equations represent momentum conservation. Then, we may expect that proper hydrodynamic solutions provide us with the full description of evaporation.

Let us try to define the velocities of the vapor near the evaporation surface. At first glance, it is easy to find velocity v_n : if we know the temperature of the liquid, we may calculate the corresponding mean velocity in a given direction, e.g., we have something like:

$$v_n = \sqrt{\frac{2T}{\pi m}} \tag{1.4.1}$$

for the Maxwell distribution function (MDF) of particles. Thus, (1.4.1) would be the normal velocity, and the mean tangential velocity would be equal to the velocity of the liquid, i.e., in the most frequent case $v_{\tau} = 0$. Done!

However, one problem faces us with this approach: the hydrodynamic description considers physical problems on large spatial scales, larger than the mean free path (MFP) of a molecule. In other words, the "mean velocity" for the hydrodynamic description implies the mean velocity of a huge amount of molecules in the volume of a specific size (~ 10 MFPs).

In a vapor, the MFP is a considerable distance, and the most interesting processes that define the evaporation phenomenon as a whole, take place at scales which are approximately equal to the MFP or even smaller, e.g., the DF of evaporated atoms is established at distances much shorter than the MFP (about several nanometers from the evaporation surface, see Chap. 5). Thereby, in the better case, velocity (1.4.1) may be adequate only directly at the evaporation surface (actually perhaps not, see Chap. 5); then, at distances approximately equal to the MFP, the DF of evaporated particles changes, and changes significantly at distances much greater than the MFP. Thus, the distribution function varies significantly in an "elementary dot" of the medium (for the scale of hydrodynamic description) near the evaporation surface, so velocity in this elementary point of the vapor is undefined.

Thus, hydrodynamics is insufficient: it cannot describe properly the evaporation process itself; it is rather the evaporation that determines the boundary conditions for hydrodynamic equations.

But hydrodynamics has a younger sister—physical kinetics.

1.4.2 Boundary Conditions for Kinetics

As always, kinetics hastens to the rescue of hydrodynamics. Boundary conditions may be obtained from the solution of the kinetic equation—the equation for the so-called DF f(v) (the velocity probability distribution function). Actually, there are many forms of the kinetic equation (see Chap. 3); almost all of them present themselves as differential (or integral—differential) equations.

Thus, one may find the boundary conditions for the Navier–Stokes equation, if one solves the kinetic equation, i.e., by calculating the mean velocity:

$$\bar{v} = \int v f(v) \, \mathrm{d}v, \qquad (1.4.2)$$

etc. However, first one has to solve the kinetic equation for DF f(v). For this operation, boundary conditions for the DF must be formulated, in turn.

The most popular boundary condition for the DF at the liquid surface is the MDF:

$$f(v) = \sqrt{\frac{m}{2\pi T}} \exp\left(-\frac{mv^2}{2T}\right),\tag{1.4.3}$$

where m is the mass of the molecule and T is temperature. Probably, the characteristic of "popular" does not sound appropriate for scientific literature, but in most works the DF (1.4.3) is accepted without any serious discussion. Sometimes, one may find the following justification of (1.4.3): the Maxwellian must be observed in a fluid, thus, because evaporated particles move from the liquid surface, they have the same DF as particles in the liquid.

Sometimes, the DF (1.4.3) is modified to take into account the average velocity of vapor V as:

$$f(v) = \sqrt{\frac{m}{2\pi T}} \exp\left(-\frac{(v-V)^2}{2T}\right). \tag{1.4.4}$$

But the DF here is not justified more strictly than the DF in (1.4.3). In both cases, the source of these DFs is rather intuition than physical analysis.

The central part of this book is devoted to determination of the DFs on the evaporation surface. In Chap. 5 we define the DF of velocities and in Chap. 6 the DF of potential energy.

1.5 Conclusion

Evaporation occurs everywhere: it governs life on Earth and rules the ever-thirsty bird toy. One may suppose that evaporation is an elementary process, but its oddity may be observed even in a glass of wine.

Evaporation is a "liquid-vapor" surface phase transition. This is a non-equilibrium process, which occurs at any temperature of a liquid's surface. Evaporation is not boiling, however, many aspects of the boiling process can be explained using aspects of evaporation.

One should avoid applying equilibrium thermodynamics relations for evaporation, because evaporation only represents the non-equilibrium part of the (eventually) equilibrium phase transition that is "liquid-vapor", which consists of both evaporation and condensation. Even here, in the conclusion, we must repeat that using the quantity of "temperature" for strong non-equilibrium processes should be avoided: you get nothing except confusion.

The hydrodynamic description of evaporation is fundamentally insufficient. Despite the fact that we can obtain some results on a macroscopic level, any refinement of the physical problem is impossible, because the spatial scale of hydrodynamic formulation is too large for the evaporation process. Indeed, during evaporation all the events occur over shorter distances, where hydrodynamics makes no sense.

Kinetics appears more suitable for the description of the evaporation phenomenon. However, kinetic equations demand boundary conditions (boundary distribution functions) too. These boundary functions represent tough opponents, so we have to move step by step.

Let us begin.

References

W. Abtew, A. Melesse, Evaporation and Evapotranspiration: Measurement and Estimations (Springer, Dordrecht, 2013)

V.S. Ajaev, Interfacial Fluid Mechanics: A Mathematical Modeling Approach (Springer, New York, 2012)

- A.A. Avdeev, Bubble Systems (Springer, Dordrecht, 2016)
- I.P. Bazarov, Thermodynamics (Vyscshaya Shkola, Moscow, 1991)
- J.D. Bernardin, I. Mudawar, J. Heat Transf. Trans. ASME 121, 894 (1999)
- W. Brenig, Statistic Theory of Heat: Nonequilibrium Phenomena (Springer, Berlin, 1989)
- D. Brutin (ed.), Droplet Wetting and Evaporation: From Pure to Complex Liquids (Elsevier, Amsterdam, 2015)
- J.D. Ford, R.W. Missen, Can. J. Chem. Eng. 46, 309 (1968)
- Y. Fujikawa, T. Yano, M. Watanabe, *Vapor–Liquid Interfaces, Bubbles and Droplets* (Springer, Heidelberg, 2011)
- S.R. German et al., Faraday Discuss. 193, 223 (2016)
- K. Hijikata, Y. Fukasaku, O. Nakabeppu, Trans. ASME 118, 140 (1996)
- A. Kryukov, V. Levashov, Yu. Puzina, Non-Equilibrium Phenomena Near Vapor-Liquid Interfaces (Springer, Heidelberg, 2013)
- L.D. Landau, E.M. Lifshitz, Fluid Mechanics (Course of Theoretical Physics, Volume VI) (Pergamon Press, Oxford, 1959)
- V. Novak, Evapotranspiration in the Soil-Plant-Atmosphere System (Springer, Dordrecht, 2012)
- P. Papon, J. Leblond, P.H.E. Meijer, The Physics of Phase Transitions (Springer, Berlin, 2002)
- S. Sazhin, Droplets and Sprays (Springer, London, 2014)
- J. Serrin, Mathematical Principles of Classical Fluid Mechanics (Encyclopedia of Physics, Volume 3/8/1) (Springer, Berlin, 1959)
- Y. Sone, *Kinetic Theory and Fluid Dynamics* (Springer, New York, 2002)
- Y. Sone, Molecular Gas Dynamics (Birkhauser, Boston, 2007)
- A.S. Tucker, C.A. Ward, J. Appl. Phys. 46, 4801 (1975)
- C.A. Ward, A. Balakrishnan, F.C. Hooper, J. Basic Eng. 92, 695 (1970)
- C.A. Ward, A.S. Tucker, J. Appl. Phys. 46, 233 (1975)
- S.-C. Wong, The Evaporation Mechanism in the Wick of Copper Heat Pipes (Springer, Cham, 2014)
- Yu.B. Zudin, Non-Equilibrium Evaporation and Condensation Processes: Analytical Solutions (Springer, Dordrecht, 2018)

Chapter 2 The Statistical Approach



An essential part of this book is computational simulation. Many analytical results will be examined by numerical calculations; for instance, we will represent the Maxwellian distribution function obtained with molecular dynamics simulations, i.e., we will present a statistical distribution function from the solution of mechanical equations. Taking into account the strengths of the mechanical and statistical approaches, we have to discuss the nuances of the statistical description itself.

Our goal is not to revive past discussions, but explain connections between mechanics and statistics, specifically, to reconcile molecular dynamics simulations results with the opinion that mechanics cannot predict the thermal equilibrium state in principal.

The second aim of this chapter is to connect the term "probability" (which often means randomness) with the deterministic character of mechanics. As we will see below, this is an easy task.

2.1 From Mechanics to Probability

2.1.1 From Mechanics ...

Any attempt to consider the world around us as a mechanical system capitulates in the face of an army of countless units—of fast, poorly known and badly predictable units—atoms. But in the middle of the 19th century physics discovered a backdoor to the problem: despite the fact that the motion of a single particle is practically unpredictable, we can predict the motion of a large group of particles. Specifically, we can predict some overall parameters of motion of a large group of atoms. These are non-mechanical parameters of a mechanical system ... so is this system really mechanical? The contradiction between the principle of least action and the 2nd law of thermodynamics led to a radical point of view that mechanics cannot describe

this world without an additional hypothesis of randomness. More precisely, the most radical point states that the randomness hypothesis represents an instrument which is sufficient for physical description.

However, mechanics has never given a reason to doubt its correctness—in cases where the laws of mechanics have been applied, reliable results are obtained every time. Sometimes it seems like something extra-mechanical has been found in a well-known mechanical system; maybe, the last example is the "Pioneer effect." However, as for these space satellites, such problems are always being solved successfully without breaking the fundamentals of mechanics.

Evidently, nature always tries to hide its mechanics from us. It could be a problem of small denominators, or the common problem of integrability of a mechanical system, or strong dependence on initial conditions, etc. Nature performs good attempts to disappoint us with its power of mechanics. At least in one case, such an attempt is almost successful.

Physics surrenders to the number of particles in a real system. We cannot track (i.e., calculate the trajectories of) even a small number of particles in a room, and, moreover, we cannot predict the motion of even a single atom over any significant time interval. However, as we know today, we can predict some integral parameters of gas in a room, and, in a general case, this is what we need (until we want to predict the weather in our common "room"—on Earth). Many areas of science were developed to describe nature on a macroscopic level, without any information of molecules and their interaction. For instance, to analyze a flow in a pipe we can neglect the atomistic structure of a fluid and use such terms as "mass density," "flow rate," etc. Even coefficients (like viscosity) which can be, theoretically, obtained with atomistic theory, are usually taken from the experimental data, i.e., in frame of the macroscopic level.

Thus, physics successfully overcomes the unpredictability of a mechanical system: we can always use a description of a higher level, such as hydrodynamics or thermodynamics ... with the next part—the analysis of the connection between the higher level and the mechanical fundament—being optional. As a rule, we tend to be satisfied with circumstances where we can describe a system, with questions of predictability of a group of molecules fading into the background.

There exists an analog in popular physics literature: we cannot predict the behavior of a single citizen, but we can predict the behavior of a mob. Of course we could argue both points, but here we have to review the possibility of prediction in nature.

2.1.2 ... Through a Chaos ...

Many physical terms come from common language, where a word means some elusive, intuitively comprehensible matter. The word "chaos" is an excellent example of such a term: originating from the Greek " $\chi\alpha\sigma\zeta$," this term means any perturbing, disordered matter of any kind. What was before the beginning of time?

Chaos. What do we see in a child's room? Chaos. What is the turbulent motion of a liquid? Chaos. Sometimes the overloading of a scientific term is not harmful, but in physics the term "chaos" has a precise meaning, and applications of this term must be adequate.

A chaotic system is a system with a strong dependence on its initial conditions. Specifically, if the fluctuation δ of a parameter x obeys the exponential law:

$$\delta(t) = \delta(0)e^{\lambda t}, \quad \lambda > 0, \tag{2.1.1}$$

then any initial deviation will increase with time. Thus, even a small disturbance $\delta(0)$ leads to a large deviation $\delta(t)$ at a sufficiently large t, and because of high δ our parameter x becomes unpredictable for long periods of time t. Such a system (a system with a strong dependence on initial conditions) is termed a chaotic system. Such a system "forgets" its initial conditions; this property is illustrated in Fig. 2.1.

In Fig. 2.1 the results of numerical 2D simulations for electron plasma are presented [method of the macroparticles was used, see Sigov (2001)]. We simulate the dynamics of plasma at time Δt , then stop the particles and recourse their velocities. The parameter $\Gamma = u^{\Sigma}/\epsilon^{\Sigma}$ —the ratio of the total potential energy of particles to the total kinetic energy of particles—is shown for the two cases and for the velocity recourse moment $\Delta t = 5$ ns and $\Delta t = 200$ ns. We see that in the first case the plasma returns to its initial state, while in the second case our stop—reverse operation does not lead to any effect: system "forgot" its initial state.

Thus, when Boltzmann said to Loschmidt "Try to recourse them!", he was partially right: it is not so easy. However, this fact has no relation to the problem that was discussed by them. Of course, the image in Fig. 2.1b has nothing to do with irreversibility.

A chaotic system is unpredictable in terms of its parameters [for the deviation of any parameter x_i we have a condition (2.1.1)], but we may introduce some new parameters for our system and try to describe our system using them.

For example, if a mechanical system is a chaotic system, then we cannot predict the motion of its particles, e.g., we cannot predict the motion of gas atoms in a

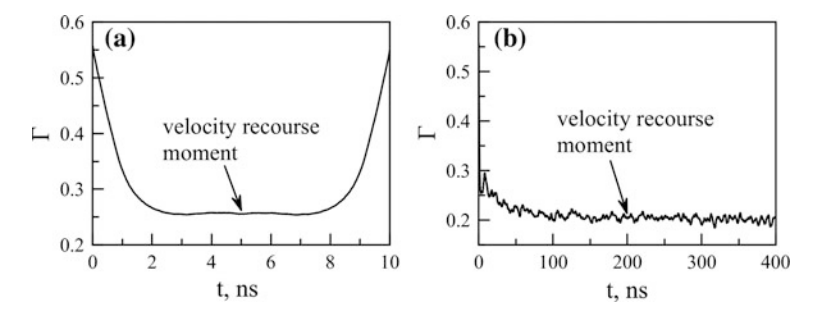


Fig. 2.1 We can return "them," but not from the distant future

room. How tragic is this fact? Usually, we are not interested in the motion of particles of a gas, we are interested in such parameters as temperature T or pressure p. However, both parameters can be evaluated for an average state of the system, without detailed information about any particle. If the velocity of particle A increases by Δv with time while the velocity of particle B decreases by Δv , then the overall result stays the same.

Thereby, if we do not need to know the velocity of any individual particle, but want to know the fraction of particles dw which have velocity from v to v + dv, we may formulate our interests in terms of a distribution function (DF):

$$f(v) = dw/dv. (2.1.2)$$

This is the function that mathematicians term as a "probability density function." Here we avoid this name for two reasons: because physicians call it (for unknown reasons) the "distribution function" and, mainly, because we want to avoid the word "probability" for as long as possible.

2.1.3 ... to Probability

How can we calculate the DF? From a mechanical standpoint, it is both easy and not very easy: one has to calculate the number of particles N_i in the room for the *i*th range of velocity Δv , corresponding to the velocity v_i , then $w_i = N_i/N$, where $N = \sum N_i$ is the total number of particles, and $f_i = w_i/\Delta v$.

Do we see any probability there? Actually, no. We see no randomness, no more randomness than the height distribution of players in a basketball team (where the player's height correlates with his role). As yet, it is only statistics: we count participators and obtain their DF.

However, one may try to construct the DF f(v) in other way. What if there exist some common principles, according to which some universal DF may be found for some universal state? If so, we may establish the DF f(v) a priori, without calculating the velocities of all the particles in a room. However, can mechanics predict the existence of such an "universal state"? In mathematical language: does a mechanical system tend to the universal attractor?

To add intrigue, we can point out that this universal state has a special name in thermodynamics: it is called a "thermal equilibrium state." Thus, the existence (specifically, the absence) of thermal equilibrium is a possible point where mechanics, considered by many, has a weakness: evidently, the existence of thermal equilibrium is an obvious empirical fact (look around). Thus, we have two choices:

- Mechanics predicts thermal equilibrium.
- Mechanics is wrong.

We cannot consider here such matters in detail (the aim of this book is to describe various regimes of evaporation, e.g., in Chap. 9), but, actually, we have

not exaggerated the fervor of this discussion. For example, you may read a popular book by Ilya Prigogine, *The End of Certainty* (with a subtitle *Time, Chaos, and the New Laws of Nature*), which is full of indeterministic ideas and critical arrows toward classical Newtonian mechanics, or other similar books.

Now, once the intrigue has been overcome, we can analyze arguments calmly.

The fact is that there are no special states in mechanics. A mechanical system is a reversible system, and the theorem of Poincare-Zermelo states that any state (determined by the coordinates and velocities of all its particles) of an isolated system must be repeated with a given accuracy. In other words, such a function as entropy (that only may increase in an isolated system, according to the most radical formulation of the 2nd law of thermodynamics) cannot exist. Let us follow the arguments of Zermelo (1896a, b).

Let x_{μ} be the 3N coordinates and 3N components of the velocity of N particles. Thereby, the Hamilton equations have the form:

$$\frac{\mathrm{d}x_{\mu}}{\mathrm{d}t} = X_{\mu}(x_1, x_2, \dots, x_n), n = 6N, \tag{2.1.3}$$

where X_{μ} does not depend on x_{μ} . For instance, for a given coordinate the time derivative $dx/dt = v \neq f(x)$. So we have:

$$\frac{\partial X_1}{\partial x_1} + \frac{\partial X_2}{\partial x_2} + \dots + \frac{\partial X_n}{\partial x_n} = 0.$$
 (2.1.4)

Let in the initial state P_0 (i.e., at t = 0) for every μ :

$$x_{\mu} = \xi_{\mu}.\tag{2.1.5}$$

Thereby, for a state P at instant t all our quantities may be represented as solutions of (2.1.3):

$$x_{\mu} = \Phi_{\mu}(t - t_0, \xi_1, \xi_2, \dots, \xi_n).$$
 (2.1.6)

This solution is as correct for $t - t_0 > 0$ as for $t - t_0 < 0$, because P_0 is an arbitrary state, in general. For the phase volume of initial states, we have:

$$\gamma_0 = \int \mathrm{d}\xi_1 \mathrm{d}\xi_2 \dots \mathrm{d}\xi_n \tag{2.1.7}$$

correspondingly, for moment t:

$$\gamma = \int \mathrm{d}x_1 \mathrm{d}x_2 \dots \mathrm{d}x_n. \tag{2.1.8}$$

However, due to the Liouville theorem, in the case of (2.1.4) $\gamma = \gamma_0$. Consequently:

$$d\gamma = dx_1 dx_2 \dots dx_n = \text{const.}$$
 (2.1.9)

Thereby, let us consider the phase region g_0 at moment t=0 (of volume γ_0) and its future images—phase regions g_t , t>0 (of volume $\gamma=\gamma_0$); i.e., all future regions of g_0 , denoted as G_0 , is the set of g_t . The volume Γ of G_0 will be of finite value if quantities x_1, x_2, \ldots, x_n are limited. Because G_0 —the future of g_0 —is fully determined by g_0 , there can be no new states in G_0 . Some states may leave G_0 , but the dimension of that set is less than the dimension of Γ itself, i.e., the states that leave G_0 cannot be represented as the finite volume in G_0 (Zermelo termed these states as "singular"). Then, g_0 is contained in G_0 , g_t is contained in G_t , thereby, g_0 is contained in G_t , and we see that $g_0 \to g_t \to g_0 \ldots$ except for the singular states, all other states will return to the initial state. Thus, there is no irreversibility. From the indeterministic point of view, mechanics signed its own death sentence with this conclusion.

In light of his work, Zermelo stated that it is impossible to prove that the Maxwell distribution represents the final state of a system.

In his immediate answer Boltzmann agreed that the theorem is true, but stated that its application is wrong. The Maxwell distribution corresponds to the most probable states of a system; there is no confrontation between a "particular function (i.e., Maxwellian) vs. all other functions," because, according to Boltzmann, "the maximum number of possible velocity distributions has specific properties of the Maxwell distribution." In other words, Boltzmann stated that there is no special limit state established in the system, but this system fluctuates around the "most probable" state. For a single molecule, this "most probable" (i.e., the most frequently observed) state corresponds to any equitable component of velocity, which leads to the Maxwellian distribution function (see Sect. 2.2.3).

The next round of discussion between Zermelo and Boltzmann (with participation of Poincare) was devoted to the H-function, its behavior with time H(t) and a correspondence between the 2nd law of thermodynamics and mechanical principles. A lot of effort was spent to prove the unprovable and to reconcile the irreconcilable. For our purposes, it is important to conclude that an agreement was achieved in this polemic: Maxwellian may be considered as the most probable velocity distribution (not as the final state of the system).

We may not doubt the Maxwellian DF—it can be obtained for a mechanical strongly chaotic system. As an illustration, in Fig. 2.2 we represent the velocity DF of macroparticles (the total number of macroparticles is 1800); see also Fig. 2.1.

Initially, all the particles were divided in two groups: 900 particles formed a uniform background and 900 particles were concentrated in the corner of a square area (see Fig. 2.3a); the initial velocity DF of all 1800 particles was uniform. With time, all particles were mixed (see Fig. 2.3b). Moments in time in Fig. 2.2 correspond to Fig. 2.1, i.e., the DF at a 300-ns instant correspond to the quasi-reverse motion.

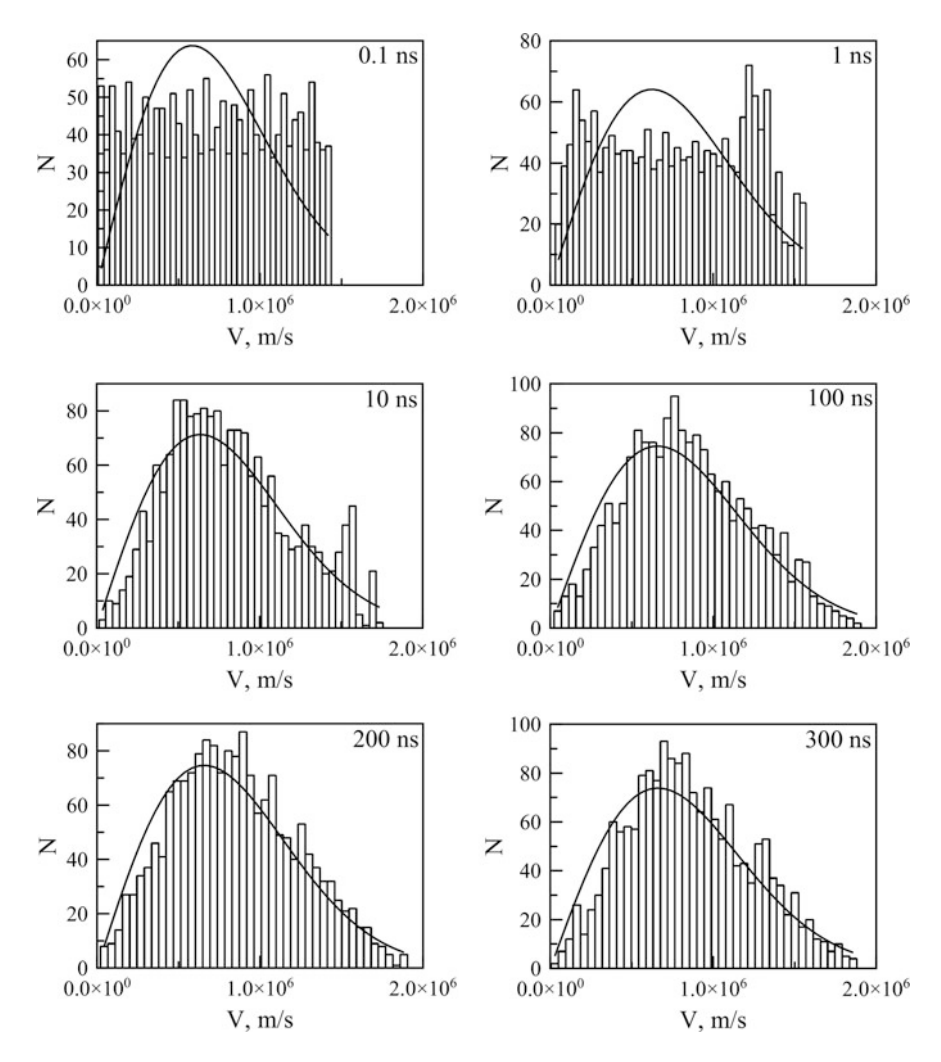


Fig. 2.2 Velocity distribution functions at different moments of time curved line represents the 2D Maxwellian distribution function

Thereby, the chaotization helps us introduce a function that may describe the distribution of particles to their velocities. The fraction of particles with velocity ν may be considered as the probability for a single particle to have a velocity ν , or for us to find a particle with such a velocity. However, in both cases probability only means a fraction of particles, nothing more. No randomness. Chaos is chaos, chance is chance. These are different things.

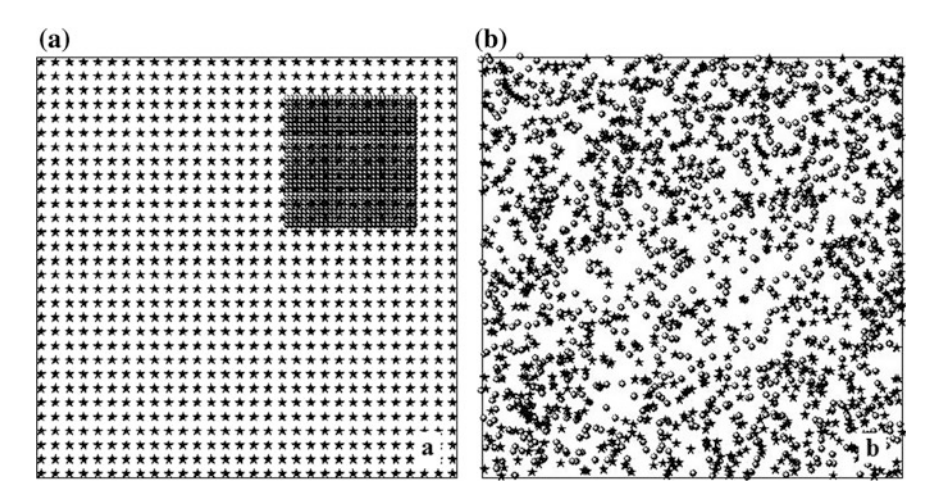


Fig. 2.3 a Initial spatial distribution and b the spatial distribution at 200 ns

2.1.4 Irreversibility Versus Unidirectionality

Newtonian mechanics describes reversible systems. For instance, in Hamiltonian equations:

$$\frac{\mathrm{d}x}{\mathrm{d}t} = v,\tag{2.1.10}$$

$$\frac{\mathrm{d}v}{\mathrm{d}t} = \frac{F}{m} \tag{2.1.11}$$

we may replace $t \to -t$ and $v \to -v$, and these equations will stay the same. Or, as Loschmidt proposed, we may recourse particles of gas in a room, and they return to their initial position. Chaoticity (i.e., strong dependence on initial conditions) prevents the observation of this process in numerical simulations. However, it does not prevent reversibility in principal: Fig. 2.1b does not illustrate any irreversibility in the system. For a demonic condition $\delta(0) = 0$ in (2.1.1), any $\delta(t) = 0$, and the system is fully predictable in a demon's mind.

However, despite the reversibility, unidirectional motion is quite possible. A stone moves toward the Earth, not back from it or in an arbitrary direction. The directionality of motion is determined by the direction of force.

Irreversibility is a thermodynamic concept. Irreversibility means that we cannot return system A to its initial state without changing environment B; a long time ago Planck explained that the process that goes in one direction may, in general, be reversed in the opposite direction. Irreversibility is a more complicated, overly mechanical property.

It looks mysterious, but sometimes concepts of irreversibility and unidirectionality are mixed even by scientists. Some process, e.g., the flight of a stone released from a sling, may be unidirectional, but it can be turned back, if we stop a stone

during this flight (by some magical force) and change the sign of its velocity. Thus, a unidirectional process may be reversible.

All that we see around us is directionality, not irreversibility. As Plato said to Diogenes during a feast: "You have the eyes to see the cup, but you don't have the mind with which to comprehend cupness;" in other words, we have eyes for directionality, but we must also have a mind for reversibility. The diffusion process is irreversible because it is described by the irreversible equation:

$$\frac{\partial n}{\partial t} = D \frac{\partial^2 n}{\partial x^2},\tag{2.1.12}$$

which is asymmetrical with replacement $t \to -t$, not because we see some irreversibility of the process of diffusion by eye.

In other words, reversibility is a scientific construction, while directionality is an observed feature. These are absolutely different matters. It is logically wrong to attempt to illustrate irreversibility with reference to any observable, unidirectional process. For instance, in his books Prigogine gives an example of a flower, which can never be seen to return to a seed. Of course, such mysterious things have never been seen, but a stone flying away from the ground has also never been seen (without external forces being applied to it, of course), while the flight of a stone obeys classical, reversible mechanics. Briefly, our eyes are bad advisers in such a complicated matter as irreversibility.

In fine, we may propose a pure mechanical "arrow of time." Let us launch a rocket named "Arrow of time" out of our solar system. On its endless voyage, the distance from this spacecraft to the Sun may be used to calculate a value of time by those who assume that reversibility is an equivalent to the absence of time.

2.1.5 "Tomorrow It Will Be Raining with 77% Probability"

Like chaos, the term "probability" has an elusive, ordinary meaning, and this domestic meaning confuses our logic. Evidently, it is better to banish the word "probability" from our everyday language forever, but the probability of success of this attempt is negligible.

Let us imagine a column of ducks crossing a street, and a mad motorcycle driver at a previous turn in the road. Observing all this tragedy with a naked eye, we may conclude that one of these ducks will be found under the wheel of that bike. From this point of view, the probability for any duck to die in this accident is 1/N. Moreover, a smart duck (intuitively feeling impending doom) may decide that with an increase in N its personal probability of dying decreases; from this point of view, this smart duck may invite more friends to cross the road. However, if we get a job calculating the trajectory of the driver and the exact position of any duck at the moment of the catastrophe, we have to conclude that for a single duck this probability is equal to unity, for other ducks—equal to zero. Can we use the term

"probability" as a measure of our incomplete knowledge? Some may answer "yes" to this question, incorporating a lot of philosophy to their conclusion. However, it is uncomfortable to realize that the term "probability" may be a measure of our laziness (our laziness to analyze and to calculate).

To introduce a probability, we have to organize a set of independent tests with the same conditions. At least, in a mental experiment. Sometimes, it is possible, but sometimes not. In an attempt to predict such mysterious things as weather or the result of a football match, we talk about probability, despite the impossibility of filling this definition with any definite content. Sometimes, probability is an inappropriate term. We cannot take thousands of tomorrows and observe the weather or sporting competitions in such cases, we cannot even imagine how this mental examination could be realized.

One girl from a famous anecdote says that the probability of meeting a dinosaur on the street is 50%: we may meet it or not. This is an example of an intuitive estimation of probability, and not the worst one by the way. Honestly, how many times have we made the same conclusions, i.e., how many times have we used the term "probability" where its definition has made no sense?

A dramatic example—with what probability will I die tomorrow? At first glance, one may construct some probability density function based on the average lifespan of people sharing my gender, social group, job, weight, and of my pernicious habits, and of the other billion parameters that, in fine, identify me as a certain person. However, in this case we cannot construct such a probability density function because of the absence of statistical material—I am a unique subject, so are you. Otherwise, for restricted description (restricted by the "gender—country" dyad, for instance) the death probability function may miss some significant information: did I mention the radiation dose that I have received up to my current age? And so on. Indeed there are no reasons to worry about such mindless questions. Actually, the grim question from the beginning of this paragraph has no more serious sense than the question "With what probability will I get married tomorrow?"

In fine, we say that the term "probability" here and below, throughout this book, means a "fraction." A fraction of particles with velocity ν , a fraction of evaporated atoms, etc. No randomness conceptions are used in this book.

2.2 Distribution Function

2.2.1 Probability Density Function

The probability density function f(x) can be determined with the probability dw that a variable has a value from x to x + dx:

$$dw = f(x)dx. (2.2.1)$$

In mathematics, the distribution function is:

$$F(y) = \int_{-\infty}^{y} f(x) dx,$$
 (2.2.2)

while traditionally in physics under the term "distribution function" the function f(x) is meant; in this book the last variation is used, i.e., DF f(x) in (2.2.1).

Note that DF does not necessarily suggest any randomness (see Sect. 2.1.3). We may use functions like f(x) when the quantity x is distributed because of a quite deterministic process, like in mechanics. In this case, the probability dw means the fraction of particles with property x (coordinates, velocities, energy, etc.).

2.2.2 Special Probability Functions

The generalized function $\chi(x)$ can be defined only inside the corresponding integrals:

$$\int_{-\infty}^{\infty} \chi(x) dx; \qquad (2.2.3)$$

they make no sense outside of it. For instance, the Dirac delta function (see Appendix B) may be defined as:

$$\int_{-\infty}^{\infty} \delta(x) dx = 1, \quad \delta(x \neq 0) = 0.$$
 (2.2.4)

Out of its integral, such a function cannot be represented analytically, but we may use some constructions to approach this (see Appendix B).

However, we can use a generalized function for the DF, because, strictly, only a probability function has a "physical meaning:" only an integral means the fraction of particles with corresponding properties (for instance, the number of particles with velocities from a to b is $\int_a^b f(v) dv$). Thus, as long as we do not use some mathematical constructions for the DF and its evolution (like differential equations), we may use any functions for the DF, including generalized functions.

For example, in the simplest case when a particle is localized at point x_0 with a probability of 100%, the DF can be expressed as:

$$f(x) = \delta(x - x_0). \tag{2.2.5}$$

For the DF of a single particle at a determined coordinate x_0 with a velocity v_0 :

$$f(x, v) = \delta(x - x_0)\delta(v - v_0).$$
 (2.2.6)

With a delta function, we have for any function g:

$$G(y) = \int_{-\infty}^{\infty} g(x)\delta(x - y)dx = g(y).$$
 (2.2.7)

2.2.3 Poisson and Gauss

Let us denote $p_n(x_1, x_2)$ as the probability of n events at interval (x_1, x_2) . For a single event we have:

$$p_1(x, x + \Delta x) = \xi(x)\Delta x, \qquad (2.2.8)$$

that is, the average number of events on (x_1, x_2) is:

$$\mu = \int_{x_1}^{x_2} \xi(x) dx. \tag{2.2.9}$$

For a chain of probabilities p_m one may obtain the system of differential equations:

$$\frac{\mathrm{d}p_0}{\mathrm{d}\mu} = -p_0, \quad \frac{\mathrm{d}p_n}{\mathrm{d}\mu} = -p_n + p_{n-1}, \ n > 1. \tag{2.2.10}$$

with conditions $p_0 = 1$ and $p_n = 0$ (n > 1). The solution of (2.2.10) is a Poisson distribution:

$$p_n = \frac{\mu^n e^{-\mu}}{n!}. (2.2.11)$$

The normal distribution (or the Gaussian):

$$f(x) = \frac{1}{\sqrt{2\pi D}} \exp\left(-\frac{(x - x_0)^2}{2D}\right)$$
 (2.2.12)

follows from the limit theorem. In the simplest formulation, this theorem establishes the distribution (2.2.12) for random independent values with limited dispersion. In other words, the distribution (2.2.12) may be obtained for a large amount of small symmetrical deviations from the mean value x_0 .

In (2.2.12) quantity x_0 is the mean value:

$$x_0 = \int_{-\infty}^{\infty} x f(x) dx, \qquad (2.2.13)$$

and the dispersion D is:

$$D = \int_{-\infty}^{\infty} (x - x_0)^2 f(x) dx.$$
 (2.2.14)

As we will see in Sect. 2.3, in the case of full chaotization (in the thermal equilibrium state) the DF of any projection of velocity satisfies (2.2.12), in this case the distribution is called "Maxwellian."

2.2.4 Spatial Scales

Thus, the DF must determine the number of particles with coordinates x and velocities v. How many particles must be taken into account to define this DF?

The extreme answer, discussed in Vlasov (1978), is as follows: the statistical approach does not restrict the amount of particles, thus, we may consider even the statistical physics of a single particle. Of course, it is easy to argue this theory, and we will not consider this method here. However, we have to answer the question.

We do not consider time or spatial scales for variation of f here; this question will be discussed in Chap. 3. In this section we provide only the preliminary consideration.

We may require two properties for spatial scale L, which must be large enough:

- To construct any DF—there must be a lot of particles on such a scale.
- To neglect fluctuations of the DF: the DF shows a fraction of particles at this
 point with certain velocity; this fraction variates because of fluctuations—
 because of thermal motion, atoms move to and from this point.

Combining these requirements, the number of particles N(x) at x must be much greater than the value N_{\min} :

$$N(x) \gg N_{\min}. \tag{2.2.15}$$

For the first condition, $N_{\min} = 1$; for the second, N_{\min} could be obtained for certain information about fluctuations. Let us consider the spatial region of volume $V = L^3$. The averaged number density of particles is $n = N/L^3$, thus, the spatial scale for the DF, according to the first requirement is:

$$L \gg n^{-1/3}$$
. (2.2.16)

For example, for an ideal gas at pressure $p = 10^5$ Pa and temperature T = 300 K, we have the left-hand side of (2.2.16) at 3.5 nm; thereby, the spatial scale only for the density calculation must be ~ 10 nm to satisfy only the simplest condition $N \gg 1$, and, moreover, the velocity DF obtained on such a small scale will be of bad resolution Δv .

Let us estimate the fluctuation of the number of particles in volume V. From each of the six sides of this volume the flux is j=nv with a characteristic velocity $v\sim \sqrt{T/m}\sim 10^2 \text{m/s}$ for $T\sim 10^2 \text{K}$ and $m\sim 1u$. Thus, the number of particles crossing one side of volume V at time Δt is defined by correlation:

$$N_{\min} = nvL^2 \Delta t, \tag{2.2.17}$$

which leads to the estimation of the spatial scale:

$$L \gg v\Delta t. \tag{2.2.18}$$

Here Δt is the timescale for a collision, thus, the product on the left-hand side of (2.2.18) is the mean free path (MFP) of the molecule (see Chap. 3). Thus, we see that fluctuations are negligible on spatial scales much larger than the MFP of the molecule. This case corresponds to the continuum medium; for a statistical (kinetic) approach the condition (2.2.16) is sufficient.

2.2.5 Example: The Debye Radius

This is an interesting example of an incorrect interpretation of the DF. Let us consider only the spatial distribution function, i.e., the number density function:

$$n(x) = \int f(x, v) dv. \qquad (2.2.19)$$

In plasma (ionized gas) we must consider three sorts of particles: neutral particles with density $n_n(x)$, electrons with $n_e(x)$ and ions (we will consider only single-charged ions, that is every ion with the charge +e) with $n_i(x)$.

From the Poisson equation for the electrostatic potential of an electric field φ :

$$\Delta \varphi = -\frac{\rho}{\varepsilon_0},\tag{2.2.20}$$

where ρ is the charge density $\rho = e(n_i - n_e)$, we have with the Boltzmann distribution function:

$$n = n_0 e^{-u/T} (2.2.21)$$

and the equation:

$$\Delta \varphi = -\frac{n_0}{\varepsilon_0} \left(\exp\left(-\frac{e\varphi}{2T} \right) - \exp\left(\frac{e\varphi}{2T} \right) \right). \tag{2.2.22}$$

One may expand the exponents of (2.2.22) into series with words about "... the small values of $e\varphi/2T$..." However, as we will see in Sect. 2.2.7, distributions (2.2.21) and, consequently, (2.2.22) have a physical sense only in the case of $|e\varphi/2T| \ll 1$; see also Ecker (1972). Thus, instead of (2.2.22) we have:

$$\Delta \varphi = \frac{n_0 e \varphi}{\varepsilon_0 T}.\tag{2.2.23}$$

The expression (2.2.23) has a common sense, and we can apply it to special problems. For example, we may consider a spatial distribution of potential around a point charge (ion or electron) in plasma. For this purpose, (2.2.23) becomes:

$$\frac{1}{r^2}\frac{\mathrm{d}}{\mathrm{d}r}r^2\frac{\mathrm{d}\varphi}{\mathrm{d}r} = \frac{n_0e\varphi}{\varepsilon_0T},\tag{2.2.24}$$

with a boundary condition at the radius of the point charge r_0 :

$$\varphi(r_0) = \varphi_0. \tag{2.2.25}$$

We may define the Debye radius as the spatial scale for the electrostatic potential that appears from (2.2.24):

$$R_D = \sqrt{\frac{\varepsilon_0 T}{n_0 e}},\tag{2.2.26}$$

and (2.2.24) has a solution:

$$\varphi(r) = \varphi_0 \frac{r_0}{r} \exp\left(\frac{r_0 - r}{R_D}\right) = \frac{A}{r} e^{-r/R_D}.$$
(2.2.27)

The equality of (2.2.26) is what we usually need from this consideration (the description of electrical potential shielding), but in some books the expression from (2.2.27) is discussed. According to this formula, the distribution of electric potential around any charge in plasma obeys (2.2.27).

Thereby, we must conclude that around any plasma particle (any ion or any electron) the electric filed is spherically symmetric. However, of course, it is an absolutely absurd conclusion. It is impossible, but where is the error in our logic in (2.2.20–2.2.27)?

Strictly, the weak (i.e., the wrong) point is the problem statement as a whole, and the weakest point is expression (2.2.25). There, we demand a certain value of electric potential at the scale of the size of a single particle r_0 . On such scales the DF (2.2.21) cannon be defined, thus, the entire consideration becomes absurd.

However, we can easily save the situation, if we consider a large (external) macroparticle of size r_0 ; for instance, it may be a charged dust grain. For this problem, the solution in (2.2.27) is correct.

2.2.6 Distribution of Potential Energy

A crucial part of Chap. 6 is where we find this DF—particularly, for an evaporating fluid. However, in this chapter, we may discuss a common question: are the kinetic energy and potential energy statistically independent quantities? That is, can we represent a DF for kinetic and potential energy multiplicatively:

$$f(\varepsilon, u) = f(\varepsilon)f(u),$$
 (2.2.28)

assuming that a particle with a kinetic energy ε may have an independent (i.e., any) value of potential energy u?

At first (mechanical) glance, it is absolutely impossible. Let us consider, for example, a pendulum: here the kinetic energy depends on the potential energy; in the lowest point with minimum u the kinetic energy has a maximum, and vice versa —for the highest (dead) points, where $u = u_{\text{max}}$ we have $\varepsilon = 0$. In common, if the total energy s is a constant:

$$s = \varepsilon + u = \text{const}, \tag{2.2.29}$$

then we cannot, of course, assume the independence of ε and u.

However, for a given particle in an N-particle system the total energy is not a constant. The quantity s fluctuates as other quantities, thus, we have no direct restriction such as (2.2.29). Thus, we may assume that any particle can have any potential energy at the given kinetic energy. With time, both ε and u of the particle variate, and it can be supposed that at $t \to \infty$ we may observe any possible value of ε accompanying any possible value of u. Thus, despite the fact that the variation of velocity (and, correspondingly, of kinetic energy) of the particle is determined by the gradient of the potential energy:

$$\frac{\mathrm{d}\vec{v}}{\mathrm{d}t} = -\frac{\nabla u}{m},\tag{2.2.30}$$

at a sufficiently long time we just observe any possible combinations of ε and u. Consequently, we may assume that (2.2.28) is correct. Results of a numerical calculation, where this representation will be verified, can be found in Chap. 6.

2.2.7 The Statistical Approach

This subsection is given only for completeness. The statistical approach led to thermodynamics in the following way (according to Gibbs).

For an adiabatic system at constant energy E the DF (probability density) of a system determined by internal parameters x and external parameters a may be written as:

$$p(x,a) = \frac{1}{B(a)}\delta(E - H(x,a)), \tag{2.2.31}$$

where δ is the Dirac function, H is the Hamiltonian of the system (total kinetic and potential energy of a system) and B(a) is the normalizing factor:

$$B(a) = \int \delta(E - H(x, a)) dx. \qquad (2.2.32)$$

The DF (2.2.31) is the so-called Gibbs microcanonical distribution. For the system in a thermostat, where one may consider two parts of the system with Hamiltonians $H_1(x_1)$ and $H_2(x_2)$, with interaction energy U_{12} we have:

$$H(x_1, x_2, a) = H_1(x_1, a) + H_2(x_2, a) + U_{12}.$$
 (2.2.33)

Assuming that $U_{12} = 0$, i.e., the interaction energy is much lower than the energy of both subsystems (we used this property above when we discussed the linearization of the exponent in the Boltzmann distribution), we have:

$$p_1(x_1, a) = \phi(H_1(x_1, a)), \quad p_2(x_2, a) = \phi(H_2(x_2, a)),$$

$$p(x_1, x_2, a) = \phi(H_1(x_1, a) + H_2(x_2, a)).$$
(2.2.34)

At last, we note that the probability density for the total system is multiplicative due to the independence of subsystems:

$$p(x_1, x_2, a) = p(x_1, a)p(x_2, a). (2.2.35)$$

Thus, if the function of the sum equals the product of the functions of the terms, then this function is the exponent:

$$p(x) = C(a)e^{-\beta H(x)}$$
. (2.2.36)

This is the canonical Gibbs distribution; inserting the expression for Hamiltonian, one may obtain the Maxwell-Boltzmann distribution. Here, the normalizing constant may be represented as:

$$\frac{1}{C(a)} = e^{-\beta F(a)} = \int e^{-\beta H(x,a)} dx,$$
 (2.2.37)

that is, we may introduce functions:

$$Z(\beta, a) = \int e^{-\beta H(x, a)} dx, \qquad (2.2.38)$$

$$F(\beta, a) = -\frac{1}{\beta} \ln Z(\beta, a). \tag{2.2.39}$$

Function (2.2.38) is the partition function. The sense of the function $F(a, \beta)$ (2.2.39) and the parameter $\beta = 1/\Theta$ may be ascertained with the equation (following from the canonical Gibbs distribution):

$$\Theta d\left(-\frac{\partial F}{\partial \Theta}\right) = d\bar{H} + Ada. \tag{2.2.40}$$

Here, the mean total energy:

$$\bar{H} = \int H(x, a) e^{\beta F(\beta, a) - \beta H(x, a)} dx \qquad (2.2.41)$$

may be treated as the internal energy of a system, the Θ is the temperature of the system and the function F is the free energy of the system; the entropy is:

$$S = -\frac{\partial F}{\partial \Theta} = \overline{\ln p} = \int \frac{F - \overline{H}}{\Theta} e^{(F - \overline{H})/\Theta} dx.$$
 (2.2.42)

In this manner, we obtained all the thermodynamics. We started from an almost mechanical consideration, and found the joined 1st and 2nd law of thermodynamics (2.2.40). Did we obtain the 2nd law in its full complexity? No, of course. As was mentioned Chap. 1, the 2nd law consists of different statements—statements of different force (see Sect. 1.2). Above, we figured out only the equilibrium equation (2.2.40), but the most interesting feature of entropy—increasing in an isolated system—cannot be explained this way. This increasing was the point of discussion between Zermelo (and Poincare) and Boltzmann, this is a point where mechanics contradicts thermodynamics (see Sect. 2.1.3).

Mechanics is based on the principal of least action; reversible mechanical equations cannot state the law of maximum entropy. However, we have seen that mechanics leads to some equations that may be interpreted as definitions (mechanical analogs) of thermodynamic functions like (2.2.41) and (2.2.42) and the connection between them in the form of (2.2.40). Can the principal of maximum entropy repeat this trick?

2.2.8 The Principle of the Maximal Entropy

This principle allows one to construct all statistical physics without appellations to other ideas, especially, to ideas taken from mechanics. Thus, it represents a self-sufficient approach. All we need is the basic statement.

We assume that the entropy S of the given system has a maximum at some additional conditions, specifically, in a closed system with a constant amount of particles N and at the constant total energy E of this system (Haken 1988).

Let us define the probability of the state with energy ε_i as the ratio of the particles with this energy to the total number of particles: $p_i = n_i/N$, then we have:

$$S = -\sum p_i \ln p_i \to \max, \tag{2.2.43}$$

$$\sum p_i = 1, (2.2.44)$$

$$\sum \varepsilon_i p_i = \bar{\varepsilon} = \frac{\varepsilon}{N}. \tag{2.2.45}$$

Then we find variations of (2.2.43-2.2.45). We have:

$$\delta S = -\sum (\ln p_i + 1)\delta p_i = 0,$$
 (2.2.46)

$$\sum \delta p_i = 0, \tag{2.2.47}$$

$$\sum \varepsilon_i \delta p_i = 0. \tag{2.2.48}$$

Multiplying (2.2.47) by $(\ln \alpha - 1)$ and (2.2.48) by $(-\beta)$ and taking the sum of all equations we see that:

$$\sum \left[-(\ln p_i + 1) + (\ln \alpha - 1) - \beta \,\varepsilon_i \right] \delta \, p_i = 0 \tag{2.2.49}$$

Due to independence of variations δp_i , any term in sum (2.2.49) must be equal to zero, thus:

$$-\ln p_i + \ln \alpha - \beta \,\varepsilon_i = 0 \tag{2.2.50}$$

$$p_i = \alpha e^{-\beta \, \varepsilon_i} \tag{2.2.51}$$

Here constant α can be obtained from (2.2.44), so:

$$\alpha^{-1} = \sum e^{-\beta \varepsilon} \tag{2.2.52}$$

Thus, we obtain the Gibbs canonical distribution. From this point on, we may continue in the manner of the previous subsection and obtain that $\beta = 1/T$, for

example. Thus, as we see, we may deduce all thermodynamics from the starting point of the principal of the maximum entropy.

This method can be applied for various systems, even for instance, for boiling (Gerasimov and Sinkevich 2004).

2.2.9 The Virial Theorem

This is a useful correlation, especially when we know two of the three parts of the pressure-kinetic energy-potential energy triad and we need to find the third part. This correlation is a kind of bridge between mechanics and statistics.

Let us consider the system of N particles; $\vec{r_i}$ and $\vec{p_i}$ are coordinates and momentum of the ith particle. The time derivation of the sum on all N particles of products $\vec{r_i}\vec{p_i}$ is:

$$\frac{\mathrm{d}}{\mathrm{d}t} \sum \vec{r}_i \vec{p}_i = \sum \frac{\mathrm{d}\vec{r}_i}{\mathrm{d}t} \vec{p}_i + \sum \frac{\mathrm{d}\vec{p}_i}{\mathrm{d}t} \vec{r}_i. \tag{2.2.53}$$

Using the Lagrange function L = E - U, we have:

$$\frac{\mathrm{d}\vec{r}_i}{\mathrm{d}t} = \frac{\partial L}{\partial \vec{p}_i} = \frac{\partial E}{\partial \vec{p}_i} = \frac{\partial}{\partial \vec{p}_i} \sum \frac{p_i^2}{2m} = \frac{\vec{p}_i}{m},\tag{2.2.54}$$

then the first term in (2.2.53) is:

$$\sum \frac{\mathrm{d}\vec{r}_i}{\mathrm{d}t}\vec{p}_i = \sum \frac{p_i^2}{m} = 2E. \tag{2.2.55}$$

Then we average (2.2.53) with (2.2.55). Under the averaging of function F we mean the operation:

$$\overline{F} = \lim_{t \to \infty} \frac{1}{t} \int_{0}^{t} F dt, \qquad (2.2.56)$$

thus, averaging the left-hand side of (2.2.53) we obtain:

$$\lim_{t \to \infty} \frac{1}{t} \int_{0}^{t} \frac{\mathrm{d}}{\mathrm{d}t} \left(\sum \vec{r}_{i} \vec{p}_{i} \right) \mathrm{d}t = \lim_{t \to \infty} \frac{\sum \vec{r}_{i}(t) \vec{p}_{i}(t) - \sum \vec{r}_{i}(0) \vec{p}_{i}(0)}{t} = 0, \qquad (2.2.57)$$

since every product in the numerator of (2.2.57) is finite for a finite volume. Then:

$$2\overline{E} + \overline{\sum_{i} \frac{d\overline{p}_{i}}{dt}} = 0, \qquad (2.2.58)$$

and with the Hamilton equation (or with the Newton's 2nd law):

$$\frac{\mathrm{d}\vec{p}_i}{\mathrm{d}t} = \vec{F}_i = \vec{F}_i^{\text{out}} - \frac{\partial U}{\partial \vec{r}_i},\tag{2.2.59}$$

with two types of forces: outer forces from outer bodies at the boundary of the system and inner forces, from other particles of the system with the potential energy U:

$$\overline{\sum \left(\vec{r}_i \frac{\mathrm{d}\vec{p}_i}{\mathrm{d}t}\right)} = -\overline{\sum_{U_r} \vec{r}_i \frac{\partial U}{\partial \vec{r}_i}} + \overline{\sum} \vec{r}_i \vec{F}_i^{\text{out}} = -\overline{U}_r - p \int \vec{r} d\vec{S} = -\overline{U} - 3pV,$$
(2.2.60)

because $\int \vec{r} d\vec{S} = \int div \vec{r} dV = 3V$. Finally:

$$2\overline{E} - \overline{U}_r - 3pV = 0. \tag{2.2.61}$$

For instance, for an ideal system of non-interacting particles $\overline{U} = 0$, and we have an analog of the Clapeyron equation:

$$p = \frac{2\overline{E}}{3V},\tag{2.2.62}$$

which leads to the normal form for $\overline{E} = \frac{3}{2}NT$. For interaction potential $U \sim \frac{1}{r^n}$ we have $\overline{U}_r = -n\overline{U}$, and (2.2.61) turns into:

$$2\overline{E} + n\overline{U} = 3pV. \tag{2.2.63}$$

For example, these correlations can be used to calculate pressure in a system if the parameter \overline{U}_r is available. Note that the introduction of pressure slightly changes the character of the description: the definition of the boundary surface S implies some hypothesis about the uniformity of pressure on it, which may lead to hypothesis of the uniform distribution of particles on S, etc.

2.3 The Maxwell Distribution Function

2.3.1 Physical Models

Possibly, the main difference between physics and mathematics is hidden in the accuracy of definitions used by these two sciences. Mathematics is based on logic while physics is led by the common experience and personal intuition of its adepts.

Every mathematical definition is precise and clear. Every physical formulation was grown in a wilderness of experimental facts known at its birth and was shaped by contemporary views.

Some physical formulae can be obtained from known physical principles with some neglections, but this fact does not mean that these neglections are an essential part of these formulae: possibly, there exists another way to establish this law without such strict circumstances. Any theorem begins from the formulation of conditions of its correctness while very rare physical contention has definitive area of its application; almost every physical law has no definite boundary of its use. Most physical laws were obtained for model systems or elementary objects (ideal gas, Newtonian fluid, mass point, etc.), thus we have an open range for applicability of these laws in real nature.

The Maxwellian distribution function (MDF) is a vivid example. It was discovered, criticized, observed in experiments and denied for complicated systems only to be resurrected later in a changed form. In physics, the MDF has a status of being the "distribution function by default:" this DF can be applied to any problem when any other DFs are not strictly proved. Of course, evaporation is not an exception (see Chap. 5).

Possibly, it is enough to say that the Maxwellian is the analog for the Gaussian (in physics): the DF on any projection of velocity in the thermal equilibrium state has a form:

$$f(v_x) = \frac{1}{\sqrt{2\pi D_v}} \exp\left(-\frac{v_x^2}{2D_v}\right)$$
 (2.3.1)

with the dispersion $D_v = T/m$.

Gabriel Lippman once said that "all scientists trust the Gaussian: physicists believe that it is proved mathematically while mathematicians thought that it was justified experimentally;" Henri Poincare cited this dictum in his "Probability Theory" with a reference to Lippman, but, as usual, details were missed and now this aphorism is attributed to Poincare.

For a physicist, there are more than enough proofs for the MDF, but from the point of view of a mathematician this is an unsolved problem (see Sect. 2.1.3): the stumbling block is the state of the thermodynamic equilibrium as it is. The Gaussian (2.3.1) can be obtained for a stochastic set of velocities (which may be interpreted as a thermal equilibrium by definition), but how does a mechanical system enter such a state? However, if one is able to jump over this stumbling block, then the rest of the proof will be direct and simple. In common, the condition for MDF is stated more or less firmly from the physicist's point of view, especially if one takes into account that the existence of the MDF was the only point of agreement between Zermelo and Boltzmann.

Below we represent the old—original—derivation of the MDF, and a nice clear modern view on a problem.

2.3.2 The Maxwellian of Maxwell

The most famous DF was born in 1859 and was re-analyzed further by its author several times. Today, we may obtain the MDF in various ways (one of them will be considered in Sect. 2.3.3) but under the same assumption: the stochastization (i.e., the isotropic property) of velocity is needed. Actually, this assumption is a kind of synonym of the "thermal equilibrium." Maxwell used this approach in an early derivation of his DF, but later he applied the principle of the detailed equilibrium to determine the MDF.

In 1959, in the work *Illustrations of the Dynamical Theory of Gases* the MDF appeared for the first time.

Let v_x, v_y, v_z be components of a velocity vector \vec{v} . Due to independence of these components from each other we have that number of particles with velocities $v_x \div v_x + dx$, $v_y \div v_y + dv_y$ and $v_z \div v_z + dv_z$ is proportional to:

$$Nf(v_x)f(v_y)f(v_z)dv_xdv_ydv_z. (2.3.2)$$

On the other hand, from the isotropic property of the velocity space, we can conclude that the number of particles can only depend on the radius from the origin in the velocity space:

$$f(v_x)f(v_y)f(v_z) = \varphi(v_x^2 + v_y^2 + v_z^2) = \varphi(v^2).$$
 (2.3.3)

From here we see that:

$$f(v_x) = C \exp(Av_x^2) \text{ and } \varphi(v^2) = C^3 \exp(Av^2).$$
 (2.3.4)

Concluding that A < 0 (otherwise the number of particles would be unlimited), and normalizing functions we obtain:

$$f(v_x) = \frac{1}{\alpha\sqrt{\pi}} \exp\left(-\frac{v_x^2}{\alpha^2}\right). \tag{2.3.5}$$

For constant α we have:

$$\overline{v^2} = \overline{v_x^2} + \overline{v_y^2} + \overline{v_z^2} = \frac{3}{2}\alpha^2.$$
 (2.3.6)

Maxwell did not state this fact in that work, but from a modern standpoint we may note that $\alpha^2 = 2T/m$.

That was Proposition IV in *Illustrations of the Dynamical Theory of Gases*. It is also interesting that in Proposition V Maxwell, in fact, establishes that his distribution is stable (to say in modern terms): the number of pairs of particles with relative velocity *w* satisfies the same distribution (see also Appendix A):

$$f(w) = \frac{1}{\sqrt{\alpha^2 + \beta^2}} \frac{1}{\sqrt{\pi}} \exp\left(-\frac{w^2}{\alpha^2 + \beta^2}\right),$$
 (2.3.7)

where α and β are parameters of distributions for particles of two sorts; in particular the case $\alpha = \beta$.

Next, Maxwell derived his DF in 1866, in the work *On the Dynamical Theory of Gases*. Later, almost the same method (except for nuances) was applied in *On the Final State of a System of Molecules in a Motion Subject to Forces of Any Kind* of 1873.

Here another approach was used. Maxwell treated a collision of particles; in common terms, Maxwell found the DF that could provide a dynamic equilibrium in such a system—or may nullify the collision integral (despite the fact that this term did not exist at that time).

Let v, v' and w,w' be the velocities of two particles before and after a collision correspondingly. The rate of direct collisions $(v, w) \rightarrow (v', w')$ in elementary volume dV between the particles of numbers $n_1 = f_1(v)dV$ and $n_2 = f_2(w)dV$ is:

$$d\gamma_1 = Ff_1(v)f_2(w)(dV)^2 dt,$$
 (2.3.8)

where F is a function of the relative velocity of particles.

For reverse collisions $(v', w') \rightarrow (v, w)$ we have a similar equation:

$$d\gamma_2 = F f_1(v') f_2(w') (dV)^2 dt, \qquad (2.3.9)$$

with the same function F. In equilibrium $d\gamma_1 = d\gamma_2$, and:

$$f_1(v)f_2(w) = f_1(v')f_2(w').$$
 (2.3.10)

We must include the energy conservation law in our consideration:

$$\frac{m_1 v^2}{2} + \frac{m_2 w^2}{2} = \frac{m_1 v^2}{2} + \frac{m_2 w^2}{2}.$$
 (2.3.11)

Because of relations (2.3.10) and (2.3.11), the only form for function f_1 and function f_2 is:

$$f_1(v) = C_1 \exp\left(-\frac{v^2}{\alpha^2}\right) \text{ and } f_2(w) = C_2 \exp\left(-\frac{w^2}{\beta^2}\right),$$
 (2.3.12)

with correlation $m_1\alpha^2 = m_2\beta^2$. Constants $C_{1,2}$ may be found from the normalizing conditions $\int f_{1,2}(v) dv = N_{1,2}$. Again, we have the same distribution functions—the MDF.

In other words, here Maxwell provided the operation that may be found in every modern textbook on physical kinetics—at the stage when the "equilibrium" DF is being found from the condition "the collision integral is equal to zero." However, Maxwell did it in a slightly more elegant and more direct way.

As we discussed in Sect. 2.2.1, some problems concerning the condition of application of the MDF were debated by mathematicians. Despite the fact that all considerations represented in this subsection look quite solid, the answer to the key question for the MDF is unclear: how can this function be obtained from mechanics? For a better understanding, we provide the mathematical method to determine the MDF in Sect. 2.3.3.

2.3.3 Modern View on Maxwellian

Returning to the beginning of Sect. 2.3.1, we may conclude that physicists, of course, have more than sufficient proof for the MDF, provided in the previous section. However, to physicists' surprise, from a mathematical point of view, the thoughts represented above are not sufficiently strict.

To the question concerning the relation between the MDF and mechanics (from which, evidently, the MDF was obtained), we may add a typical "physicist's" question: where the mount begins? We mean, how many particles must be in an ensemble to provide sufficient accuracy of the MDF? Usually, physicists rely on their intuition, when they named some great numbers as "ten in Nth degree." However, probably, we may derive a more common relation under the same assumption about thermal equilibrium, which has the MDF as the asymptotic function for $N \to \infty$?

Below we will follow Kozlov (2002).

Let each *i*th particle of *N* particles in *n*-dimensional space have components of velocity $v_{i,1}, v_{i,2}, ..., v_{i,n}$. The total kinetic energy of all particles is:

$$\sum_{i=1}^{N} \frac{m\vec{v}_i^2}{2} = \sum_{i=1}^{N} \sum_{j=1}^{n} \frac{mv_{i,j}^2}{2} = E = \bar{\epsilon}N,$$
(2.3.13)

where $\bar{\epsilon}$ is the mean kinetic energy of a single particle. The state of the medium is defined by the point:

$$\{v_{i,1}, v_{i,2}, \dots, v_{i,n}; \dots; v_{N,1}, v_{N,2}, \dots, v_{N,n}\} \in \Re^{nN}$$
 (2.3.14)

on the (nN-1)-dimensional hypersphere S of radius:

$$R = \sqrt{\frac{2E}{m}} = \sqrt{\frac{2\bar{\varepsilon}N}{m}}.$$
 (2.3.15)

Then, we have to define the probability measure p on this sphere S. This is always a problematic step; in Kozlov (2002) p is defined as a volume of S, i.e., the

probability measure for a given velocity projection of the given particle may be defined as:

$$p(a < v_{i,j} < b) = \frac{\text{mes}(a < v_{i,j} < b)}{\text{mes}S},$$
 (2.3.16)

where:

$$\operatorname{mes}\left(a < v_{i,j} < b\right) = \int_{a}^{b} \left(1 - \frac{mx^2}{2\overline{\epsilon}N}\right)^{\frac{nN-3}{2}} dx, \tag{2.3.17}$$

$$\operatorname{mes} S = \int_{-R}^{R} \left(1 - \frac{mx^2}{2\overline{\epsilon}N} \right)^{\frac{nN-3}{2}} dx. \tag{2.3.18}$$

Thus, the probability density function (in our language, the DF) may be represented in an *N*-particle system as:

$$f^{N}(v) = \left(1 - \frac{mv^{2}}{2\bar{\epsilon}N}\right)^{\frac{mN-3}{2}}.$$
 (2.3.19)

For n=1 and $N\to\infty$ one can obtain the regular form of the Maxwell distribution:

$$f^{\infty}(v) = \sqrt{\frac{m}{4\pi\bar{\varepsilon}}} e^{-\frac{mv^2}{4\bar{\varepsilon}}}.$$
 (2.3.20)

Hear the quantity $\bar{\epsilon}$, as usual, is:

$$\bar{\varepsilon} = \int_{-\infty}^{\infty} \frac{mv^2}{2} f(v) dv = \frac{T}{2}.$$
 (2.3.21)

Thus, from this consideration we may see a more common form of the MDF is (2.3.19); this function is represented in Fig. 2.4.

However, the function f^N was obtained at the same condition of thermal equilibrium represented by the correlation for the measure of probability (2.3.17), this condition may be also explained as an equality of velocities (specifically, the equality of each velocity projection of each particle).

Returning to the previous consideration, and replacing the term "probability" with the term "fraction," we may conclude that for a sufficiently disordered system the MDF may be expected. Note also that the absence of the potential energy in this consideration does not mean that this method can be applied only for ideal gas. Contrary to this, from a physical consideration it follows that only the interaction of particles may lead to disorder in a system.

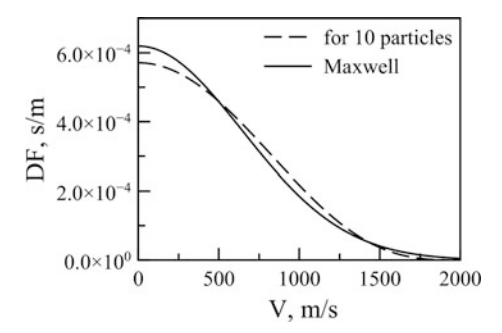


Fig. 2.4 The distribution function (2.3.19) for N = 10 particles and the Maxwellian distribution function (T = 300 K). DF—distribution function

2.3.4 The Maxwellians for 2D and 3D Cases

In 2D geometry, on a plane, the MDF is:

$$f(v) = \frac{mv}{T} \exp\left(-\frac{mv^2}{2T}\right), \quad v > 0.$$
 (2.3.22)

This DF follows from (2.3.20) written for $f(v_x)f(v_y)dv_xdv_y$, considering that $v_x^2 + v_y^2 = v^2$ and replacing $dv_xdv_y = 2 \pi v dv$. Analogically, for a 3D case:

$$f(v) = \left(\frac{m}{2\pi T}\right)^{3/2} 4\pi v^2 \exp\left(-\frac{mv^2}{2T}\right), \quad v > 0.$$
 (2.3.23)

In a general case, for ND geometry (why not? especially for numerical simulations) we have:

$$f(v) = \frac{2^{(2-n)/2}}{\Gamma(n/2)} \left(\frac{m}{T}\right)^{n/2} v^{n-1} \exp\left(-\frac{mv^2}{2T}\right), \quad v > 0$$
 (2.3.24)

There is no contradiction between (2.3.24) for n = 1 and (2.3.20) because of the different definition area of v in these formulae.

2.3.5 The Maxwellian Distribution Function of Kinetic Energy

Expression (2.3.23) represents the velocity distribution function. However, one also may need a DF for kinetic energy. Such a DF—which can also be termed the MDF—can be obtained from the corresponding velocity DF for $\varepsilon = mv^2/2$:

$$f(\varepsilon)d\varepsilon = \frac{1}{\sqrt{\pi \varepsilon T}} \exp\left(-\frac{\varepsilon}{T}\right)d\varepsilon, \text{ for 1D};$$
 (2.3.25)

$$f(\varepsilon) = \frac{1}{T} \exp\left(-\frac{\varepsilon}{T}\right), \text{ for 2D};$$
 (2.3.26)

$$f(\varepsilon)d\varepsilon = \frac{2\sqrt{\varepsilon}}{\sqrt{\pi T^3}} \exp\left(-\frac{\varepsilon}{T}\right)d\varepsilon, \text{ for 3D.}$$
 (2.3.27)

The average kinetic energy for function (2.3.27) is, of course:

$$\varepsilon_m = \int_0^\infty \varepsilon f(\varepsilon) d\varepsilon = \frac{2}{\sqrt{\pi T^3}} \int_0^\infty \varepsilon \sqrt{\varepsilon} e^{-\varepsilon/T} d\varepsilon = 1.5T.$$
 (2.3.28)

The dispersion of the MDF (2.3.27) is:

$$D_{\varepsilon} = \overline{(\varepsilon - \varepsilon_m)^2} = \frac{2}{\sqrt{\pi T^3}} \int_{0}^{\infty} (\varepsilon - \varepsilon_m)^2 \sqrt{\varepsilon} e^{-\varepsilon/T} d\varepsilon = 1.5T^2.$$
 (2.3.29)

We will use these correlations further in Chap. 6.

2.3.6 The Meaning of the Maxwellian Distribution Function

This problem was discussed in Sect. 2.2.1, but here we repeat and emphasize key aspects.

The MDF is not the pinnacle of evolution of a dynamic system. We do not state that at any instant the velocity DF of molecules in the system obeys the Maxwellian; it would be a wrong and confusing assertion. The velocity DF oscillates (non-regularly) around the MDF which represents a weak attractor for a chaotized system. In the common case, a deviation of the DF from Maxwellian at a given moment of time depends on the number of particles N in the system, but even when $N \to \infty$ the DF does not turn into the MDF forever, because, generally, the "fluctuations" in a dynamic system may be of any intensity. Note that the term "fluctuations" is non-mechanical in its nature; this definition belongs to another set of physical terminology (that of thermodynamics). A dynamic system does not "fluctuate," it performs perpetual motion. Due to the chaotization of velocities, we may (specifically, Maxwell did) note some special property of the averaged velocity DF: in this case any projection of velocity must satisfy the Gaussian, which is named here as the MDF.

In another formulation, the DF f(v,t), even for $t \to \infty$, is not Maxwellian; the MDF can be observed only for function:

$$\lim_{\Delta t \to \infty} \frac{1}{\Delta t} \int_{t}^{t+\Delta t} f(v, t) dt.$$
 (2.3.30)

In turn, this equation can be easily proven. On a "physicist severity level," it is sufficient to point out that the measure (2.3.17) can be used for mean values of velocities. In correlated systems (and other systems, of course) we may expect that any particle would repeat the fate of any other particle, i.e., particles are indistinguishable on their kinetic energy spectrum. In this case, we have (2.3.17) and (2.3.20) as a consequence.

2.4 Conclusion

In this observation chapter we discussed some important problems facing the upcoming results obtained and presented in this book.

We cannot obtain any results from a numerical calculation of a real system, consisting of $10^{[\text{very much}]}$ particles. This is a super complicated task, which will probably remain unrealizable. Thus, we have to turn to statistical science. Instead of the coordinates and velocities of all the particles, we may use the probability density function (the DF)—a function which determines the fraction of particles at corresponding coordinates with corresponding velocities.

The statistical approach uses the term "probability" as a rule. For our purposes—for the description of a mechanical system of many particles—the probability does not mean "chance;" it is synonymous with the word "fraction." We never involve any randomness concept in our considerations. However, on several pages of this chapter chaos is discussed.

Chaos is not chance, a chaotic system is a deterministic system. Due to a strong dependence on initial conditions, a chaotic system forgets its initial state. We may also observe even a quasi-irreversibility in such a system, however, this is not an irreversibility in its direct sense, but a mirage of it.

The MDF may be obtained in numerical simulations without any additional factors such as stochastic forces, etc. The chaotization of particle velocities—even in a deterministic system—is a sufficient condition to obtain the MDF; there are no contradictions with principles of mechanical reversibility in this result. At sufficient chaotization, we may expect that the velocity distribution function of particles will oscillate around the Maxwellian. This is something we have observed.

References

- G. Ecker, Theory of Fully Ionized Plasmas (Academic Press, New York-London, 1972)
- D.N. Gerasimov, O.A. Sinkevich, High Temp. 42, 489 (2004)
- H. Haken, Information and Self-organization (Springer, Berlin-Heidelberg-New York, 1988)
- V.V. Kozlov, *The Heat Equilibrium by Gibbs and Poincare* (Institute of Computer Science, Moscow-Izhevsk, 2002)
- Y.S. Sigov, Numerical Experiment: The Bridge between the Past and the Future (Fismatlit, Moscow, 2001)
- A.A. Vlasov, Nonlocal Statistical Mechanics (Nauka, Moscow, 1978)
- E. Zermelo, Ann. Phys. 57, 485 (1896a)
- E. Zermelo, Ann. Phys. 59, 797 (1896b)

Recommended Literatures

- L. Boltzmann, Ann. Phys. 57, 773 (1896)
- J.W. Gibbs, Elementary Principles in Statistical Mechanics (Charles Scribner's Sons, New York, 1902)
- J.C. Maxwell, The Scientific Papers of James Clerk Maxwell (Dover Publications Inc, New York, 1965)
- D. Ruelle, Chance and Chaos (Princeton University Press, Princeton, NJ, 1993)

Chapter 3 The Kinetic Approach



This chapter further develops Chap. 2. The dynamics of the distribution function (DF) may be represented with various methods and different equations. Despite the fact that the Boltzmann kinetic equation is the most popular expression, there are many other correlations that can do the same.

This chapter describes several kinetic approaches.

3.1 Dynamics of Probability

3.1.1 Kinetic Equations

The DF f(x, v), introduced in Chap. 2, describes a static picture: the number of particles at point x with velocity v. However, for transient processes we have to evaluate the variation of DF, i.e., we must consider the function f(t, x, v).

Correlations for the dynamics of f(t, x, v) are referred to as the kinetic equations. The most famous equation is the Boltzmann kinetic equation, but it is not the only one, and is not even the best construction for many practical purposes. Many kinds of kinetic equations may be used; some of them are discussed in this chapter.

A common way to determine an expression of time evolution of a DF can be explained by analogy with the continuity equation (the law of mass conservation):

$$\frac{\partial \rho}{\partial t} + \operatorname{div} \rho \, \vec{v} = S. \tag{3.1.1}$$

In normal conditions the mass source S = 0 (if we do not consider a pair production by gamma-quants, for example), however, in a mixture the density of a component of the said mixture can be expressed by (3.1.1) with a non-zero source

term (due to chemical reactions). For a pure substance, with S = 0, (3.1.1) states that mass may flow to this point or from it, but cannot be produced in any way.

As we remember, a DF, by its nature, is a number density in expanded space (not only in the usual coordinate space, but also in the velocity space), thus, we can formulate the dynamic equation for a DF similar to (3.1.1):

$$\frac{\partial f}{\partial t} + \vec{v} \frac{\partial f}{\partial \vec{x}} + \vec{a} \frac{\partial f}{\partial \vec{v}} = I. \tag{3.1.2}$$

The last two terms on the left-hand side may be written as the divergence term $\operatorname{div} \vec{V} f$ in the phase space (\vec{x}, \vec{v}) , where the vector \vec{V} unites vectors \vec{v} and \vec{a} . Such a "derivation" of the kinetic equation provides many questions; some of them may be unexpected, and we will consider the nuances of the kinetic approach, as a whole, later in Sect. 3.4.

The single question concerning (3.1.2) must be settled here: the source term on the right-hand side, denoted as I. This is the collision integral; its form defines the type of kinetic equation. The oldest versions of the collision integral were obtained by Maxwell and Boltzmann, and the corresponding equation is referred to as the Boltzmann equation.

The Boltzmann kinetic equation may be obtained in various ways; it can be written almost immediately with simple consideration of collisions between particles with a DF $f(\vec{x}, \vec{v})$, and, actually, it was almost written in Chap. 2. However, from a certain point of view, such an approach raises more questions than provides answers.

We prefer the most common approach, which demands that we first redetermine the DF.

3.1.2 The Liouville Theorem

The DF $f(\vec{x}, \vec{v})$ that was used previously defines the probability to find a single particle at coordinates \vec{x} with a velocity \vec{v} . However, one may use another approach: to obtain the probability to find particle #1 with \vec{x}_1 and \vec{v}_1 , then find particle #2 with \vec{x}_2 and \vec{v}_2 , etc., for all N particles. This approach might make sense when particle #1 at (\vec{x}_1, \vec{v}_1) influences the probability to find particle #2 at (\vec{x}_2, \vec{v}_2) .

Let us introduce a multiparticle DF that describes the probability that the first particle has coordinate \vec{x}_1 and velocity \vec{v}_1 , the second particle has coordinate \vec{x}_2 and velocity \vec{v}_2 , and so on:

$$dw^{N} = f^{N}(t; \vec{x}_{1}, \vec{v}_{1}; \dots; \vec{x}_{N}, \vec{v}_{N}) d\vec{x}_{1} d\vec{v}_{1} \dots d\vec{x}_{N} d\vec{v}_{N}.$$
(3.1.3)

Of course, the DF f^N is normalized:

$$\int f^N d\vec{x}_1 \dots d\vec{x}_N d\vec{v}_1 \dots d\vec{v}_N = 1.$$
 (3.1.4)

The DF of N-1 particles may be obtained with (3.1.3) as:

$$f^{N-1}(\vec{x}_1, \vec{v}_1; \dots; \vec{x}_{N-1}, \vec{v}_{N-1}) = \iint f^N d\vec{x}_N d\vec{v}_N.$$
 (3.1.5)

In such a manner, we may continue to integrate forever, until we find a single-particle DF $f(\vec{x}, \vec{v})$.

Then, we introduce the "probability conservation equation" for a DF in the form that was discussed above:

$$\frac{\partial f^N}{\partial t} + \operatorname{div}_{2N} \vec{V} f^N = 0, \tag{3.1.6}$$

where \vec{V} is the vector of generalized velocities, consisting of N regular velocities \vec{v}_i and of N accelerations \vec{a}_i . Equation (3.1.6) represents the discontinuity equation for DF f^N . In a slightly more traditional representation:

$$\frac{\partial f^N}{\partial t} + \sum_{k=1}^N \vec{v}_k \frac{\partial f^N}{\partial \vec{x}_k} + \sum_{k=1}^N \vec{a}_k \frac{\partial f^N}{\partial \vec{v}_k} = 0.$$
 (3.1.7)

Equation (3.1.6) can be substantiated by many ways; for instance, in Cercignani (1969) a mechanical analog of f^N was used:

$$f^{N} = \prod_{i=1}^{N} \delta(\vec{x} - \vec{X}(t)) \delta(\vec{v} - \vec{X}(t)), \qquad (3.1.8)$$

where $\vec{X}(t)$ and $\vec{X}(t)$ are coordinates and velocities of particles, correspondingly, which are determined by mechanical equations (the Hamilton equations), and $\delta(x)$ are the Dirac delta functions (see Appendix B). Actually, to use the generalized function for such purposes, we have to define its derivative; in fine, in this modus, (3.1.6) can be obtained.

Equation (3.1.6) is only a starting point for the derivation of kinetic equations. This equation means that, across the whole system of N particles, probability is a conserved quantity (in contrast to the single-particle DF, it obeys (3.1.2) when $I \neq 0$).

In Sect. 3.2 we briefly provide a real show—considering such exercises which are analogous to a short program in figure skating.

3.2 The Bogoliubov–Born–Green–Kirkwood–Yvon Chain

3.2.1 Kinetic Equations

The Bogoliubov–Born–Green–Kirkwood–Yvon (BBGKY) chain (or hierarchy) defines the kinetic equation for the DF f^k through the DF f^{k+1} .

The acceleration \vec{a} in the kinetic equation may be of dual nature: this may be the acceleration in the external force \vec{F} or the result of an interparticle interaction. In the latter case, the quantity \vec{a} depends on the coordinates of interacting particles, i.e., each term $\vec{a}_k \frac{\partial f}{\partial \vec{v}_k}$ in the sum of (3.1.7) may be represented with the pair interaction potential $\varphi_{ik}(|\vec{x}_i - \vec{x}_k|)$ as:

$$\vec{a}_k \frac{\partial f^N}{\partial \vec{v}_k} = \frac{\vec{F}_k}{m} \frac{\partial f^N}{\partial \vec{v}_k} - \frac{1}{m} \sum_{i \neq k} \frac{\partial \varphi_{ik}}{\partial \vec{x}_k} \frac{\partial f^N}{\partial \vec{v}_k}, \tag{3.2.1}$$

where m is the mass of the particle.

Integrating (3.1.7) for coordinates \vec{x}_N and velocities \vec{v}_N of the Nth particle, we have:

$$\int \frac{\partial f^{N}}{\partial t} d\vec{x}_{N} d\vec{v}_{N} = \frac{\partial f^{N-1}}{\partial t};$$
 (3.2.2)

$$\int \sum_{k=1}^{N} \vec{v}_{k} \frac{\partial f^{N}}{\partial \vec{x}_{k}} d\vec{v}_{N} d\vec{v}_{N} = \sum_{k=1}^{N-1} \vec{v}_{k} \frac{\partial f^{N-1}}{\partial \vec{x}_{k}} + \underbrace{\int \vec{v}_{N} \frac{\partial f^{N}}{\partial \vec{x}_{N}} d\vec{x}_{N} d\vec{v}_{N}}_{0}.$$
(3.2.3)

Analogically, the last term in (3.1.7) may be represented as:

$$\int \sum_{k=1}^{N} \vec{a}_k \frac{\partial f^N}{\partial \vec{v}_k} d\vec{x}_N d\vec{v}_N = \sum_{k=1}^{N-1} \int \vec{a}_k \frac{\partial f^N}{\partial \vec{v}_k} d\vec{x}_N d\vec{v}_N + \underbrace{\int \vec{a}_N \frac{\partial f^N}{\partial \vec{v}_N} d\vec{x}_N d\vec{v}_N}_{0}.$$
(3.2.4)

We may rewrite (3.2.1) as follows:

$$\sum_{k=1}^{N-1} \frac{\vec{F}_k}{m} \frac{\partial f^{N-1}}{\partial \vec{v}_k} - \frac{1}{m} \sum_{k=1}^{N-1} \sum_{j \neq k} \int \frac{\partial \varphi_{ik}}{\partial \vec{x}_k} \frac{\partial f^N}{\partial \vec{v}_k} d\vec{x}_N d\vec{v}_N. \tag{3.2.5}$$

Integrating (3.1.7) for variables $\vec{x}_{N-1}, \vec{x}_N, \vec{v}_{N-1}, \vec{v}_N$, we get the corresponding equation for function f^{N-2} . Actually, (3.1.7) may be integrated further and further; for the DF f^i one may obtain:

$$\frac{\partial f^{i}}{\partial t} + \sum_{k=1}^{i} \vec{v}_{k} \frac{\partial f^{i}}{\partial \vec{x}_{k}} + \sum_{k=1}^{i} \frac{\vec{F}_{k}}{\partial \vec{v}_{k}} \frac{\partial f^{i}}{\partial \vec{v}_{k}} \\
= \frac{1}{m} \sum_{k=1}^{i} \sum_{j \neq k} \int \frac{\partial \phi(\left|\vec{x}_{k} - \vec{x}_{j}\right|)}{\partial \vec{x}_{k}} \frac{\partial f^{i+1}}{\partial \vec{v}_{k}} d\vec{x}_{i+1} d\vec{v}_{i+1}$$
(3.2.6)

In fine, after integrating for all variables $\vec{x}_2, ..., \vec{x}_N$ and $\vec{v}_2, ..., \vec{v}_N$, we obtain the kinetic equation for the single-particle DF f^1 :

$$\frac{\partial f^{1}}{\partial t} + \vec{v}_{1} \frac{\partial f^{1}}{\partial \vec{x}_{1}} + \frac{\vec{F}_{1}}{m} \frac{\partial f^{1}}{\partial \vec{v}_{1}} = \frac{1}{m} \sum_{k=2}^{N} \int \frac{\partial \varphi(|\vec{x}_{1} - \vec{x}_{k}|)}{\partial \vec{x}_{1}} \frac{\partial f^{2}}{\partial \vec{v}_{1}} d\vec{x}_{k} d\vec{v}_{k}, \tag{3.2.7}$$

or, to simplify, and to avoid confusion, removing index "1" and denoting the two-particle DF as f_{1k} , then taking the derivate $\partial/\partial \vec{v}$ out of the integral, we may rewrite (3.2.7) as:

$$\frac{\partial f}{\partial t} + \vec{v} \frac{\partial f}{\partial \vec{x}} + \frac{\vec{F}}{m} \frac{\partial f}{\partial \vec{v}} = \frac{1}{m} \sum_{k=2}^{N} \frac{\partial}{\partial \vec{v}} \int \nabla \varphi f_{1k} d\vec{x}_k d\vec{v}_k. \tag{3.2.8}$$

Thus, to obtain a certain equation for the single-particle DF, we have to include the two-particle DF f_{1k} , but we cannot obtain such an expression directly from the BBGKY chain because this function is represented through the three-particle DF, etc. Therefore, we may design some correlation for the function f_{1k} immediately, based on some physical assumptions.

We will use this approach in Sect. 3.3 and obtain the Boltzmann equation.

3.3 The Boltzmann Kinetic Equation

3.3.1 Derivation from the BBGKY Chain

As we mentioned in Sect. 3.1, the Boltzmann equation may be constructed with the "physical" consideration of the collision processes, but we prefer a more formalistic way.

Kinetic equations of Boltzmann type can be obtained from the BBGKY hierarchy; this is the kinetic equation for a single-particle DF. As it follows from the previous section, for function f we have a kinetic equation, which has a two-particle DF on its right-hand side (under the integral). Usually, this operation—derivation of the Boltzmann equation—is executed in a pair of pure mathematical steps. Here we follow the method of Vlasov; which is a deeper and more interesting approach.

The kinetic equation for the single-particle DF f can be obtained under seven assumptions (Vlasov 1966).

- 1. There is no spread of accelerations. This means the absence of the term $\sim \partial f/\partial a$ in the kinetic equation; see discussion in Sect. 3.4.
- 2. The system must be restricted with regular conditions for the convergence of integrals [e.g., for (3.2.3)].
- 3. Collisions take place at a spatial scale much smaller than the mean distance between particles in a gas. In other words, the scale of interactions named "collisions" is very short, i.e., these are local point interactions. This is an important remark because of Sects. 3.4 and 3.5.
- 4. The interaction between particles is reduced to pair collisions.
- 5. In the kinetic equation:

$$\frac{\partial f}{\partial t} + v \frac{\partial f}{\partial x} = I \tag{3.3.1}$$

on a time arrow the left-hand side describes events that follow the collision, i.e., the event described in the right-hand side.

- 6. The time taken for the collision is small, i.e., this time is negligible, and we may assume that the collision is a momentary process in which the velocities of collided particles change their values and directions.
- 7. The two-particle DF is multiplicative: $f_{1s} = f_1 f_s$. This assumption is the main requirement from a mathematical point of view. It allows us to obtain certainty from of the integral on the right-hand side of the kinetic equation. Note that usually this condition is the only condition discussed during the derivation of the Boltzmann equation.

We need the first two assumptions to obtain the BBGK chain, and then we have:

$$I = \frac{1}{m} \sum_{k=2}^{N} \frac{\partial}{\partial \vec{v}} \iint \nabla \varphi f_{1k} d\vec{x}_k d\vec{v}_k. \tag{3.3.2}$$

Here the term $\nabla \varphi$ means the force acting between the particles during the time of collision; at the time gap between two successive collisions $\nabla \varphi = 0$.

This integral can be represented using correlation:

$$\operatorname{div}_{v}(f_{1k}\nabla\varphi) = \operatorname{div}_{x}(f_{1k}\vec{v}) \tag{3.3.3}$$

in a form:

$$I = \frac{1}{m} \sum_{k=2}^{N} \iint \xi \nabla f_{1k} d\vec{v}_k d\vec{v}_k, \qquad (3.3.4)$$

where $\xi = |\vec{v} - \vec{v}_k|$ is the relative velocity of the colliding particles. How many terms must be taken into account in the sum? That depends on the timescale τ for derivative $\partial f/\partial t$ relative to the time between two successive collisions t_{col} .

The first limiting case is $\tau < t_{col}$. If so, either all terms in the sum are equal to zero, or one term is non-zero. The second choice assumes n collisions at time $\tau > t_{col}$. In the last case, for non-correlated collisions, we will have n identical terms from the sum. Renormalizing the single-particle DF $f \to nf$, we obtain the same result, i.e., the same final equation.

Then we represent the integral in coordinate space in a cylindrical system with axis z and radius a:

$$d\vec{x} = a da dz d\vartheta. \tag{3.3.5}$$

where a has the role of an impact parameter and axis z is directed along the vector $\vec{v} - \vec{v}_k$. Thus, the integral is:

$$\int a da d\vartheta d\vec{v}_k \int \xi \frac{\partial f_{1k}}{\partial z} dz. \tag{3.3.6}$$

The last integral of z must be taken from "before the collision" up to "after the collision." Using assumption 6, we can take out ξ from the integral, so:

$$\int \xi \frac{\partial f_{1k}}{\partial z} dz = \xi \int \frac{\partial f_{1k}}{\partial z} dz = \xi (f'_{1k} - f_{1k}). \tag{3.3.7}$$

where the apostrophe denotes the two-particle DF after the collision.

Finally, with assumption 7 we obtain:

$$\frac{\partial f}{\partial t} + \vec{v} \frac{\partial f}{\partial \vec{x}} + \frac{\vec{F}}{m} \frac{\partial f}{\partial \vec{v}} = \frac{1}{m} \int \xi (f' f'_k - f f_k) a da d\vartheta d\vec{v}. \tag{3.3.8}$$

This is the Boltzmann equation. To use this equation, we have to establish one more additional condition for the existence of derivatives in (3.3.8) and, consequently, for the existence of (3.3.8) as a whole.

3.3.2 The Differentiability

We formulate physical laws in mathematical language, and this is the language of differential equations. Sometimes we add integral terms to these equations (e.g., the collision integral in the kinetic equation), but one can say without much exaggeration that mathematical physics is the theory of differential equations: we formulate a theory by applying various derivatives to physical quantities and combining them into equations. This theoretical method seems to be the only one that can be used, but indeed it is not.

The alternative way is the formulation of a physical problem in the language of maps. Actually, this is not a bad way considering the dominative role of numerical

simulations in modern theoretical physics: it looks reasonable to omit the phase of a differential equation, formulating a problem as a map $x_{i+1} \leftarrow F(x_i)$ immediately. However, this method is used vary rarely, in extraordinal models (e.g., in the Fermi acceleration problem). Mathematical descriptions of physical problems and differential equations become almost synonymous.

Many mathematicians are convinced that physics (in its theoretical part) contains nothing more than equations. It is not true: theoretical physics consists not only of equations, but also of variables within these equations. An adequate formulation of a physical description implies correctness of the chosen scale of these variables, and this is a difficult task.

To apply a derivative to a physical variable, the variable representing a physical quantity must be:

- Well defined at a given point in a medium.
- Discontinuous.
- · Smooth.

We may start the discussion about these matters by considering the example of temperature.

First, this means that temperature exists. In the simplest case, temperature can be determined as the mean kinetic energy of chaotic motion, i.e., for a 1D case:

$$\frac{T}{2} = \bar{\varepsilon} = \frac{1}{N} \sum_{k=1}^{N} \frac{m(v_k - \bar{v})^2}{2},$$
(3.3.9)

where $\bar{v} = \frac{1}{N} \sum_{k=1}^{N} v_k$. A single particle (i.e., for N=1) has zero mean kinetic energy $\bar{\varepsilon}$ (because $\bar{v}_1 = \bar{v}$), thus, we see that T=0, and some may say that the temperature of a single particle is absent. Then we take two particles and notice that $\bar{\varepsilon} > 0$ in such a system. Does this system have such a quantity as temperature? Actually, no. The thermodynamic arguments behind this were considered in Chap. 1; briefly, the "equilibrium distribution function" is the key phrase here. Here we provide alternative reasoning.

Temperature is a quantity which appears in various physical relations. For certainty, we will consider Fourier's law:

$$q = -\lambda \frac{\partial T}{\partial x}. (3.3.10)$$

On the left-hand side of this equation we see the heat flux q, on the right-hand side we see the heat conductivity λ and the gradient of temperature T. Thereby, temperature is a quantity, the gradient of which determines the heat flux (with a proportional coefficient that may be found in references). In the case of two particles in each of two neighboring elementary volumes, obviously, the heat flux from

one volume to another does not obey the correlation in (3.3.10); consequently, we cannot replace $T \to \bar{\epsilon}$ and hope to obtain reasonable results.

How many particles do we need in order to introduce temperature? Of course, this question has no certain answer. We can be sure of the correctness of (3.3.9), if and only if it provides the same results for limited N and for $N \to \infty$ at the accepted accuracy δ , i.e.:

$$\frac{\left|\frac{1}{N}\sum_{k=1}^{N}\frac{m(\nu_{k}-\bar{\nu})^{2}}{2} - \lim_{N\to\infty}\frac{1}{N}\sum_{k=1}^{N}\frac{m(\nu_{k}-\bar{\nu})^{2}}{2}\right|}{\lim_{N\to\infty}\frac{1}{N}\sum_{k=1}^{N}\frac{m(\nu_{k}-\bar{\nu})^{2}}{2}} < \delta.$$
(3.3.11)

Of course, (3.3.11) is a kind of theoretical estimation, because it is difficult to obtain $N \to \infty$ in a real system. The requirement of (3.3.11) is suitable for various physical quantities (such as pressure, density, etc.), but temperature is a special case: in addition to the common relation in (3.3.11), we have to demand that any value of temperature—obtained with different physical methods—must be the same.

We mean that temperature is the parameter that determines the equilibrium state (according to the 0th law of thermodynamic, see Chap. 1). Any energy distribution must have the same module (here and below under the term "module" we understand the parameter of the probability density function that determines the scale of the distributed quantity). For instance, in the equilibrium medium:

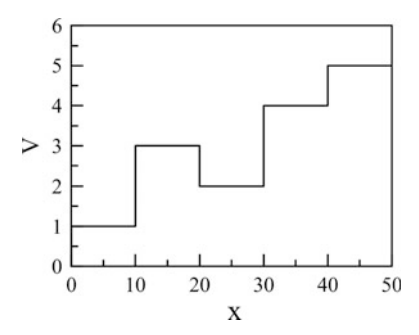
- Temperature determines all the distribution functions.
- A body placed in this medium takes this temperature.
- Radiation emitted by this medium has the same temperature; we do not mean
 that any medium emits thermal radiation, e.g., it can be impossible for a thin
 optic layer of gas, but the rotational and vibrational temperatures of gas must
 coincide with the transitional temperature.

Therefore, we have discussed the first requirement: the existence of the physical quantity. As for discontinuity, there are no problems at first glance: any physical quantity exists at any point in space. "Nature abhors a vacuum," and so on. However, for extraordinary cases, for rarefied medium, defining the quantity uniformly (at the same spatial scale in every point of the medium), we may have a problem in some (more rarefied) areas. The next counterexample is the temperature of a non-uniformly heated liquid (see Sect. 9.3). Actually, this second item in the list of requirements must not be missed.

The last requirement is more serious. As we know from L. F. Richardson, "wind has no velocity:" because of the irregular motion of liquid particles, their trajectory may be interpreted as a non-differentiable function, i.e., the quantity v = dx/dt does not exist.

For instance, in Fig. 3.1 the variation of velocity V of a particle is presented. This particle collides with other particles through an equal distance L (of, course, this is a model). In each collision, the value of velocity varies drastically on discrete random values ΔV .

Fig. 3.1 The step function V(x) has no derivatives at several points

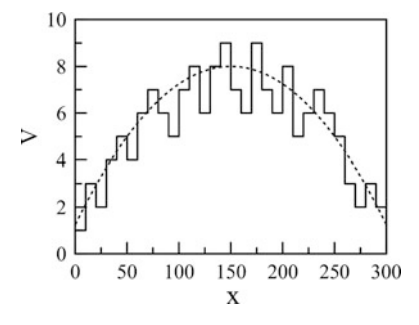


Can we determine the operator dV/dx? Of course not. The derivative does not exist at any point of the collision (at any "step" in the "stairs" in Fig. 3.1), thus, the function presented in Fig. 3.1 is non-differentiable. We cannot compose any differential equation for such a function, but we can average our "stairs" over many "steps" (see Fig. 3.2) and obtain a smooth "hill" (i.e., a differentiable function) in that way. Using this smooth function on that "hill" we cannot pretend to calculate the exact value of V at a given point: we can only find an averaged value. In other words, on a large scale we may replace the real step function V(x) with the smoothed function $V^s(x)$, represented in Fig. 3.2. From a physical point of view, there are no serious problems here: this replacement demands some variations in the physical model describing the variation of $V^s(x)$, but no dramatic changes. However, at this price, we gain a benefit: we now can compose a differential equation for the function $V^s(x)$, in contrast to function V(x).

Thus, by replacing $V(x) \to V^s(x)$ we have the advantage of a differential equation, with the disadvantage being the value $V^s(x)$ represents the averaged quantity V on some spatial interval Δx around the coordinate x.

This example explains the restrictions for the physical quantity that arise when we formulate a differential equation for this quantity. Now we are ready to discuss the spatial scale specifically for the DF obtained as a solution to the Boltzmann equation.

Fig. 3.2 The step function and its "smoothed" variant



3.3.3 Spatial Scales for the Distribution Function

There are three types of spatial scales that can be separated:

- 1. The scale where the physical quantity exists: L_A .
- 2. The scale where the physical quantity varies: L_R .
- 3. The scale where the physical quantity can be described by a smooth, differentiable function: L_C .

As we noticed in Chap. 2, the scale L_A of the number of particles that determines the DF is sufficiently large, i.e., $N(L_A) \gg 1$.

The spatial scale L_B is obviously the distance l—the mean free path (MFP) of the particle. At distance L_B the velocity of a single particle undergoes drastic variations; thus, strictly, we may have problems with the differential equation for f.

Of course, the DF f(x,v) does not repeat the velocity function of the single particle V(x) from Fig. 3.2: the DF represents the number density of many particles, and one may hope that the averaged (over many particles) velocity $\bar{V}(x)$ is a more "smoothed" function than V(x). Indeed, some particles undergo collisions directly at the MFP, whilst others undergo collisions at MFP/2 or at π -MFP, etc. Alas, the possibility to construct a differentiable DF for gas is questionable anyway (the answer depends on a small-scale model of collisions), and the problem depicted in the previous subsection remains. In the common case, we have to conclude that the calculated DF is a function smoothed on scales approximately equal to the MFP. In other words, the spatial resolution of our DF is approximately equal to the scale of the MFP—we cannot predict the exact values of the DF at smaller scales with differential equations for the DF.

However, we may use a differential equation for the "smoothed" DF f. In this case, the spatial scale L_C for the function f is around a few MFPs of the particle (in the general case it is impossible to be more precise; the minimal scale is $\sim l$): $L_C \sim L_B \sim l$.

By the way, we may remember from Chap. 2 that there exists the spatial scale $L_D \gg l$, where fluctuations of the DF are small, and we have a continuous approach.

3.3.4 Temporal Scale for the Distribution Function

An interesting property of the collision integral is the issue that $I(f_M) = 0$, where f_M is the Maxwellian distribution function (MDF). We showed this in Chap. 2 (when we obtained the Maxwellian from conditions $f_1'f_2' = f_1f_2$ at $v_1'^2 + v_2'^2 = v_1^2 + v_2^2$). Thus, the kinetic equation predicts the Maxwellian as the final state of the non-equilibrium system.

However, we saw (in Chap. 2) that this statement contradicts the mechanical nature of the system: the Maxwellian is the most frequent state of the system, not

the destination point of the system's evolution. The simplest way to reconcile both approaches is to consider the evolution of a DF on timescales much longer than the period of the DF fluctuations, i.e., at times where many collisions take place.

Thus, from another point of view, we again obtain the condition $\tau \gg t_{col}$ that we used above in Sect. 3.3.1.

3.4 The Vlasov Approach: No Collisions

3.4.1 Collisionless

At first glance, it is easy to understand (and explain to somebody else) what a "collision" is. Actually, it is a much harder task in physical terms. Molecules are not elastic dots, and "collision" implies, from a strict point of view, interaction between two (or more) molecules by means of physical forces. These forces are conditioned by an interaction potential, and, strictly, "collision" means a motion with alternating acceleration at the field of these forces. For the given particle from the system, these forces are caused by other particles from this very system. Since our goal is to find the DF for particles, then perhaps a "collision"—we mean motion with alternating accelerations, the forces which cause this acceleration, the instant distribution of particles which provide these forces—can be described by means of this DF itself (along with the potential of intermolecular interaction). How far can we go in this direction?

Anatoly Vlasov had his own ideas about every aspect of physical kinetics. In his books *Many-Particle Theory*, *Statistical Distribution Functions* (of special interest) and *Nonlocal Statistical Mechanics* he presented many original ideas. His kinetic equation for plasma became a classical implementation of the statistical approach to a strongly coupled system, and this success meant that he tended to generalize this approach to all types of systems. As we know now, this was too brave a move and incorrect in some nuanced situations, but anyway ... The kinetic theory of Vlasov deserves much more attention than it has today. We bet that 9 out of 10 physicists would find something new in the theory described below. Here we decline all the previous considerations from Sects. 3.1–3.3 and start from the very beginning.

Let us introduce the multiparametric DF $f(t, \vec{x}, \vec{v}, \dot{\vec{v}}, \ddot{\vec{v}}, \ldots)$, which depends, as one can see, not only on coordinates and velocities, but also on \vec{v} (acceleration), on \vec{v} , etc. That is, the number of particles at corresponding parameters is defined as:

$$dn = f(t, \vec{x}, \vec{v}, \vec{v}, \vec{v}, \vec{v}, \dots) d\vec{x} d\vec{v} d\vec{v} d\vec{v} d\vec{v}. \dots$$
(3.4.1)

Note that to unify all the independent variables $\vec{x}, \vec{v}, \dot{\vec{v}}$... we can use notification $\dot{\vec{x}}, \ddot{\vec{x}}, \ddot{\vec{x}}, \dots$ However, in fine, we get a more or less regular kinetic equation, thus, we distinguish the coordinates and velocities.

With the DF in (3.4.1), density, for example, can be calculated as an integral:

$$\rho(t, \vec{x}) = \int f\left(t, \vec{x}, \vec{v}, \dot{\vec{v}}, \dot{\vec{v}}, \dots\right) d\vec{v} d\vec{v} d\vec{v}...$$

$$= \int f(t, \vec{x}, \vec{v}) d\vec{v} = \int \left(\int f\left(t, \vec{x}, \vec{v}, \dot{\vec{v}}\right) d\vec{v}\right) d\vec{v} = \dots,$$
(3.4.2)

with appropriate limits for its corresponding variables (usually these limits may be put as $\pm \infty$). In such a way, every DF of *N* parameters $\vec{x}, \vec{v}, \dot{\vec{v}}, \ldots$ can be expressed through the function of the larger number of parameters.

Then we establish a conservation law—a sort of discontinuity equation—for function $f(t, \vec{x}, \vec{v}, \dot{\vec{v}}, \dot{\vec{v}}, \dots)$ in the same manner as the mass conservation law equation for $\rho(t, \vec{v})$:

$$\frac{\partial f}{\partial t} + \operatorname{div}_{x} \vec{v} f + \operatorname{div}_{v} \dot{\vec{v}} f + \operatorname{div}_{\dot{v}} \ddot{\vec{v}} f + \dots = 0. \tag{3.4.3}$$

Here we take divergences in appropriate spaces. For example:

$$\operatorname{div}_{v}\dot{\vec{v}}f = \frac{\partial \dot{v}_{x}f}{\partial v_{x}} + \frac{\partial \dot{v}_{y}f}{\partial v_{y}} + \frac{\partial \dot{v}_{z}f}{\partial v_{z}}.$$
(3.4.4)

How many terms must be left in (3.4.4)? To truncate the series of divergences in (3.4.3) we need additional information about the average value of \vec{v} , \vec{v} or \vec{v} , etc., i.e., a certain expression for a term like:

$$\left\langle \vec{v} \right\rangle = \int \vec{v} f\left(t, \vec{x}, \vec{v}, \dot{\vec{v}}\right) d\dot{v},$$
 (3.4.5)

or with any other quantities of dots above \vec{v} .

Usually, we know a specific expression exactly for (3.4.5): from the 2nd law of Newton it follows that:

$$\left\langle \dot{\vec{v}} \right\rangle = \vec{a} = \frac{\vec{F}}{m}.\tag{3.4.6}$$

The force acting on the particle \vec{F} must be determined by the external closing relation. In this case, we have the usual kinetic equation (3.4.3) for function $f(t, \vec{x}, \vec{v})$ that follows from (3.4.3):

$$\frac{\partial f}{\partial t} + \operatorname{div}_{x} \vec{v} f + \operatorname{div}_{v} \left\langle \dot{\vec{v}} \right\rangle f = 0. \tag{3.4.7}$$

Is the truncation performed above unique? No. For instance, in a system of particles emitting electromagnetic radiation, the reaction of radiation is:

$$\vec{F}_{rr} = \frac{e^2}{6\pi\varepsilon_0 c^3} \ddot{\vec{v}},\tag{3.4.8}$$

so we have a different closing correlation instead of (3.4.6):

$$\left\langle \ddot{\vec{v}} \right\rangle = \frac{6\pi\varepsilon_0 c^3}{e^2} \left(m\dot{\vec{v}} - \vec{F}_{\text{other}} \right),$$
 (3.4.9)

where \vec{F}_{other} represents all sorts of other forces. Thus, the kinetic equation in this case is:

$$\frac{\partial f}{\partial t} + \operatorname{div}_{r} \vec{v} f + \operatorname{div}_{v} \dot{\vec{v}} f + \operatorname{div}_{\dot{v}} \left\langle \vec{v} \right\rangle f = 0. \tag{3.4.10}$$

Usually radiation forces are small, so the spread of accelerations is also narrow, as it follows from (3.4.9): still $\vec{v} \sim \vec{F}_{\text{other}}/m$. However, the fact that we may (or must?) take into account the DF depending on accelerations deserves attention.

Now let us return to (3.4.7). In many cases, force \vec{F} can be represented through the pair potential $\varphi(|\vec{x}_1 - \vec{x}_2|)$ —the energy of interaction between two particles, which depends only on the coordinate difference. Therefore, the total force acting on a given particle is:

$$\vec{F} = \sum_{i} -\nabla \varphi(|\vec{x} - \vec{x}_{i}|) = -\nabla \int_{V} \int_{-\infty}^{+\infty} \varphi(|\vec{x} - \vec{x}'|) f(t, \vec{x}', \vec{v}') d\vec{v}' d\vec{x}'$$

$$= -\nabla \int_{V} \varphi(|\vec{x} - \vec{x}'|) \rho(t, \vec{x}') d\vec{x}' = -\nabla U(t, \vec{x}).$$
(3.4.11)

Equation (3.4.11) means that:

- The energy of the interaction between two particles does depend on a third particle.
- The distribution of particles which influence this given particle can be described by the required DF $f(t, \vec{x}, \vec{v})$.

We can use any pair potential in (3.4.11), for instance, the regular Coulomb potential:

$$\varphi(r) = -\frac{e^2}{4\pi\varepsilon_0 r},\tag{3.4.12}$$

or the exotic potential for two grains in a dusty plasma (Gerasimov and Sinkevich 1999):

$$\varphi(s = r/r_0) = Ae^{-s} \left(\frac{B}{s} - 1\right),$$
(3.4.13)

where $r_0 = \sqrt{\frac{ne^2}{\epsilon_0 T}}$ is the Debye radius (see also Sect. 2.2.5).

Moreover, we can try to construct a potential which describes a "collision" between two particles (a sort of potential with sharp dependence on coordinates in a repulsive term). In any case, it seems that the kinetic equation:

$$\frac{\partial f}{\partial t} + \vec{v} \frac{\partial f}{\partial \vec{r}} - \frac{\nabla_r U(r)}{m} \frac{\partial f}{\partial \vec{v}} = 0$$
 (3.4.14)

provides an adequate description of our physical problem. Or does it? We will discuss this question later in Sect. 3.4.4. Here we want to extrapolate on some other ideas of Vlasov.

3.4.2 The Hamiltonian of the Macrosystem

Everybody knows that the Hamiltonian of a system can depend only on coordinates and velocities of particles with this system, right? Well, this is not so, because of the reason noted above: electromagnetic forces (3.4.8).

The second reason, specifically, the second example that may be considered, is the potential of interaction shown in (3.4.13). This relation was used for two dust grains in thermal plasma, and, as we see, this pair potential depends on temperature. Thus, the Hamiltonian of a system of macroparticles depends on temperature.

The first question to address is how may this be possible? How might the potential energy of a system depend on such a parameter as temperature? It is impossible for dot particles, but when we consider a macroscale system, we may obtain such a result. Briefly, the interaction of two macroparticles in plasma consists of two forces:

- The repulsion of charged dust particles.
- The attraction between the dust particle and the plasma cloud surrounding another dust particle; actually, the dust grain in plasma is a kind of "macroatom" (the dust grain is a nucleus, the plasma cloud is a shell), thus, the interaction of these atoms is a sort of a covalent bond.

The second type of force depends on the plasma conditions and, therefore, depends on temperature.

The second question to address is how can we deal with H(T)? Are we able to use traditional statistical physics (see Sect. 2.2.7) to obtain all the results in the same manner?

The answer is no. Indeed, if the Hamiltonian is the function of temperature, then we have to change all of the theory. We may do it here, however, Vlasov already obtained the solution (it is not a very hard problem, by the way). Finally, we may conclude that the internal energy in all thermodynamic equations must be replaced by the function:

$$U = \overline{H(T)} - T \frac{\overline{dH}}{dT}.$$
 (3.4.15)

Thus, it is a question of taste regarding what we call the "intrinsic energy:" the function U or the function $\overline{H(T)}$. For example, the Gibbs-Helmholtz equation has the form:

$$U = F - T \frac{\partial F}{\partial T},\tag{3.4.16}$$

where U is defined by (3.1.15) and free energy of the system is the function from the Gibbs canonical distribution (2.2.36).

3.4.3 Crystallization

Another result obtained by Vlasov is crystallization theory; below we will follow his original treatise.

Let us return to the Vlasov equation. In its simplest form, equation:

$$\frac{\partial f}{\partial t} + v \frac{\partial f}{\partial x} + a(x) \frac{\partial f}{\partial v} = 0 \tag{3.4.17}$$

has a stationary solution for any function Φ of the total energy of the particle $E = \frac{mv^2}{2} + U(x)$. Indeed:

$$\frac{\partial f}{\partial x} = \frac{\mathrm{d}f}{\mathrm{d}\Phi} \frac{\partial \Phi}{\partial x} = -ma \frac{\mathrm{d}f}{\mathrm{d}\Phi}; \tag{3.4.18}$$

$$\frac{\partial f}{\partial v} = \frac{\mathrm{d}f}{\mathrm{d}\Phi} \frac{\partial \Phi}{\partial v} = mv \frac{\mathrm{d}f}{\mathrm{d}\Phi},\tag{3.4.19}$$

and (3.4.17) is satisfied with (3.4.18) and (3.4.19). For instance, one may choose $\Phi_1 = e^{-E}$, $\Phi_2 = \ln E^2$ or $\Phi_3 = \sin E$. So, which function of $\Phi(E)$ should be preferred?

The answer follows from the statistical independence of coordinates and velocities. The stationary DF must be represented as:

$$f(\vec{x}, \vec{v}) = f_x(\vec{x}) f_v(\vec{v}). \tag{3.4.20}$$

If so, then we have the DF in exponential form $f(E) = Ae^{-E/T}$, where potential energy is defined with (3.4.11) as:

$$U(\vec{x}) = \int \varphi(|\vec{x} - \vec{x}'|)\rho(\vec{x}')d\vec{x}', \qquad (3.4.21)$$

where ρ is the number density (3.4.2). Thereby, for a stationary case we have the following condition for potential energy:

$$U(\vec{x}) = A \int \varphi(|\vec{x} - \vec{x}'|) e^{-U(\vec{x}')/T} d\vec{x}'.$$
 (3.4.22)

Equation (3.4.22) has the solution U(0) = const, where:

$$U(0) = \int \varphi(|\vec{x} - \vec{x}'|)\rho(0)d\vec{x}'$$
 (3.4.23)

The last integral may be represented in spherical coordinates in the form:

$$U(0) = \rho(0) 4\pi \int_{0}^{\infty} \varphi(r)r^{2} dr. \qquad (3.4.24)$$

Then we introduce function:

$$u(\vec{x}) = -\frac{U(\vec{x}) - U(0)}{T},$$
(3.4.25)

Equation (3.4.22) may be written as:

$$u(\vec{x}) = \lambda \int \varphi^*(|\vec{x} - \vec{x}'|) e^{u(\vec{x}')} d\vec{x}', \qquad (3.4.26)$$

where $\varphi^*(r) = \frac{\varphi(r)}{4\pi \int_0^\infty \varphi(y)y^2 dy}$.

For constant potential energy $\varphi(r) = \text{const} = C$ we have the condition for the existence of the spatial uniform solution from (3.4.26):

$$C = \lambda e^C \tag{3.4.27}$$

This equation has a solution for $\lambda < 1/e$ (two real roots) and has no solutions for $\lambda > 1/e$. For $\lambda = 1/e$ the only solution is C = 1; in this case $\rho = Ae = \rho_0$ and we have the condition:

$$-\frac{4\pi\rho_0}{T} \int_{0}^{\infty} \varphi(r)r^2 dr = 1.$$
 (3.4.28)

In other words, relation (3.4.28) determines the limit of the existence of the spatial uniform distribution. On the other hand, this condition defines the beginning of periodic solutions of (3.4.26) in form:

$$u(r) = C + Be^{ikr}. (3.4.29)$$

After linearization and the assumption that $B \ll C$, we obtain the relation determining the existence of the periodic structure with wave vector k:

$$1 = 4\pi\lambda e^C \int_0^\infty \varphi^*(r) \frac{\sin kr}{kr} r^2 dr.$$
 (3.4.30)

Thus, the Vlasov equation predicts the existence of periodic solutions, the range and validity of which are defined by (3.4.30). However, we also have to determine the range of validity of the Vlasov equation itself.

3.4.4 Limitations of the Vlasov Approach

Vlasov's arguments look so logical that it is hard to argue with them. Previously, we ignored collisions. But what are collisions? Any interaction between particles can be described in terms of forces and, consequently, with an interaction potential. We can represent this in the kinetic equation of form:

$$\int \varphi(|\vec{x} - \vec{x}'|)\rho(\vec{x}')d\vec{x}', \qquad (3.4.31)$$

(see above for details). This description satisfies any physical model with the given $\varphi(r)$: the Coulomb interaction, Van der Waals forces or any other sort of forces. Collisions can be interpreted as short-scale interactions with corresponding form $\varphi(r)$ or as a short repulsive potential in the form r^{-n} , with a high value of n. It is difficult to expect that a single term in a differential equation would make all the approaches incorrect when we use many possible kinds of interaction potentials.

What else could it be? What physical reasons can restrict the Vlasov approach?

To answer these questions, we must return to the discussion about scales for quantities and their derivatives in kinetic equations. The DF was defined on a spatial scale L and this fact means that our "spatial resolution" is restricted by sufficiently large scales: an elementary volume L^3 must contain a lot of particles. Equation (3.4.31) means that we consider, at a given moment in time, an interaction between the given particle at the point \vec{x} and a large amount of particles at point \vec{x}' , i.e., the corresponding averaged force acting on the given particle from point \vec{x}' is:

$$\vec{F} = -\nabla \varphi(|\vec{x} - \vec{x}'|) \underbrace{\rho(\vec{x}')d\vec{x}'}_{dN'}. \tag{3.4.32}$$

Thus, the Vlasov equation initially implies a collective interaction. The source of the applied force is a smeared point in space, and we cannot localize it more precisely to the scale of the size of the given particle. The integrating procedure of (3.4.31) amplifies the effect of collectivization.

Thereby, even taking the initial position held at the start of this section, we may see that the approach of the self-consisted field is restricted: we cannot consider short-scale instantaneous interactions (collisions). One may also add arguments from the viewpoint of the correlation function, two-particle DF, etc.

3.5 The Kinetic Equation for Practical Purposes

3.5.1 The Split Decision

As we have seen, we may represent the interaction between particles by two limiting methods:

- As collisions: the local instantaneous interaction—before and after this interaction one may assume that particles are uncorrelated.
- As long-range interactions, when a given particle is effected by others according to the single-particle DF.

These approaches lead to different forms of the kinetic equation: the Boltzmann equation for the first case, the Vlasov equation for the second. The Boltzmann equation is suitable for gases, where collisions are an adequate representation of this type of interaction. Contrary to this, for strong-coupled plasma, collective interactions play the main role.

However, sometimes we have intermediate conditions: both long-range correlations and collisions are insufficient as approaches in their own separate ways. Usually, the kinetic equation for such a case may be composed directly as the combination of the two basic equations:

$$\frac{\partial f}{\partial t} + \vec{v} \frac{\partial f}{\partial \vec{x}} + \frac{\vec{F}}{m} \frac{\partial f}{\partial \vec{v}} = I, \tag{3.5.1}$$

where I is the collision integral and \vec{F} is the total force that affects the particle—this is the sum of the external force \vec{F}^{ext} and forces which influence all other particles:

$$\vec{F}(\vec{x}) = \vec{F}^{ext}(\vec{x}) - \int \nabla \varphi(|\vec{x} - \vec{x}'|) f(\vec{x}') d\vec{x}'$$
 (3.5.2)

Of course, we see that if $\varphi = 0$ (without interactions) then (3.5.1) turns into the Boltzmann equation, and vice versa for I = 0. It is more interesting to discuss the physical meaning of Frankenstein's monster (3.5.1) and to figure out alternative approaches.

3.5.2 Interactions at Intermediate Scales

Actually, (3.5.2) can be obtained from the BBGKY chain if we separate the forces according to the scales they acting across, i.e., separate all types of interactions into two limiting cases described at the beginning of this section. In this method, we obtain two types of term:

$$\vec{a}^{long} \frac{\partial f}{\partial \vec{v}} + \vec{a}^{short} \frac{\partial f}{\partial \vec{v}},$$
 (3.5.3)

and we obtain the Vlasov relation for \vec{a}^{long} and the Boltzmann integral from the second term. This method may be rather more suitable to correct the kinetic equation for plasma (by taking short-range correlations into account).

However, for dense gases or liquids this approach is problematic. In this case, we have no long-range collective effects in their pure form (3.4.30), because a short-range interaction potential like the Lennard-Jones does not provide such a type of interaction. For liquids, we have another starting point: we have short-range correlations, but we also have to take medium-range ones into account.

The correct method is to find the two-particle DF directly from the BBGKY chain (i.e., to also consider the kinetic equation for f_{1k}), or deny the multiplicative approximation for this DF:

$$f_{1k} = f_1 f_k + g_{1k}, (3.5.4)$$

and compose some relations for the correlation function g_{1k} ; this function plays the main role in the kinetic theory of liquids (Croxton 1974).

3.5.3 The Relaxation Approach

Of course, practical purposes imply simplicity as one of the main advantages (at least) of the mathematical description of the problem. From this point of view, the collision integral must provide the transition to the equilibrium state, i.e., the transition to the DF f_0 , which corresponds to the MDF of velocities. In this case, the collision integral may be represented in the form $\sim (f_0 - f)$, i.e., the kinetic equation has the form:

$$\frac{\partial f}{\partial t} + \vec{v} \frac{\partial f}{\partial \vec{x}} + \frac{\vec{F}^{\text{ext}}}{m} \frac{\partial f}{\partial \vec{v}} = -\frac{f - f_0}{\tau}.$$
 (3.5.5)

Sometimes this equation is referred to as the Bhatnagar-Gross-Krook approach. This relation found wide application in condensed media physics—first of all, because of its rusticity.

3.6 The Evolution of Probability: The Mathematical Approach

One can imagine two ways to apply theoretical physics.

The first way is to have universal equations that hold all the answers within them; any solution can be obtained from these perfect equations. The second way, almost forgotten now, is to construct an equation for a given problem. Here we open the door leading to kinetics.

3.6.1 The Master Equation

Here we will use function p instead of function f, which is used everywhere in this book, to distinguish this approach from other, more traditional equations. We obtain some results for a 1D case only for clarity; it is not difficult to generalize these results for 3D equations.

First of all, we will consider the function describing the probability to be at instant t, at coordinate x with velocity v, which can be named formally the "probability density function" p(t, x, v), but, as with everywhere else, we will call it the "distribution function." This function describes a fraction of the particles at parameters (t, x, v).

Then we have to formulate the equation for the evolution of p(t, x, v). Assuming that particles cannot appear or disappear, we can write:

$$p(t+\tau,x,v) = \iint p(t,x-\Delta,v-\Omega)w(\tau,\Delta,\Omega)d\Delta d\Omega. \tag{3.6.1}$$

Here, function $w(\tau, \Delta, \Omega)$ defines the probability of a change in the coordinate Δ and velocity Ω at time interval τ ; of course, this probability is normalized:

$$\iint w(\tau, \Delta, \Omega) d\Delta d\Omega = 1. \tag{3.6.2}$$

The double integral in (3.6.1) and (3.6.2) must be taken at all ranges of Δ and Ω . In adjacent areas of science (such as non-linear dynamics) (3.6.1) is known as the Fokker-Plank-Kolmogorov (FPK) equation. In its integral form it does not contain any serious assumptions. For instance, there is no special assumption on the differentiability of function p(t,x,v). Further, in Chap. 7, we will apply (3.6.1) directly. Here we choose another path.

Then, supposing a sufficiently short time step τ , we can represent our DF in series:

$$p(t+\tau, x, v) = p(t, x, v) + \tau \frac{\partial p}{\partial t} + \dots,$$
 (3.6.3)

$$p(t, x - \Delta, v - \Omega) = p(t, x, v) - \Delta \frac{\partial p}{\partial x} + \frac{\Delta^2}{2} \frac{\partial^2 p}{\partial x^2} - \Omega \frac{\partial p}{\partial v} + \dots,$$
(3.6.4)

and so on, including mixed derivatives.

Keeping a sufficient number of terms in (3.6.3) and (3.6.4), and inserting these expansions into (3.6.1), one can obtain a kinetic equation for the given problem, identified by the certain function of probability $w(\tau, \Delta, \Omega)$. In general, function $w(\tau, \Delta, \Omega)$ can be designed in various forms. For instance, it can be multiplicative like $w(\tau, \Delta, \Omega) = w_x(\tau, \Delta)w_v(\tau, \Omega)$, or not. This function may even depend on the probability distribution function itself, thus, in the common case, w is a function of all parameters.

The next sections are devoted to such problems: by choosing one or another function w, we will obtain various forms of the kinetic equation.

3.6.2 The Kinetic Equation in an External Field

We hold only the first derivatives in (3.6.3) and (3.6.4). Then, the right-hand side of (3.6.1) is:

$$\iint p(t, x, v) w d\Delta d\Omega - \iint \Delta \frac{\partial p}{\partial x} w d\Delta d\Omega - \iint \Omega \frac{\partial p}{\partial v} w d\Delta d\Omega
= p(t, x, v) - \frac{\partial p}{\partial x} \iint \Delta w d\Delta d\Omega - \frac{\partial p}{\partial v} \iint \Omega w d\Delta d\Omega.$$
(3.6.5)

Combining (3.6.5) and (3.6.3) in (3.6.1), we have:

$$\frac{\partial p}{\partial t} + \frac{\partial p}{\partial x} \iint \frac{\Delta}{\tau} w d\Delta d\Omega + \frac{\partial p}{\partial v} \iint \frac{\Omega}{\tau} w d\Delta d\Omega = 0.$$
 (3.6.6)

The second term in (3.6.6) contains the mean value of displacement of a particle during time interval τ :

$$\bar{\Delta} = \iint \Delta w(\tau, x, \nu) d\Delta d\Omega, \qquad (3.6.7)$$

divided by this time step τ . This ratio is the velocity of the particle $\nu = \bar{\Delta}/\tau$. The third term, analogically, has a factor of the mean acceleration:

$$a = \frac{\bar{\Omega}}{\tau} = \frac{F}{m} = -\frac{1}{m}\nabla U. \tag{3.6.8}$$

where U is the potential of external forces. Thus, we see a regular form of the kinetic equation for particles at the external field U:

$$\frac{\partial p}{\partial t} + v \frac{\partial p}{\partial x} - \frac{\nabla U}{m} \frac{\partial p}{\partial v} = 0. \tag{3.6.9}$$

There is nothing new here. There is nothing new in the next section either, but we must demonstrate how it works.

3.6.3 The Kinetic Equation for a Self-consisted Field

When the probability of the displacement of a particle (in both spaces: coordinates and velocities) depends on the configuration of all particles, we observe a more complicated situation.

At first, we consider the interaction of a given particle with others through a self-consisted field: the field of potential forces created by other particles with the same DF p(t, x, v). The "probability" of displacement in Ω (in velocity space) is now fully determined by the Newton's 2nd law, thus:

$$w(\tau, \Delta, \Omega) = w(\Delta)\delta\left(\frac{\Omega}{\tau} - \frac{F(x)}{m}\right). \tag{3.6.10}$$

Here we can represent forces through the function p, as in Sect. 3.4:

$$F(x) = -\int \int \nabla \varphi p(t, x', v) dx' dv, \qquad (3.6.11)$$

where $\varphi(|x-x'|)$ is a pair potential function. Then we obtain the Vlasov equation:

$$\frac{\partial p}{\partial t} + v \frac{\partial p}{\partial x} - \frac{\iint \nabla \varphi p dx' dv}{m} \frac{\partial p}{\partial v} = 0. \tag{3.6.12}$$

This description is incorrect for sufficiently small spatial scales. As we discussed above, we cannot define forces from other particles at this point in this manner. The spatial resolution for the forces in the Vlasov approach is about the spatial scale where the probability function is defined. In some cases, for long-range forces (for objects like plasma, where long-range electromagnetic forces dominate) this description may be sufficient.

However, usually, especially for gases, we need a more detailed circumscribing. For these purposes, another form of the function $w(\tau, \Delta, \Omega)$ must be used; now this function must depend on the DF itself.

3.6.4 The Kinetic Equation for Collisions

An interesting situation appears when the probability function w, which describes displacements of a given particle at point $(x - \Delta)$, is determined by other particles at this very point. It is a radically different problem, and we will solve it in several steps.

First, for simplicity, we will consider only the function p(t,v), i.e., we neglect the spatial distribution. Next we exclude the time step τ from the probability function w. This function is now determined by interaction at this very point with "scattered centers"—particles with the same DF p. Let the probability $\omega(v,v',\Omega)$ define the transfer of velocity Ω in one collision between two particles with velocities v and v'. The probability of such a collision is determined by the fraction of atoms with velocity v': p(v') dv'. To take into account all possible collisions—with particles at various velocities—one must consider an integral of all v'. Finally, we have:

$$p(t+\tau,v) = \int p(t,v-\Omega) d\Omega \underbrace{\int \omega(v-\Omega,v',\Omega) p(t,v') dv'}_{w(\Omega)}.$$
 (3.6.13)

Expanding $p(t+\tau, v)$ into series (3.6.3), we obtain a kinetic equation in the form:

$$\frac{\partial p}{\partial t} = \frac{P - p}{\tau}. (3.6.14)$$

where P is the right-hand side of (3.6.13).

Moreover, we can conclude that in equilibrium $p = p_0$ and, consequently, in equilibrium $P = p_0$ too (the right-hand side must vanish at equilibrium; this is one of the possible definitions of the equilibrium state). Of course, this circumstance does not mean that $P \equiv p_0$: a more correct formulation is $P(p_0) = p_0$; but, assuming that near the equilibrium state $P \approx p_0$, we obtain a kind of kinetic equation in relaxation form.

In addition to (3.6.14), we may choose another path. Considering that:

$$p(t,v) = \int p(t,v)w(\Omega)d\Omega = \iint \omega(v-\Omega,v',\Omega)p(t,v)p(t,v')d\Omega dv', \quad (3.6.15)$$

we may represent (3.6.14) with (3.6.13) and (3.6.15) in a more "Boltzmannian" form, especially after some manipulations with probability function $\omega(\nu - \Omega, \nu', \Omega)$. However, we are not going rewrite the same equation here a thousand times; we must show other forms of the kinetic equation.

3.6.5 The Diffusion Equations

One of the first applications of the FPK equation was a derivative of a diffusion equation (Einstein 1905). Neglecting all velocity parts of (3.6.1) (by integrating velocities, for example), and assuming that the mean displacement is equal to zero:

$$\int \Delta w(\tau, \Delta) d\Delta = 0. \tag{3.6.16}$$

If we hold the second spatial derivative in (3.6.4); then we have:

$$\frac{\partial p}{\partial t} = \underbrace{\frac{1}{2\tau} \int \Delta^2 w(\tau, \Delta) d\Delta}_{P} \cdot \frac{\partial^2 p}{\partial x^2}.$$
 (3.6.17)

The first factor on the right-hand side of (3.6.17) is the diffusion coefficient—the ratio of the mean-square displacement to the corresponding doubled time step:

$$D = \frac{\overline{\Delta^2}}{2\tau}.\tag{3.6.18}$$

The final, well-known form of the equation—the diffusion equation—is:

$$\frac{\partial p}{\partial t} = D \frac{\partial^2 p}{\partial r^2}.$$
 (3.6.19)

It is more interesting to obtaining same equation in velocity space. Assume that the variation of velocity is determined by collisions with particles of another nature, for instance, with particles with different masses. In one such collision the velocity of our particle changes its direction while the absolute value of velocity stays (assumingly) the same: in a single collision of particles with masses $m_1 \ll m_2$ only energy of the order $\sim m_1/m_2$ can be transferred. Thus, in many collisions (the number of collisions must be fewer than m_2/m_1) the particle velocities only change direction chaotically.

Performing the same operations, we have:

$$\frac{\partial p}{\partial t} = D_v \frac{\partial^2 p}{\partial v^2}.$$
 (3.6.20)

In the literature, this equation is referred to as the Fokker-Planck equation too. Here the diffusion coefficient D_{ν} , of course, differs from the usual analog D: these quantities determine diffusion in different spaces.

3.6.6 The Stationary Equations

We are free to use (3.6.1) in a slightly different manner. Instead of the time–coordinate–velocity triad we may consider a stationary (or quasi-stationary) problem and write the following correlation:

$$p(x + \Delta, v) = \int p(x, v - \Omega)w(\Delta, \Omega)d\Omega.$$
 (3.6.21)

Thus, we consider a stationary probability density function along axis x and find a dependence on its velocity. This equation may be useful when we try to establish the variation of the velocity DF along a selected direction; for instance, at the boundary surface.

Adopting results from previous sections, we can rewrite it as:

$$p(x + \Delta, v) = \iint p(x, v - \Omega)p(x, v')\omega(v - \Omega, v', \Omega)dv'd\Omega, \qquad (3.6.22)$$

and follow the previous consideration. Otherwise, for example, we can expand (3.6.21) into series of Δ and Ω . Thus, we have on the left-hand side:

$$p(x + \Delta, v) = p(x, v) + \Delta \frac{\partial p}{\partial x} + \dots$$
 (3.6.23)

We can leave the right-hand side of (3.6.23) as it is, assuming that this function is $\sim p_0$, and obtain the equation in relaxation form:

$$\frac{\partial p}{\partial x} = \frac{p_0 - p}{\Lambda}. (3.6.24)$$

Thus, we may find the simplest representation:

$$p(x, v) = p_0(v) - (p_0(v) - p(0, v))e^{-x/\Delta},$$
(3.6.25)

where Δ is about the MFP. This simplest relation is suitable for a problem when the DF at the origin is defined as p(0, v), and we know that $p(x \to \infty, v) = p_0$. We may estimate fluxes at any coordinate x this way, but, to be fair, there are too many simplifications here.

3.7 The Kinetics of Gas Near the Evaporation Surface

At the vicinity of the evaporation surface, the region may be divided into several zones (see Fig. 3.3), which will be referred to in the following text.

3.7.1 The Liquid

The first zone (<A) is liquid—the condensed phase, where the density of particles is high, and the "elementary volume" of the medium is low in comparison to the gaseous phase. In the liquid, the characteristic spatial scale is about σ —the parameter of the interatomic interaction. For instance, in argon $\sigma \approx 0.34$ nm (the parameter of the Lennard–Jones potential), while the density ~ 1300 kg/m³, corresponding to 100 K, and we have an interparticle distance of 0.6 nm, i.e., of similar order.

In such a dense substance we may expect the quasi-equilibrium state to be on a scale of approximately 1–10 nm: we may define the temperature of a part of the liquid to this size, and we may expect that the temperature of that part is close to the temperature of the neighboring part of the liquid. In most cases these remarks are valid, however, even in a liquid we may produce strong non-equilibrium conditions, where the temperature of the liquid would be an inappropriate quantity (see Chap. 9).

3.7.2 The Region of Vapor-Liquid Interaction

In layer A–B the vapor molecules of gases are not free, they interact with the liquid. We mean direct interaction of vapor particles with molecules of the liquid: at long

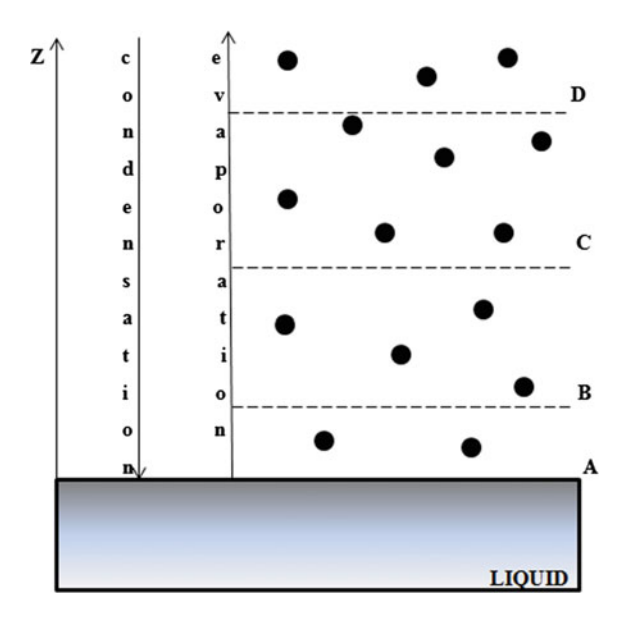


Fig. 3.3 Areas considered during the processes of evaporation and condensation. Planes: A—Vapor—liquid interface, B—Boundary of area where evaporated atoms interact with a liquid; there are problems with the DF in A–B; if one would desire to solve the kinetic equation here, it must contain external forces (if the DF for evaporated atoms is considered separately) or a self-consisted field (for a total distribution function), C—Boundary of the Knudsen layer B–C; here we can construct some kind of DF f(z), but this function is averaged at several MFPs, D—Boundary of the medium that can be considered as a boundary layer; in C–D we can use macroscopic parameters and, in the absence of other restrictions (non-equilibrium in nature), formulate an equation such as the Navier—Stokes or the heat conduction equation. Here the DF is not strictly a MDF, because there are fluxes present

ranges atoms attract one another. As the spatial scale of the interatomic potential is 0.34 nm, then the width of the layer A–B is about 1 nm (actually, more: several nanometers, see Chap. 5 for results from numerical simulations).

For non-superdense vapor the number of vapor atoms in A–B is small; the width of this layer is much smaller than the MFP of a molecule. Of course, the continuous medium approach cannot be applied on such scales; moreover, the correctness of the kinetic equation is subject to doubt too, because of an insufficient amount of particles in this layer.

If, anyway, someone needs to calculate the DF in this layer, one must take into account the interaction with a liquid of external forces, at least. We have no such goal in this book; however, in Chap. 5 we will find the DF at plane B. We think that it is sufficient for any practical purpose; it is hard to imagine the reason to calculate the DF inside zone A–B.

3.7.3 The Knudsen Layer

Layer *B–C* is a layer with a width of about several MFPs of a molecule; this is the so-called Knudsen layer—a thin but very important zone at the surface of the phase transition.

The MFP of a particle in a medium with number density n, i.e., the path length of free motion between two successive collisions, may be estimated as:

$$l \sim \frac{1}{n\sigma^2}.\tag{3.7.1}$$

In an ideal gas n = p/T, and we have:

$$l \sim \frac{T}{p\sigma^2}. (3.7.2)$$

For example, for temperature $T=100~\rm K$, $p=10^5~\rm Pa$ and $\sigma=0.34~\rm nm$ the MFP $l\sim0.1~\rm \mu m$. In such conditions, the mean interparticle distance is $\sim4~\rm nm$. Thereby, on scales of approximately 10 nm (we mean several tens of nanometers) we may introduce the DFf, but a substance on such a scale is not a continuous medium. For example, we cannot use Fourier's law here, or any other macroscopic equation.

Kinetic equations must be used in the Knudsen layer. The simplest version (the relaxation equation) may be applied, as well as more complicated versions of the Boltzmann equation. However, for our purposes in Chap. 7 we will use kinetic equations from Sect. 3.6.

3.7.4 The Boundary Layer

In this layer the hydrodynamic description can be applied. This is a thick layer, and we may enter large "elementary volumes" here, the size of which are greater than the MFP of a molecule. Thus, the macroscopic description is possible (Navier-Stokes equations, etc.).

Indeed, macroscopic circumscribing is what we usually need. The flow of gas near the liquid surface is an ordinary physical problem, which can be considered with continuous media equations. As we know, this description demands boundary conditions for the gas flow—conditions for macroscopic parameters of a gas near the interface, i.e., on plane C, while we have to connect these conditions with parameters of a liquid, i.e., at plane A.

As we see in Fig. 3.3, planes A and C are separated by two particular regions: zone A-B, where particles "unbound" from the liquid, and the Knudsen layer B-C, where macroscopic definitions do not exist. Thus, we cannot immediately equate, for example, the temperature of the liquid T_C at plane C to the temperature of the liquid T_A at plane T_A , because, at first, $T_A \neq T_C$. The temperature difference between

the vapor and the liquid—the so-called temperature jump—is the matter of Chap. 8 of this book; this problem is even more interesting than it looks at the first glance.

Also, we cannot connect mass fluxes J_A and J_C directly, because even fluxes J_B and J_C must be associated with others through parameters of the Knudsen layer. Some aspects of this problem will be considered in Chap. 7.

Indeed, the boundary conditions for a boundary layer are a complicated problem, and there full solution may only come in time.

3.7.5 The Bulk of the Gas

In some problems, there may exist a region of equilibrium vapor, where T = const, and the macroscopic velocity of the vapor is equal to zero; this steady bulk volume of the vapor is the limiting case of layer C–D. Otherwise, the steady flow may be defined at this region, etc.

In common, far away from the interface, specific external macroscopic conditions may be formulated, however, these formulations would be hydrodynamic in nature and, therefore, outside of the scope of this book.

3.8 Conclusion

The kinetic equation may be written in various forms, the most important fact being that these forms are, in fact, different equations. We cannot say that one form of the kinetic equation is more convenient for a certain problem, while another form of the equation is more suitable for another case. It is more likely that the kinetic equation suitable for a given problem is absolutely inappropriate for another one.

For practical purposes, the kinetic equation for the single-particle DF must be used. It may be designed in various ways, but the most promising and the least used representation follows directly from the Kolmogorov equation. By formulating a kinetic equation in integral form (not as a differential equation), we may, at least, avoid some problems concerning the scales of the DF, which may distort the solution obtained by the differential equation. This approach is not a panacea, but can be applied to a wider class of physical problems.

As for differential kinetic equations, there are two limiting forms: the Boltzmann approach and the Vlasov equation. Of course they can be combined and applied for some physical systems too. Both these approaches are characterized by the special scales of forces that these models take into account.

The spatial scale of the DF itself is a specific problem. This function may be introduced for scales L where the number of particles is high: $N_L \gg 1$. However, the scale where the DF varies more or less smoothly may be somewhat greater. Indeed, the spatial scale is the bane of interphase problems. The macroscopic flow of gas cannot be described properly, because it is impossible to formulate boundary

3.8 Conclusion 91

conditions based on same-scale physics: the statistical and kinetic approach, which consider problems on much smaller scales, are items required for physical descriptions.

Throughout this book we will analyze all the problems only on the small-scale level, even in Chap. 9, where we will discuss problems of boiling and cavitation. Despite the common difficulty—the results of small-scale considerations needing to be linked to the original problem—we may say that many issues of macroscopic processes can be described on the microscopic level.

Moreover, the macroscopic problem can be fully modelled by the microscopic system; this is the matter of the next chapter.

References

C. Cercignani, Mathematical Methods in Kinetic Theory (Springer, US, 1969)

C.A. Croxton, Liquid State Physics (Cambridge University Press, Cambridge, 1974)

A. Einstein, Ann. Phys. 17, 549 (1905)

D.N. Gerasimov, O.A. Sinkevich, High Temp. 37, 823 (1999)

A.A. Vlasov, Statistical Distribution Functions (Nauka, Moscow, 1966)

Recommended Literatures

L. Boltzmann, Wissenschaftliche Abhandlungen von Ludwig Boltzmann (Verlag von Johann Ambrosius Barth, Leipzig, 1909)

A.A. Vlasov, Many-Particles Theory (GITTL, Moscow, 1950)

Chapter 4 Numerical Experiments: Molecular Dynamics Simulations



It is very hard to solve kinetic equations directly. Thus, if we want to obtain information about the dynamics of a complicated system, we have to find another way.

One of these ways is to analyze the dynamics of a small amount of particles ($\sim 10^3$ to 10^4 , sometimes more, sometimes even less) and to consider them as the representative set, from which we can obtain the properties of the real system.

Thus, now we shall return to the very beginning: to mechanics.

4.1 From Statistics to Mechanics: There and Back Again

4.1.1 From Kinetics to Mechanics

As we discussed in Chap. 2, the evolution of a real mechanical system is impossible now and, most likely, will remain impossible forever.

So physics invented another way: to represent parameters of the real system with statistical characteristics: through distribution functions (DFs), etc. However, the statistical approach describes a static picture of the system, while we need information about the dynamics of the system—about its evolution.

The area of science that considers the evolution of DFs is called "kinetic theory." Based on the early works of Maxwell and Boltzmann, this theory derives a set of integral-differential equations—kinetic equations.

However, it is very hard to solve a kinetic equation analytically; actually, it is impossible. After the cycle that is "mechanics-statistics-kinetics" we find ourselves at the starting point: we must select one of two impossibilities, the impossibility of mechanics or the impossibility of kinetics.

Of course, as usual, there exists a third way: to solve the kinetic equation numerically. Sometimes, this way leads to interesting (from the conceptual point of view) results.

Let us consider, for example, the Vlasov equation:

$$\frac{\partial f}{\partial t} + \vec{v} \frac{\partial f}{\partial \vec{x}} + \vec{a}(\vec{x}) \frac{\partial f}{\partial \vec{v}} = 0. \tag{4.1.1}$$

Here, as we remember from Chap. 3, the acceleration is determined by the distribution of particles themselves:

$$\vec{a}(t,\vec{x}) = -\frac{1}{m} \int \nabla \varphi(|\vec{x} - \vec{x}'|) f(t,\vec{x}',\vec{v}') d\vec{x}' d\vec{v}'. \tag{4.1.2}$$

From the mathematical point of view, (4.1.1) represents the hyperbolic equation for function f. This equation has characteristics:

$$\frac{d\vec{x}}{dt} = \vec{v}; \quad \frac{d\vec{v}}{dt} = \vec{a} = \frac{q\vec{E}}{m},\tag{4.1.3}$$

where the electric field strength \vec{E} acting on the charge q may be found from the Poisson equation.

Thus, actually, the solution of (4.1.1) through its characteristics is similar to the consideration of the dynamics of the mechanical system. Originally, this interpretation led to the consideration of the dynamics of so-called macroparticles—clouds of regular particles (Sigov 2001). Since the Vlasov approach suits plasma dynamics, these clouds consist of charged particles—ions or electrons; moreover, usually even the distribution of particles inside such clouds is considered in this method (for instance, the Gaussian, of course).

The method of macroparticles was used in Chap. 2 as an illustration of (ir) reversibility. Thus, one may say that the results of the solution of the Vlasov equation were indeed presented in that chapter.

However, in problems of such condensed matter as liquids, the Vlasov equation does not provide adequate results, because of the different spatial scales of forces in liquid dynamics problems. Thus, we need to find another foundation for the approach based on the Newtonian dynamics equation.

4.1.2 The Statistics for the Boltzmann Case

This method—the method of molecular dynamics (MMD)—is, strictly speaking, not just for the Boltzmann equation, but is adequate for various types of problems where the interaction potential is known for given types of particles.

The idea of the MMD is to model the mechanical system with a number of particles of the order "unity with several zeros." Of course, this is much less than the number of particles in the real system, or even in a part of the real system. However, we have no goal to model the real system itself, we want to consider a "sufficient amount" of particles to model the essential properties of the real system with an appropriate accuracy.

Then, what amount of particles is "sufficient?" Sometimes, it is possible to meet estimations as 1 mol, 10^{20} or some similar value; these estimations are based on the number of particles in some real system (for instance, in a microdroplet), i.e. reflects the reason described above. However, the valuation of the number of particles must follow from the statistical and kinetic arguments.

To model a property of volume (such as density), we must consider a region of the medium of a size where the surface deviation of energy is negligible: boundary conditions contribute to the MMD analysis, even for periodic boundary conditions. Then, the spatial scale of the considered volume must be much greater than the interparticle distance $l_{\rm ip}$ (which is the scale for the surface). For instance, in a liquid $l_{\rm ip} \sim \sigma$ (see Sect. 3.7), thus, the scale of the model system must be $\gg \sigma$. Translating this assertion into the language of the "required number of particles," we obtain an old demand $N \gg 1$ (see Chap. 2; note that this amount of particles is sufficient for the Maxwellian distribution function (MDF)).

To model the vapor phase, we have to take into account the mean free path (MFP) of the molecule: only on such scales does a gas represent a continuum; this requirement rather concerns the volume of the molecular dynamics (MD) cell rather than the number of particles.

It follows from this consideration, that setting the number of particles to $\sim 10^3$ looks adequate for a simple problem, when one needs to calculate properties of an evaporating liquid, for example. Not all aspects can be taken into account with such a number of particles, e.g., the liquid layer is quite thin and, therefore, is isothermal, so we cannot treat the influence of evaporation on the liquid surface's temperature properly (because this surface has the temperature of the solid surface beneath it). However, again, for *simple* problems setting the number of particles to $\sim 10^3$ is satisfactory. It is hard to imagine what new results can be obtained for such ordinary problems with $\sim 10^6$ particles (excluding the wow effect from colleagues). Results that are much more adequate can be obtained by "ensemble averaging," i.e., repeating the calculations for small MD cells ($\sim 10^3$ particles) over and over.

Of course, there are problems where a great amount of particles is necessary, e.g., if we want to model a bubble in a liquid. We do not state that it is enough to consider 10³ particles for any possible case. Special problems demand special solutions.

The technique of the MMD is described in Sect. 4.2. Below this section, we discuss some principal aspects of MD simulations.

4.1.3 Interaction Potential

One may say that the MD simulation is a direct numerical investigation of the given problem. This is not exactly true, but this statement is close to the truth.

The interaction potential of Lennard-Jones type, which may be written as:

$$\varphi(r) = 4\varepsilon \left[\left(\frac{\sigma}{r} \right)^{12} - \left(\frac{\sigma}{r} \right)^{6} \right], \tag{4.1.4}$$

is usually applied for rare gases. Here the second term $\sim r^{-6}$ describes the attraction of two dipoles; this formula can be obtained theoretically. The first, repulsive term $\sim r^{-12}$, reflects only our imagination about its "sharp" form. There is no solid theory beneath (4.1.4) as a whole. Moreover, the dipole-interaction term $\sim r^{-6}$ in (4.1.4) was obtained for two isolated particles; in vicinity of the third particle this expression, generally, must have another form. In other words, the potential (4.1.4) is not as fundamental as we like to think. We may repeat these arguments for almost any interaction potential, except for the Coulomb interaction of dot charged particles.

Thus, the MD simulation represents the exact method with the non-exact function of the interaction potential. This means that it is difficult to obtain precise quantities of the physical system, while qualitative properties or parameters of dynamics of the given system may be examined quite correctly.

As for the interaction potential, we have the old problem: to cut or not to cut? Cutting the potential (4.1.4) at some certain radius (for instance, at 3σ), means that we receive many bonuses in terms of calculations, because the calculation of the total potential energy (i.e., of the forces acting on the particle) is the most time-consuming procedure in the MMD. Practically, the truncation of $\varphi(r)$ is the most popular scheme in the MMD. However, such a direct sort of cutting leads to problems which are common in mathematical nature, because the function of the potential energy has a special point at the cutting radius. One may provide arguments about the negligible influence of such a small contribution to the total energy (the part which has been cut may be of the order of size of rounding errors, etc.), but, anyway, this non-differential point spoils the clear picture of MD simulations.

4.1.4 The Wrong Method to Solve Equations

Let us consider a 1D system (in order to write fewer symbols) of N particles. The dynamics of this system are described by the Hamilton equations:

$$\frac{\mathrm{d}x_i}{\mathrm{d}t} = \frac{p_i}{m_i}, \frac{\mathrm{d}p_i}{\mathrm{d}t} = -\sum_{\substack{k=1\\k\neq i}}^{N} \frac{\partial \varphi_{ik}}{\partial x_i}, \quad i = 1...N,$$
(4.1.5)

where function $\varphi_{ik}(x_{ik})$ is the pair potential of interaction between the *i*th and *k*th particles, placed at a distance x_{ik} from one another.

The system (4.1.5) can be solved only numerically. The simplest method to solve the differential equation:

$$\frac{\mathrm{d}f}{\mathrm{d}t} = F(f) \tag{4.1.6}$$

is the explicit scheme. According to this method, we may represent a derivative through a finite difference, and express the function F(f) on the right-hand side with f at the previous time step:

$$\frac{f^{n+1} - f^n}{\tau} = F(f^n),\tag{4.1.7}$$

for each nth time step. This scheme allows one to evaluate the function f recursively, if one knows the initial condition f^0 :

$$f^{n+1} = f^n + \tau F(f^n). \tag{4.1.8}$$

The explicit scheme (4.1.8) applied to the Hamilton equations (4.1.5) gives:

$$x_i^{n+1} = x_i^n + \tau \frac{p_i^n}{m},\tag{4.1.9}$$

$$p_i^{n+1} = p_i^n + \tau F(x_i^n). \tag{4.1.10}$$

However, this method is wrong, as shown by Tabor (1989). From the mathematical point of view, the system (4.1.9)–(4.1.10) represents the map $(x_i^n, p_i^n) \rightarrow (x_i^{n+1}, p_i^{n+1})$. Mechanics demands we save the phase volume; thus, this map must satisfy this requirement too. For this, the Jacobian J of this transformation must be equal to unity. However, from (4.1.9) and (4.1.10) we have:

$$J = \begin{vmatrix} 1 & \tau/m \\ -\tau F'(x_i^n) & 1 \end{vmatrix} = 1 - \frac{\tau^2}{m} F'(x_i^n), \tag{4.1.11}$$

where $F' = dF/dx_i$.

We see that if $F'\neq 0$, then $J\neq 1$ for any time step $\tau>0$. Thus, the explicit numerical scheme is the non-conservative map for the initial Hamilton system; so, there are no appropriate time steps, which may correct this problem—any numerical solution of the Hamilton system by the explicit method will be wrong.

Thereby, we have to use another numerical method to obtain the solution for (4.1.5). This method will be explained in Sect. 4.2.

4.1.5 The Results of Numerical Simulations

After the calculations, we get all the coordinates $\vec{x_i}$ and velocities $\vec{v_i}$ for all N particles in our system. We rarely need these quantities directly (e.g., we explore the trajectories of individual particles during the condensation process in Chap. 7). Usually, we look for averaged, statistical parameters of the system, such as the DF, temperature, pressure, heat flux, etc.

The single-particle DF can be constructed as the histogram $f_i(v_i)$:

$$f_j = \frac{N_j}{N}, \quad j = 1...M,$$
 (4.1.12)

where N_j is the number of particles with the corresponding projection of velocity from $v_j - \Delta v/2$ to $v_j + \Delta v/2$. The interval of velocity Δv is connected with the number of intervals M as $\Delta v = (v_{\text{max}} - v_{\text{min}})/M$, where v_{min} and v_{max} are the limiting values of the calculated velocities of all particles.

The number of intervals M can be adopted more or less arbitrarily. There are several estimations of M, following from mathematical statistics, probably, the most convenient relation between M and N is:

$$M = \sqrt{N}. (4.1.13)$$

For example, for 1000 particles the number of intervals is about 30. As we see, the number of particles in the system determines the "resolution" of the DF obtained in numerical simulations.

4.1.6 How to Calculate Temperature

When the solution of (4.1.5) is (somehow) obtained, and we have the set of coordinates and velocities of all N particles, we may calculate the temperature of the system with the relation $\bar{\epsilon} = \eta \, T/2$, where η is the number of degrees of freedom and $\bar{\epsilon}$ is the kinetic energy of the chaotic motion of particles. For a 3D system $\eta = 3$, and we have:

$$T = \frac{1}{3N} \sum_{i=1}^{N} \sum_{k=1}^{3} (v_{i,k} - \bar{v}_k)^2,$$
(4.1.14)

where index k denotes the projection of the velocity, and the mean velocity is:

$$\bar{v}_k = \frac{1}{N} \sum_{i=1}^{N} \bar{v}_{i,k}.$$
(4.1.15)

Correlation (4.1.14) shows that we should remember the average velocity of particles: when particles move in one direction with the same velocity, the temperature of this group is zero. From another viewpont, practically, the velocity (4.1.15) is much less than the chaotic velocity, and often the term \bar{v}_k is omitted in (4.1.14).

4.1.7 How to Calculate Pressure

The pressure corresponding to the Clapeyron equation p = nT follows from the ideal gas approach, as the integral:

$$p = \int 2mv^2 f(v) dv, \qquad (4.1.16)$$

with the MDF for f(v). However, this is not a single part of the total pressure, which also contains the contribution corresponding to the interaction of particles. The total pressure is usually calculated as:

$$p = nT + \frac{1}{3V} \sum_{i} \sum_{j} \vec{r}_{ij} \vec{F}_{ij}, \qquad (4.1.17)$$

where \vec{r}_{ij} is the interparticle distance and \vec{F}_{ij} is the pair force. However, for a non-equilibrium case, it is more appropriate to consider integral representation (4.1.16) instead of the first term in (4.1.17).

Note that the pressure can also be calculated with the virial theorem (see Sect. 2.2.9).

4.1.8 How to Calculate Heat Flux

Actually, this is not a trivial problem. The flux of energy can be calculated in a simple form:

$$q = \int \frac{mv^2}{2} v f(v) dv \tag{4.1.18}$$

only for an ideal gas. Expression (4.1.18) contains only the flux of kinetic energy, but in the common case the interaction of particles is also significant, especially in such a condensed medium as a liquid.

In solid-state physics, the energy flux is described by phonons—quasi-particles that have no mass but have energy and momentum (Kittel 2005). This theory (or, specifically, this language) can also be used for disordered media like liquids, but it is not the best approach, especially for numerical experiments.

Another approach can be used in MD simulations (Ohara 1999). Considering two particles, one may obtain the relation for the energy that transfers from one particle to another (interparticle energy exchange rate) per unit of time:

$$\frac{\partial Q}{\partial t} = \frac{\vec{F}_{12}}{2} (\vec{v}_1 + \vec{v}_2). \tag{4.1.19}$$

The energy flux may be obtained from (4.1.19), taking the sum of all particles and dividing it by the corresponding surface area.

Let us consider this problem from another angle. The total kinetic energy of all particles in the given volume V is:

$$E = \sum_{i=1}^{N} \frac{m\vec{v}_i^2}{2}.$$
 (4.1.20)

The time derivative of (4.1.20) is:

$$\frac{\partial E}{\partial t} = \sum_{i=1}^{N} \vec{v}_i \underbrace{m \frac{d\vec{v}_i}{dt}}_{\vec{F}_i} = \sum_{i=1}^{N} \vec{v}_i (\vec{F}_i^{\text{in}} + \vec{F}_i^{\text{out}}), \tag{4.1.21}$$

where \vec{F}^{in} is the force from the particles inside the volume V and \vec{F}^{out} is the force from the particles outside. Relation (4.1.21) is a well-known mechanical theorem about the variation of kinetic energy in a system.

Thus, even when not a single particle crosses the boundary of the volume V, the kinetic energy of the particles inside this volume varies with time, because of the interaction between particles. Taking the limit $V \to 0$, we may introduce (4.1.21) into the balanced equation for kinetic energy (or the total energy) in two ways. We may represent (4.1.21) as the source term in this equation, but also we may interpret (4.1.21) as the energy flux through the boundary of that volume, in the manner described above (considering the flux into and out of the volume V, corresponding to the time derivative $\partial E/\partial t$).

4.1.9 From Mechanics to Statistics, Part Two

Briefly, up to this point we have taken the following journey:

- A real system cannot be described as a mechanical system, because we cannot solve a system of $\sim 10^{23}$ equations.
- We have to use statistics to define some macroscopic properties of the given system, i.e., we have to use DFs.
- To treat the dynamics of the system, we must consider the time dependence of the DF, i.e., solve the kinetic equation.

- There are many forms of kinetic equations, with most of them being very hard to solve.
- Thus, we have to return to the mechanical system of a small amount of particles: we obtain statistical characteristics from this diminished system, and hope to attribute the obtained results to the real (large) system.

It was discussed above that the volume properties of the diminished system may be adequate to be used as parameters of the real system. Is this enough?

Not just yet. The key word here is "fluctuations."

The fluctuation of any property of an *N*-particle system is usually estimated as the quantity proportional to $1/\sqrt{N}$. For instance, we may obtain such an estimation from the dispersion:

$$D = \frac{1}{N} \sum_{i=1}^{N} (X_i - \bar{X})^2, \tag{4.1.22}$$

with the estimation of error $\Delta X \sim 1/\sqrt{N}$. Thus, at first, fluctuations in a small (model) system are higher than in a big (initial) system. Based on this consideration, one may conclude that the role of fluctuations is overestimated in numerical simulations, even if $\sqrt{N} \gg 1$.

However, the opposite statement does not make sense either. Small-scale simulation principally omits long-scale fluctuations, but many processes in nature are based on such fluctuations; for instance, our world and the people living in it are long-scale fluctuations. We cannot describe a large-scale process properly if we suspect that long-scale (or long-time) deviations play a crucial role in the process.

From a technical point of view: in the MMD, we can obtain results for a small system ($\sim 10^3$ particles) for certain conditions (for instance and simplicity, at a given boundary temperature). We realize that our results (the average values) are representative for the large system under the same conditions; see above. However, how can we be sure that the boundary conditions for any small sub-system of the large system are the same, i.e., T = const at any side of this volume? It is difficult to find a small volume in a sea with constant temperatures at its boundaries; it is more probable that the temperature of different boundaries would be different. If so, we would see energy fluxes through our sub-volume of sea, with a distorted DF in this volume, etc.

Thus, in any sub-volume of a real, large system the DF differs from the DF in our small "representative" volume, the representativeness of which, actually, is reduced by negligible surface effects. How can we make sure that the Maxwellian obtained in our numerical simulation for 1,234 particles can be attributed to the real system?

The answer to this question may be based on the considerations made in Chap. 2 (the chaotization of velocities leads to the Maxwellian), but here we require a solution from another point of view. The Maxwellian is a Maxwellian everywhere, of course, but we have to understand how the DF varies with the size of the system: it should be noted that the MDF is only the "most frequent" distribution (in terms of

L. Boltzmann), nothing more. But what about the deviations from the most frequent distribution?

Thus, answering the previous question, we may say that:

- The equilibrium DF (Maxwellian) of the small system with 1234 particles corresponds to the equilibrium (averaged) DF of the large system.
- The momentary DF of the small system may be absolutely inadequate as a sub-system of the large (the whole) system.
- Note that usually we have to deal not with the whole system, but with a part of it.

The Fourier series for a MD distribution function:

$$f(t, v) = \sum_{k} \hat{f}_{k}(v) \exp\left(\frac{i2\pi kt}{T}\right)$$
 (4.1.23)

differs from the series for the real system due to a significantly different period T of decomposition: coefficients $\hat{f}_k(v)$ vary with T, i.e., with the size of the system. Theoretically, the justification of the correctness of the MMD must contain the estimation of coincidence (4.1.23) for a certain number of particles N and for $N \to \infty$, i.e., it must describe the tendency:

$$\hat{f}_k^N(v) \to \hat{f}_k^\infty(v). \tag{4.1.24}$$

In simple words, when Alice (the experimenter) determines the DF in a gas volume, she obtains results different from Bob's calculations (MD simulations), because the experimental conditions are not "the equilibrium" found in the MD cell of size $10 \times 10 \times 10$ nm. Local but macroscopic fluxes may distort the surgically clear picture explored by the MMD. For instance, Bob obtained that the heat transfer coefficient is equal to zero, because in his numerical simulations the mean velocity of the gas is absent. However, Alice noticed that the mean velocity of a gas is non-zero at any moment in time (this velocity fluctuates periodically with a large period around the averaged zero value), and the heat transfer coefficient is non-zero too. What might Bob do? There is not much sense in artificial simulations of long-scale modeling by variations of boundary conditions at opposite sides of the MD cell: the result obtained in such a simulation will be fully determined by artificial external conditions.

Finally, we may state that we can obtain the equilibrium properties of a large system by considering the diminished system in numerical simulations, but we cannot obtain full information about fluctuations with MD simulations without additional methods, i.e., without applying the tricks involving these fluctuations in the numerical simulation artificially. However, such tricks do not seem to be very useful, and it is difficult to compare the MMD results to experiments: this circumstance causes problems when we try to translate the results from the MMD to the real system; see Chap. 9 where we discuss some of the problems of boiling (the macroscopic process).

4.1.10 The Role of Molecular Dynamics Simulations

Perhaps, we overcriticized the MMD in the previous section. The MMD is only an instrument, like combination pliers: we may use them only for the purposes for which they are intended.

First, the MMD lets us establish properties of the equilibrium system. By the way, the fact that we were able to obtain the MDF from the MD simulation is worth something too.

Then, the MMD lets us analyze elementary processes that cannot be explored experimentally, e.g., the interaction of a single incoming particle with a liquid surface. Such applications make the MMD a useful testing device for any theory.

The MMD also helps us to understand some principals of evolution of a mechanical system; we will use the MD for such a purpose in Chap. 6, finding the DF of potential energy.

Definitely, the MMD may be applied to various problems. If we do not raise our expectations of the MMD too high, we may easily find appropriate applications for it: in the frame of its validity.

4.2 Techniques of Molecular Dynamics

B. Alder and T. Wainwright's work (Alder and Wainwright 1957) is known as the first work dedicated to MD. They analyzed phase transitions in systems containing 32 and 108 hard spheres with periodic boundary conditions. Even in systems that small they observed an equilibrium velocity distribution. The MD method was then described in their further work (Alder and Wainwright, 1959).

In 1964, A. Rahman studied the properties of liquid argon (Rahman 1964) using a system of 864 particles interacting with Lennard–Jones (LJ) potential (Jones 1924).

4.2.1 Motion Equations

Motion equations for N interacting particles are defined as follows (Landau and Lifshitz 1960):

$$\begin{cases} \vec{X}_i = \vec{V}_i \\ \vec{V}_i = \vec{a}_i \end{cases} \tag{4.2.1}$$

where i is the sequence number of the particle, 1...N; \vec{X}_i is the radius vector of the ith particle; and \vec{V}_i and \vec{a}_i are the velocity and acceleration of the ith particle.

To numerically solve this problem, a sequence $t = \tau \Delta t$ is considered, where τ is the sequence number of the time step Δt . The velocity of the *i*th particle is denoted as $\vec{V}_i^{\tau+1/2}$, then the differential equation is discretized:

$$\vec{\vec{X}}_i = \frac{d\vec{X}_i}{dt} = \frac{\vec{X}_i^{\tau+1} - \vec{X}_i^{\tau}}{\Delta t} = \vec{V}_i^{\tau+1/2}$$
(4.2.2)

The velocity at time step $\tau + 1/2$ corresponds to a particle change of position between time steps $\tau + 1$ and τ . Then the second derivative of \vec{X} in time step $\tau + 1/2$ is:

$$\vec{\vec{V}}_i = \frac{d\vec{V}_i}{dt} = \frac{\vec{V}_i^{\tau + 1/2} - \vec{V}_i^{\tau - 1/2}}{\Delta t} = \vec{a}_i^{\tau}$$
 (4.2.3)

The method for solving motion equations using a system where position and velocity are calculated at interleaved time points that "leapfrog" each other (Skeel 1993) is called the "leapfrog integration:"

$$\begin{cases} \frac{\vec{X}_{i}^{\tau+1} - \vec{X}_{i}^{\tau}}{\Delta t} = \vec{V}_{i}^{\tau+1/2} \\ \frac{\vec{V}_{i}^{\tau+1/2} - \vec{V}_{i}^{\tau-1/2}}{\Delta t} = \vec{a}_{i}^{\tau} \end{cases}$$
(4.2.4)

It is also useful to know the velocity and position at integer steps:

$$\vec{V}_i^{\tau} = \frac{\vec{V}_i^{\tau + 1/2} + \vec{V}_i^{\tau - 1/2}}{2},\tag{4.2.5}$$

or

$$\begin{cases} \frac{\vec{X}_{i}^{\tau+1} - \vec{X}_{i}^{\tau}}{\Delta t} = \vec{V}_{i}^{\tau} + \frac{1}{2}\vec{a}_{i}^{\tau} \cdot \Delta t \\ \frac{\vec{V}_{i}^{\tau+1} - \vec{V}_{i}^{\tau}}{\Delta t} = \frac{\vec{a}_{i}^{\tau+1} + \vec{a}_{i}^{\tau}}{2} \end{cases}$$
(4.2.6)

Eventually, in MD, the following equations are solved at each time step:

$$\begin{cases} \vec{X}_{i}^{\tau+1} = \vec{X}_{i}^{\tau} + \vec{V}_{i}^{\tau} \cdot \Delta t + \frac{1}{2} \vec{a}_{i}^{\tau} \cdot \Delta t^{2} \\ \vec{V}_{i}^{\tau+1} = \vec{V}_{i}^{\tau} + \frac{\vec{a}_{i}^{\tau+1} + \vec{a}_{i}^{\tau}}{2} \Delta t \end{cases}$$
(4.2.7)

Such an integration is known as the "velocity Verlet" (Swope et al. 1982). Despite these methods being similar, the second one is more convenient due to the position and velocity being calculated at the same time step.

The Verlet method (Verlet, 1967) involves expanding \vec{X} in Taylor series; by expanding in the second power we obtain:

$$\vec{X}_i(t+\Delta t) = \vec{X}_i(t) + \dot{\vec{X}}_i(t) \cdot \Delta t + \ddot{\vec{X}}_i(t) \cdot \vec{a}_i^{\tau} \cdot \Delta t^2 / 2 + O(\Delta t^3). \tag{4.2.8}$$

Considering (4.2.1) and the expression for the discrete time step Δt :

$$\vec{X}_{i}^{\tau+1} = \vec{X}_{i}^{\tau} + \vec{V}_{i}^{\tau} \Delta t + \vec{a}_{i}^{\tau} \Delta t^{2} / 2. \tag{4.2.9}$$

The series expansion for $\vec{X}_i(t - \Delta t)$ is:

$$\vec{X}_{i}^{\tau-1} = \vec{X}_{i}^{\tau} - \vec{V}_{i}^{\tau} \Delta t + \vec{a}_{i}^{\tau} \Delta t^{2} / 2. \tag{4.2.10}$$

It is shown that velocity reversion gives the position at the previous time step. Velocity is expressed from the previous equations as:

$$\vec{V}_i^{\tau} = \frac{\vec{X}_i^{\tau+1} - \vec{X}_i^{\tau-1}}{2\Delta t}.$$
 (4.2.11)

However, this is an obvious way to take the derivative. In addition, these equations give:

$$\vec{X}_i^{\tau+1} = 2\vec{X}_i^{\tau} - \vec{X}_i^{\tau-1} + \vec{a}_i^{\tau} \Delta t^2. \tag{4.2.12}$$

It should be noted that the last expression allows us to solve motion equations without using the velocity variable. We use it though to obtain the numerator in the velocity expression:

$$\vec{V}_{i}^{\tau} = \frac{2\vec{X}_{i}^{\tau} - 2\vec{X}_{i}^{\tau-1} + \vec{a}_{i}^{\tau} \cdot \Delta t^{2}}{2\Delta t}.$$
(4.2.13)

For the next time step:

$$\vec{V}_i^{\tau+1} = \frac{2\vec{X}_i^{\tau+1} - 2\vec{X}_i^{\tau} + \vec{a}_i^{\tau+1} \cdot \Delta t^2}{2\Delta t}.$$
 (4.2.14)

Taking into account (4.2.9) in order to calculate $\vec{X}_i^{\tau+1}$, we get the expression for velocity:

$$\vec{V}_i^{\tau+1} = \vec{V}_i^{\tau} + \frac{\vec{a}_i^{\tau} + \vec{a}_i^{\tau+1}}{2} \Delta t. \tag{4.2.15}$$

Evidently, (4.2.9) and (4.2.15) set the desired system (4.2.7).

The above-mentioned algorithm requires the calculation of acceleration.

According to Newton's 2nd law:

$$\vec{a}_i^{\tau} = -\frac{1}{m_i} \nabla \sum_{j \neq i} \varphi_{ij}. \tag{4.2.16}$$

In this equation, the force that affects the *i*th particle from the *j*th particle is written using the interaction potential φ_{ij} .

4.2.2 Interatomic Potential

As we already discussed, to calculate the force, one needs to define the potential φ . A common method is the LJ potential, which accurately describes the interaction between atoms in noble gases:

$$\varphi_{ij} = 4 \cdot \varepsilon \cdot \left[\left(\frac{\sigma}{r_{ij}} \right)^{12} - \left(\frac{\sigma}{r_{ij}} \right)^{6} \right],$$
(4.2.17)

where ε and σ are interaction parameters, which depend on the particle type; and $r_{ij} = |\vec{X}_i - \vec{X}_j|$ is the distance between the *i*th and *j*th particles.

The second term is in charge of atomic attraction as a result of the London dispersion force. The first term represents atomic repulsion at small distances due to exchange interaction. Figure 4.1 shows the LJ potential. Minimal energy corresponds to $r = \sigma \sqrt[6]{2}$, so at larger distances particles attract one another while at shorter distances they repel.

The interaction potential in the form of (4.2.17) is suitable for pure substances and, strictly, can be applied only for rare gases: Ar, Ne, etc. However, this relation can be applied to determine the interaction between different atoms. In this case we replace $\sigma \to \sigma_{ij}$ and $\varepsilon \to \varepsilon_{ij}$, i.e., we consider different parameters for different atoms: parameters for the interaction of i-j particles (e.g., Ar–Xe) are calculated according to the Lorentz–Berthelot rule (Lorentz 1881; Berthelot 1898):

Fig. 4.1 The Lennard–Jones potential

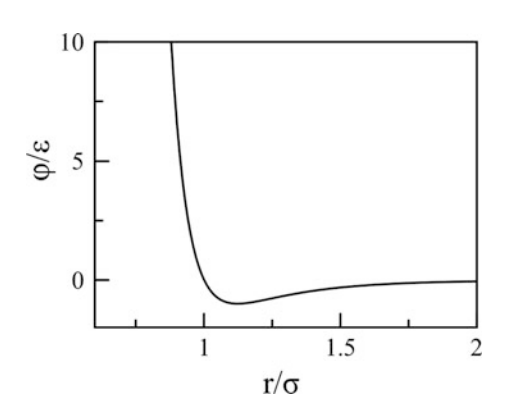


Table 4.1 Parameters of atoms in the simulation

Atom	m (kg) 10 ⁻²⁶	σ (Å)	ε (Κ)
Ar	6.633543	3.345	125.7
Cu	10.5521	2.33	3168.8
Xe	21.8018	4.568	225.3

$$\sigma_{ij} = \frac{\sigma_i + \sigma_j}{2},\tag{4.2.18}$$

$$\varepsilon_{ij} = \sqrt{\varepsilon_i \varepsilon_j}. \tag{4.2.19}$$

Moreover, this representation can be used for the interaction of various atoms—not only for noble gases. For instance, below we will consider the interaction of liquid Ar with a Cu solid surface (see Chap. 9).

Using the divergence of the LJ potential, the acceleration is defined as:

$$\vec{a}_{i}^{\tau+1} = \sum_{j \neq i} \frac{\varepsilon_{ij} \cdot \left(\vec{X}_{i}^{\tau+1} - \vec{X}_{j}^{\tau+1}\right)}{m_{i} \cdot \left(r_{ij}^{\tau+1}\right)^{2}} \left[48 \cdot \left(\frac{\sigma_{ij}}{r_{ij}^{\tau+1}}\right)^{12} - 24 \cdot \left(\frac{\sigma_{ij}}{r_{ij}^{\tau+1}}\right)^{6} \right]. \quad (4.2.20)$$

To complete the molecular dynamics method, one needs to specify the interaction parameters of potential, boundary and initial conditions.

In this simulation, we used atoms of three types: argon (White 1999), xenon (Whalley and Shneider 1955) and copper (Seyf and Zhang 2013). Interaction parameters are given in Table 4.1.

Note that these parameters are different in different reference works. For example, for Ar we have from White (1999): $\varepsilon = 119.8$ K and $\sigma = 0.3405$ nm.

As an alternative to the LJ potential, one may also use, for example, the Buckingham potential (it features exponents instead of terms raised to the power 12) (Buckingham 1938). The potentials of harmonic, torus and angular interactions are used to simulate polyatomic molecules (Morse 1929; Dau and Baskes 1984; Tersoff 1988). However, here we confine ourselves to considering simulations of monatomic substances.

4.2.3 Initial and Boundary Conditions

To calculate system (4.2.7), one needs to place particles in the computational region and set their velocities, i.e., set their initial conditions.

One should specify the type of system under consideration. If it is a solid body, then atoms are placed corresponding to the chosen lattice (e.g., the face-centered lattice). More complicated schemes are sometimes used: the properties of nanostructured surfaces were studied in Seyf and Zhang (2013), Diaz and Guo (2015) and Shavik et al. (2016) (surfaces with various macrostructures built upon them for heat

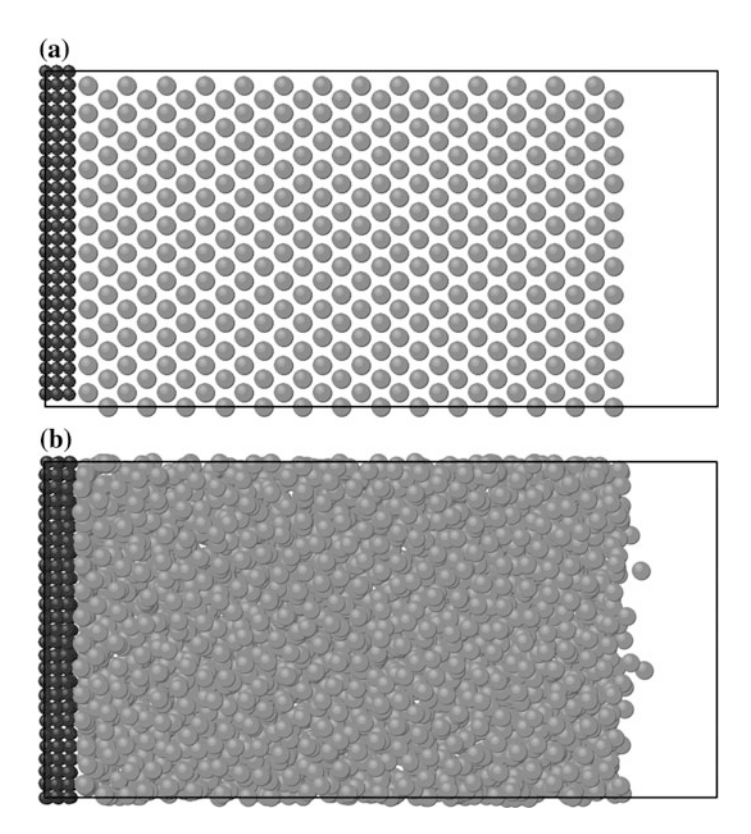


Fig. 4.2 a Initial positions (Cu atoms in face-centered cubic (FCC) lattice and Ar atoms in body-centered cubic (BCC) lattice). b 100 time steps later (crystal Cu and liquid Ar)

transfer enhancement). In liquid and vapor, atoms are not set in a regular structure and their position is rather chaotic. However, they should not be placed randomly—at least they should not be too close to each other. In fact, to form a liquid, atoms can be placed at lattice positions—the structure will be lost after hundreds of time steps if the initial velocities (i.e., temperature) are chosen properly (see Fig. 4.2).

As for velocities, their values should correspond to the chosen temperature. For N monoatomic molecules with mass m and at time step τ , the instant value of temperature can be calculated neglecting the average velocity (see Sect. 4.1):

$$T^{\tau} = \sum_{i} \frac{m \cdot \left(V_{i}^{\tau}\right)^{2}}{3 \cdot N}.$$
 (4.2.21)

In other words, the mean square velocity should be equal to 3 T/m. The simplest way to reach it is to set the velocity projections $\pm \sqrt{T/m}$ for each particle. Although this arrangement does not provide the Maxwellian distribution, the equilibrium distribution will be certainly settled this way. A more complicated method suggests

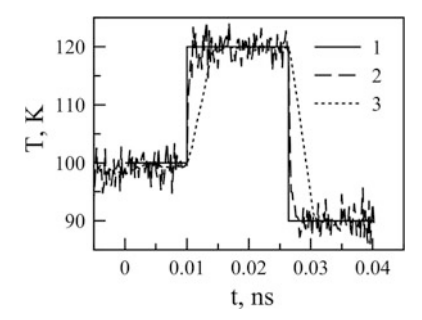


Fig. 4.3 Setting temperature by the velocity rescaling method; 1—predetermined temperature T^* ; 2—actual temperature T^* ; 3—mean temperature

generating a set of velocity projections that correspond to the Maxwell-Boltzmann distribution at a specified temperature.

Many problems require either to change or maintain temperatures in the computational region—and there are a lot of ways to perform this. Here we mention the easiest one, called the "velocity rescaling" method. Let us assume that at time step τ the temperature is equal to T^{τ} . Then, to set the temperature T^{*} , one should multiply all velocities by a $\sqrt{T^{*}/T^{\tau}}$ factor. Now, the temperature calculated according to (4.2.21) will be equal to T^{*} .

An example of the application of this algorithm is given in Fig. 4.3. The temperature is corrected every 20 time steps. The initial temperature is equal to 100 K, and is then set to $T^* = 120$ and 90 K.

Setting the boundary conditions and temperature is not enough to solve the problem—one should also select the computational region. A common computational region is represented by a parallelepiped (with face lengths $L_{x,y,z}$), with boundary conditions set at its faces.

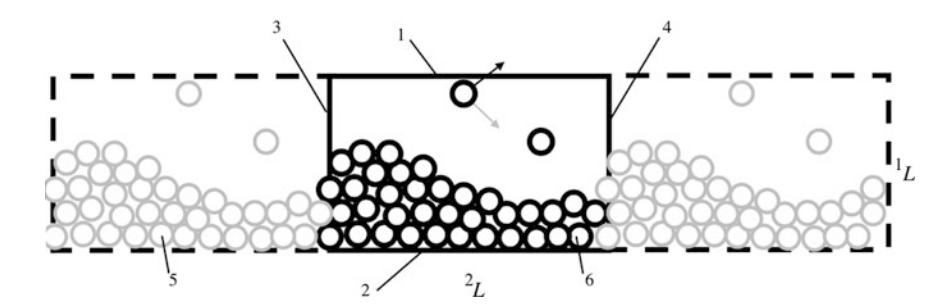


Fig. 4.4 Boundary conditions. 1, 2—side with reflection boundary conditions; 3, 4—side with periodic boundary conditions; 5—the "phantom" particle; 6—particle from the computational region

The reflection boundary condition is rather simple: when a particle reaches the side it bounces and changes its velocity vector. An example of a computational region that includes sides with reflection boundary conditions (with sides of length ^{2}L) and periodic boundary conditions (with sides of length ^{1}L) is given in Fig. 4.4.

Periodic boundary conditions ought to save (somehow) the situation with an insufficient number of particles. The molecular dynamics method allows one to simulate systems of thousands (and even millions) of particles, but in fact there are far more of them, as one cubic millimeter contains about 10^{16} molecules (not to mention liquid). To simulate a large/infinite volume (of gas or liquid), periodic boundary conditions are used (Xiong et al. 1996), that are represented by additional particles moving simultaneously with the main ones. The positions and velocities of these particles are known and do not need to be calculated, however, main particles interact with these additional ("phantom") particles too. In Fig. 4.4, periodic boundary conditions are set on two sides of the computational region.

Note that Fig. 4.4 represents a 2D projection of the computational region. Usually, periodic boundary conditions are also set on two further sides, so there are eight phantom computational regions.

In this case, the periodicity for the X coordinate is represented: a particle that crossed a side of the computational region comes to the other side (the coordinate of this particle shifts either by $\vec{P}_1 = (0, -^2L, 0)$ or by $\vec{P}_2 = (0, ^2L, 0)$, see Fig. 4.4). One also needs to take into account the interaction between the particles and boundaries that simulate periodicity. Each particle has copies shifted by \vec{P}_1 and \vec{P}_2 (phantom particles), the interaction with which is considered:

$$\vec{a}_{i}^{\tau+1} = \sum_{j \neq i} \frac{\varepsilon_{ij} \cdot \left(\vec{X}_{i}^{\tau+1} - \vec{X}_{j}^{\tau+1}\right)}{m_{i} \cdot \left(r_{ij}^{\tau+1}\right)^{2}} \left[48 \cdot \left(\frac{\sigma_{ij}}{r_{ij}^{\tau+1}}\right)^{12} - 24 \cdot \left(\frac{\sigma_{ij}}{r_{ij}^{\tau+1}}\right)^{6} \right]$$

$$+ \sum_{n} \sum_{j} \frac{\varepsilon_{ij} \cdot \left(\vec{X}_{i}^{\tau+1} - \vec{X}_{j}^{\tau+1} + \vec{P}_{n}\right)}{m_{i} \cdot \left(\vec{X}_{i}^{\tau+1} - \vec{X}_{j}^{\tau+1} + \vec{P}_{n}\right)^{2}}$$

$$\times \left[48 \cdot \left(\frac{\sigma_{ij}}{\left|\vec{X}_{i}^{\tau+1} - \vec{X}_{j}^{\tau+1} + \vec{P}_{n}\right|}\right)^{12} - 24 \cdot \left(\frac{\sigma_{ij}}{\left|\vec{X}_{i}^{\tau+1} - \vec{X}_{j}^{\tau+1} + \vec{P}_{n}\right|}\right)^{6} \right].$$

$$(4.2.22)$$

It is worth mentioning again the problem of the initial conditions: while placing particles, they should not be too close to each other. For periodic boundary conditions the distance between the real and "phantom" particles should be controlled.

4.2.4 Step-by-Step Guide for Simple Modeling

To perform MD calculations, one should select a substance (with parameters m, σ and ε for the LJ potential, for example). Based on this, the integration step is adjusted, which may be estimated as:

$$\Delta t = \frac{\sigma}{32} \sqrt{\frac{m}{48 \cdot \varepsilon}} \tag{4.2.23}$$

For argon, we have $\Delta t = 10$ fs. Examination of the energy conservation for the set integration step should be performed anyway.

Hereafter, the initial conditions must be set: the positions and velocities of all the particles. Consequently, the algorithm at $(\tau + 1)$ time step is:

•
$$\vec{X}_i^{\tau+1} = \vec{X}_i^{\tau} + \vec{V}_i^{\tau+1} \cdot \Delta t + \frac{1}{2} \cdot \vec{a}_i^{\tau} \cdot \Delta \tau^2$$
.

•
$$\vec{a}_i^{\tau+1} = \sum_{j \neq i} \frac{\varepsilon_{ij} \cdot (\vec{X}_i^{\tau+1} - \vec{X}_j^{\tau+1})}{m_i \cdot (r_{ij}^{\tau+1})^2} \left[48 \cdot \left(\frac{\sigma_{ij}}{r_{ij}^{\tau+1}} \right)^{12} - 24 \cdot \left(\frac{\sigma_{ij}}{r_{ij}^{\tau+1}} \right)^6 \right].$$

$$\bullet \quad \vec{V}_i^{\tau+1} = \vec{V}_i^{\tau} + \frac{\vec{a}_i^{\tau} + \vec{a}_i^{\tau+1}}{2} \Delta t.$$

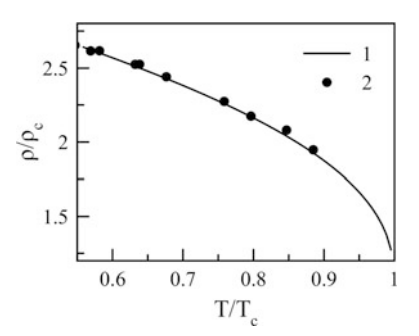
- Calculation of new boundary condition.
- Repetition for the next time step.

It is inconvenient to solve this system in dimensional form, because the characteristic times and distances are small (femtoseconds and angstroms) while velocities are large. For this reason, all the equations translate to the dimensionless form with corresponding scales:

- For coordinates— σ .
- For velocities— $\sigma/\Delta t$ or $\sqrt{\frac{48\varepsilon}{m}}$;
- For time— Δt or $\sigma \sqrt{\frac{m}{48s}}$.

At each time step, the macroscopic properties such as temperature, density, pressure, heat flux, etc., are calculated.

Fig. 4.5 Saturation liquid argon density: line—National Institute of Standards and Technology data; dots—results of molecular dynamics calculations



The algorithm is verified by performing an analysis of liquid density at the saturation line. Density is calculated for a system where liquid and vapor exist in equilibrium, using the mean kinetic energy (temperature) and number of atoms (density). A comparison of the calculated and reference density of argon is given in Fig. 4.5.

At each time step, one should calculate 3 N acceleration projections: in other words, calculate the expression under the sum in (4.2.22) about N^2 times. For 1 ns with step 10 fs, there will be 100,000 time steps. Let us assume that the system contains 1000 particles. Then, at each time step, the interaction between particles is evaluated about 1 million times, and for 1 ns this calculation repeats 100 billion times. The same calculation for 10,000 particles demands 100 times higher the number of operations. So, researchers always try to speed up the calculation process.

Using a cut-off radius seems to be the most effective way to do this, as it eliminates the quadratic dependence of computation complexity. A cut-off radius $(r_{\rm cut})$ is a distance where the interaction potential becomes zero and interaction with particles that are farther away is not taken into account. If there are n particles in the $r_{\rm cut}$ radius, one can use the linear dependence nN instead of the quadratic one. To apply this method, one should zero out the interaction potential at the $r_{\rm cut}$ distance, i.e.:

$$\varphi_{ij} = \begin{cases} 4 \cdot \varepsilon_{ij} \cdot \left[\left(\frac{\sigma_{ij}}{r_{ij}} \right)^{12} - \left(\frac{\sigma_{ij}}{r_{ij}} \right)^{6} \right] - 4 \cdot \varepsilon_{ij} \cdot \left[\left(\frac{\sigma_{ij}}{r_{\text{cut}}} \right)^{12} - \left(\frac{\sigma_{ij}}{r_{\text{cut}}} \right)^{6} \right], r \leq r_{\text{cut}} \\ 0, r_{ij} > r_{\text{cut}} \end{cases}$$

$$(4.2.24)$$

Cut-off radius values usually lie in the range from 2.5 σ to 6 σ . However, this method is rather specific: depending on the $r_{\rm cut}$, for the same ε and σ , properties of the system will differ (pressure, density, etc.) Also, since the vapor particles without any other particles in their vicinity are attracted by the liquid at a distance of about one nanometer anyway, the "cut-off radius method" should be used with caution.

4.3 Compute Unified Device Architecture

The problem mentioned above appears to be extremely time-consuming to solve, especially if the cut-off radius is not applied. Computational power of a device is usually measured in "flops" (floating-point operations per second) the number of which mostly depends on the clock frequency of the central processing unit (CPU), its size and architecture. In 2000s, the development of classic CPUs hit the ceiling: clock frequency reached a value of 3–4 GHz (without special coolers) and performance—about 10 Gflops. However, the industry managed to improve the performance by using multicore CPUs. Consequently, performance can be increased with parallel calculations. Although we initially mention the the CPU, it is the graphics processing unit (GPU) that shows the highest performance.

High demand for computer graphics encouraged the development of the GPU as a powerful multithreaded, multiprocessor computing device. The GPU was built for massively parallel computing in graphic rendering, so chips in it contain way more transistors than for data processing.

In the problem described in Sect. 4.2, at each time step the same set of operations is performed to calculate coordinates, velocities and accelerations for each particle. Besides this, to obtain these parameters for *i*th particle on the $(\tau +1)$ th time step, one does not need to know the coordinates of the rest of the particles on the $(\tau +1)$ th time step.

This means that at each time step, coordinates, velocities and accelerations for N particles can be calculated independently of one another—simultaneously and parallel. The advantage in time consumption is obvious: hypothetically, if N devices are employed, they complete the task N times faster. Let us recall that in molecular dynamics N amounts to thousands and millions. Of course, common GPUs are not capable of performing so many operations simultaneously, but even speeding up the process by 100 times is beneficial.

One of the technologies allowing the use of GPUs for performing calculations is known as CUDA (Compute Unified Device Architecture) and was developed by the NVIDIA Corporation for GPUs they produced in 2006.

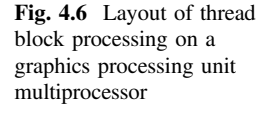
This section deals with CUDA, as it is the first and probably the most common architecture that speeds up MD calculations with GPUs and greatly simplifies handling them. Back in 2006 and 2007, Elsen (2006) published work where accelerated MD calculations using GPUs, using shader language, were performed. However, with the release of CUDA by NVIDIA in 2007, the use of GPUs became available to a wider audience, because the CUDA programming interface is based on a slightly modified C language.

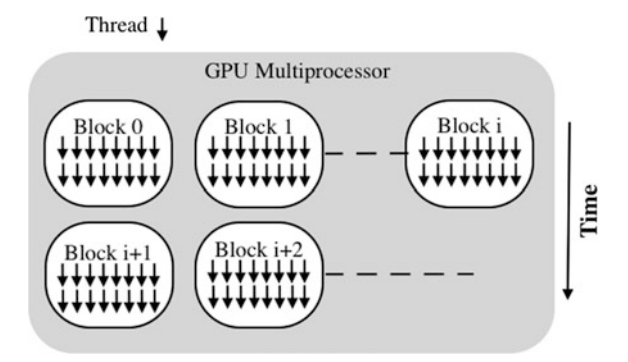
At the moment of writing this chapter, CUDA is used in programming languages such as C, C++, Fortran, Java, Python, Wrappers, DirectCompute and Directives. The capabilities of CUDA are embedded in such apps as MATLAB and Mathematica. All modern MMD programs use the GPU; particularly NAMD (NAnoscale Molecular Dynamics) (NAMD 2016), GROMACS (Groningen Machine for Chemical Simulations) (Abraham et al. 2015) and LAMMPS (Large-scale Atomic/Molecular Massively Parallel Simulator) (LAMMPS 2018) allow the use of CUDA technologies.

This section includes an overview of the possible ways one might use a GPU for the MMD. For a more detailed study, one should refer to the original guides (CUDA 2018). It should be noted that the NVIDIA company considered the problem of *N*-body simulation in 2008 (Mittring 2008).

The smallest sequence of programmed instructions in a program unit is called a thread. It usually means that threads are implemented in parallel, but actually this is not the case in every instance. Code that is performed in threads is called a kernel, which contains a set of instructions that are to be implemented in parallel, but with different data elements.

In CUDA, threads are combined in blocks. Threads in blocks are processed using warps. Actually, only warps are performed in a block simultaneously





(usually, the warp size is 32). Blocks, in turn, are combined into a grid. Blocks and grid sizing can be 1D, 2D or 3D. This multilevel structure is very convenient. While processing a thread, its address is defined—so, each thread corresponds to a particular data array.

Such an approach allows us to process huge data arrays in parallel (actually, a certain number of warps is processed). Also, data is not manually divided into pieces according to a certain GPU and number of processed elements. CUDA became widespread not only because of its interface, but also thanks to the scalable programming model. Actually, GPUs have different numbers of multiprocessors and are able to complete different data arrays. A multithreaded program is divided into blocks of threads that are performed independently from one another, thus the GPUs with more multiprocessors automatically run programs faster than GPUs with fewer multiprocessors.

All aforementioned terms (threads, blocks, warps and grids) refer to software. Blocks are processed on a streaming multiprocessor (that refers to a hard), each of which can process several blocks (Fig. 4.6).

To sum up, now we know how to speed up the calculation process using GPUs: one should create a kernel containing operations that are to be performed in parallel. In this case, the calculation of the accelerations for N particles seems to be the most time-consuming operation. To process N data sets, n threads for m blocks should be defined, so as $n \cdot m = N$ (generally $n \cdot m > N$).

A GPU works with its own memory: first, it is necessary to allocate the required amount of GPU memory. In our case, there are arrays of acceleration, velocities and coordinates. It hardly makes sense to generate initial conditions on a GPU, since it is a one-time definition that does not require large computational cost. So, when initial arrays are formed, they should be transferred to the GPU memory.

Next, the required parallel operations are performed on the GPU (in the so-called CUDA function). To process/save data, the results of the CUDA function calculation are transferred back to the CPU, i.e., the GPU data is copied to the CPU DRAM (Dynamic Random Access Memory).

Upon completion of the program, the GPU allocated memory is cleared.

The general calculation algorithm is:

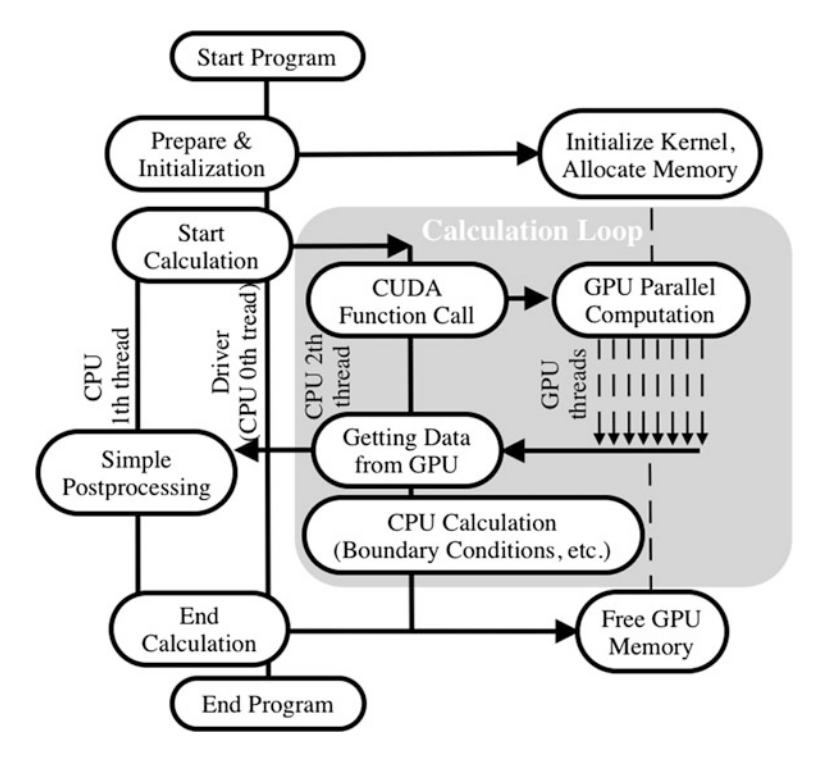


Fig. 4.7 Layout of the program structure. CUDA—compute unified device architecture; GPU—graphics processing unit; CPU—central processing unit

- To define the source data: to declare variables and pointers (for the source module and for the GPU); to initialize the required variables (including the initial condition).
- To allocate the place for the variables processed by the CUDA function, in the GPU memory.
- To configure and invoke the CUDA function.
- To copy the necessary data from the GPU memory.
- To clear the GPU memory.

Actually, when modeling molecular dynamics, it becomes necessary to analyze the results. This can be more laborious than the calculations themselves, e.g., the construction of the potential energy DF or calculation of the energy flux (which also requires calculating the energy value). Therefore, it is efficient to collect arrays of coordinates and velocities during the calculation. Then, in post-processing, it will be possible to calculate any interesting quantities and, if necessary, interrupt and resume the calculation.

Often there is a need to adjust the program (change the boundary conditions, temperature, etc.) during the execution, and not with a rigidly defined scenario. For such time-consuming calculations, any unnecessary recounting is an unattainable

luxury. Therefore, our code saves data on velocities and coordinates with a certain periodicity (which allows rolling back the calculation in the case of an error), and the main calculation is executed in parallel on the CPU and controlled by the driver. The layout of the program structure is provided in Fig. 4.7.

As for the acceleration achieved by the presented method, we should consider the ratio of the time spent on the same calculation on the same PC with and without using the GPU. In fact, this comparison makes clear whether it is expedient to use the GPU.

Most of the authors' calculations were performed on a monoblock PC with a relatively weak, mobile-grade GPU and a powerful multicore processor at the same time. Using a GPU on such a PC speeds up calculations by a dozen times. However, in comparison, for example, with a minimal MacBook Air (with a rather weak CPU) gives an acceleration of more than 20 times. In fact, as it was already mentioned, using the GPU not only speeds up the calculations, but also frees up the CPU (which can be used for post-processing).

The obtained results are neither record-setting nor indicative in terms of the potential of the video card. However, they show the expediency of using GPUs on ordinary PCs. For calculations that last about a day, the acceleration represents the difference between calculations done in a day and in a week.

It should be noted that in 2009 Open Computing Language (OpenCL) was introduced. It allows the user to create instructions not solely for use on GPUs produced by NVIDIA. Also, this language is supported by CUDA. The aforementioned parallel calculations on the MacBook were performed using OpenCL.

4.4 Conclusion

The MMD simulations is often referred to as the direct numerical simulation method, keeping in a mind that one may obtain a final answer to any question using the MMD. This is not true because:

- The interaction potential used in the MMD is a model correlation that neglects many nuances such as the influence of a third particle on the two-particle interaction, etc.
- The MMD increases short-range fluctuations.
- The MMD cannot take into account large-scale or long-time fluctuations.

However, the MMD is a very useful instrument for the analysis of local processes. When we do not require the exact quantitative calculations, but want to consider the physical nature of the given process, MD is a convenient and, actually, an indispensable instrument.

The most frequent question answered by the MMD is how many particles must be taken into account? The simplest answer: $\sqrt{N} \gg 1$, this condition follows from the requirement of negligible fluctuations and may be obtained in other ways. In other words, a number of particles approximating to 1000 is quite sufficient. Of

4.4 Conclusion 117

course, when you want to, for example, consider a bubble in a liquid, the number of particles must be correspondingly large, but this is a special case.

Anyway, we have to solve the system of the corresponding number of equations (specifically, 6 *N* equations in a 3D case). Moreover, we cannot use the simplest (explicit) scheme, and have to consider methods that are more complicated. Numerical simulations of even 1000 particles demands time-consuming calculations, so it is not superfluous to boost them somehow.

The most direct way to speed up the calculations is to parallelize them. Despite the fact that the MMD is not a very suitable object for program parallelism, we may organize simultaneous computations on several computing devices (note that even the summation of the series can be parallelized). The most evident devices for such calculations are CPUs, but we chose another way.

In our calculations, we used the CUDA technique: computations on graphics cards. For domestic conditions, this the most convenient way to boost the speed of calculations by an order or two.

The results of these computations will be presented in the Chaps. 5–9.

References

M.J. Abraham, D. Spoel, E. Lindahl, B. Hess, The GROMACS Development Team, in *User manual* (2015). www.gromacs.org

B.J. Alder, T.E. Wainwright, J. Chem. Phys. 27, 1208 (1957)

B.J. Alder, T.E. Wainwright, J. Chem. Phys. 31, 459 (1959)

D. Berthelot, Comptes rendus hebdomadaires des séances de l'Académie des Sciences 126, 1703 (1898)

R.A. Buckingham, Proc. R. Soc. London A 168, 264 (1938)

M.S. Dau, M.I. Baskes, Phys. Rev. B 29, 6443 (1984)

R. Diaz, Z. Guo, in Proceedings of CHT-15, 033 (2015)

E. Elsen, M. Houston, V. Vishal, E. Darve, P. Hanrahan, V. Pande, in *Proceedings of the 2006 ACM/IEEE Conference on Supercomputing* (2006)

J.E. Jones, Proc. R. Soc. A 106, 463

C. Kittel, Introduction to Solid State Physics. (Wiley, New York, 2005)

LAMMPS Documentation (2018). http://lammps.sandia.gov/doc/Manual.html

L. D. Landau, E. M. Lifshitz, Mechanics (Volume 1 of Course of Theoretical Physics) (1960)

H.A. Lorentz, Ann. Phys. 248, 127 (1881)

M. Mittring, in The GPU Gems series features a collection of the most essential algorithms required by next-generation 3D engines (2008). https://developer.nvidia.com/gpugems/ GPUGems/gpugems_pref01.html

P.M. Morse, Phys. Rev. 34, 57 (1929)

NAMD, in NAMD user's guide (2016). http://www.ks.uiuc.edu/Research/namd/

NVIDIA, in CUDA C programming guide (2018). www.nvidia.com

T. Ohara, J. Chem. Phys. 111, 9667 (1999)

A. Rahman. Phys. Rev. 136A, 405

H.R. Seyf, Y. Zhang, J. Heat Trans. 135, 121503 (2013)

S.M. Shavik, M.N. Hasan, A.K.M.M. Morshed, J. Electron. Packag. 138, 010904 (2016)

YuS Sigov, Computational Experiment: The Bridge Between the Past and the Future of Plasma Physics (Nauka, Moscow, 2001)

R.D. Skeel, BIT Numer. Math. 33, 172 (1993)

W.C. Swope, H.C. Andersen, P.H. Berens, K.R. Wilson, J. Chem. Phys. 76, 637 (1982)

- M. Tabor, Chaos and Integrability in Nonlinear Dynamics (Wiley, New York, 1989)
- J. Tersoff, Phys. Rev. B 37, 6991 (1988)
- L. Verlet, Phys. Rev. 159, 98 (1967)
- E. Whalley, W.G. Schneider, J. Chem. Phys. 23, 1644 (1955)
- J.A. White, J. Chem. Phys. 111, 9352 (1999)
- D.X. Xiong, Y.S. Xu, Z.Y. Guo, J. Therm. Sci. 5, 196 (1996)

Recommended Literatures

- S.I. Anisimov, D.O. Dunikov, V.V. Zhakhovski, S.P. Malyshenko, J. Chem. Phys. 110, 8722 (1999)
- A. Arkundato, Z. Su'ud, M. Abdullah, W. Sutrisno. Turkish J. Phys. 37, 132
- H.J.C. Berendsen, J.P.M. Postma, W.F. Gunsteren, A. DiNola, J.R. Haak, J. Chem. Phys. 81, 3684 (1984)
- P.H. Berens, K.R. Wilson, J. Chem. Phys. 76, 637 (1982)
- F. Calvo, F. Berthias, L. Feketeova, H. Adboul-Carime, B. Farizon, M. Farizon, Europ. Phys. J. D 71, 110 (2017)
- B. Cao, J. Xie, S.S. Sazhin, J. Chem. Phys. 134, 164309 (2011)
- F. Chen, B.J. Hanson, M.A. Pasquinelli, AIMS Mater. Sci. 1, 121 (2014)
- S. Cheng, G.S. Grest, J. Chem. Phys. 138, 064701 (2013)
- R. Diaz, Z. Guo, Int. J. Comput. Method. 72, 891 (2017)
- Y. Dou, L.V. Zhigilei, N. Winograd, B.J. Garrison, J. Phys. Chem. A 105, 2748 (2001)
- D.O. Dunikov, S.P. Malyshenko, V.V. Zhakhovskii, J. Chem. Phys. 115, 6623 (2001)
- A. Frezzotti, AIP Conf. Proc. 1333, 161 (2011)
- T. Fu, Y. Mao, Y. Tang, Y. Zhang, W. Yuan, Nanoscale Microscale Thermophys. Eng. 19(1), 17 (2015)
- T. Fu, Y. Mao, Y. Tang, Y. Zhang, W. Yuan, Heat Mass Transfer 52, 1469 (2016)
- J.B. Gibson, A.N. Goland, M. Milgram, G.H. Vineyard, Phys. Rev. 120, 1229 (1960)
- K. Gu, C.B. Watkins, J. Koplik, Phys. Fluids 22, 112002 (2010)
- J. Guobin, L. Yuanyuan, Y. Bin, L. Dachun, Rare Met. 29, 323 (2010)
- H.Y. Hou, G.L. Chen, G. Chen, Y.L. Shao, Comput. Mater. Sci. 46, 516 (2009)
- T. Ishiyama, T. Yano, S. Fujikawa, Phys. Fluids **16**, 2899 (2004)
- E.K. Iskrenova, S.S. Patnaik, Int. J. Heat Mass Transfer 115, 474 (2017)
- Khronos Group, in OpenCL 1.1 quick reference (2015)
- K. Kobayashi, K. Hori, M. Kon, K. Sasaki, M. Watanabe, Heat Mass Transfer 52, 1851 (2016)
- K. Kobayashi, K. Sasaki, M. Kon, H. Fujii, M. Watanabe, Microfluid. Nanofluid. 21, 23 (2017)
- M. Kon, K. Kobayashi, M. Watanabe, AIP Conf. Proc. 1786, 110001 (2016)
- A.P. Kryukov, VYu. Levashov, Heat Mass Transfer 52, 1393 (2016)
- A.P. Kryukov, VYu. Levashov, N.V. Pavlyukevich, J. Eng. Thermophys. 87, 237 (2014)
- AYu. Kuksin, G.E. Norman, V.V. Pisarev, V.V. Stegailov, A.V. Yanilkin, Hight Temp. 48, 511 (2010)
- AYu. Kuksin, G.E. Norman, V.V. Stegailov, High Temp. 45, 37 (2007)
- L. Li, J. Pengdei, Y. Zhang, Appl. Phys. A 122, 496 (2016)
- L.N. Long, M.M. Micci, B.C. Wong, Comput. Phys. Commun. 96, 167 (1996)
- A. Lotfi, J. Vrabec, J. Fischer, Int. J. Heat Mass Transf. 73, 303 (2014)
- P. Louden, R. Schoenborn, C.P. Lawrence, Fluid Phase Equilib. 349, 83 (2013)
- M. Matsumoto, Fluid Phase Equilib. 144, 307 (1998)
- R. Meland, A. Frezzotti, T. Ytrehus, B. Hafskjold, Phys. Fluids 16, 223 (2004)
- I.V. Morozov, G.E. Norman, A.A. Smyslov, High Temp. 46, 768 (2008)
- G. Nagayama, M. Takematsu, H. Mizuguchi, T. Tsuruta, J. Chem. Phys. 143, 014706 (2015)
- Z. Ru-Zeng, Y. Hong, Chin. Phys. B 20, 016801 (2011)
- D. Sergi, G. Scocchi, A. Ortona, Fluid Phase Equilib. 332, 173 (2012)

Recommended Literatures 119

- B. Shi, S. Sinha, V.K. Dhir, J. Chem. Phys. 124, 204715 (2006)
- W.B. Streett, D.J. Tildesley, G. Saville, Mol. Phys. 35, 639 (1978)
- T. Tokumasu, T. Ohara, K. Kamijo, J. Chem. Phys. 118, 3677 (2003)
- T. Tsuruta, G. Nagayama, J. Phys. Chem. B 108, 1736 (2004)
- T. Tsuruta, H. Tanaka, T. Masuoka, Int. J. Heat Mass Transf. 42, 4107 (1999)
- M.E. Tuckerman, B.J. Berne, G.J. Martyna, J. Chem. Phys. 94, 6811 (1991)
- P. Varilly, D. Chandler, J. Phys. Chem. B 117, 1419 (2013)
- J. Vrabec, J. Stoll, H. Hasse, Mol. Simul. 31, 215 (2005)
- J. Wang, T. Hou, J. Chem. Theory Comput. 7, 2151 (2011)
- W. Wang, H. Zhang, C. Tian, X. Meng, Nanoscale Res. Lett. 10, 158 (2015)
- T. Werder, J.H. Walther, R.L. Jaffe, T. Halicioglu, F. Noca, P. Koumoutsakos, Nano Lett. 1, 697 (2001)
- J. Xie, S.S. Sazhin, B. Cao, J. Therm. Sci. Technol. 7, 288 (2012)
- K. Yasuoka, M. Matsumoto, Y. Kataoka. J. Mol. Liquids 65/66, 329 (1995)
- K. Yasuoka, M. Matsumoto, Y. Kataoka, J. Chem. Phys. 101, 7904 (1994)
- J. Yu, H. Wang, Int. J. Heat Mass Transf. 55, 1218 (2012)
- V.V. Zhakhovskii, S.I. Anisimov, J. Exp. Theor. Phys. 84, 734 (1997)
- S. Zhang, F. Hao, H. Chen, W. Yuan, Y. Tang, X. Chen, Appl. Therm. Eng. 113, 208 (2017)

Chapter 5 Velocity Distribution Function of Evaporated Atoms



Some scientists perceive all situations around the distribution function (DF) of evaporated particles as a sort of gamble; the title of the article by Knox and Phillips (1998) is eloquent: *Maxwell versus non-Maxwell Velocity Distributions for Molecules Emitted from a Liquid Surface*. We may admit that this fight continues to this day.

5.1 The Maxwellian Distribution Function?

5.1.1 Our Expectations

Due to the specific structure of human mind we always expect familiar things to happen even when we are facing absolutely new matters. We prefer to use standard physical descriptions for investigated objects and we invent many circumstances to keep this situation as it is.

Probably, the most dramatic illustration took place in 1899–1900 when the black body spectrum was studied. In the previous decade (during the 1890s) it had been "firmly" proven that Wien's law was absolutely correct—because, as we now know, only a range of sufficiently high values of quantity hv/T had been treated in experiments. Max Planck was assured that Wien's law was absolutely correct and aimed his theory in this direction; actually, Planck wanted to explain the irreversibility of the fundament of electromagnetic field theory. His first work, published in the beginning of 1900, contains the phrase that "the area of application of the [Wien] law coincides with the area of application of the second law of thermodynamics" (see end of §23 in this work). And this confusion took place not only in theory. As it became known later, experimental investigations in 1899 (e.g., by Lummer and Pringsheim) showed clearly that Wien's law did not describe experimental data for sufficiently large T, i.e., for relatively low hv/T. Only in March of

1900 were the first observations of the deviation from Wien's law officially reported.

Max Planck applied tremendous force to correct his mistake; no less than a new scientific area—quantum mechanics—arose from his subsequent work. However, the moral of the story is clear: an open mind is always needed.

The Maxwellian distribution function (MDF) has become almost a synonym for the term "equilibrium state." We expect the MDF to be everywhere, at least to be bundled in with the equilibrium state; in non-equilibrium, we expect a shifted MDF. Usually, there are no serious discussions precluding the choice of the MDF for any problem. We have an equilibrium state for liquid—oh, yes, we may use a Maxwellian there.

Of course, it is peculiar for anyone to doubt. Proofs are needed always and everywhere, especially for obvious things (at least in physics). The proofs were sought, and evidence was not obtained. Thus, the story begins.

5.1.2 Experimental Results

It is not easy to determine the DF of velocity (or of kinetic energy) experimentally. In fact, to find such a function by measuring is a very hard job. The usual experimental method—the so-called time-of-flight method (TOF), where we actually use time (that was spent to reach a detector) instead of velocity, must exclude any interaction of evaporated molecules with a gas, otherwise all the measurements lose their value.

As we know, the first work where the DF of evaporated atoms was treated, was in the article written by Otto Stern in 1920. To be precise, there were two papers: the first paper with experimental results, and the second one with discussions about them (in polemics with Einstein, by the way). In these experiments, the evaporation of silver wire was treated and agreement with the MDF was obtained; in many works from the middle of the Twentieth century these results were referred to if necessary as an experimental confirmation of the MDF. As an example, take a look at an excellent review by Knake and Stranskii (1959), where the question about the MDF arises several times only to be faded out (with a positive answer).

Many works were devoted to the DF in sorption/desorption processes. This problem has some relation to evaporation, however, it is hardly possible to transfer results obtained for desorption directly to evaporation, due to differences in types of intermolecular forces in these cases.

Possibly, the first experimental report regarding the non-MDF for desorbed molecules was by Dabirli et al. (1971); the desorption of D_2 molecules from a nickel polycrystalline surface was investigated with the TOF method. While the temperature of the surface was 1073 K, the observed spectrum corresponded to a shift-Maxwellian with a temperature of ~ 1500 K.

In Cardillo et al. (1975), for desorbing atoms of H_2 from a nickel surface, a non-MDF, skewed to a high-velocity range, was obtained. The same results—an increasing number of high-energy particles—were later observed in Matsushima (2003).

However, everything is not that clear (of course). In Hurst et al. (1985) the obtained DF was not the MDF, but was shifted toward a low-energy range, as were the results of Rettner et al. (1989). In both cases the desorption of argon was investigated, from platinum and tungsten, correspondingly.

We recommend the paper by Comsa and David (1985) for those who want to delve more deeply into experimental problems—both methodological and technical; this work also contains a wide discussion concerning the non-MDF for desorbed particles.

In Hahn et al. (2016) the evaporation of rare gases from water was treated. There were reports about the MDF in the case of the evaporation of argon and about "super-Maxwellian" evaporation of helium both from fresh and saline water.

Finally, we refer the reader to an important result for the DF of evaporated molecules of the same substance (Faubel et al. 1988; Faubel and Kisters 1989). In the first of these works an agreement with the shifted MDF was obtained:

$$f \sim v^2 \exp\left(-\frac{m(v-V)^2}{2T}\right).$$
 (5.1.1)

For water evaporation, it was determined that $T=210\,\mathrm{K}$ —the lowest temperature that has been observed ever for a liquid surface. It is also interesting that DFs measured at different distances from the surface (at 4 and 8 mm) were quite different. Note that the authors admit that a collision-free regime was not achieved; evidently, it is the only reason for different DFs at different distances.

In the next work (Faubel and Kisters 1989) the authors reported a double result. The MDF was observed for monomers of carboxylic acid, but a non-MDF observed for dimers.

In fine, M. Faubel and T. Kisters concluded that "it would be interesting to investigate these phenomena further with realistic molecular-dynamics simulation." Let us follow this advice.

5.1.3 Numerical Simulation Results

Today we have a big database of numerical simulation results. Contrary to natural experiments, numerical simulations allow us to obtain clearer results for such a complicated problem as a DF.

While experimental data can be divided into two sets—Maxwellian or non-Maxwellian—the results of numerical simulations can be divided also into two groups, but based on another DF.

The DF:

$$f(v) = \frac{mv}{T} \exp\left(-\frac{mv^2}{2T}\right) \tag{5.1.2}$$

is often used to describe the results of numerical simulations. The most recent paper where this function was used was Kobayashi et al. (2017). A DF of the same kind was also obtained by Tsuruta and Nagayama (2004), Cheng et al. (2011), Frezzotti (2011) and especially—Varilly and Chandler (2012), and the DF has been (almost) obtained analytically by Kon et al. (2016) and Kobayashi et al. (2016). We will not represent DF (5.1.2) here, because we will treat this function in the next section in detail.

However, in other works DFs of different forms have been obtained. Below we present results from Ishiyama et al. (2004) and Lotfi et al. (2014); see Figs. 5.1 and 5.2, correspondingly.

To these works we may add Meland et al. (2004), Kryukov and Levashov (2011) and Xie et al. (2012) where various DFs for evaporation were obtained.

Analyzing all these results, it is important to understand in what nearby region of a liquid surface this velocity DF has been constructed. Unfortunately, not all articles contain this information. In Zhakhovskii and Anisimov (1997) DFs in various liquid layers were calculated; we provide the same operation with the same results

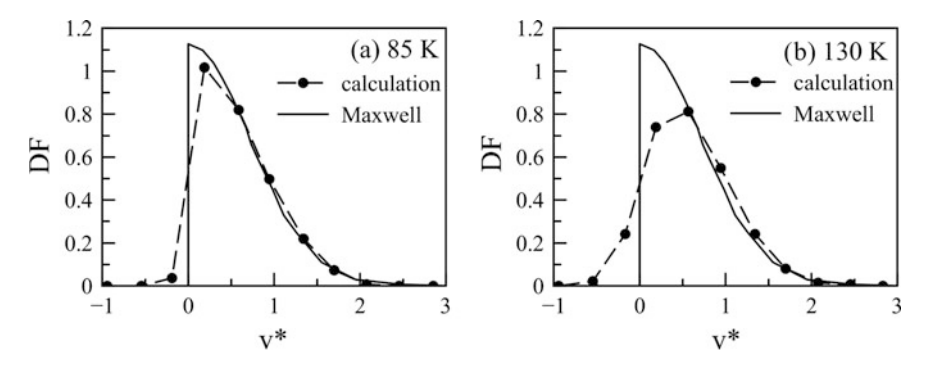


Fig. 5.1 Distribution functions from Ishiyama et al. (2004). DF-distribution function

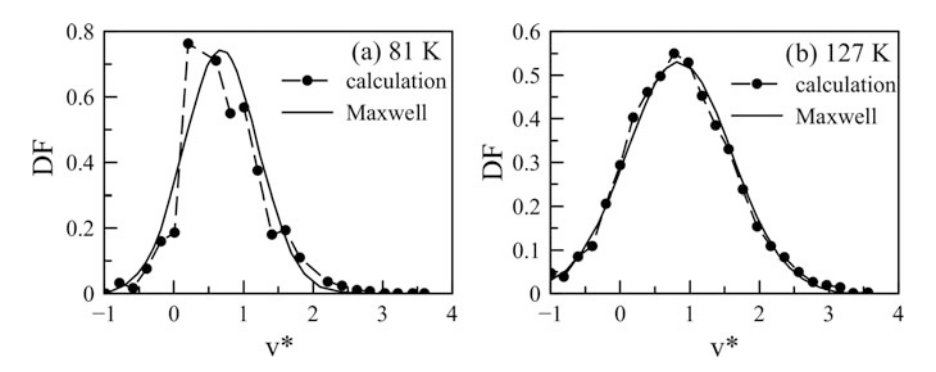
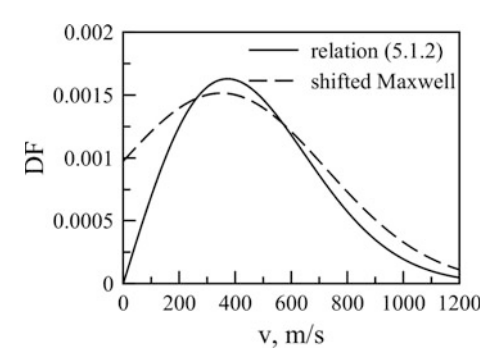


Fig. 5.2 Distribution functions from Lotfi et al. (2014). DF—distribution function

Fig. 5.3 Distribution (5.1.2) versus the shifted Maxwellian distribution function. DF—distribution function



in the next section. Here we may briefly conclude that DFs in a liquid are Maxwellian, but this function is being strongly distorted if we include a region of a gas, i.e., of the evaporated molecules themselves. Thus, it is logical to remove all the liquid particles from the consideration, however, sometimes it is hard to say whether the authors of the given paper have performed this operation or not.

In fine, we want to compare function (5.1.1), which is a popular function in analytical solutions, and function (5.1.2) (see Fig. 5.3).

This figure gives us a lot of food for thought, especially if we take inevitable errors of calculations into account. There is a good chance to confuse these two. Thereby, we have to move on from the question that was asked in the beginning of this section and restate it in a more solid form. We asked a shrewd question "What DF is observed in experiments (natural or numerical)?" As we can see, different answers are possible.

But this is absolutely the wrong approach.

We need an answer to the question "What is the DF for evaporated particles?" We need a theory here. Not some speculation or reasoning, we need a strict derivation. Only in that case we can surely define which function is correct—(5.1.1) or (5.1.2). Or, possibly, a third option.

5.2 Theoretical Calculation of the Distribution Function

5.2.1 The Simplest Form of Velocity Distribution Function

It is hard to name the author who addressed the most direct approach to the problem of evaporation, where the work function U of the evaporated atom was considered for the first time. Possibly, it was Jakov Frenkel who introduced U for evaporated atoms in his fundamental book *Kinetic Theory of Liquids*. However, the idea looks rather evident.

Let us consider a DF in an evaporating liquid. If we assume an equilibrium state, then we may expect that the MDF can be applied:

$$f(v) = \sqrt{\frac{m}{2\pi T}} \exp\left(-\frac{mv^2}{2T}\right). \tag{5.2.1}$$

There is no doubt that this function is correct for the bulk of the liquid. But by applying (5.2.1) for an evaporation problem, we assume that the atoms at the surface obey Maxwellian law too; this assumption is merely brave and, strictly, demands a proof. One can identify two problems concerning the application of (5.2.1) for a liquid surface:

- 1. Due to the evaporation, atoms with high kinetic energy leave the liquid, so the temperature of a liquid tends to decrease; the deficit of fast atoms repairs because of the energy drift from the dipper layer of a liquid. In the common case, we can say that the temperature of the surface is lower than the temperature of the bulk of the liquid; one question to address is "by how much?" Thus, the parameter *T* from (5.2.1) is (somewhat) undefined.
- 2. The influence of evaporation on a DF is not restricted by the uncertainty of *T*. In the general case, because of evaporation, a liquid can be far out of equilibrium state, and all arguments from Chap. 2 in favor of the Maxwellian may be eliminated in such a case. Thus, even the form of a DF of velocity may be undefined.

Both problems are serious and it is very difficult to provide any certain answers. However, we may partly overcome function (5.2.1) in both objections:

- 1. The temperature of the surface differs from the bulk temperature indeed (see Chaps. 6 and 8). However, the temperature of the liquid surface may actually be an external parameter defined by experimental data.
- 2. Liquid is a condensed matter. There are many collisions between atoms of liquid at the surface layer, thus, we can expect that equilibrium conditions will be stated. As for the escaping high-energy particles, one may hope that for an intermediate evaporation rate the "high-energy tail" of the DF will recover rapidly due to the collisions between atoms. The bulk of a liquid transfers energy to its surface, thus, at least a stationary state can be achieved at the interface.

However, this consideration is not a proof, it is only an eventual explanation. Below we will use the MDF for a liquid surface—the first thing that will be checked in the next section (with results from a computer simulation) is the DF for atoms in the liquid.

Thus, we have (by agreement) that the DF of liquid atoms is Maxwellian. The next point to consider—or, in fact, that Frenkel considered—is the fact that to leave a surface an atom of a liquid must overcome the binding energy that holds it inside a liquid. If a particle leaves a surface in the direction of the z axis (axes x and y are tangential to the liquid's surface), then the positive binding energy U (or the negative potential energy u = -U) will lead to a decrease in the normal projection

of velocity (i.e., of the v_z). Formally, the total energy of a particle before (we denote corresponding quantities with an prime) and after a detachment is:

$$\frac{mv_x'^2}{2} + \frac{mv_y'^2}{2} + \frac{mv_z'^2}{2} - U = \frac{mv_x^2}{2} + \frac{mv_y^2}{2} + \frac{mv_z^2}{2}.$$
 (5.2.2)

Because of the absence of forces in directions x and y the corresponding projections of velocity stay the same: $v'_x = v_x$ and $v'_y = v_y$, and we have to deal only with the normal projection of velocity. For this reason, in this subsection we omit index "z" for velocity.

We are interested in the DF of evaporated atoms, i.e., of atoms which lose their kinetic energy on value U; with (5.2.2) we have a relationship between velocities before and after evaporation:

$$v' = \sqrt{v^2 + \frac{2U}{m}}. (5.2.3)$$

Thus, under an "evaporated atom" we mean an atom which becomes absolutely free, i.e., its potential energy is equal to zero. Thereby, we find the DF of velocities on the evaporation surface not directly on the very interface, because the atom is bound with other particles there; we construct our DF at some distance from the evaporation surface (~ 1 nm) where atoms unbound from their neighbors (see Fig. 3.3). All this consideration may look obvious, of course. Considering the fact that usually the DF is needed as a boundary condition for a kinetic equation, we may depict that if someone wants to use the MDF in a liquid (5.2.1) as this boundary condition, then one must solve not a Boltzmann kinetic equation (consisting of a hyperbolic differential operator in the left-hand part of the equation and a collision integral in the right-hand part), but a kinetic equation with a self-consisted field, or with a collision integral and an external field, etc.: somehow, one must consider the potential forces influencing the particles.

Further we will use velocity v_0 which is defined from the equality $U = \frac{mv_0'}{2}$. Then, for the DF f(v) we must reconstruct the MDF for atoms in a liquid, remembering that $dv \neq dv'$:

$$f(v) = f(v')\frac{dv'}{dv} = f(v')\frac{v}{\sqrt{v^2 + v_0^2}}.$$
 (5.2.4)

So, we must replace v' with v in (5.2.1) and (5.2.2), and then the DF of the velocity of evaporated atoms will be obtained in accordance with (5.2.4). We have:

$$f(v)dv = A \frac{v}{\sqrt{v^2 + v_0^2}} \exp\left(-\frac{mv^2}{2T}\right) \exp\left(-\frac{mv_0^2}{2T}\right) dv,$$
 (5.2.5)

where factor A provides normalization $\int_0^\infty f(v) dv = 1$:

$$A = \sqrt{\frac{2m}{T}} \frac{1}{\Gamma(\frac{1}{2}, \frac{mv_0^2}{2T})}.$$
 (5.2.6)

We emphasize that our DF (5.2.5) is defined for $v \in [0, \infty]$; this is the reason for normalization being in the form \int_0^∞ rather than $\int_{-\infty}^\infty$.

The function (5.2.5) can be simplified. Suppose that the work function is huge, that is, $U \gg T$ and $v_0 \gg v$ in all intervals of significant v, i.e., where $v \sim \sqrt{T/m}$. In such conditions we get a simple and convenient expression instead of (5.2.5):

$$f(v) = \frac{mv}{\bar{\epsilon}} \exp\left(-\frac{mv^2}{2\bar{\epsilon}}\right),\tag{5.2.7}$$

with the mean kinetic energy $\bar{\epsilon}$ of an atom in a vapor phase (i.e., after evaporation) that can be obtained from the balance of energy (5.2.3). Of course, one may see directly from the expression (5.2.5) that $\bar{\epsilon} = T$, but, keeping in the mind the next sections, we should point out that this equation also follows from (5.2.3) in the general case after the averaging procedure:

$$\bar{\varepsilon} = \frac{\overline{mv^2}}{2} = \frac{\overline{mv'^2}}{2} - U. \tag{5.2.8}$$

Note that to calculate $\frac{\overline{mv^2}}{2}$ we must take into account only $v' > v_0$, because only these particles may be detached, and change the normalized factor to consider only the particles that are of interest. Thus, the mean kinetic energy of all the particles in liquid with v > 0 is:

$$\frac{\int_0^\infty \frac{mv'^2}{2} e^{-\frac{mv'^2}{2}} dv'}{\int_0^\infty e^{-\frac{mv'^2}{2}} dv'} = \frac{T}{2},$$
(5.2.9)

while only for detached particles their averaged kinetic energy is:

$$\frac{\overline{mv'^2}}{2} = \frac{\int_{v_0}^{\infty} \frac{mv'^2}{2} e^{-\frac{mv'^2}{2T}} dv'}{\int_{v_0}^{\infty} e^{-\frac{mv'^2}{2T}} dv'} = T \frac{\Gamma(\frac{3}{2}, \frac{U}{T})}{\Gamma(\frac{1}{2}, \frac{U}{T})}.$$
 (5.2.10)

For $U/T \gg 1$ we have (see Appendix B):

$$\Gamma\left(\frac{3}{2}, \frac{U}{T}\right) \approx \sqrt{\frac{U}{T}} \left(1 + \frac{T}{2U}\right) e^{-U/T},$$
 (5.2.11)

$$\Gamma\left(\frac{1}{2}, \frac{U}{T}\right) \approx \sqrt{\frac{T}{U}} \left(1 - \frac{T}{2U}\right) e^{-U/T},$$
 (5.2.12)

so, for the mean kinetic energy of evaporated particles we have:

$$\bar{\varepsilon} = \lim_{U/T \to \infty} T \left[\frac{\Gamma(\frac{3}{2}, \frac{U}{T})}{\Gamma(\frac{1}{2}, \frac{U}{T})} - \frac{U}{T} \right] = T.$$
 (5.2.13)

Thus, the mean kinetic energy that corresponds to the z projection of the velocity of the detached particles is the temperature of the liquid T, while the average kinetic energy corresponding to all Maxwellian-distributed particles is T/2. One may note that the escaped particles (i.e., the tail of the MDF for $v > v_0$) have the average kinetic energy U + T in a liquid.

In fine, we can rewrite the DF for the velocity of atoms after evaporation as:

$$f(v) = \frac{mv}{T} \exp\left(-\frac{mv^2}{2T}\right). \tag{5.2.14}$$

This DF for vapor particles is a non-equilibrium DF. Here the parameter T is not the temperature of these particles but the temperature of the liquid which emitted these vapor particles.

From some points of view, the DF (5.2.14) is very interesting: it contains some confusing issues. This function coincides with a well-known DF—the MDF function for absolute velocity in a 2D case. In our case we have $\bar{\epsilon} = T$ in (5.2.14) for the mean flux energy: the so-called mean value for the quantity Q(v) is calculated as:

$$\overline{Q} = \frac{1}{\{j = m\overline{v}\}} \int_{0}^{\infty} Q(v) mv f(v) dv.$$
 (5.2.15)

For $Q(v) = \frac{mv^2}{2}$ and the MDF f(v) we get $\bar{\varepsilon} = T$.

However, of course, this is only a confusing coincidence. The function (5.2.14) describes the distribution of velocities in a 1D case. The mean kinetic energy $\bar{\epsilon}$ was calculated based on the number density DF, not on the flux DF with (5.2.15). And, certainly, $\bar{\epsilon}$ represents the mean energy for a single translational degree of freedom: due to its value, it may be confused with the mean energy for the vibrational degree of freedom. Any resemblances are random and should not be processed further.

As already obtained, the DF for the normal velocity can be described by the simple relation (5.2.14) if $U \gg T$. Practically, "much larger" here means that U must be several times larger than T. In Fig. 5.4 the DFs (5.2.5) for various ratios of U/T are presented: from U/T=0, which corresponds to the MDF, to $U/T\to\infty$ with function (5.2.14).

5.2.2 Probability of Evaporation

The probability of evaporation can be calculated for the MDF of atoms in a liquid. To leave the surface, an atom must have a kinetic energy higher than its binding

energy U, or a longitude velocity higher than v_0 . Thus, the total number of such atoms is:

$$N = N_0 \int_{v_0}^{\infty} \sqrt{\frac{m}{2\pi T}} \exp\left(-\frac{mv^2}{2T}\right) dv, \qquad (5.2.16)$$

where N_0 is the total number of atoms with any velocity: $-\infty < v < \infty$. Defining probability as $w = N/N_0$, we get:

$$w = \frac{1}{2\sqrt{\pi}} \Gamma\left(\frac{1}{2}, \frac{U}{T}\right). \tag{5.2.17}$$

Obviously, if the work function vanishes $\frac{U}{T} = 0$ then $w = \frac{1}{2}$: one half of the particles—which have velocities towards a vapor phase—would leave the surface, in this case we also have the MDF for evaporated atoms. However, we always have U > 0, thus, the DF of evaporated particles has the property f(0) = 0, i.e., there are no particles with zero velocity in the evaporation flux (however, see Sect. 5.2.5).

5.2.3 Distribution of Tangential Velocities

After detachment from the surface, particles hold their tangential components of velocities, that is, axes x and y DFs for velocities v_x and v_y stay the same as in the liquid (MDF):

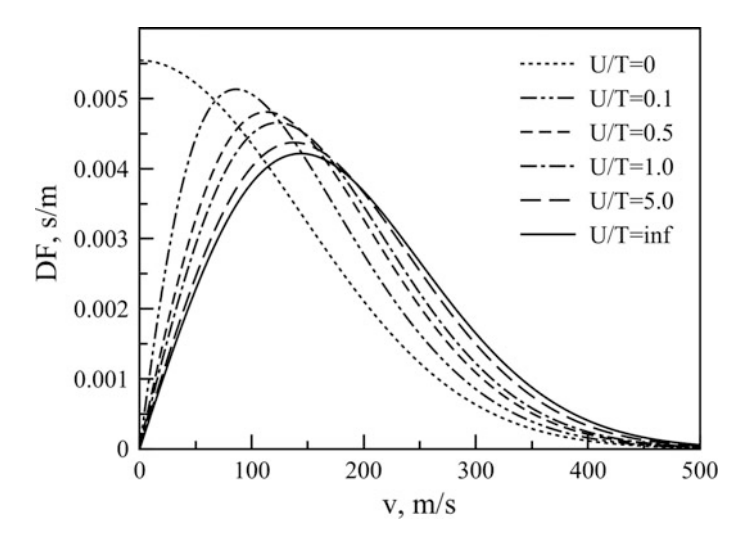


Fig. 5.4 Distribution functions for the different binding energy of particles. DF—distribution function

$$f(v_{x,y}) = \sqrt{\frac{m}{2\pi T}} \exp\left(-\frac{mv_{x,y}^2}{2T}\right), \quad -\infty < v < \infty.$$
 (5.2.18)

As we know, the mean kinetic energy corresponding to distribution (5.2.18) is T/2, therefore, the sum of the mean kinetic energy for projections of velocities x and y is T. Thereby, the total mean kinetic energy of the atom after evaporation is:

$$\bar{\varepsilon} = 2T \tag{5.2.19}$$

Possibly, this is the most important result that we have obtained. It means that:

- The flux of evaporated atoms is "overheated:" while atoms of a liquid at equilibrium have kinetic energy 1.5T, evaporated atoms have an energy which is higher by 0.5T.
- One may expect that an object placed close to the evaporation surface tends to
 obtain an increased temperature; the spatial scale of such an effect is approximately equal to the mean free path (MFP); we will discuss the consequences of
 this issue in Chap. 8.

Again, the total DF of the evaporated atom has no such parameter as a temperature; for instance, it is incorrect to compose a "temperature" corresponding to any direction, such as $T_{x,y} = T$, $T_z = 2T$. Temperature is not a vector!

5.2.4 Some Thoughts Concerning Condensation

This book is devoted to evaporation, not to condensation. The process of condensation is not a process of "evaporation with a reversed sign:" many nuances arise when an atom moves from vapor toward an interface, through a mob of its colleagues, and attaches to a liquid surface. For example, we can consider evaporation in vacuum—this is a comfortable and convenient model which allows us to exclude interactions with atoms of a surrounding gas. However, we cannot, of course, consider condensation from a vacuum; the condensation process is necessarily tied to an interaction between atoms.

Nevertheless, we are forced to treat some aspects of condensation from time to time. Here, we must discuss the problem of attachment itself. We have obtained a DF (5.2.15) which considers how to overcome the potential barrier U. For the attached particle, we must consider the same factor: when an atom "falls" on an evaporation surface, its energy rises to the value of U. Thus, because of condensation, the surface of the liquid obtains additional energy, something which must be kept in mind for the many problems that will be discussed in this book later.

For instance, this effect may define the different temperatures of evaporation surfaces under conditions of a contemporary condensation process, or the absence of it.

5.2.5 Distribution Function on an Irregular Surface

As usual, the reality is slightly more complicated than the simple theoretical model. The evaporation surface may not be absolutely flat (see Fig. 5.5). What will the black atom do on this figure if it has sufficient kinetic energy to leave the interface? It cannot move straight up in the direction of the z axis, because its neighbors prevent its motion in this direction: its upper neighbor would repel it. In such a case the preferred direction for escape from the surface is to move to one side, as is shown in Fig. 5.5. Here the normal component of velocity (normal to the local area of the surface) does not coincide with the z axis (normal to the "averaged" surface). Consequently, the binding energy will be overcome in the direction at an angle θ relative to the z axis.

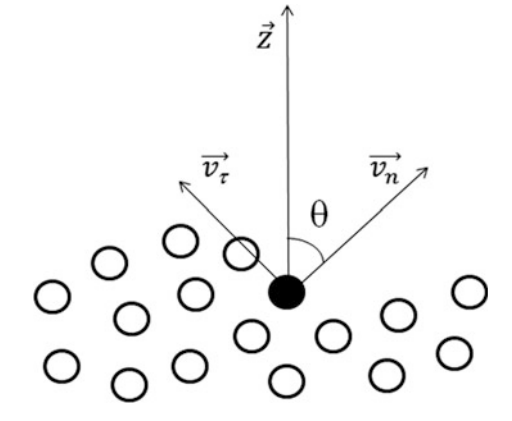
Then, the DF (5.2.14) describes velocities in some new, local direction. Different local areas have different angles θ with the z axis, and an overall DF for velocities must be obtained by averaging all possible values of θ . To provide this averaging we must have a probability density function $p(\theta)$ which describes the probability of a local tilt of angle θ :

$$f(v_z) = \int_{0}^{\theta_{\text{max}}} f(v_z, \theta) p(\theta) d\theta$$
 (5.2.20)

Here the DF (5.2.20) describes the probability of velocity v_z when the atom leaves the surface at an angle θ .

Gerasimov and Yurin (2014) wrote that there is no good hypothesis about the function $p(\theta)$; today we still do not have such a hypothesis. We still use an equal probability of tilt for any angle from zero to the maximal angle θ_{max} , thus, our problem is reduced to the determination of the function $f(v_z, \theta)$. Consequently, the solution to the problem is $f(v_z) = f(v_z, \theta)$ with $\theta \sim \theta_{\text{max}}$ (note that quantity θ_{max} is unknown too).

Fig. 5.5 An irregular evaporation surface. The white circles represent steady atoms in a liquid and the black circle represents an atom which is ready to escape



As one can see in Fig. 5.5, the z projection of velocity for that black particle is:

$$v_z = v_n \cos \theta + v_\tau \sin \theta. \tag{5.2.21}$$

The corresponding DF of the *z*-directed velocity can be found with (5.2.21) if we put the DF for the normal component of velocity according to (5.2.14), denoting it as $f_n(v_n)$, and the DF for the tangential projection of velocity as the MDF, denoting it as $f_{\tau}(v_{\tau})$.

Summarizing, we have:

$$f(v_z, \theta) = \int_{v_{\tau}^{\min}}^{v_{\tau}^{\max}} f_n \left(\frac{v_z - v_{\tau} \cos \theta}{\sin \theta} \right) f_{\tau}(v_{\tau}) dv_{\tau}.$$
 (5.2.22)

As for the upper limit of this integral, we see that $v_{\tau}^{\text{max}} = v_z / \sin \theta$. Previously, we put the lower limit to zero: $v_{\tau}^{\text{min}} = 0$; we are going to discuss this convenient, but poorly corrected, move later.

Omitting all the manipulations, we get a solution for (5.2.22):

$$f(v_z, \theta) = \frac{a}{2c_1} \exp\left(-\left(A - c_1 c_2^2\right) v_z^2\right) \left[\exp\left(-c_1 v_z^2 (1/a - c_2)^2\right) - \exp\left(-c_1 v_z^2 c_2^2\right)\right]$$

$$+ (1 - ac_2) \frac{v_z}{\sqrt{c_1}} \exp\left(-\left(A - c_1 c_2^2\right) v_z^2\right) \left[\exp\left(v_z \sqrt{c_1} (1/a - c_2)\right) + \exp\left(v_z c_2 \sqrt{c_1}\right)\right]$$

$$(5.2.23)$$

where:

$$a = \sin \theta$$
, $A = \frac{m}{2T \cos^2 \theta}$, $B = \frac{m}{2T}$, $c_1 = Aa^2 + B$, $c_2 = \frac{aA}{c_1}$. (5.2.24)

Of course, expression (5.2.23) is absolutely huge; this construction does not suit any analytical consideration. However, two limiting cases can be considered. The first one is the case of small angles $\theta \to 0$, that is, for $a \to 0$ and $A \to m/2T$, where we have a DF (5.2.14) representing an obvious result. In the opposite case, for large θ , we represent (5.2.23) in the form:

$$f(v_z) = Cv_z^2 \exp\left(-\frac{mv_z^2}{2\Upsilon_z}\right),\tag{5.2.25}$$

where constant C must be determined from the normalized condition.

Functions (5.2.25) and (5.2.14) in comparison to (5.2.23) are shown in Fig. 5.6 for different values of angle θ .

By finding a constant we can finally represent the DF for the z projection of velocity for a strongly irregular surface:

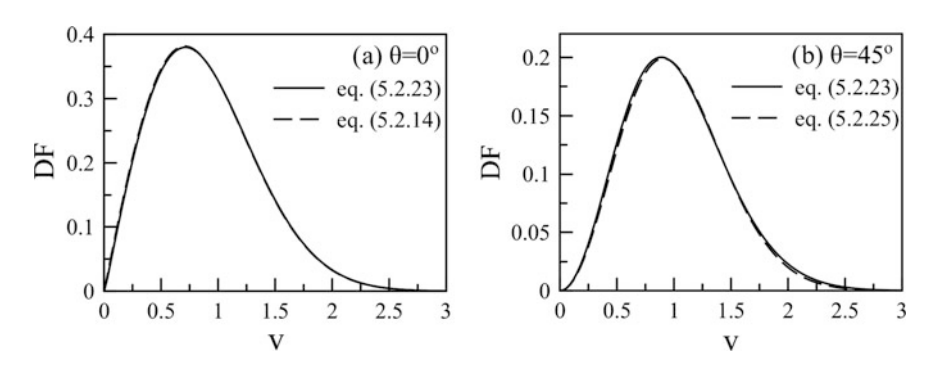


Fig. 5.6 Distribution function (5.2.23) for different values of angle θ . DF, distribution function

$$f(v_z) = \sqrt{\frac{2}{\pi}} \left(\frac{m}{\Upsilon_z}\right)^{3/2} v_z^2 \exp\left(-\frac{mv_z^2}{2\Upsilon_z}\right). \tag{5.2.26}$$

It is also worth noting that we choose the lower limit $v_{\tau}^{\min} = 0$ for integral (5.2.22) in some arbitrary manner. From Fig. 5.5 one may see that the black atom can leave the liquid even with a (small) value $v_{\tau}^{\min} < 0$. The corresponding DF [calculated numerically with integral (5.2.22)] is shown in Fig. 5.7. Now we can see that f(0) > 0; this fact may be useful for the analysis of DFs presented in the previous section.

The module of distribution (5.2.26), quantity Υ_7 , is:

$$\Upsilon_z = \frac{2}{3} \frac{\overline{mv_z^2}}{2},\tag{5.2.27}$$

that is, 2/3 of the mean kinetic energy.

According to our model, the DF for tangential projections of velocities v_x and v_y must keep the Maxwellian form, but with different mean kinetic energy:

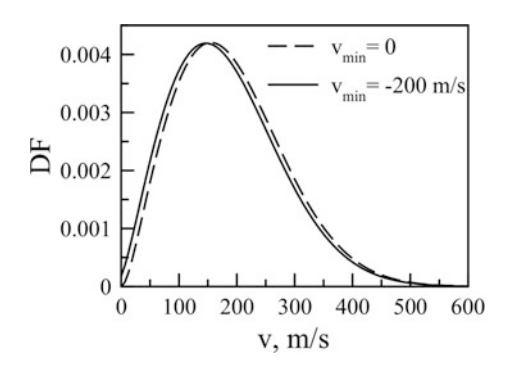
$$f(v_{x,y}) = \sqrt{\frac{m}{2\pi \Upsilon_{x,y}}} \exp\left(-\frac{mv_{x,y}^2}{2\Upsilon_{x,y}}\right). \tag{5.2.28}$$

Despite any oscillations of the evaporation surface, the total kinetic energy of the detached atom must be the same, i.e., 2*T*:

$$\frac{\overline{mv_x^2}}{2} + \frac{\overline{mv_y^2}}{2} + \frac{\overline{mv_z^2}}{2} = 2T,$$
 (5.2.29)

that is, for all our parameters Υ_k we have the condition:

Fig. 5.7 Distribution function with v_{τ} <0 (see Fig. 5.5). DF—distribution function



$$\Upsilon_x + \frac{3}{2}\Upsilon_z = 2T,\tag{5.2.30}$$

because $\Upsilon_x = \Upsilon_y = \overline{mv_x^2}$.

Distinct from the results for a plain evaporation surface, here, parameters Υ_x and Υ_z depend on the unknown angle θ in (5.2.23), and, as we understand, can be calculated only with numerical simulations. The test for correctness of all these considerations is correlation (5.2.30).

However, before the results of the numerical simulations are presented, we discuss some important questions.

5.2.6 A Generalization

We may generalize all our DFs for the z projection of velocity in a form that combines both DFs and allows approximation for a common case:

$$f(v_z) = Cv_z^n \exp\left(-\frac{mv_z^2}{2\Upsilon_z}\right),\tag{5.2.31}$$

where the normalizing constant is:

$$C = \frac{m^{(n+1)/2}}{2^{(n-1)/2} \Upsilon_z^{(n+1)/2} \Gamma((n+1)/2)}$$
 (5.2.32)

and the mean kinetic energy is:

$$\frac{\overline{mv_z^2}}{2} = \frac{n+1}{2}\Upsilon_z. \tag{5.2.33}$$

There is not a lot of physics here, but a bit of mathematics. Note that parameter n here is not necessarily an integer.

5.2.7 About Fluxes from an Evaporation Surface

Fluxes from the evaporation surface may be calculated with our DFs from the previous section, but not completely.

For example, the mean velocity of the atoms evaporated from the flat surface is:

$$\bar{v}_z = \int_0^\infty v_z f(v_z) dv_z = \sqrt{\frac{\pi T}{2m}}.$$
 (5.2.34)

Thus, the flux from the surface is:

$$j = n\sqrt{\frac{\pi T}{2m}}. (5.2.35)$$

We may also calculate fluxes for DF (5.2.26) (see Sect. 5.2.9). One problem remains: we do not know the number density of evaporated atoms n. For the approach presented in this section, this quality is absolutely external; we have no idea about it. Possibly, we may find n with (5.2.17), however, the work function U is required.

5.2.8 The Binding Energy: Preliminary Remarks

The work function U that has been introduced at the early stage of our consideration in this section disappeared in a mystical manner in the normalizing constants. However, this is not a reason to forget this quantity, since this is probably the most important parameter concerning the process of evaporation.

It is evident that U may depend on spatial coordinates: in different zones of the evaporation surface the work function can be different due to fluctuations in number density of surface atoms, etc. How may this fact affect our consideration?

As we see from the formulae in this section—it has no affect. Both our DFs—for a flat surface and for an irregular one—keep the form:

$$f(v, U) = f(v)f(U).$$
 (5.2.36)

This multiplicative form allows us to consider both parts of the DF independently. In other words, even if the work function depends on coordinates U(x, y, z), we can have no worries about the final results: in such a case, our normalizing factors are averaged for the whole surface (both for coordinates and time, in general the case).

Thus, the question about quantity U is rather a question about its physical nature. If it is not a constant, then fluctuations of this quantity may have an effect on the

evaporation flux; thus, we have to find this parameter ... When some fluctuating quantity is unknown, it always tempting to use a Gaussian for its DF. This approach was discussed in Frenkel (1946), but in next chapter we try to establish a real expression for the DF on U.

5.2.9 Fluxes at the Surface

Here we briefly give the expressions for evaporation fluxes at different distances from the evaporation surface (see Fig. 3.3):

• At the liquid surface (plane A in Fig. 3.3):

$$j = n_0 \sqrt{\frac{T}{2\pi m}} e^{-U/T}, (5.2.37)$$

$$q = n_0 T \sqrt{\frac{T}{2\pi m}} e^{-U/T} \left(2 + \frac{U}{T} \right).$$
 (5.2.38)

• In the vapor (plane *B* in Fig. 3.3):

$$j = n_{\rm e} \sqrt{\frac{\pi T}{2m}};\tag{5.2.39}$$

$$q = n_{\rm e}T \sqrt{\frac{25\pi T}{8m}}. (5.2.40)$$

The correlation between the number of particles in the liquid n_0 and the number of evaporated particles n_e will be discussed in next chapter.

5.2.10 Atoms or Molecules?

Strictly speaking, our approach can only be applied to the evaporation of atoms. Molecules have inner degrees of freedom, which can be excited during interactions with their neighbors. During the process of evaporation, in detaching from the surface (i.e., from other molecules) some energy may be transferred from transitional degrees of freedom to the inner ones. Because of this nuance, the whole detachment phenomenon is an inelastic process, and (5.2.2) must be written with inner energy: vibrational, rotational and probably more. There are many experimental works

where excitations of the inner degrees of freedom during evaporation or desorption were observed (e.g., Michelsen et al. 1993; Maselli et al. 2006).

On the other hand, accounting for other types of energy would significantly complicate our approach. Actually, all that we need is the binding energy, which can be determined from experimental data. In Chaps. 7 and 8 we will compare our results with experimental data for water, and an agreement between calculations and experiments will be achieved.

Anyway, we can always consider our approach as an approximation.

5.3 Molecular Dynamics Simulations

5.3.1 A Classification

We do not claim this classification to be of any completeness, obviously, it is only our opinion. However, we are able to distinguish several approaches to numerical simulation.

For some, this is a method which can be used to calculate the properties of the medium (or of a process), which cannot be measured in experiments. It could be a P–V–T diagram for extreme conditions, calculations of kinetic coefficients of plasma, wrapping of bodies by supersonic flow, etc. Here the digits are the main, and often the only, results of calculations. No new physical problems are considered, no new physical (we mean, conceptually) results are obtained. This approach is widespread in technical physics.

Other scientists use numerical simulation as a part of theoretical analysis. Here snip-snap methods of numerical simulations are combined with, for example, approximate solutions of the Boltzmann kinetic equation. As a rule, this approach is used for uncertain problem statements because of its complexity. If we cannot formulate a problem solidly, thus, we cannot pretend to have a direct solution to it. Some numerical simulations of the evaporation problem can be attributed to this class; for instance, we may also refer to the works devoted to approximated solutions of the Boltzmann equation.

We assume that numerical simulation has a value in its pure performance. For us, molecular dynamics simulation (MDS) helps us to understand the fundamental problems of physics, which cannot be predicted analytically or obtained in experiments. Of course, MDS is not a direct numerical experiment in the strictest meaning of the term (because of problems with interaction potential; see Chap. 4), however, results of numerical simulations can verify the theoretical considerations of the previous section very well. With numerical simulations, we can observe processes that are not available for experimental setups, but it is important to consider clear tasks for these purposes. For instance, perhaps a certain value of a cut radius for the interaction potential provides a better agreement between the calculated saturation curve and experimental data; however, we assume that

exceptional points in a flux may influence the integrability property of a system; thus, we use the uncut Lennard-Jones (LJ) potential.

Below we present the numerical simulation results for the evaporation of liquid argon.

5.3.2 Numerical Simulation of Evaporation

We considered the evaporation of argon in a vacuum, i.e., initially only one (liquid) phase was placed in the calculation region. The LJ potential was used:

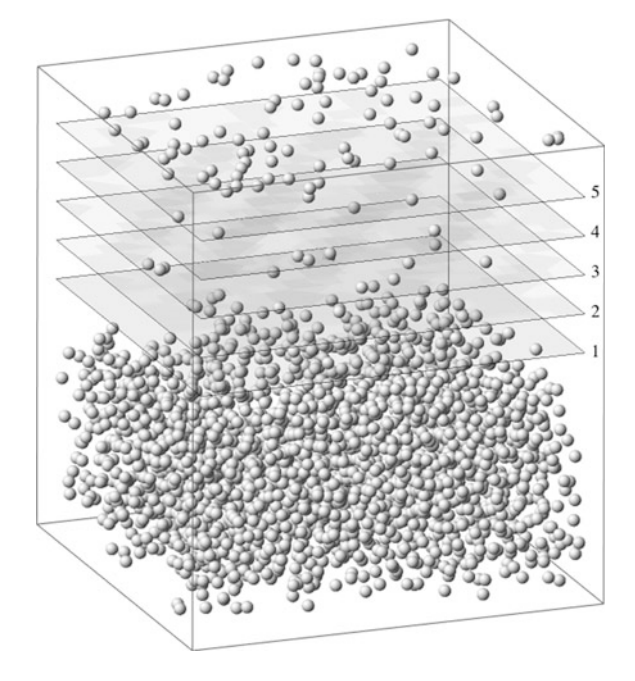
$$\varphi(r) = 4\varepsilon \left[\left(\frac{\sigma}{r} \right)^{12} - \left(\frac{\sigma}{r} \right)^{6} \right]. \tag{5.3.1}$$

with parameters $\varepsilon = 119.8 \text{ K}$ and $\sigma = 3.405 \text{ Å}$.

The calculation region is shown in Fig. 5.8. This is a cube with an edge of 6.5 (for 2000 particles in the region) or 11 nm (for 10,000 particles). Periodic boundary conditions were used for the side faces of this cube; on the bottom of the cube a layer of immobile particles holds the liquid inside. The upper face is open: when particles reach this side they "disappear" from calculations.

The liquid argon (depth ~ 2 nm) was initially heated to a temperature ~ 120 K (see below for specific conditions). We consider the evaporation process during a

Fig. 5.8 The calculation region; at the upper face of the cube we see evaporated particles (excluded from the calculation)



period of $\sim 10^{-1}$ ns, then we repeat the calculations, and so on. In each simulation mode, only ~ 100 particles were evaporated with the temperature of the liquid dropping by several degrees. Due to the repetition of calculations, we obtained an number of escaping particles that was sufficient for treatment, namely, to construct a DF for evaporated atoms.

First, we have to make sure that the DF of the velocities in a liquid corresponds to the MDF. In Fig. 5.9 we represent the velocity DF in a liquid for all three projections of velocity; good coincidence can be seen for every component. Here we represent DFs averaged on spatial scales of ~ 2 nm; this is a rather thick layer. In the next section we present a DF calculated for a thin surface layer of ~ 0.5 nm thickness; the results stay the same, i.e., the MDF describes the results of numerical simulations with sufficient accuracy.

The potential energy of the interaction of an evaporating particle (i.e., of an atom in a process of detachment) with others (i.e., with a bulk of a liquid) is shown in Fig. 5.10.

We can see that the binding energy decreases at the rate of approximately two orders of a magnitude for 1 nm. This is the scale of the thickness of the surface layer; we also have to understand that for any coordinate on Fig. 5.10 the detaching atom must have a non-zero longitude velocity v_z in order to escape. In other words: strictly speaking, there is not a single point on the graph where the atom cannot be

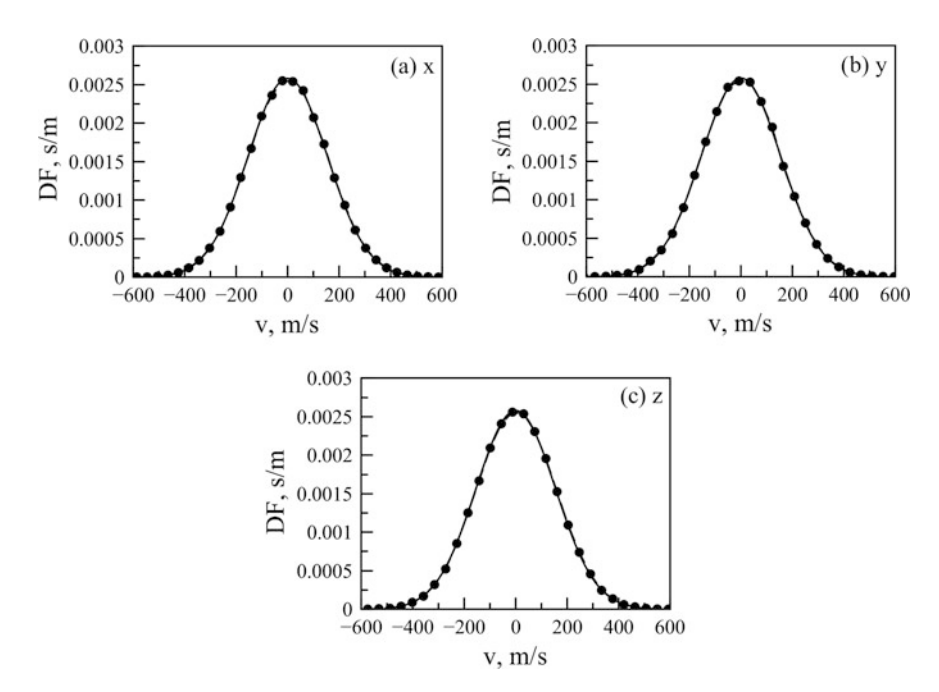


Fig. 5.9 Velocity distribution functions in a liquid (dots) and the Maxwellian distribution function at the temperature of the liquid (curve). DF—distribution function

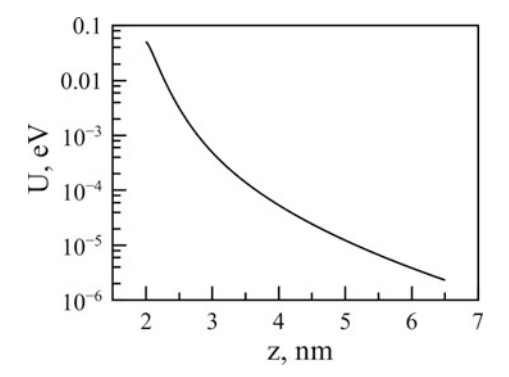


Fig. 5.10 The binding energy of an evaporated atom as a function of the distance from the liquid surface

considered as a free particle; but practically, at the upper side of the calculated region, where the interaction energy is $\sim 10^{-2}$ K, one may neglect such a binding energy and assume that particles are free.

5.3.3 Velocity Distribution Function for Evaporated Particles

Next we calculate the DF of velocity for particles that cross planes at some distances from the evaporation surface (see Fig. 5.8). Note that the term "evaporation surface" is unclear: this is an irregular surface, so some plains that were considered

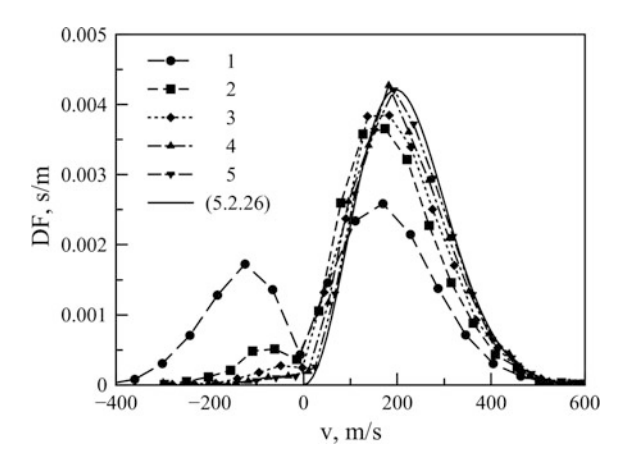


Fig. 5.11 The distribution function at different distances from the surface (see corresponding planes in Fig. 5.8). DF—distribution function

can be crossed by particles in both directions, i.e., both out from the bulk and toward it; in the latter case, we see particles that cannot fly out and return back.

The velocity DF at different distances from the surface is shown in Fig. 5.11.

One may see that at short distances from the surface the DF of velocities "consists of two parts." Some particles have a velocity sufficient to escape $(v_z > 0)$, some of them return to the liquid after an ineffective attempt to escape $(v_z < 0)$. Of course, the number of returning particles decreases with the distance from the surface (i.e., with the number of corresponding planes in Fig. 5.8). Far from the evaporation surface, on the upper side of the cube, we can calculate the DF for particles which may be considered as free atoms.

We will compare the DF obtained from numerical simulations with our formulae from the previous section; specifically, with (5.2.26) and (5.2.30).

The first regime that was considered was 2000 particles, with an initial temperature of the liquid argon of 125 K; during evaporation, the temperature was decreased to 115 K. For calculations, using (5.2.30), we accepted a mean temperature of 120 K. Results of numerical simulations are presented in Fig. 5.12.

The second regime considered had 10,000 particles; during evaporation the temperature was decreased from 120 to 110 K; for calculations we used 115 K. Results are presented in Fig. 5.13.

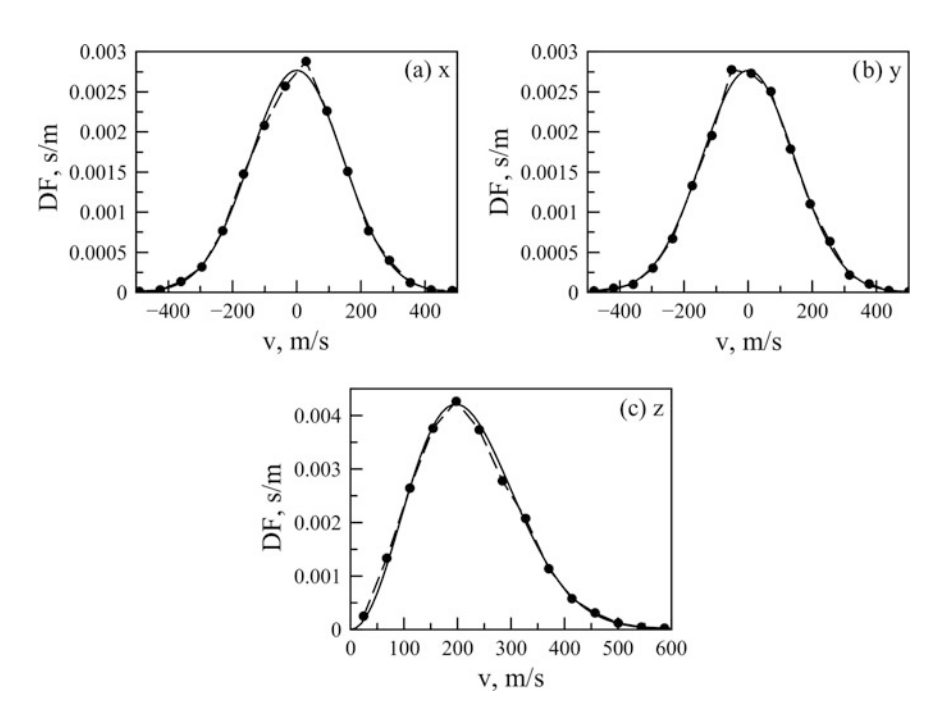


Fig. 5.12 The calculated distribution function (dots) and analytical curves—(5.2.28) for x and y projections and (5.2.26) for the z projection. The system contained 2000 particles. DF—distribution function

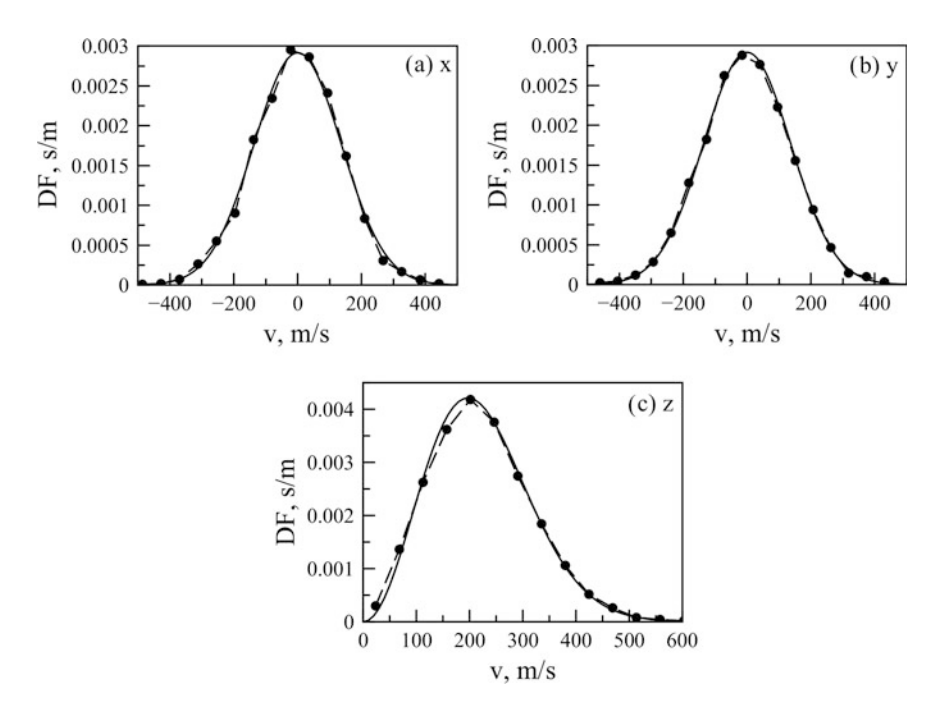


Fig. 5.13 The calculated distribution function (dots) and analytical curves—(5.2.28) for x and y projections and (5.2.26) for the z projection. The system contained 10,000 particles. DF—distribution function

Table 5.1 Parameters for distribution functions presented in Figs. 5.12 and 5.13

NN	Υ_x (K)	Υ _y (K)	Υ_z (K)	2T, K	$\bar{\varepsilon}_{\Sigma}^{NS}$ (K)
#1	100	100	93	240	239
#2	90	90	93	230	231

All parameters for DFs were calculated with DFs obtained in numerical simulations; there are two aspects of theory that can be tested in such conditions:

- Agreement of calculated DFs with results from numerical simulations.
- Agreement with correlation (5.2.30).

The parameters for theoretical DFs (5.2.26) are presented in Table 5.1, along with the average energy of particles \bar{e}_{Σ}^{NS} calculated in the numerical simulations.

Thus, we see that the theory presented in the previous section works well. It has two uncertainties: first, we cannot establish a priori what kind of velocity DF must be chosen for the given situation; second, the work function U is undefined as yet. The last problem is considered in next chapter.

5.4 Conclusion

Maxwellian or not? This is the first question that must be answered. Many analytical solutions work on the assumption of a positive answer to this question, and use the MDF as a boundary condition for a liquid surface. However, despite the "obviosity" of such an approach, some proof is needed. They say that physics is an experimental science, thus, one may expect that the velocity DF of atoms from an evaporation surface can be obtained directly from experiments. Indeed, the first measurements were provided in 1920.

However, this task is not very simple. A few experiments—a significant number that is—obtained contradictory results. In some experiments the MDF was confirmed, in others it was refuted. Actually, it is hard to make a definitive conclusion, especially if we take into account that particles registered in the TOF method must originate from a liquid surface and cannot interact with other molecules, solid surfaces, etc., on their path to the detector. Finally, one may conclude that more new questions have arisen from experiments than have been answered. It is a rare thing, when in a paper with experimental data an author says that numerical simulation is needed. Usually, we meet the opposite scenario: after long and difficult calculations simulators state that natural experiments would not be superfluous ...

Thus, we have to turn our attention to theoretical considerations.

Despite the fact that intuition suggests the MDF for evaporated atoms, the real DF differs significantly from this equilibrium correlation. In the simplest case, the DF for normal velocities for detached particles from a liquid surface at temperature T is:

$$f(v) = \frac{mv}{T} \exp\left(-\frac{mv^2}{2T}\right).$$

In following chapters we will use this DF for almost all analytical approaches, because this formula represents all the significant issues concerned with an evaporation DF. This is a non-symmetric function which provides non-zero total fluxes.

The main property of this DF and, probably, the main result of this chapter is the fact that the average kinetic energy of evaporated atoms is $\bar{\epsilon}=2T$. The evaporated flux is a non-equilibrium, high-energy flux; this fact determines many issues of evaporation that will be discussed further in this book.

However, it is worth remembering that the DF is only an approximation of the real DF; this relation is correct if and only if:

- The energy barrier U is very high, if not, function (5.2.16) must be used. Indeed, this condition "works" when the ratio $U/T \sim 5$ (see Fig. 5.4).
- The evaporation surface is "flat," i.e., particles overcome the energy barrier at a direction which is normal to the surface. If not—if this barrier is overcome at some angle $\theta > 0$ to the normal of the surface—then the DF is determined by (5.2.25). Moreover, the property f(0) = 0 may be disturbed in this case. Anyway, $\bar{\varepsilon} = 2T$ here too.

5.4 Conclusion 145

Numerical simulations confirm that the DF for evaporated particles is not Maxwellian. This is an asymmetric function with a non-zero total flux (in opposition to the MDF). In most articles the results of numerical simulations correspond with our calculations.

Thus, the DF for evaporated atoms at a liquid surface is not Maxwellian. Considering how many analytical solutions were composed with MDF as a boundary condition for evaporating liquid, we feel that a kind of resistance to such a function to be an eventual reaction.

Let us try to save the MDF as a boundary condition for an evaporated liquid anyway.

An attempt

Non-MDF for evaporated atoms? May be so; it is hard work to parse calculations, but it is evident that for short distances from the interface a flux from the surface is thermalized due to collisions with atoms of gas. In this case we may use the MDF at other distances from the surface.

An answer

Thermalization occurs at long spatial scales, much longer than the MFP of a molecule. Then, it is difficult to imagine an application where the boundary conditions for an interface would actually be established within a vapor phase.

An attempt

What about the condensation flux? It may also change the DF of evaporation particles. Collisions with them change the DF to its Maxwellian form right at the interface.

An answer

Again, collisions take place on large scales. The condensation flux cannot turn a non-Maxwellian function into a MDF at the evaporation surface.

In fine, let us allow ourselves a forecast. The MDF for evaporation will still be used for decades to come. Let us see which of these will happen first: a human to step on Mars or the MDF for evaporated particles be banished forever.

References

- M.J. Cardillo, M. Balooch, R.E. Stickney, Surf. Sci. 50, 263 (1975)
- S. Cheng et al., J. Chem. Phys. 134, 224704 (2011)
- G. Comsa, R. David, Surf. Sci. Rep. 5, 145 (1985)
- A.E. Dabirli, T.J. Lee, R.E. Stickney, Surf. Sci. 26, 522 (1971)
- M. Faubel, T. Kisters, Nature 339, 527 (1989)
- M. Faubel, S. Schlemmer, J.P. Toennies, Z. für Phys. D Atoms Mol. Clust. 10, 269 (1988)
- J. Frenkel, Kinetic Theory of Liquids (Oxford University Press, Oxford, 1946)
- A. Frezzotti, AIP Conf. Proc. 1333, 161 (2011)
- D.N. Gerasimov, E.I. Yurin, High Temp. **52**, 366 (2014)

- C. Hahn et al., J. Chem. Phys. 144, 044707 (2016)
- J.E. Hurst et al., J. Phys. Chem. 83, 1376 (1985)
- T. Ishiyama, T. Yano, S. Fujikawa, Phys. Fluids 16, 2899 (2004)
- O. Knake, I.N. Stranskii, Phys. Usp. 68, 261 (1959)
- C.J.H. Knox, L.F. Phillips, J. Phys. Chem. 102, 10515 (1998)
- K. Kobayashi et al., Heat Mass Transf. 52, 1851 (2016)
- K. Kobayashi et al., Microfluid. Nanofluidics 21, 53 (2017)
- M. Kon, K. Kobayashi, M. Watanabe, AIP Conf. Proc. 1786, 110001 (2016)
- A.P. Kryukov, VYu. Levashov, Int. J. Heat Mass Transf. 54, 3042 (2011)
- A. Lotfi, J. Vrabec, J. Fischer, Int. J. Heat Mass Transf. 73, 303 (2014)
- O.J. Maselli et al., Aust. J. Chem. 59, 104 (2006)
- T. Matsushima, Surf. Sci. Rep. **52**, 1 (2003)
- R. Meland et al., Phys. Fluids 16, 223 (2004)
- H.A. Michelsen et al., J. Chem. Phys. 98, 8294 (1993)
- M. Planck, Ann. Phys. 1, 69 (1900)
- C.T. Rettner, E.K. Schweizer, C.B. Mullins, J. Chem. Phys. 90, 3800 (1989)
- T. Tsuruta, G. Nagayama, J. Phys. Chem. B 108, 1736 (2004)
- P. Varilly, D. Chandler, J. Phys. Chem. 117, 1419 (2012)
- J.-F. Xie, S.S. Sazhin, B.-Y. Cao, J. Therm. Sci. Technol. 7, 288 (2012)
- V.V. Zhakhovskii, S.I. Anisimov, J. Exp. Theor. Phys. 84, 734 (1997)

Recommended Literatures

- S.I. Anisimov, V.V. Zhakhovskii, JETP Lett. 57, 91 (1993)
- A. Charvat, B. Adel, Phys. Chem. Chem. Phys. 9, 3335 (2007)
- W.Y. Feng, C. Lifshitz, J. Phys. Chem. 98, 6075 (1994)
- T. Hansson, L. Holmlid, Surf. Sci. Lett. 282, L370 (1993)
- T. Kondow, F. Mafune, Annu. Rev. Phys. Chem. 51, 731 (2000)
- O.J. Maselli et al., Chem. Phys. Lett. 513, 1 (2011)
- N. Musolino, B.L. Trout, J. Chem. Phys. 138, 134707 (2013)
- G.M. Nathanson, Annu. Rev. Phys. Chem. 55, 231 (2004)
- E.H. Patel, M.A. Williams, S.P.K. Koehler, J. Phys. Chem. B 121, 233 (2016)
- D. Sibold, H.M. Urbassek, Phys. Fluids A 3, 870 (1991)
- O. Stern, Z. für Phys. 2, 49 (1920a)
- O. Stern, Z. für Phys. 3, 417 (1920b)
- T. Tsuruta, G. Nagayama, Energy 30, 795 (2005)

Chapter 6 Total Fluxes from the Evaporation Surface



The distribution function (DF) of velocities obtained in Chap. 5 gives us a guiding thread to solve some problems of evaporation, but, as they say this is only "the smaller part" of the problem. We still cannot calculate absolute values of evaporation fluxes, we have no idea about the work function for surface atoms and do not know how deviations of this parameter might affect evaporation processes.

In this chapter we will provide answers to these questions.

6.1 Distribution Function for Potential Energy in Condensed Media

6.1.1 Work Function as a Distribution Function

In Chap. 5 we obtained important relationships for the velocity DF of atoms detached from the interface. Consequently, we have expressions for fluxes at the evaporation surface, but with an unknown parameter n—number density of evaporated particles—which could be calculated, in principal, through balance correlations at the interfacial surface. However, the number of evaporated atoms can be calculated analytically, without any additional assumptions for the fluxes on the interface or even the existence of balanced equations of any kind. If the total number density at the surface of a liquid is n_0 , then the density of particles which have sufficient kinetic energy is:

$$n = n_0 \int_{U}^{\infty} f(\varepsilon) d\varepsilon, \tag{6.1.1}$$

where U is the work function—the energy that must be overcome by an atom to leave the surface.

To calculate n analytically we must add parameter U in (6.1.1)—the binding energy of an atom at the surface. It is indeed obvious that U is not a constant. As with any energy in a mechanical system, the binding energy fluctuates, i.e., particles on the interfacial surface have different potential energy to one another. Thus, the problem is not to establish a single value of U: we have to find the DF g(U)—the DF of the binding energy of an atom at the surface of a liquid. Specifically, we have to find the probability:

$$dw = g(U)dU (6.1.2)$$

that the atom has binding energy from U to $U + \mathrm{d}U$. Note that we are not interested in the DF in phase space in the form $g'(U)\mathrm{d}\Gamma$, instead we have to find g(U) from (6.1.2). Thus, Boltzmann with his distribution cannot help us here. We must find the DF g(U) independently.

6.1.2 Potential Energy Distribution Function

Further, we will use the potential energy of the particle u = -U, that is, u < 0 and U > 0 (generally, it is important to note that, at least theoretically, there may be u > 0; these particles would leave a surface independently of their kinetic energy).

Of course, the potential energy DF g'(U) can be represented as the Maxwell-Boltzmann DF, but this is a dead-end approach because we cannot establish a correlation for $\frac{d\Gamma}{dU}$ in the general case. To find a function g(U) we will use another approach here based on mechanical principles: the possibilities of mechanics might not be exhausted yet.

In mechanics, a fundament of all constructions is the principal of least action. The integral of the function L (termed the Lagrange function or Lagrangian) tends to be minimal:

$$\int_{t_1}^{t_2} L dt \to \min. \tag{6.1.3}$$

It can be shown [for instance, see Landau and Lifshitz (1976)] that the Lagrange function is the difference between the kinetic energy E and the potential one U:

$$L = E - U. ag{6.1.4}$$

Now we transform (6.1.3) for statistical purposes. At first, we must use the statistical approach: a consideration which involves DFs for every mechanical quantity, that is:

- $f(\varepsilon)$, the DF of kinetic energy ε , $\varepsilon \in [0, \infty]$.
- g(u), the DF of potential energy $u, u \in (-\infty, \infty)$.
- h(l), the DF of the Lagrangian l = ε u, which can be expressed through f and g as:

$$h(l) = \int_{0}^{\infty} g(\varepsilon - l) f(\varepsilon) d\varepsilon. \tag{6.1.5}$$

• j(s), the DF for the total energy $s = \varepsilon + u$:

$$j(s) = \int_{0}^{\infty} g(s - \varepsilon) f(\varepsilon) d\varepsilon.$$
 (6.1.6)

Thus, we suppose that a particle can have any value of potential energy at a given kinetic energy, or—in statistical language—the DFs $f(\varepsilon)$ and g(u) are statistically independent functions. Thereby, we assume that both ε and u of any particle take on a continuous series of values. At such conditions the mean-time value of the Lagrangian in (6.1.3) can be replaced by its statistical analog:

$$\int_{l_1}^{l_2} lh(l) dl \to \min, \tag{6.1.7}$$

which reflects the minimum condition of the mean Lagrangian on its statistical trajectory. At first, we may consider an infinite trajectory, because only in that case can one expect that all possible states, with all possible ε and u energy values, will be realized. Therefore, in (6.1.7) we have $l_1 = -\infty$ and $l_2 = \infty$. This is a simple part of our treatment.

The difficult part is this. Equation (6.1.6) alone is insufficient to define a certain function h(l); we have to impose restrictions on the form of this function. For this assumption, we suppose that *the most probable value* of the Lagrangian l_0 [which corresponds to the maximum of the function h(l)] is defined. Then we see from (6.1.7) that l_0 must coincide with *the probable value* l_m of the Lagrangian [the mean value of l with DF h(l)]:

$$l_0 = l_m = \int_{-\infty}^{\infty} lh(l)dl, \qquad (6.1.8)$$

that is, at our assumption:

$$\int_{-\infty}^{\infty} (l - l_0)h(l)dl = 0, \tag{6.1.9}$$

and the DF h(l) is a symmetrical function on the argument $l-l_0=l-l_m$.

We emphasize that our consideration rather reflects some intuitive properties of the Lagrangian than provides a strict proof of the symmetry of the h(l) function. Some additional evidence of this property must be provided; further we present the results of a numerical simulation.

We find a DF g(u) in the following form:

$$g(u) = \int_{0}^{\infty} g_{\varepsilon}(\varepsilon, u) f(\varepsilon) d\varepsilon, \qquad (6.1.10)$$

where function $g_{\varepsilon}(\varepsilon, u)$ is the conditional DF of potential energy u for a particle with a certain kinetic energy ε , and the DF of kinetic energy is the Maxwellian distribution function (MDF):

$$f(\varepsilon) = \frac{2}{\sqrt{\pi T^3}} \sqrt{\varepsilon} \exp\left(-\frac{\varepsilon}{T}\right). \tag{6.1.11}$$

For example, in the case of a certain total energy $s = \varepsilon + u = \text{const}$, function $g_{\varepsilon}(\varepsilon, u)$ degenerates into the Dirac function, and the DF of potential energy represents the DF of kinetic energy f(s-u) (with restrictions for u in this case: $u \le s$). However, the total energy of a particle, of course, is uncertain: a particle might have any value of s. The connection between the kinetic energy of a particle and its potential energy follows from the principal of least action, i.e., from the condition of the symmetric form of h(l), as we discussed above.

To achieve the symmetricity of the DF of the Lagrangian, function $g_{\varepsilon}(\varepsilon, u)$ should have a form $g_{\varepsilon}(\varepsilon - u)$, if:

$$g_{\varepsilon}(\varepsilon - u - l_m) = g_{\varepsilon}(l_m - \varepsilon + u),$$
 (6.1.12)

then:

$$h(l-l_m) = \int_0^\infty \int_0^\infty g_{\varepsilon}(\varepsilon - \xi + l - l_m) f(\xi) f(\varepsilon) d\xi d\varepsilon$$

$$= \int_0^\infty \int_0^\infty g_{\varepsilon}(\xi - \varepsilon + l - l_m) f(\xi) f(\varepsilon) d\xi d\varepsilon$$

$$= \int_0^\infty \int_0^\infty g_{\varepsilon}(\varepsilon - \xi - l + l_m) f(\xi) f(\varepsilon) d\xi d\varepsilon = h(l_m - l).$$
(6.1.13)

Q.E.D: at condition (6.1.12) we see from (6.1.13) that h(l) is symmetric, as was discussed above.

The function $g_{\varepsilon}(\varepsilon - u) = g_{\varepsilon}(l)$ for certain ε describes a distribution of the potential energy of a given particle (at a defined value of kinetic energy). This potential energy is the sum of the energy of interaction between this particle and many, many others. Thus, one can expect that $g_{\varepsilon}(\varepsilon - u)$ is the stable DF (see Appendix A). Finally, we have:

$$g_{\varepsilon}(\varepsilon, u) = \frac{1}{\sqrt{2\pi\theta^2}} \exp\left(-\frac{(\varepsilon - u - l_m)^2}{2\theta^2}\right). \tag{6.1.14}$$

Parameter θ of the DF has a clear purpose. It determines the fluctuations of potential energy which are "additional" to the fluctuations caused by variations in kinetic energy. Possibly, its meaning can be understood by the following analogy. Let us imagine a pendulum in an external random potential field. When this pendulum is placed at a certain point (with fully defined mean potential energy), variations in its potential energy are uniquely connected with variations of its kinetic energy; these fluctuations are described by parameter T of the DF (6.1.11). However, the location of our pendulum variates, and the value of the mean potential energy determines additional variations of the total potential energy of the pendulum; these fluctuations are described by parameter θ .

At equilibrium state, all fluctuations are expected in the Gaussian form. We may refer to common principles like "the Boltzmann principle" (Einstein 1904) or "the Gauss principle" (Lavenda 1991). Thus, we may suppose that for an equilibrium state $\theta = T$, because temperature is the measure of fluctuations.

However, for an equilibrium state only, we have some arguments to set $\theta = T$, and both parameters can be referred to as a "temperature." In the common case, there may be $\theta \neq T$; we will hold the term "temperature" for T and introduce a new term "fluctura" (because this parameter describes fluctuations) for θ . There are not many chances that this term will survive, but we have to refer to the parameter θ someway other than "the parameter θ ." Fluctura, its value and calculation in numerical experiments will be discussed below, in Sect. 6.1.5.

The dispersion of potential energy can be obtained in two ways. As we see, the DF of potential energy is determined as:

$$g(u) = \int_{0}^{\infty} f(\varepsilon)g_{\varepsilon}(\varepsilon - u)d\varepsilon. \tag{6.1.15}$$

In fact, according to (6.1.15), potential energy can be determined as a difference between two independent random values: $u = \varepsilon - z$, and the DF for ε is $f(\varepsilon)$, while the DF for z is $g_{\varepsilon}(z)$. Because the dispersion of the sum (or of the difference) of two random independent quantities is the sum of their dispersions, we see that $D_u = D_{\varepsilon} + D_z$, or:

$$D_u = 1.5T^2 + \theta^2. (6.1.16)$$

Another way to obtain (6.1.16) is more complicated. By definition:

$$D_{u} = \int_{-\infty}^{\infty} (u - u_{m})^{2} g(u) du = \int_{-\infty}^{\infty} \int_{0}^{\infty} (u - u_{m})^{2} f(\varepsilon) g_{\varepsilon}(\varepsilon - u) d\varepsilon du. \quad (6.1.17)$$

With some rearrangement, we get:

$$D_{u} = \int_{0}^{\infty} f(\varepsilon) \left[\int_{-\infty}^{\infty} (u - u_{m})^{2} g_{\varepsilon}(\varepsilon - u) du \right] d\varepsilon$$

$$= \int_{0}^{\infty} f(\varepsilon) \left[\int_{-\infty}^{\infty} (\varepsilon - \varepsilon_{m} - z + z_{m})^{2} g_{\varepsilon}(z) dz \right] d\varepsilon.$$
(6.1.18)

Because $\int_0^\infty \int_{-\infty}^\infty (\varepsilon - \varepsilon_m)(z - z_m) f(\varepsilon) g_{\varepsilon}(z) = 0$ and functions $f(\varepsilon)$ and $g_{\varepsilon}(z)$ are normalized: $\int_0^\infty f(\varepsilon) d\varepsilon = 1$, $\int_{-\infty}^\infty g_{\varepsilon}(z) dz = 1$, we have:

$$D_{u} = \int_{0}^{\infty} (\varepsilon - \varepsilon_{m})^{2} f(\varepsilon) d\varepsilon + \int_{-\infty}^{\infty} (z - z_{m})^{2} g_{\varepsilon}(z) dz = D_{\varepsilon} + D_{z}, \qquad (6.1.19)$$

that is, correlation (6.1.16) again.

The dispersion of the total energy of a particle $s = \varepsilon + u$ can be obtained easily with the consideration given above, and:

$$D_s = D_{\varepsilon} + D_u = 3T^2 + \theta^2. \tag{6.1.20}$$

The same correlation is quite true for the dispersion of the Lagrangian $D_l = D_u$. Now, to establish a DF of potential energy we have to take integral (6.1.10) with functions $f(\varepsilon)$ (6.1.11) and $g_{\varepsilon}(\varepsilon, u)$ (6.1.14), that is:

$$g(u) = \int_{0}^{\infty} 2\sqrt{\frac{\varepsilon}{2\pi^{2}\theta^{2}T^{3}}} \exp\left(-\frac{\varepsilon}{T}\right) \exp\left(-\frac{(\varepsilon - u - l_{m})^{2}}{2\theta^{2}}\right) d\varepsilon.$$
 (6.1.21)

As it follows from (6.1.21), the DF actually depends on the relation $\frac{u}{\theta}$. This scaling property is important in the analysis of numerical simulation data: the tradition to normalize energy on the parameter of interaction potential (Lennard-Jones (LJ), etc.), possibly, played a confusing role previously.

Using dimensionless parameters:

$$\tilde{\varepsilon} = \frac{\varepsilon}{\theta}, \tilde{u} = \frac{u}{\theta}, \tilde{l}_m = \frac{\varepsilon_m - u_m}{\theta}, \tilde{t} = \frac{\theta}{T}, \tilde{g}(\tilde{u}) = g(\tilde{u})\theta, \tag{6.1.22}$$

we can represent integral (6.1.21) in the form:

$$\tilde{g}(\tilde{u}) = \frac{\sqrt{2}\tilde{t}^3}{\pi} \int_{0}^{\infty} \sqrt{\tilde{\varepsilon}} \exp(-\tilde{\varepsilon}\tilde{t}) \exp\left(-\frac{\left(\tilde{\varepsilon} - \tilde{u} - \tilde{l}_m\right)^2}{2}\right) d\tilde{\varepsilon}. \tag{6.1.23}$$

Here, the sub-integral function can be rewritten as:

$$\sim \exp\left(\frac{\ln \tilde{\varepsilon}}{2} - \tilde{\varepsilon}\tilde{t} - \frac{\left(\tilde{\varepsilon} - \tilde{u} - \tilde{l}_{m}\right)^{2}}{2}\right),\tag{6.1.24}$$

which is suitable for the saddle-point method. The sub-exponential function has a maximum at the point:

$$\tilde{\varepsilon}_0 = \frac{1}{2} \left[\tilde{u} + \tilde{l}_m - \tilde{t} + \sqrt{2 + \left(\tilde{u} + \tilde{l}_m - \tilde{t} \right)^2} \right], \tag{6.1.25}$$

and (6.1.23) can be approximately represented in the form:

$$\sim \exp(a - b(\tilde{\varepsilon} - \tilde{\varepsilon}_0)^2),$$
 (6.1.26)

where $a = \ln \sqrt{\tilde{\epsilon}_0} - \tilde{\epsilon}_0 \tilde{t} - 0.5 (\tilde{\epsilon} - \tilde{u} - l_m)^2$ and $b = \frac{1}{2} (1 + \frac{1}{2\tilde{\epsilon}_0^2})$. Thus, we have:

$$\tilde{g}(\tilde{u}) = \sqrt{\frac{\tilde{t}^3 \tilde{\varepsilon}_0}{2\pi b}} \left(1 + \operatorname{erf}\left(\sqrt{b}\tilde{\varepsilon}_0\right) \right) \exp\left(-\tilde{\varepsilon}_0 \tilde{t} - \frac{\left(\tilde{\varepsilon}_0 - \tilde{u} - \tilde{l}_m\right)^2}{2}\right). \tag{6.1.27}$$

Function (6.1.27) provides a simplified answer—the DF of potential energy in the general case. Actually, because of approximation, the integral of $\int_{-\infty}^{\infty} \tilde{g}(\tilde{u}) d\tilde{u} \neq 1$: it is slightly less than unity, so a correctness factor should be used. A multiplicator $1.05\tilde{t}^{0.25}$ corrects this problem for $\tilde{t} \in [1,2]$: the discrepancy between the analytical DF and the calculated one is less than 3%.

The DF (6.1.27) with a correctness factor $1.05\tilde{t}^{0.25}$ is shown in Fig. 6.1. The coincidence with the curve obtained by the numerical integration of (6.1.21) is good, but it is worth nothing since our analytical function is too complicated for analytical analyses.

In a more complicated form, we can obtain the solution of (6.1.21) by expanding $f(\varepsilon)$ into series:

$$f(\tilde{\varepsilon}) = \sum_{n=0}^{\infty} Q_n(\tilde{\varepsilon} - \tilde{\varepsilon}')^n, \tag{6.1.28}$$

with $\tilde{\epsilon}' = \tilde{u} + \tilde{l}_m$. This expansion may be provided only for $\tilde{\epsilon}' > 0$, i.e., for sufficiently small (on absolute values) potential energy \tilde{u} —for the right tail of the DF in

Fig. 6.1 The distribution function of potential energy: numerical integration of (6.1.21) in comparison to analytical expression (6.1.27)

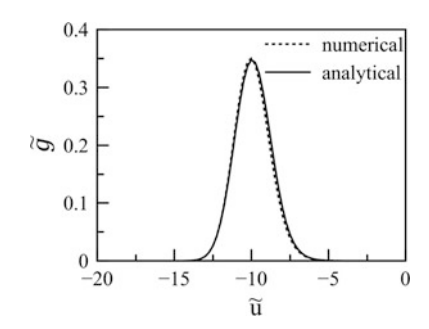


Fig. 6.1. This tail is "more important" in applications of the evaporation problem because usually particles with relatively low binding energy leave the surface.

Thereby, one can find coefficients for (6.1.28):

$$Q_n(\tilde{\varepsilon}') = \frac{2\tilde{t}^{3/2}}{\sqrt{\pi}} \frac{(-1)^n}{n!} \exp(-\tilde{\varepsilon}'\tilde{t}) \left[\tilde{t}^n \sqrt{\tilde{\varepsilon}'} - \sum_{i=1}^n K_{i,n} \frac{\tilde{t}^{n-i}}{\tilde{\varepsilon}'^{(2i-1)/2}} \right], \tag{6.1.29}$$

$$K_{i,n} = \frac{(2i-3)!!C_n^i}{2^i},\tag{6.1.30}$$

 $C_n^i = \frac{n!}{i!(n-i)!}$ is a binomial coefficient, and N!! is the so-called double factorial: the multiplication of all even numbers smaller than N, i.e., here:

$$(2i-3)!! = (2i-3) \cdot (2i-5) \cdot (2i-7) \cdot \dots \cdot 5 \cdot 3 \cdot 1, (-1)!! = 1.$$
 (6.1.31)

Thus, we have integral (6.1.23) in the form:

$$\frac{\sqrt{2\tilde{t}^3}}{\pi} \sum_{n=0}^{\infty} \int_{0}^{\infty} Q_n(\tilde{\epsilon}')(\tilde{\epsilon} - \tilde{\epsilon}')^n \exp\left(-\frac{(\tilde{\epsilon} - \tilde{\epsilon}')^2}{2}\right) d\tilde{\epsilon}. \tag{6.1.32}$$

Integrating carefully, we obtain the DF of potential energy as:

$$\tilde{g}(\tilde{u}) = \frac{\sqrt{2\tilde{t}^3}}{\pi} \sum_{n=0}^{\infty} Q_n(\tilde{\epsilon}') 2^{(n-1)/2} \left[\Gamma\left(\frac{n+1}{2}\right) + (-1)^n \gamma\left(\frac{n+1}{2}, \frac{\tilde{\epsilon}'^2}{2}\right) \right].$$
 (6.1.33)

Here, the incomplete gamma-functions (see Appendix B) are:

$$\Gamma(a,b) = \int_{b}^{\infty} t^{a-1} e^{-t} dt, \gamma(a,b) = \int_{0}^{b} t^{a-1} e^{-t} dt.$$
 (6.1.34)

Again, we should note that function (6.1.33) may be used only for $\varepsilon' > 0$, i.e., for $\tilde{u} > \tilde{u}_m - \tilde{\varepsilon}_m$.

Later, we will use the DF of potential energy in our problem—evaporation—but some parameters of (6.1.21) must be defined first. In (6.1.21) $\tilde{l}_m = \frac{\varepsilon_m - u_m}{\theta}$, and, obviously, $\varepsilon_m = 1.5T$ (see Chap. 2). We also need information about:

- The mean potential energy u_m .
- The fluctura θ .

As for fluctura, the question is complicated. In the following sections we establish some common principles for it, but do not provide full information. We hope that the final answers about this parameter will be understood sooner or later.

The determination of the average potential energy is a much simpler problem. Of course, this value could be obtained from numerical simulations. But can the information about \tilde{u}_m possibly be obtained from existing experimental data? Actually, the answer is not very complicated (and affirmative), but we will establish it in a long manner.

6.1.3 Analytical Description of Vaporization

First, we apply our theory—or, to be exact, consider a fact that not all of our initial arguments were quite solid, our ideas concerning the form of the potential energy DF are appropriate—for vaporization, which is a phase transition inside a volume.

Returning to the last question from the previous section, one may note that the answer is simple: it is easy to conclude that the average potential energy of a single particle is $\tilde{u}_m/2$ (because the mean potential energy of a given particle with other particles is \tilde{u}_m , and the calculation of the total potential energy of the system involves any pair of particles twice). Thus, it is clear (at first glance) that the latent heat of vaporization per a single particle, i.e., the binding energy, is $-\tilde{u}_m/2$. Consequently, $\tilde{u}_m = -2\Delta \tilde{H}$, where $\Delta \tilde{H}$ was measured in experiments.

Some people may object to this consideration.

In the simplest case of equilibrium $\theta = T$ (see above), i.e., $\tilde{t} = 1$. The DF of the binding energy for vaporized atoms (i.e., for the freed particles—for particles with positive total energy) must be obtained on account of the probability of particles being free $\int_U^\infty f(\varepsilon) d\varepsilon$. The corresponding DF is:

$$p(U) = g(-U) \int_{U}^{\infty} f(\varepsilon) d\varepsilon = g(-U) \frac{2}{\sqrt{\pi}} \Gamma\left(\frac{3}{2}, \frac{U}{T}\right).$$
 (6.1.35)

This function indicates the distribution of the binding energy for particles with s > 0. Thus, it is logical to assume that the average binding energy for such

particles (the vaporization energy per particle) must be calculated as the average value of the DF p(U):

$$\overline{U} = \int_{-\infty}^{\infty} Up(U) dU. \tag{6.1.36}$$

We try to obtain the mean value (6.1.36) analytically under some assumptions. At first, we will not find the average value directly: instead of the probable value of U [which is determined by (6.1.36)] we will find the most probable value, i.e., the value of U which corresponds to the maximum of the distribution p(U). This substitution is possible in our case because of the sharp peak of this DF. Thereby, we will find U_0 such that $\frac{\partial p(U)}{\partial U}\Big|_{U} = 0$.

Then, we represent the incomplete gamma function (see Appendix B) as:

$$\Gamma\left(\frac{3}{2}, \tilde{U}\right) \approx \sqrt{\tilde{U}} \exp(-\tilde{U}).$$
 (6.1.37)

For $|\tilde{u}_m| \gg 1$ we see from (6.1.25) that $\tilde{\epsilon}_0 \approx \tilde{u} + \tilde{l}_m = \tilde{l}_m - \tilde{U}$, and the last multiplier in expression (6.1.27) is:

$$\exp\left(-\tilde{\varepsilon}_0 - \frac{\left(\tilde{\varepsilon}_0 - \tilde{u} - \tilde{l}_m\right)^2}{2}\right) \sim \exp(\tilde{U} - \tilde{l}_m). \tag{6.1.38}$$

Consequently, combining (6.1.25), (6.1.35), (6.1.37) and (6.1.38), we have:

$$p(\tilde{U}) \sim \sqrt{\frac{\tilde{U}(\tilde{l}_m - \tilde{U})}{\frac{1}{2} + \frac{1}{4\tilde{\epsilon}_0^2}}} \left(1 + \operatorname{erf}\left(\sqrt{\frac{1}{4} + \frac{\tilde{\epsilon}_0^2}{2}}\right)\right). \tag{6.1.39}$$

At sufficiently large values of $\tilde{\epsilon}_0$ one may see that $\frac{1}{4\tilde{\epsilon}_0^2} \approx 0$ and $\operatorname{erf}(\sqrt{\frac{1}{4} + \frac{\tilde{\epsilon}_0^2}{2}}) \approx 1$. In other words, the dependence (6.1.39) actually has a form $p(U) \sim \sqrt{\tilde{U}(\tilde{l}_m - \tilde{U})}$, and the maximum of this function is reached at:

$$\tilde{U}_0 \approx \frac{\tilde{l}_m}{2} \approx -\frac{\tilde{u}_m}{2},$$
(6.1.40)

because $\tilde{\varepsilon}_m = 1.5 \ll \tilde{l}_m \approx -\tilde{u}_m$.

Thus, we finally obtain the result that had been predicted at the beginning of this section: the binding energy \tilde{U}_0 may be interpreted as the specific latent heat of vaporization. Consequently, the value of $-2u_m$ may be found in any reference data under the term "the specific enthalpy of vaporization."

In Sect. 6.1.6, the results of numerical simulations will be presented. From the National Institute of Standards and Technology (NIST) database, for argon at 100 K, we obtain $\Delta H/T = \tilde{U}_0 = 7.24$ K, thus, we will use $\tilde{u}_m = -14.5$ K in the following sections.

However, first we have to discuss an interesting question.

6.1.4 Sidestep: Trouton's Rule

In this section we provide a common consideration without any concretization of the DF. We think that it may be useful. To obtain some results we do not need to know any certain details of the DF; results may be obtained by common consideration. For this problem, only the following circumstances are related to an interesting feature of the average value of binding energy:

- The binding energy of a particle inside a liquid has a universal form for any substance.
- The spread of binding energy may be described by the scaling parameter U/T for any substance.

If the binding energy is parametrized by temperature, then the corresponding DF has the form p(U/T) with a normalizing factor A that can be found from the condition:

$$\int Ap(U/T)dU = 1, \qquad (6.1.41)$$

that is, A = C/T (where C is a constant). Thereby, for the mean value of U we have:

$$\overline{U} = \int AUp(U/T)dU = T^2 \int \frac{C}{T} \frac{U}{T} p\left(\frac{U}{T}\right) d\left(\frac{U}{T}\right) = CT \underbrace{\int xp(x)dx}_{\overline{x}}. \quad (6.1.42)$$

$$\frac{\overline{U}}{T} = C\bar{x}.\tag{6.1.43}$$

Thus, in the common case we see that the ratio \overline{U}/T is defined only by the constant C and the mean-integral value \bar{x} . For a universal DF p(U/T) both C and \bar{x} are the same for any substance. Consequently, (6.1.43) means that the ratio of the average binding energy to the temperature is the universal constant for any liquid.

A similar expression is known from experimental results under the name "Trouton's rule". For the latent heat of vaporization ΔH :

$$\frac{\Delta H}{T} = B. \tag{6.1.44}$$

Note that there also exists an analog for melting; the corresponding rule is named after Richard (Swalin 1972). Sometimes correlations of the kind in (6.1.44) are described as obvious, in style "it's evidently the latent heat of vaporization must be proportional to the temperature," but, in our opinion, such a consideration is only a half truth. The meaning of Trouton's rule is not the proportionality $\Delta H \sim T$, but the fact that the constant of proportionality is the same (of course, nearly the same) for any substance.

Is the constant B truly the same for any substance? For instance, in Swalin (1972) one may find the value B=87.9 J/(mol K). However, this "constant" is not strictly a constant. This parameter slightly depends on the substance: in Table 6.1 we present the parameter B for liquids of inert substances (calculated from NIST data). We may also calculate that parameter in numerical simulations, but there is no point here: the coincidence with experimental data will be tested by comparison of the simulation results with analytical expressions containing an experimental value of $u_m=-2\Delta H$.

First, as we see, B differs from the "universal" value presented above; the difference is huge for helium, but helium is a special liquid in many aspects. For other elements variations are not dramatic.

Next, the ratio \overline{U}/T slightly varies with temperature for the same substance. This fact can be easily predicted: really, the mean value of binding energy \overline{U} (hidden in constant C) depends on temperature, because the binding energy depends on the distance between particles, which depends on temperature.

Trouton's rule, of course, is only a rule—not a law. However, the ability of the theory presented above to predict such formulae make us sure that the method of DFs can be used for a more complicated problem—evaporation.

However, one parameter is still undefined and unexplained.

6.1.5 Fluctura

As we have seen above, in equilibrium the DF for the additional fluctuation of potential energy (see Sect. 6.1.2) can be represented in the form:

$$g_{e}(u) = \frac{1}{\sqrt{2\pi\theta}} \exp\left(-\frac{(u - u_{m})^{2}}{2\theta^{2}}\right).$$
 (6.1.45)

Table 6.1 Parameter *B* in Trouton's rule

Substance	Не	Ne	Ar	Kr	Xe	Rn
B, J/(mol K)	19.8	65.8	74.5	75.4	76.5	79.5

We termed parameter θ here as a "fluctura" because θ determines additional fluctuations of potential energy. In this section we try to establish the value of fluctura both in the equilibrium liquid and in the evaporated one.

At equilibrium, fluctura determines the magnitude of the potential energy fluctuations. Usually, temperature *T* plays an analogic role in statistical mechanics. We may mention "the Boltzmann principle" or "the Gauss principle" from which the condition:

$$\theta = T \tag{6.1.46}$$

follows for normal-distributed fluctuations. Indeed, if we return to our analogy with the pendulum, we may conclude that the average energy on this vibrational degree of freedom is *T*.

Formula (6.1.45) is obtained for homogenous systems. However, in the evaporated fluid one may expect the parameters of a liquid to be different at various distances from the evaporation surface: significant heat flux brings the liquid out of equilibrium. Thus, parameters u_m and θ of the DF (6.1.45) are not constants, and here we establish a connection between them.

There are two reasons for variations of θ :

- A physical reason. Due to non-equilibrium, fluctura may differ from temperature and, moreover, may differ from point to point in the non-equilibrium liquid.
- A calculation-based reason. We always determine statistical parameters of a medium by averaging across a spatial volume or time interval (or both). Thus, we may mix the variations of mean potential energy u_m with the general parameter θ that describes fluctuations of u.

For the last option, the correlation of u_m and θ is clear. Fluctura θ describes fluctuations around the average level of energy u_m . Variations of level u_m itself—for example, between two neighboring points—leads to an increase of these fluctuations: the range of values u is wider now. Thus, if u_m varies then θ increases (independently of the sign of Δu_m between these two points) relative to the homogenous case $u_m = \text{const.}$

Let us turn these physical ideas into mathematical formulae. At first, from the consideration provided above, it follows that $\Delta \theta = f\left(\left(\Delta u_m\right)^2\right)$. The deviation of fluctura cannot depend on the sign of Δu_m without depending on an increase or decrease of u_m in two consequent layers.

Let us suppose that in two neighboring layers the parameters in (6.1.45) are u_m^a and u_m^b , and the difference between them is small: $|\Delta u_m| = |u_m^b - u_m^a| \ll |u_m^a|, |u_m^b|$. Thus, we consider two infinitesimal narrow layers at constant average potential energy. Note that these conditions are needed only for the correctness of approximation using the resultant distribution function: the main conclusion—the expression for variation of fluctura—stays the same even for large deviations of Δu_m .

For certainty, let $\Delta u_m > 0$. Let the fluctura in each of these two separated layers be θ , i.e., in each layer we have DF (6.1.45) with θ and u_m^a or u_m^b . Thus, the DF of

potential energy for the particle which may be found with equal probability both in layer a and layer b is:

$$g_{\varepsilon}(u) = \frac{1}{2\sqrt{2\pi}\theta} \left[\exp\left(-\frac{(u - u_m + \xi)^2}{2\theta^2}\right) + \exp\left(-\frac{(u - u_m - \xi)^2}{2\theta^2}\right) \right], \quad (6.1.47)$$

where $u_m = \frac{u_m^a + u_m^b}{2}$ and $\xi = \frac{u_m^b - u_m^a}{2}$.

We will try to approximate DF (6.1.47) using the normal DF with the new fluctura Θ (since we can state right now that $\Theta > \theta$):

$$g_{\varepsilon}'(u) = \frac{1}{\sqrt{2\pi}\Theta} \exp\left(-\frac{(u - u_m)^2}{2\Theta^2}\right). \tag{6.1.48}$$

Formally, we must define Θ in (6.1.48) with (6.1.47), i.e.:

$$\Theta^2 = \int_{-\infty}^{\infty} (u - u_m)^2 g_\varepsilon(u) du.$$
 (6.1.49)

Substituting (6.1.47) into (6.1.49), we get for each term of kind:

$$\int_{-\infty}^{\infty} (u - u_m)^2 \exp\left(-\frac{(u - u_m \pm \xi)^2}{2\theta^2}\right) du = \int_{-\infty}^{\infty} (x \mp \xi)^2 \exp\left(-\frac{x^2}{2\theta^2}\right) dx (6.1.50)$$

three integrals:

$$\int_{-\infty}^{\infty} x^2 \exp\left(-\frac{x^2}{2\theta^2}\right) dx = \sqrt{2\pi}\theta^3, \tag{6.1.51}$$

$$\int_{-\infty}^{\infty} 2x\xi \exp\left(-\frac{x^2}{2\theta^2}\right) dx = 0, \qquad (6.1.52)$$

$$\int_{-\infty}^{\infty} \xi^2 \exp\left(-\frac{x^2}{2\theta^2}\right) dx = \sqrt{2\pi}\theta \,\xi^2. \tag{6.1.53}$$

Finally, we have dispersion (6.1.49):

$$\Theta^2 = \theta^2 + \xi^2. \tag{6.1.54}$$

Thus, if the mean energy in two neighboring layers differs by 2ξ , then the average dispersion in the combined layer is determined by (6.1.54) (and it depends

on ξ^2 , of course). Note again that there are no principal restrictions for ξ there (i.e., for Δu_m), only from the viewpoint of the correctness of (6.1.45).

We may—moreover, we must—generalize our result on many layers with different energy values u_m . Suppose that we have 2N layers with a linear distribution of energy u_m between them: from u_m^{\min} to u_m^{\max} . That is, the mean potential energy in these layers is $u_m = \frac{u_m^{\min} + u_m^{\max}}{2}$, and we want to approximate the DF of potential energy for a particle which may be found in any of these layers with equal probability:

$$g_{\varepsilon}(u) = \frac{1}{2N} \sum_{i=1}^{N} \frac{1}{\sqrt{2\pi\theta}} \exp\left(-\frac{(u - u_m \pm i\xi)^2}{2\theta^2}\right),$$
 (6.1.55)

[where $\xi = \frac{u_m^{\text{max}} - u_m^{\text{min}}}{2N}$; both signs in the exponent must be accounted for in each term of the sum in (6.1.55)] by the normal DF (6.1.48) with dispersion (6.1.49). Analogically with previous considerations, this method gives us:

$$\Theta^2 = \theta^2 + \frac{1}{N} \sum_{i=1}^{N} (i\xi)^2.$$
 (6.1.56)

Finally, me must take limits for $N \to \infty$. Because:

$$\lim_{N \to \infty} \sum_{i=1}^{N} i^2 = \lim_{N \to \infty} \frac{N(N+1)(2N+1)}{6} = \frac{N^3}{3},$$
 (6.1.57)

we finally obtain:

$$\Theta^2 = \theta^2 + \frac{(\Delta u_m)^2}{12},\tag{6.1.58}$$

where $\Delta u_m = u_m^{\text{max}} - u_m^{\text{min}}$.

Thus, we may approximate the DF of potential energy in layers with different u_m by a single Gaussian function with the extended dispersion—the significantly increased dispersion Θ^2 .

In Fig. 6.2 we represent DF (6.1.55) with $u_m^{\min} = 8$, $u_m^{\max} = 12$, $\theta = 1$ and the Gaussian (6.1.48) with $u_m = 10$ and $\Theta = 1.53$ [according to (6.1.58)]. One can see that the agreement is rather good, and it is possible to use the Gaussian DF even for such a large difference Δu_m between average energy in this layer. Note that this method can be applied also for cases when mean energy varies in the same spatial layer over time: all our calculations stay the same, only the sense of DF (6.1.55) changes. By the way, it is difficult to say what kind of averaging is more important at the vicinity of the evaporation surface: the spatial averaging or the temporal one. In such an irregular area, both sorts of averaging may be applied.

In fine, we must discuss the value θ in the infinitely thin layer (or at the single instant). It is hard to give a certain instruction to calculate this quantity for a

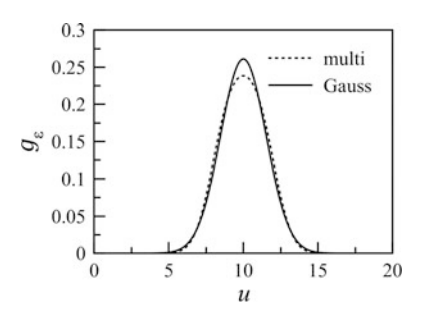


Fig. 6.2 Averaging of the distribution functions: single Gaussian as the approximation of the distribution function of potential energy in the non-uniform layer. The dashed curve represents distribution function (6.1.55) obtained by averaging many distribution functions with different mean potential energy from $u_m^{\min} = 8$ to $u_m^{\max} = 12$. Solid curve represents the Gaussian (6.1.48) with $u_m = 10$ and increased dispersion Θ^2 from (6.1.58)

non-equilibrium case. Possibly, it would differ from temperature T significantly, but we have no theory to define θ in terms of its dependence on a heat flux or gradient of the number density, etc.

Numerical simulations seem to be useless for solving this problem, because the layers, in which the DF has been calculated, are significantly wider, and in these thick layers:

- The difference Δu_m always exists.
- The distribution of u_m along the layer is likely non-linear; i.e., correlation (6.1.58) is only an approach here, because we cannot define the exact probability for a particle to be in each layer with certain u_m .

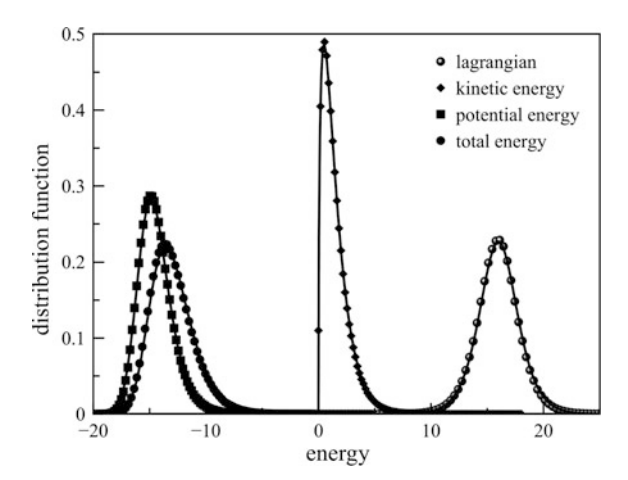
Thereby, the "calculation disturbance" of the calculated parameter θ is strong, and θ can only be evaluated approximately with (6.1.58) through the calculated value Θ . In other words, it is hard to extract θ from the calculated (in numerical experiments) value Θ with an appropriate accuracy.

In any way, numerical simulations are necessary to test many details of the model. Questions have been accumulated. Is the DF of the Lagrangian symmetrical? Does the DF of potential energy obey the (6.1.21)? Can fluctura really be put as $\theta = T$ in an equilibrium system? How does the DF of potential energy vary at the vicinity of the surface of the evaporated liquid?

6.1.6 Numerical Simulations

The method of molecular dynamics (MMD) is almost an exact equivalent to real experiments. Nuances of construction of the interaction potential do not matter if we want to examine such basic features of the system.

Fig. 6.3 Distribution functions from this chapter for an equilibrium liquid. Energy is given as the ratio of the temperature of the system *T*. DF, distribution function



In this section we present our results of numerical simulations for liquid argon (see Chap. 4 for details of the numeric scheme, etc.).

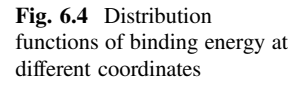
First, we investigate the equilibrium liquid at temperature T=100 K, without evaporation. The results of numerical simulations are compared to DF (6.1.21) with $\theta=T$ and $\tilde{u}_m=-14.5$; thus, there are no adjustment parameters in our analytical function. The results are presented in Fig. 6.3.

There are four DFs shown in Fig. 6.3: the DF of the Lagrangian of a particle $\tilde{l}=\tilde{\epsilon}-\tilde{u}$ (6.1.5); the DF of the kinetic energy (6.1.11); the DF of the potential energy (6.1.21); and the DF of the total energy (6.1.6) $\tilde{s}=\tilde{\epsilon}+\tilde{u}$. All the DFs are normalized on unity. Despite the fact that the aim of this section is the DF of potential energy, the main DF in Fig. 6.3 is the DF of the Lagrangian: the assumption about its symmetricity is the fundament for all other DFs.

Two of the four DFs from Fig. 6.3 were obtained under the assumption about independent quantities ε and u. Actually, this fact is not so obvious, and this question was the subject of discussion between Loschmidt and Boltzmann: in his work (Loschmidt 1876) Loschmidt argued that kinetic energy is independent of potential; now only a single paragraph of this work is remembered—the one about the reverse motion of particles. Thus, we may see that these two types of energy are indeed independent, because the calculated DF of the total energy and of the Lagrangian coincide with the results of numerical simulations.

The inferences of the good coincidence between numerical and analytical DFs are:

- The DF of the Lagrangian is symmetrical.
- That $\theta = T$ for equilibrium, condensed media.
- The kinetic energy and potential energy are independent, as established by (6.1.5–6.1.6).
- The DF of the potential energy (6.1.21) is correct.
- The MDF is also correct.



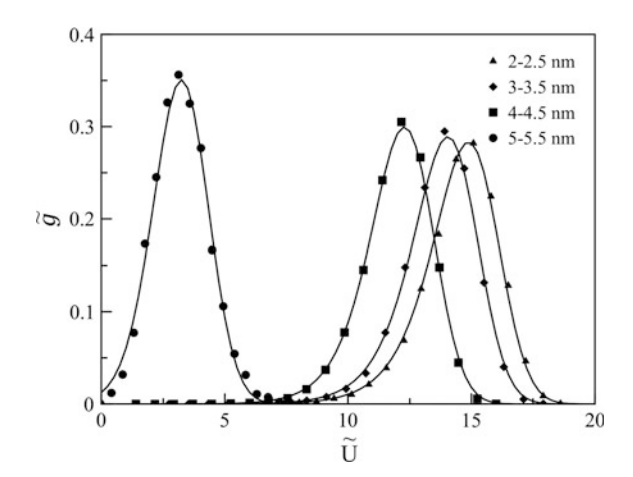


Table 6.2 Parameters for distribution function (6.1.18) for different layers in the liquid

z (nm)	2-2.5	3–3.5	4-4.5	5-5.5
Θ (Κ)	100	105	115	200
\tilde{u}_m	-14.5	-13.7	-12.0	-3.2

Next, we provide the results of numerical simulations for an evaporated liquid. We calculate the potential energy DFs in the 0.5-nm layer—from the solid surface to the evaporation surface. The results are presented in Fig. 6.4. To compare analytical results with these simulations, parameters \tilde{u}_m and Θ were calculated from the numerical simulations for each layer; the results are presented in Table 6.2; note that z=2 nm corresponds to the solid surface and z=5 nm corresponds to the liquid surface. Quantities U are values u_m from Table 6.2 multiplied by Θ .

It should be remembered that $\tilde{u}_m = u/\Theta$, not u/T.

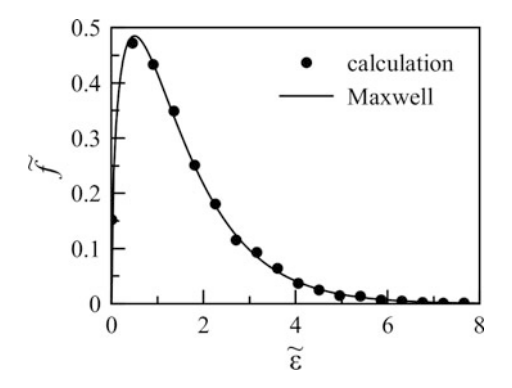
As we see from Fig. 6.4, we can sufficiently describe all "experimental" numerical functions with (6.1.21) with Θ derived from the same numerical experiment. On the other hand, as was discussed in the previous section, it is important to calculate the "true" value of fluctura θ . Let us try here.

From the data in Table 6.2 we can find that in the last layer the mean potential energy varies from $U_m^{\text{max}} = 13.7T$ to $U_m^{\text{min}} = 6.4T$. Thereby, we can see from (6.1.55) that the assumption for any layer that $\theta = T$ gives:

$$\Theta = \sqrt{T^2 + \frac{7.3^2 T^2}{12}} \approx 2.3T,\tag{6.1.59}$$

which is close to the value in Table 6.2 (where $\theta = 2T$, so the difference is $\sim 10\%$), especially considering the fact that we do not know for certain the value of Δu_m in this layer (other uncertainties were discussed above). We cannot pretend we have better accuracy; thus, we may conclude that the assumption $\theta \approx T$, for a non-equilibrium system, does not contradict numerical simulations.

Fig. 6.5 Distribution function of kinetic energy nearby the evaporation surface. The Solid curve is the Maxwellian distribution function at the temperature of the bulk of the liquid



The DF of the kinetic energy at the surface layer is presented in Fig. 6.5: we see that the calculated DF coincides with the MDF at temperature *T*. Thus, the temperature of the surface does not differ significantly from the temperature in the "bulk" of the liquid: one of the reasons for this is a thin layer of liquid on the heated solid surface.

We see that for the last layer $\Theta \approx 2T$. It is also interesting how the potential energy of a particle depends on its number of neighbors in this layer. We divide the ensemble from the near-surface layer into two groups:

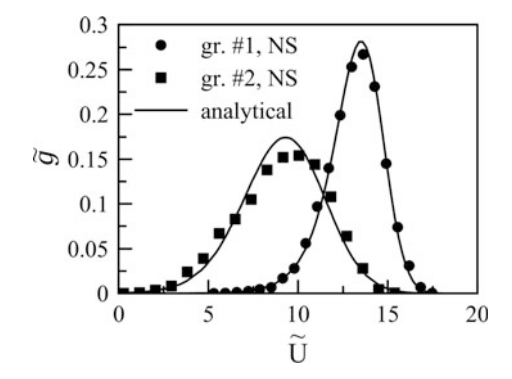
- Particles with ≥ 10 neighbors (group #1).
- Particles with <10 neighbors (group #2).

Next we construct DFs separately for each group of particles (each group consists of $\sim 10^4$ particles); the result of numerical simulations is shown in Fig. 6.6. Analytical DFs were calculated with parameters:

$$\tilde{U}_m = 13.7$$
 and $\Theta = T$ for group #1.
 $\tilde{U}_m = 4.6$ and $\Theta = 2T$ for group #2.

One can see that the sub-ensembles of particles have significantly different parameters, especially \tilde{U}_m . This issue has a clear explanation: the binding energy of a

Fig. 6.6 Distribution functions for particles with different numbers of neighbors: $N \ge 10$ (circles) and N < 10 (squares). Results obtained using numerical simulations



particle is associated with its number of neighbors, thus, the perceptible deviations in the binding energy may be observed only if the particle has a significantly different number of neighbors nearby, i.e., for a relatively low number density—for group #2. One may see that for these particles Θ coincides with the existing value (see above).

In the dense sub-system, for a large number of particles in the vicinity of a given particle (group #1), strong fluctuations of potential energy are impossible and we see the usual picture: $\Theta = \theta = T$.

To avoid misunderstanding, we have to note that the results in Fig. 6.6 were not obtained from the same numerical simulations as the data in Fig. 6.4: a thicker surface layer was considered in the first case. Among other inferences, the diversity of the numerical simulation results indicates a problem concerning the definition of the term "surface of a liquid" (see next sections).

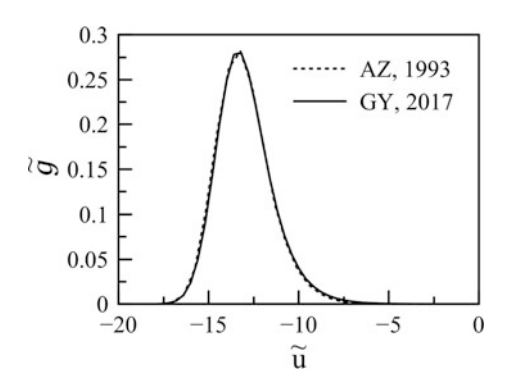
Finally, we may conclude that the results of the comparison are encouraging. All our theoretical results provided confirmation of the following good aspects, i.e., the DF of the Lagrangian, the DF of the potential energy g(U), the fluctura $\theta = T$; as well as the not so good aspects, i.e., at the surface the averaged DF for changing u_m may be approximated by g(U) but with an enlarged value of Θ , and there is no way to as yet avoid this averaging or to extract the exact value of θ from Θ). The bad news is really not all that bad, and hopefully sometime in the future the problems associated with g(U) may be solved.

We are almost ready to solve problems of evaporation itself. One additional step remains.

6.1.7 Numerical Simulations (Continued)

Actually, this section should be titled "Numerical simulation (beginning)" because the work by Anisimov and Zhakhovskii (1993) was a predecessor to our work. In their article the DF of the potential energy was obtained in standard (for a numerical simulation) coordinates. However, after recalculation, we can represent this numerical simulation data with our traditional variables $\tilde{u} = u/T$; the result is shown in Fig. 6.7.

Fig. 6.7 The dashed curve represents the distribution function of the potential energy from 2. The solid curve represents distribution function (6.1.21) from this book



Note that from a technical point of view, the method of numerical simulation in Anisimov and Zhakhovskii (1993) significantly differs from ours. However, as we see, the coincidence of the results is good. Unfortunately, we do not know of other works where the DF of the potential energy has been obtained: an additional comparison would not be out of place here.

There is an additional moral to this story: the dimensionless variables must be chosen carefully. The traditional manner to construct scales from the parameters of the LJ has, at least, two weak points:

- The results are unclear for a direct physical analysis.
- LJ-derived scales may not hold real physical invariants of the problem.

6.2 Number of Evaporated Particles

6.2.1 The Possibility to Escape

As was shown in Chap. 5, the probability to leave a liquid surface may be expressed as:

$$w = \frac{1}{2\sqrt{\pi}} \Gamma\left(\frac{1}{2}, \frac{U}{T}\right),\tag{6.2.1}$$

where U is the work function and T is the temperature of the surface. For U=0, we see that w=1/2: the particle leaves the liquid with a 50% probability (if its velocity is directed away from the liquid). Of course, this value has no sense for a given particle: in the next moment in time a particle, which had a negative z-projection velocity, may obtain the "correct" direction and escape (but, it might not—see below). Function (6.2.1) establishes a ratio of the total number of particles which leave the surface at this moment.

To use (6.2.1), we must know two parameters: U and T. As for the last quantity, the following chapters will show that it is not obvious what exactly we should insert into (6.2.1) for T. However, here we are only concerned about the binding energy U. Previously, in Chap. 5, we thought that it was sufficient to find (in reference) a certain value of U, and thereby solve the problem. However, in the previous section we found that the work function is indeed a DF, and the function g(U) was constructed there. Thus, one may suppose that it is enough to calculate the mean value $\overline{U} = \int Ug(U) dU$, with the function $w(\overline{U})$ providing an answer: the probability for a particle to escape.

However, the problem is still not that simple. The probability to escape cannot be found so easily. The total DF—distribution of the velocity \vec{v} (i.e., of kinetic energy ε) and the binding energy U—may be expressed under the assumption of the independence of \vec{v} and U:

$$dn = n_0 g(U) f(\vec{v}) dU d\vec{v}, \tag{6.2.2}$$

where *n* is the number density of particles in a liquid. Consequently, the number density of particles with sufficient velocity on the *z* axis $v_z \ge v_0 = \sqrt{\frac{2U}{m}}$:

$$n = n_0 \int_{-\infty}^{\infty} g(U) \left[\int_{v_0}^{\infty} \int_{-\infty}^{\infty} \int_{-\infty}^{\infty} f(v_x) f(v_y) f(v_z) dv_x dv_y dv_z \right] dU, \qquad (6.2.3)$$

where we integrate for U from $-\infty$, that is, we also consider particles with positive potential energy. For such particles the probability to escape is 1/2 (these particles leave the surface if their velocity $v_z > 0$); finally, we have:

$$n = n_0 \int_{-\infty}^{\infty} g(U)w(U)dU.$$
 (6.2.4)

Thus, according to (6.2.4), we need the function:

$$\overline{w(U)} = n/n_0 = \int_{-\infty}^{\infty} w(U)g(U)dU$$
 (6.2.5)

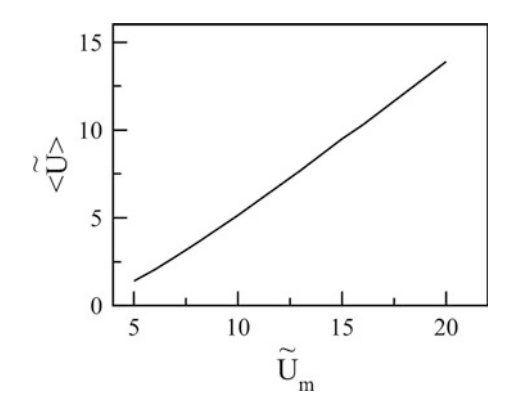
rather than $w(\overline{U})$. However, we can always avoid this difficulty with a standard trick: defining the mean binding energy $\langle U \rangle$ from the equality $w(\langle U \rangle) = \overline{w(U)}$; with such redefining we can use a much more convenient correlation (6.2.1) for our estimations.

Which value is greater: $w(\overline{U})$ or $\overline{w(U)}$? This is an easy question to answer; one may solve this without any calculations. Function $w(\overline{U})$ defines the probability of escaping from the surface for particles with the same energy \overline{U} . The mean value $\overline{w(U)}$ considers the probability of detachment both for particles with high binding energy $U > \overline{U}$ [with low and very low values of w(U)] and low binding energy $U < \overline{U}$ [with high values of w(U)]. It is obvious, that due to the strong non-linearity of function w(U) the main contribution to $\overline{w(U)}$ is defined by low values of W(U). Consequently, one may conclude that $\overline{w(U)} > w(\overline{U})$ or even $\overline{w(U)} \gg w(\overline{U})$.

To strengthen these considerations with calculations we might consider, e.g., the case for $\overline{U}=14.5$ where we have $w(\overline{U})=3.6\times 10^{-8}$ while $\overline{w(U)}=4.6\times 10^{-6}$, i.e., it is 100 times greater. Using definitions for $\langle U\rangle$ (see above), we obtain $\langle U\rangle\approx 9.5$ —this binding energy corresponds to a value $w(\langle U\rangle)=\overline{w(U)}$; see also Fig. 6.8.

Thus, due to the DF of potential energy, the flux from the interface is determined par excellence by the particles with low binding energy. The mean value \overline{U} determines only the shape of the DF of binding energy, not the probability w itself.

 $\begin{array}{l} \textbf{Fig. 6.8} \quad \text{The dependence of} \\ \frac{\left<\tilde{U}\right>}{w(\tilde{U})} \text{ , such that } w(\left<\tilde{U}\right>) = \\ \hline {w(\tilde{U})} \text{ , on the mean value of} \\ \text{potential energy } \tilde{U}_m \end{array}$



Can we now conclude that we have enough information to calculate the probability of detachment? We have a DF of potential energy (6.1.21) and we have correlation (6.2.5) which determines this probability. Are we done with our consideration?

No, not at all. Not all the nuances have been discussed yet. Actually, on the surface of the liquid, the DF of the binding energy differs from g(U) because of an interesting reason which will be discussed further on in this chapter.

However, first, let us consider the terms "surface" and "detachment" more closely.

6.2.2 The Surface Layer of a Liquid

What is the surface? This is the real question. In numerical simulations one may construct a correlation function for particles and try to extract the coordinates of the interface from it. However, this method is insufficient for us, because we are interested in the probability of a particle leaving a liquid, not in the abstract "surface" itself. Thus, we mean that the "surface" is the area of a liquid from which the escape of a particle may be possible. This means that other particles on the surface do not prevent this escape directly by colliding with the escaping particles on their way out.

The particles of a liquid surface have finite lifespan because of evaporation, but this time is sufficiently long because of the small probability of escape. Atoms from deep in a liquid arrive at its surface, where they may be evaporated sooner or later. Thus, we must take into account that particles "move through" a surface layer: they enter the surface with a significant binding energy, but, with time, this energy decreases as the particle moves toward a more "hollowed" zone at the surface. Note that any motion—in the literal sense of the word—is not necessary: the number of neighbors also may vary with the same result—decreasing or increasing potential energy. We showed earlier (see Sect. 6.1.6), that at the surface layer some particles have a lower number of neighbors; these particles are the first candidates to escape.

Thus, we have a problem: the DF at the liquid surface is probably poor in terms of low-energy particles—particles may leave a liquid with higher binding energy, they cannot decrease their energy further because they leave a liquid earlier, with larger binding energy.

This scheme becomes significant for a small binding energy U [with large probabilities (6.2.1)] and prevents establishing a stable DF with a tale of negative U (i.e., with positive potential energy) or even with a significantly smaller positive U. However, as was discussed above, this part of the DF is the most important for evaporation. Consequently, we cannot determine g(U) for a surface directly, without complementary assumptions. Additional treatment is needed.

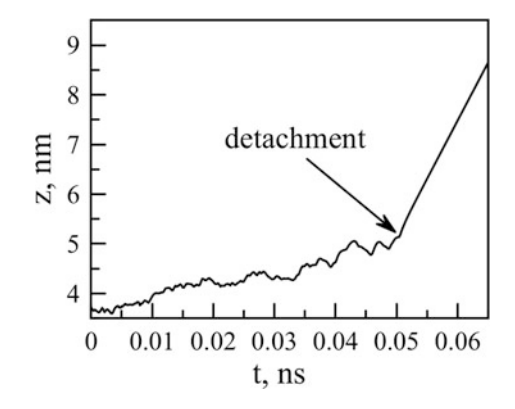
However, before we proceed with this treatment we have to consider an unexpected object. To the "low-energy tail" problem we may add the problem of uncertainty of the term "escape." Do we understand what the "work function for the particle of the liquid" really is?

6.2.3 The Moment of Escape

This sudden problem concerns the fact that an atom in a liquid does not have a stable binding energy. An atom moves, atoms around it move, thus, the binding energy of the atom variates. If this atom leaves a liquid, from which moment of time must we consider the process of detachment? That is, which value of binding energy must be put in formulae like (6.2.1)?

The work function may be defined as the work needed to remove a particle from condensed phase to infinity. This definition looks logical until we take into account the distribution of potential energy in the condensed phase. A given particle has different potential energy at different points and at different moments in time. In order to try to determine a work function in a numerical experiment, for example, we must clearly define the moment of detachment.

Fig. 6.9 A particle moves toward the surface and evaporates; the moment when z(t) becomes a linear function may be accepted as the moment of detachment (approximately)



Let us look at Fig. 6.9, where coordinate z of the particle (axis \vec{z} is directed normally to the liquid surface) is shown to be dependent on time. Details of the numerical simulation (argon at T = 100 K) can be found in the previous section; we represent the function z(t) for the particle that has been evaporated.

As we see in Fig. 6.9, a particle moves toward the surface. One may note the absence of clear separation between the oscillations and the jumps: the dependence z(t) is quite uniform. The question raised at the beginning of this section may be asked in other way: what point on the graph in Fig. 6.9 corresponds to the moment of detachment? Generally, one may choose—arbitrarily—any point on this graph as the "detachment point," but one method is preferred.

It is logical to assume that after evaporation the particle becomes free (no forces affect it), and its velocity is a constant. We can establish this point in Fig. 6.9, but actually we need to look for some moment before this—when the particle was part of the liquid (the first moment of time when the total energy of the particle becomes a constant).

In Fig. 6.10 the evolution of the potential energy of a particle is presented (here $\tilde{u} = u/T$). There is no straight correlation between $\tilde{u}(t)$ and z(t) in Fig. 6.9 until the moment $t \sim 0.04$ ns, when a particle arrives in the zone with high fluctuations both of potential energy and coordinates; evidently, this is a "rarefied" region where such fluctuations are possible.

Of course, not every particle that reaches the surface leaves it. Perhaps, the most dramatic situation is illustrated in Fig. 6.11: a particle gets very close to the surface, but in this case "very close" is not close enough. As we see in Fig. 6.11, this unsuccessful atom returns to the bulk of the liquid; possibly, it will receive a second chance at some other moment in time.

To illustrate the term "surface" in our sense (i.e., the place from which detachment is possible), let us look at Fig. 6.12. Here, one particle leaves the surface at coordinate $z\approx 4.7$ nm, while another atom at $z\approx 5.2$ nm. Thus, the width of the surface layer ~ 0.5 nm: this is a wide layer, considering all the previous results for the DF. The potential energy DF in the evaporation region represents a combination of various DFs with different mean energy; this DF is widened relative to the DF which is unique to the mean potential energy because of the averaging of different DFs (see previous section). This widening is not artificial as a whole: we cannot really establish a single DF with $\Theta=\theta$ here.

The next problem concerning the determination of the detachment moment is shown in Fig. 6.12. One may see deviations from the linear dependence z(t) after the moment of detachment: this atom interacts with another atom; thus, its potential energy variates. Only after ~ 0.01 ns does this atom become absolutely free.

Thus, we may conclude that the moment of departing cannot be fully formalized. We can determine this moment only approximately, but it is difficult to turn this explanation into an algorithm. On the other hand, in the frame of our approach, we do not need a certain value of the work function derived from numerical simulations. We need a DF of binding energy and we must take into account all the nuances of the process of evaporation that have been discussed in this and previous sections.

6.2.4 Deformation of the Distribution Function

Now we will try to take into consideration the scheme that was described above: the particle has two opportunities at the evaporation surface—to decrease its binding energy or to escape at its existing binding energy (of course, a third one—to increase its binding energy—exists too, but here we consider only the most probable situations).

Two issues have to be accounted for:

- At a surface, a particle may obtain a lesser binding energy U_2 only if it has larger energy $U_1 > U_2$ prior to that.
- At a surface, a particle may leave a liquid with a larger binding energy U_1 .

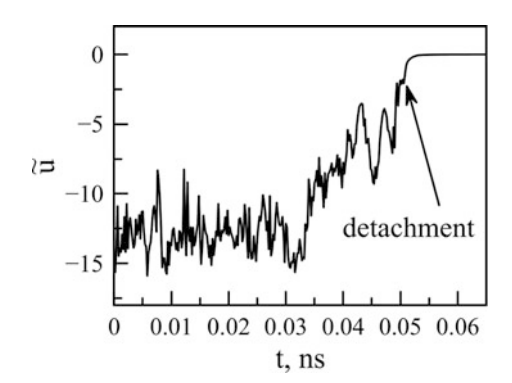
This is a simplified construction, of course. However, under this assumption we may redesign the surface DF of binding energy. Let the number of particles with binding energy be $U + \Delta U$ with $g(U + \Delta U) \mathrm{d} U$. Thus, the number of particles that can obtain lesser energy is $(1 - w(U + \Delta U))g(U + \Delta U)\mathrm{d} U$; we consider only non-escaped particles. Finally, assuming that $\Delta U \to 0$ we have:

$$g^{\rm sf}(U) = g(U)(1 - w(U)). \tag{6.2.6}$$

Thus, we take the DF (6.1.16) and reform it using factor (1 - w), which takes into account the probability of staying at the surface. This is a model approach, and we believe that it may be significantly improved in the future.

An interesting question is what probability of escape w must be used in (6.2.6). The answer depends on the kinetic energy of a particle near the surface: if any change in the velocity is accompanied by variation in the binding energy, then this probability may be expressed by (6.2.1); otherwise—if the particle can change its velocity (especially, the direction of its velocity) and hold its binding energy at the same value—we must double the probability (6.2.1) to obtain w for (6.2.6). Based on the material from the previous subsection, we prefer the first choice: the

Fig. 6.10 The evolution of the potential energy of a particle (this figure corresponds to Fig. 6.9)



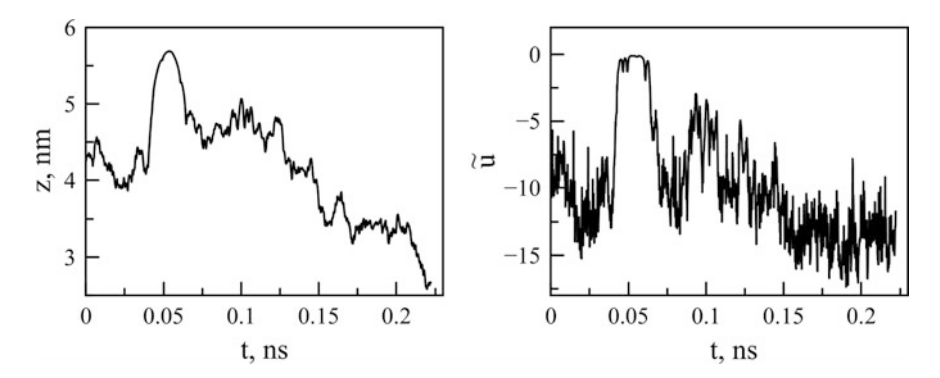


Fig. 6.11 A particle at the surface; its maximum potential energy was $\tilde{u} \approx -0.1$. However, in fine, it was an unsuccessful attempt to escape: the particle returning to the inner layers of the liquid

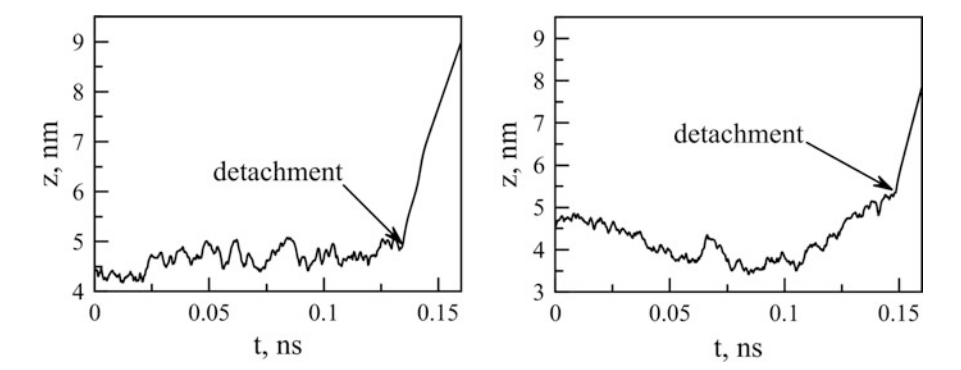


Fig. 6.12 Various coordinates for detachment. Look at the left-hand picture: here detachment does not mean the absence of any interaction with other atoms

probability of the departure from any state at the surface cannot exceed 1/2; we cannot suppose that at the next moment of time the velocity changes direction and the act of detachment becomes possible: that will be a new state with a different binding energy. For example, take a look at the fate of the unhappy particle in Fig. 6.11: not quite taking its chance.

We present the surface DF (6.2.6) in Fig. 6.13. As we see, the deviations from DF (6.1.16) may be distinguished only for a small binding energy. However, despite this fact, deviations between the total number of evaporated particles in different DFs is significant: for DFs in Fig. 6.13 the difference is $\sim 15\%$.

In fine, we may repeat that the scheme described in this section is far from ideal, of course. Improvements are needed; a more complicated model for the DF of binding energy near the evaporation surface may be achieved later.

6.2.5 Number of Particles at the Surface

We discussed the probability of escaping w in detail above. However, one problem remains: what is the number density of particles at the surface? If we want to calculate the number of evaporated particles with an equation like (6.2.4), i.e., $n = n_0 w$, then we also need $n_0 = n^{\rm sf}$ —the number density on the evaporation surface. As was considered in the previous section, the number of neighbors a surface particle has may be lower than for particles within the bulk of a liquid. Thus, the number density at the surface $n^{\rm sf}$ differs from the bulk value $n^{\rm b}$ that may be calculated with reference data through density ρ and mass of molecule m:

$$n^{\rm sf} \neq n^{\rm b} = \rho/m. \tag{6.2.7}$$

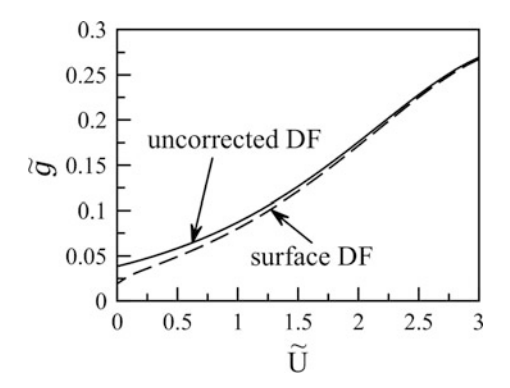
Moreover, numerical simulations are not much help because the surface layer is tiny and irregular; it is hard to distinguish the surface layer and to count the particles in this layer, but it is much harder to define the volume of this surface layer. We suppose that the error in the estimation of $n^{\rm sf}$, by numerical simulations, is $\sim 10\%$ at least; in the worst case an uncertainty of $\sim 100\%$ may be expected: these problems ruin all possible attempts to eject $n^{\rm sf}$ from the numerical simulation results. The last reason to decline the numerical simulation as a source of such uncertain information: definitely, in this way $n^{\rm sf}$ becomes an additional free parameter.

We may choose another way, however.

To estimate the number density of particles at the surface, we assume that the binding energy of a particle is proportional to the number density at this region of a liquid. Thus, we suppose that $U = U_1 n$, where U_1 is a constant. Therefore, we have that in the bulk of the liquid $U^b = U_1 n^b$, while at the surface $U^{sf} = U_1 n^{sf}$. Thereby, we obtain a correlation:

$$n^{\rm sf} \approx n^{\rm b} \frac{U^{\rm b}}{U^{\rm sf}}.\tag{6.2.8}$$

Fig. 6.13 The low-energy tail of distribution functions: for the standard uncorrected distribution function (6.1.20) and for distribution function (6.2.6). DF, distribution function



Here, we replace the symbol "=" with " \approx " because this consideration is, of course, based on assumptions. In (6.2.8) the energy of the surface layer may be determined with much higher accuracy than the volume V of such an undefined structure as the liquid surface (to calculate the number density n = N/V).

The second advantage of the approach in (6.2.8) is that we have one fewer free parameter, because now only U^{sf} will be determined in numerical simulations.

However, we may use (6.2.8) in another way. If we represent the surface of a liquid as a rough cut of the condensed medium, then we may conclude that the number of neighbors at the surface is N/2, where N is the number of neighbors in the bulk of the liquid. Consequently, the binding energy at the surface must be half the binding energy in the depth of the liquid, i.e., $U^{\rm sf} = U^{\rm b}/2$. This expression may be a simple estimation of the binding energy at the surface; indeed, we see from our numerical simulations (see Sect. 6.1) that $U^{\rm sf} \approx 6.4T$ while $U^{\rm b} = 7.24T$. Not bad for such a simple estimation.

6.3 Mass and Energy Fluxes from an Evaporation Surface

6.3.1 Evaporation, Condensation and Their Sum

Let us forget, for a minute, all the information from the previous chapter and from the beginning of this chapter, i.e., suppose that we do not know anything about the DFs of the velocities of evaporated particles. All that we have now are the expressions for the fluxes corresponding to the MDF.

In gas with a MDF the total flux is equal to zero, but this zero consists of two parts: of equal fluxes in opposite directions with each of them being easily evaluated according to the Hertz formula $j = n\bar{\nu}/4$. Thus, in such a manner we may calculate a flux from a vapor on a surface, i.e., try to calculate a condensation flux on a surface.

Take a closer look at the values that follow from this equation. For the mass flux of water vapor (molecular mass $m = 3 \times 10^{-26}$ kg) we have, e.g., at a pressure $p = 10^3$ Pa temperature T = 300 K:

$$J = p\sqrt{\frac{m}{2\pi T}} \approx 1 \frac{\text{kg}}{\text{m}^2 \text{s}}.$$
 (6.3.1)

In equilibrium, or in the vicinity of an equilibrium state, one may expect a value of the same order of magnitude for a reverse flux, i.e., for an evaporation flux. These are enormous fluxes, actually. In experiments, the total mass of the fluxes for both p and T is less than $1 \text{ g/m}^2/\text{s}^1$. From the discrepancy between the calculation flux (6.3.1) and experimental value, one may make one of two conclusions:

• If it is assumed that the total flux has the same order of the evaporation or condensation flux; then we obtain that the real fluxes on an interface are $J^{\text{cond}} =$

 γJ , where $\gamma \ll 1$ is the so-called condensation (or the evaporation) coefficient, i.e. the flux of particles absorbed by the interface differs significantly from the flux of particles dropped on a surface.

• If it is assumed that the total flux J^{tot} is the difference between two close quantities J^{ev} and J^{cond} , then the value of the total flux is very sensitive to the variation of the parameters of the liquid or of the gas.

These alternatives are very unpleasant. As for the first alternative, we will consider such a problem with the evaporation/condensation coefficient in Chap. 7. The condensation coefficient is the property of the interface, this is an external parameter for Molecular Kinetic Theory (MKT): we cannot calculate the condensation flux without this quantity, and it is impossible to extract γ from the solution of the kinetic equation. One may suppose that this quantity can be obtained by experimentation. Yes, there exists a large volume of experimental data for the condensation coefficient ... with many values of γ ; for water there exists are range of values $\gamma = 0.01-1$; this uncertainty is appropriate only if you want to set γ equal to any value you want, for serious calculations such a spread is a problem. The last chance is to find the condensation coefficient from the results of numerical simulations (see Chap. 7), but here this is a forbidden trick. Thus, we cannot determine yet, whether the value for the condensation coefficient $\gamma \ll 1$ or not.

However, we may calculate (at least, estimate) the evaporation flux with all the formulae from Chap. 5 and this chapter without any additional parameters like γ (see next sections). Consequently, we may determine which estimation is correct: $J^{\rm tot} \sim J^{\rm ev}$ or $J^{\rm tot} \ll J^{\rm ev}$.

Note that if $J^{\rm tot} \ll J^{\rm ev}, J^{\rm cond}$ then it would be very difficult to measure the coefficient γ because of the strong sensibility of $J^{\rm tot}$ to $J^{\rm ev}$ or $J^{\rm cond}$. Let the absolute deviation of the flux be ΔJ ; then the relative deviation of the total flux is:

$$\frac{\Delta J^{\rm tot}}{J^{\rm tot}} \sim \frac{\left(J^{\rm ev} + J^{\rm cond}\right)}{|J^{\rm ev} - J^{\rm cond}|} \max\left(\frac{\Delta J^{\rm ev}}{J^{\rm ev}}, \frac{\Delta J^{\rm cond}}{J^{\rm cond}}\right). \tag{6.3.2}$$

This well-known expression determines the relative error of calculation $J^{\rm tot}$ by subtraction $(J^{\rm ev}-J^{\rm cond})$. Of course, nature runs this mathematical operation without any calculation errors; expression (6.3.2) demonstrates the sensibility of the total flux to the values of the evaporation or condensation flux. In the case of $|J^{\rm ev}-J^{\rm cond}| \ll (J^{\rm ev}+J^{\rm cond})$ the relative oscillations of a total flux will be enormous.

The fact that the mass flux (6.3.1) is huge may also be understood with the following consideration. The mass balance for the droplet may be written as the balance equation:

$$\frac{\mathrm{d}m}{\mathrm{d}t} = -JS,\tag{6.3.3}$$

where *m* is the mass of the droplet and *S* the surface area. With $dm/dt = d(\rho V)/dt = \rho S dm/dt$ we have:

$$\rho \frac{\mathrm{d}R}{\mathrm{d}t} = -J,\tag{6.3.4}$$

that is, the dependence of the radius of our droplet on time and the time of the full evaporation are:

$$R(t) = R(0) - Jt/\rho,$$
 (6.3.5)

$$t_{\text{max}} = \frac{R(0)\rho}{I}.$$
 (6.3.6)

Let us consider a droplet of ~ 1 mm size (i.e., with a surface area of $\sim 10^{-6}$ m² and mass of $\sim 10^{-3}$ g). For the flux $J \sim 1$ $\frac{\text{kg}}{\text{m}^2 \text{s}}$ we get $t_{\text{max}} = 1$ s. Thus, a droplet with such a radius will be fully evaporated in ~ 1 s.

However, here we have assumed that the evaporation flux is a constant, i.e., the temperature of the surface has not varied during the evaporation process. One can imagine two opportunities:

- The surface temperature must continuously drop during the evaporation process because the most "hot" particles have left it.
- The surface temperature is constant, because a stationary state of evaporation is established with time, i.e., the temperature of the surface may be found through the equality of the conductive heat flux $q^c = \lambda \frac{T T_{sf}}{\delta}$ and that of evaporation $q^{ev}(T_{sf})$; from this point of view the temperature of the interface will be constant due to the heat flux from the bulk of the liquid.

The stationary state of evaporation is a problematic matter (see next section), and the energy balance strictly depends on the conditions of the solid surface under the liquid. However, the second option to address the dilemma presented above looks more adequate. The temperature of the interface tends to decrease due to evaporation, but also tends to increase due to the heat flux from deep layers in the liquid. Atoms at the surface receive energy from their neighbors, and one may expect that the temperature of the evaporation surface will not drop continuously, unless the liquid holds heat within itself. Thus, the temperature of the evaporated liquid drops, but there is a limit to this decrease.

Anyway, the temperature of the interface differs from the temperature of the main mass of a liquid, and this is an interesting point.

6.3.2 Temperature of the Evaporation Surface

The following fact may be confusing if it is the first time you have stumbled upon it. From the early work of T. Alty and co-workers in the 1930s we know that the temperature of the surface of evaporated water may be ~ 0 °C or even lower (see

Chap. 7). For example, in Fang and Ward (1999) a minimum temperature was established of -12 °C and in Duan et al. (2008) the temperature of the water's surface was measured as low as -16 °C.

Thus, the temperature of the interface may reach values significantly below zero, and one may expect that at such temperatures the liquid must freeze. However, experiments show that this tiny surface layer would still be in a liquid state.

In our numerical simulations (results presented in Sect. 6.1) the heated solid surface was at a distance of ~ 1 nm from the liquid surface, thus, a significant temperature drop was not observed: the temperature difference between the bulk of the liquid and the surface was ~ 1 K. When calculating the parameters of the evaporating liquid we neglected this difference.

However, in real life, when you pour a glass of water and leave it in open air at room temperature, it is naive to expect that the evaporation flux must be determined for 25 $^{\circ}$ C: the temperature of the surface may be significantly lower than this value; see below for details of how the evaporation flux varies when the temperature of the surface changes by 10 $^{\circ}$ C.

Practical tip: because evaporation is a very efficient cooling process, you may leave an open can of Coca-Cola outside the fridge and expect the temperature of the drink to remain lower than the room temperature by several degrees. In cold season, this may be enough.

6.3.3 Fluxes from the Evaporation Surface

With all our knowledge, let us return to the method of derivation of the DF of velocity from Chap. 5. For a liquid phase we have:

$$dn = n_0 f(v_x) f(v_y) f(v_z) g(U) dv_x dv_y dv_z dU$$
(6.3.7)

with MDFs f(v); n_0 is the number density of atoms at the liquid surface. The DF of velocity \vec{V} in a vapor can be obtained if we replace the velocities in (6.3.7) (axis z is directed normally from the surface of a liquid to vapor):

$$v_x = V_x, v_y = V_y, v_z^2 = V_z^2 + \frac{2U}{m} = V_z^2 + v_0^2.$$
 (6.3.8)

Thereby, (6.3.7) becomes:

$$dn = n_0 f(V_x) f(V_y) \frac{f(V_z) V_z}{\sqrt{V_z^2 + v_0^2}} g(U) dV_x dV_y dV_z dU.$$

$$(6.3.9)$$

If we only want to obtain the DF of velocity V_z , as in Chap. 5, then we have to integrate the DF F from (6.3.8) for all other variables, keeping in mind that $V_z > 0$ and U > 0. Because $\int_{-\infty}^{\infty} f(V_{x,y}) dV_{x,y} = 1$, one may obtain:

$$f(V_z) = n_0 \sqrt{\frac{m}{2\pi T}} V_z \exp\left(-\frac{mV_z^2}{2}\right) \int_0^\infty \frac{\exp(-U/T)}{\sqrt{V_z^2 + 2U/m}} g(U) dU.$$
 (6.3.10)

Thus, for the case of large $V_z^2 \ll 2U/m$ we have the integral:

$$f(V_z) = n_0 \frac{mV_z}{2\sqrt{\pi T}} \exp\left(-\frac{mV_z^2}{2T}\right) \int_0^\infty \frac{\exp(-U/T)}{\sqrt{U}} g(U) dU, \qquad (6.3.11)$$

or, with dimensionless variable $\hat{U} = U/T$:

$$f(V_z) = n_0 \frac{mV_z}{2T\sqrt{\pi}} \exp\left(-\frac{mV_z^2}{2T}\right) \int_0^\infty \frac{\exp(-\hat{U})}{\sqrt{\hat{U}}} g(\hat{U}) d\hat{U}. \tag{6.3.12}$$

Considering the fact that for $\hat{U}\gg 1$ —the condition that was practically used above, because $V_z^2\sim T/m$ —we may represent $e^{-\hat{U}/T}/\sqrt{\hat{U}}\approx \Gamma(1/2,\hat{U})$ (see Appendix B), we see that (6.3.11) is equivalent for:

$$f(V_z) = \frac{mV_z}{T} \exp\left(-\frac{mV_z^2}{2T}\right) n_0 \int_0^\infty \underbrace{\frac{1}{2\sqrt{\pi}} \Gamma\left(\frac{1}{2}, \hat{U}\right)}_{w(U/T)} g(\hat{U}) d\hat{U}. \tag{6.3.13}$$

Function (6.3.13) differs from its analog (5.2.14) by the normalizing factor. Function (5.2.14) was normalized on unity, while (6.3.12) was normalized on the number density of the escaped particles n; one may compare n from (6.3.13) with expressions from Sect. 6.2 (of course, we may replace g(U) in (6.3.13) with a more complicated function discussed in Sect. 6.2.4). In other words, in this section we have obtained the same formulae as in previous sections: here, more directly from the mathematical point of view, and previously, from the physical point of view.

Note that we may also use the DF of the irregular surface (5.2.23) instead of the first component of (6.3.13).

Thereby, we are ready to calculate fluxes from the evaporation surface. All components for this were obtained in Chap. 5 and earlier sections of this chapter.

For the mass flux in the common case we have the expression:

$$J = mn\bar{V},\tag{6.3.14}$$

with the mean velocity for the flat evaporation surface:

$$\bar{V} = \sqrt{\frac{\pi T}{2m}},\tag{6.3.15}$$

or for the irregular surface:

$$\bar{V} = \sqrt{\frac{8\Upsilon_z}{\pi m}}. (6.3.16)$$

For the heat flux we obtain for the flat surface:

$$q = nT\sqrt{\frac{25\pi T}{8m}},\tag{6.3.17}$$

while for the irregular surface:

$$q = n[\Upsilon_x + 2\Upsilon_z] \sqrt{\frac{8\Upsilon_z}{\pi m}},\tag{6.3.18}$$

where Υ_x and Υ_z are parameters of the DF of velocity at the irregular surface.

Let us estimate the value of the evaporation flux, e.g., for water at 300 K; here we mean the temperature of the surface. For the number of the evaporated particles $n=\frac{n_0}{2\sqrt{\pi}}\Gamma(\frac{1}{2},\frac{U}{T})$ we have $U\approx 3700\,\mathrm{K}$ (see Sect. 6.2.1) and $n_0\approx 3\times 10^{28}\,\mathrm{m}^{-3}$, so $n\approx 10^{22}\,\mathrm{m}^{-3}$ (for simplification, we use the number density n_0 in the bulk of the liquid). Then, the average velocity (6.2.15) is $\bar{V}\approx 460\,\mathrm{m/s}$ and the mass flux (6.2.14) $J\approx 140\,\frac{\mathrm{g}}{\mathrm{m}^2\,\mathrm{s}}$. As a comparison, for a temperature 310 K we have $J\approx 220\,\frac{\mathrm{g}}{\mathrm{m}^2\,\mathrm{s}}$.

For the heat flux, we have from (6.2.17) $q \approx 1.6 \times 10^4$ W/m² for 300 K and $q \approx 2.5 \times 10^4$ W/m² for 310 K.

Thus, the "clean" evaporation flux is huge. At this rate, a glass of water of mass 200 g and surface area $\sim 4 \times 10^{-3}$ m² would fully evaporate in 6 min. Of course, in reality that would not be the case due to the condensation process. Therefore, the total flux would be much lower than the value calculated above.

The high evaporation (and condensation) fluxes cause some problems to the description of condensation. Let us consider the mixture of water vapor and air (under "air" here and below we mean "dry air"), then suppose the absence (for some reasons) of evaporation. Vapor molecules condense—and do it intensively. Due to condensation, the concentration of vapor decreases near the surface. In a gas, pressure levels itself at the speed of sound, but it does not concern the number density of components: the concentration of water vapor molecules recreates

because of a much slower process—diffusion. This process of diffusion controls the number density of vapor molecules close to the interface and, consequently, the condensation flux. As stated, condensation is a more complicated problem than evaporation.

In fine: we see that the evaporation flux exceeds the total flux by a few orders of magnitude. In real situations the evaporation process always runs alongside condensation and we may expect that in equilibrium the total flux is equal to zero: the evaporation flux is counterbalanced by the condensation flux. Is this really the case?

6.4 Evaporation and Condensation: the Balance Equations

In this section we discuss a fundamental problem. This is not a problem about te special conditions at the interfacial surface. This problem does not concern the fluxes of evaporation and condensation and the balance between them. This problem is whether balanced equations actually exist?

This is partially a provocative question. There exists an equilibrium state when the total fluxes of a given quantity vanish and the quantity itself does not vary with time. However, is there really a state where the fluxes are constant, or does a fluctuating regime exist with a total flux operating as a periodic function of time with a zero mean?

6.4.1 Attractors of a Dynamic System

It is a well-known fact that a dynamical system may have different types of ultimate trajectory (attractor).

The first type of attractor is a stable point: the system goes to its limiting parameters, and once these parameters have been achieved, the system "stops:" there being no further variations. Inevitable fluctuations cannot drive this system out of equilibrium: these deviations fade with time, and the system returns to a stable state.

The second type of attractor is a cycle: parameters of the system vary periodically. There may be one independent frequency or more, it does not matter: any quality of a system undergoes oscillations.

The third type of attractor is a strange (chaotic) attractor. This is a very unusual thing, which has been discovered at least twice (by Lorenz in 1963 for the first time and later by Ruelle and Takens in 1971). This type of attractor may possibly describe a phenomenon called "turbulence" (but it might not)—this subject is absolutely out of the scope of this book.

Possibly, the simplest example of a dynamic system which demonstrates all three types of attractors is:

$$\frac{dx}{dt} = yz - ax,$$

$$\frac{dy}{dt} = by - xz,$$

$$\frac{dz}{dt} = xy - cz.$$
(6.4.1)

This dynamic system was discussed, for instance, in Turner (1996). System (6.4.1) may have clear physical explanations: each pair of quantities affects the third quantity, while this third quantity tends to increase (the "+" sign in (6.4.1) on the right-hand side at the corresponding term for y) or decrease (a "-" sign for x and z) by itself.

This is a dissipative system if -a+b-c<0. The type of attractor depends on parameters a, b and c. There is a stable point (0,0,0) at b<0 and fixed but unstable points $(\pm\sqrt{bc},\pm\sqrt{ac},\pm\sqrt{ab})$ (for each stable point the number of pluses is odd) at, for example, a=5,0< b<0.71 and c=1. Dynamical system (6.4.1) has limiting cycles (for instance, see Fig. 6.14 for a=5,b=1.2 and c=1) or a strange attractor (for a=5,b=1.9 and c=1 see the attractor in Fig. 6.14).

This is only an example: non-linear dynamic systems have reach dynamics as a rule. Despite this fact, for unknown reasons, physicists almost always expect a stable point as a unique solution for any problem they encounter. Many analytical treatments of dynamic systems begin with the words "now we will find a stationary solution for system X ...," but rarely is the stability of the point or the uniqueness of the attractor studied (except for special problems where instability is the very point of the study). From this position, any non-point attractor should be considered as a confusing abnormal special case.

However, of course, there may be other types of attractors than the stable point. Periodic attractors may be expected for various physical problems; one of these being evaporation.

6.4.2 What We May Expect for Phase Transitions

As discussed above, one should distinguish the evaporation flux (i.e., the flux of the evaporated particles) and the flux on the evaporation surface (i.e., the total flux, consisting of evaporation and the condensation fluxes).

We expect equilibrium and, consequently, we expect zero total fluxes on the evaporation surface. In the language of DFs, we expect equalities in the moments of DFs for evaporation and the condensation fluxes.

$$\int_{0}^{\infty} mv f^{\text{ev}}(v) dv = \int_{0}^{\infty} mv f^{\text{cond}}(v) dv, \qquad (6.4.2)$$

$$\int_{0}^{\infty} 2mv^{2} f^{\text{ev}}(v) dv = \int_{0}^{\infty} 2mv^{2} f^{\text{cond}}(v) dv, \qquad (6.4.3)$$

$$\int_{0}^{\infty} \frac{mv^2}{2} v f^{\text{ev}}(v) dv = \int_{0}^{\infty} \frac{mv^2}{2} v f^{\text{cond}}(v) dv.$$
 (6.4.4)

We added condition (6.4.3) for the equality of the pressures (with a little variation, it can be interpreted as the equality of temperatures); thus, we expect that the first three moments of the evaporation distribution function (EDF) $f^{\text{ev}}(v)$ and the condensation distribution function (CDF) $f^{\text{cond}}(v)$ will coincide.

To analyze these equations in the common case we must take into account the fact that DFs for the evaporated particles and for the condensed ones can be different functions of velocity. The EDF was defined in Chap. 5, but here we cannot give a specific expression for the CDF (see also Chap. 7, where we also cannot give a specific expression for the CDF, because this book is about the "kinetics of evaporation", not the "kinetics of condensation"), so will consider the general case for uncoinciding DFs.

The EDF is fully determined by two parameters: the number density of the evaporated particles n^{ev} and the temperature of the liquid surface T; for the simplest case this function is:

$$f^{\text{ev}}(v) = n^{\text{ev}} \frac{mv}{T} \exp\left(-\frac{mv^2}{2T}\right). \tag{6.4.5}$$

Thereby, only two parameters of the EDF may be defined. Suppose that the pressure and the fluxes of mass and energy in the vapor phase are determined, thus, in this case, it is impossible to satisfy (6.4.2)–(6.4.4) completely: one or more expressions in these equations will turn to inequalities.

For instance, let us assume that the DF in a vapor phase is a MDF. Thus, we desire the balanced equations for the fluxes on the interface:

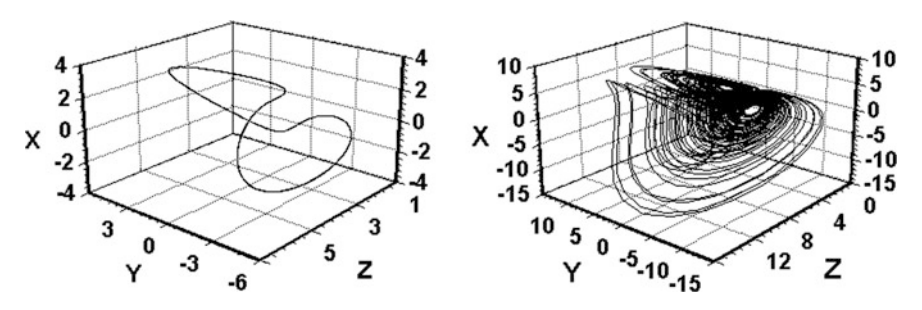


Fig. 6.14 The limiting cycle (left) and the strange attractor (right) for (6.4.1)

$$n_l \sqrt{\frac{\pi T_l}{2m}} \equiv j^{\text{ev}} = j^{\text{cond}} \equiv n_v \sqrt{\frac{T_v}{2\pi m}},$$
 (6.4.6)

$$4n_l T_l \equiv p_l = p_v \equiv n_v T_v, \tag{6.4.7}$$

$$n_l T_l \sqrt{\frac{25\pi T_l}{8m}} \equiv q^{\text{ev}} = q^{\text{cond}} \equiv n_\nu T_\nu \sqrt{\frac{2T_\nu}{\pi m}}$$
 (6.4.8)

We may put $T_l = T_v$ and $n_l = n_v/4$ (from (6.4.7), see Chap. 7 for details), but in this case we see that $j^{\rm ev} \neq j^{\rm cond}$ and $q^{\rm ev} \neq q^{\rm cond}$; the fluxes differ by tens of percent. There may be various speculations made from balanced (6.4.6–6.4.8), but the simplest conclusion is the inexistence of them in principle.

Thus, if it is difficult (moreover, impossible) to satisfy all conditions (6.4.2–6.4.4) for different DFs f^{ev} and f^{cond} , then we are inclined to suppose that the equilibrium is a state where only average fluxes are equal: $\overline{j^{\text{ev}}} = \overline{j^{\text{cond}}}$, $\overline{q^{\text{ev}}} = \overline{q^{\text{cond}}}$, but where momentary quantities fluctuate.

In the following subsections we try to estimate the period of such fluctuations.

6.4.3 Timescale from the Viewpoint of a Vapor

The period of oscillations may be estimated in various ways and, strictly, there may exist numerous specific time frames for this problem. Actually, a full theoretical picture must be painted first, including all equations, boundary conditions, etc. However, this is too complicated a task for us now; many aspects of the near-interface processes must be solved first. We restrict ourselves here with a much simpler problem: here we want to estimate only the period of oscillations of the condensation flux at the interface.

Assume that the limiting process at the interface is establishing an "equilibrium" value for vapor density, e.g., when evaporation is too intensive, then the density of the vapor will increase until the condensation flux equalizes the evaporation one, and vice versa. In other words, if the evaporation (or condensation) flux spontaneously varies, then a new value of density will be established after a certain period of time; this time is the point of our treatment here, because the timescale for the establishment of a vapor density value may be considered as the characteristic time for the evaporation-condensation problem as a whole.

Let us consider an evaporating droplet of surface area *S* in the vapor phase of volume *V*. The vapor obeys the Clapeyron equation, i.e.:

$$p = \frac{NT}{V}. (6.4.9)$$

Assume that due to some fluctuation the flux on the interface increased (or decreased). The number of vapor particles that appear due to evaporation (or disappear because of condensation) is:

$$\frac{\mathrm{d}N}{\mathrm{d}t} = jS,\tag{6.4.10}$$

because, as was discussed in the previous section, the total flux is much less than the momentary evaporation (or condensation) flux.

The flux on the interface—both of evaporation and of condensation—may be estimated as:

$$j \sim \frac{p}{\sqrt{2\pi mT}},\tag{6.4.11}$$

where strong equality arises between the condensation of vapor and the Maxwellian distribution of velocities. Thus, we may estimate the timescale from the equation $\frac{dN}{dt} \sim \frac{N}{\tau}$, and from (6.4.7) with (6.4.6) and (6.4.8) we have for the required timescale the estimation:

$$\tau \sim \frac{N}{iS} \sim \frac{V}{S} \sqrt{\frac{2\pi m}{T}}.$$
 (6.4.12)

For example, for a water $(m \sim 3 \times 10^{-26} \text{ kg})$ droplet of size $\sim 1 \text{ mm}$ (i.e., $S \sim 10^{-6} \text{ m}^2$) in a volume of $\sim 1 \text{ L}$ (i.e., $V \sim 10^{-3} \text{ m}^3$) we obtain $\tau \sim 7 \text{ s}$. Considering all the approximations, it is more appropriate to state that for real conditions this timescale is $\sim 1-10 \text{ s}$.

Returning to the beginning of this section, we may conclude that τ may serve as an estimation for the period of oscillations due to the slow "adjustment" of a vapor phase to variations of fluxes at the interface.

Note that only a pure vapor in the absence of a buffering gas was treated above. If diffusion of vapor molecules is a vital part of a process (for instance, for a vapor in the air, see Sect. 6.3), then the timescale may be estimated directly through the diffusion coefficient *D*:

$$\tau_{\text{diff}} \sim \frac{L^2}{D}.\tag{6.4.13}$$

Usually, in gases $D \sim 0.1 \, \mathrm{cm^2/s}$, and for spatial scales of $L \sim 1-10 \, \mathrm{mm}$ we obtain $\tau_{\mathrm{diff}} \sim 0.1-10 \, \mathrm{s}$. Thus, we may conclude that the gaseous phase may provide oscillations with periods of $\sim 1 \, \mathrm{s}$ (with an order of magnitude spread).

At least for completion's sake, we should examine the timescale for processes in the liquid phase.

6.4.4 Timescale from the Viewpoint of a Liquid

The limiting process in the evaporating liquid is the cooling caused by evaporation. The variation of the temperature of the liquid mass m due to the heat flux q through the surface area S is:

$$c_p m \frac{\mathrm{d}T}{\mathrm{d}t} = qS. \tag{6.4.14}$$

Let us consider variations of temperature at the surface: fast atoms leave the surface, and the temperature of the surface decreases. Then, because of the heat flux from the bulk of the liquid to the liquid surface, the temperature of the surface will increase; evaporation rate grows, and so on.

As was discussed in Sect. 6.3, the heat fluxes on the interface are huge, so we may assume that the limiting process (i.e., the slowest process) is the heat conductance from the liquid. Thus, from (6.4.14) we have the timescale of the process directly:

$$\tau \sim \frac{c_p \rho}{\lambda} \delta^2 = \frac{\delta^2}{a}.$$
 (6.4.15)

where ρ is the density, λ is the thermal conductivity of the liquid and $a = \frac{\lambda}{\rho c_p}$ is the thermal diffusivity; the last quantity is $\sim 10^{-7}$ m²/s, thus, the value of τ depends on δ —the "thickness of the interface."

We must note that:

- The parameter δ is small; it may be $\sim 1\text{--}10$ nm or even 100 nm. Anyway, the answer for τ would be the same in any case: this timescale is very small and these time variations may be better observed in numerical simulations (where the total time interval for calculations may be ~ 1 ns) than in experiments.
- Any estimations like (6.4.15), which imply a definite scale for a diffusion process, strictly, are not fully acceptable, because the character of the time-space variations have a self-similar form for their Boltzmann variable x^2/t , i.e., due to (1) the non-linear character of dependence (6.4.15) and (2) the uncertainty of the spatial scale we have significant uncertainty for the timescale.

Comparing results from this section with results from the previous one, it is easy to conclude that the condensed phase briefly "adjusts" to the variation in external (or, as in this case, of eternal) conditions. However, the gaseous phase cannot repeat such a trick, consequently, changes to its parameters lead to a significant lag for any dynamic processes.

6.4.5 The Simple Experiment

All philosophers and some physicists believe that a theory must be supported by experiments. This optimistic positivism excludes such a factor as vitality, which usually is a feature of any non-contradictory theory. As a rule, a single experiment tests only a single point of a theory, and this one-to-one combat adds nothing to a theory as a whole. Even in the worst case, a theory may survive by mutating, holding its basic principles untouched. Indeed, it is very hard to kill a theory with an

experiment, despite the idealistic view of philosophers. Moreover, sometimes a theory strikes back, see Chap. 8.

Here, we present some experimental results for the temperature of a wet thermocouple. Here we used a chromel–alumel thermocouple with a radius of 0.5 mm, its inertial time was determined as ~ 0.5 s.

We put the thermocouple's tip into hot water (\sim 40 °C) and then released it from the vessel, holding it at a height of \sim 1 cm above the interface for minutes. A droplet with a radius of \sim 1 mm on the tip of the thermocouple was allowed to evaporate, but, because of the vicinity of the hot evaporating liquid surface, vapor condensed on the droplet too. Thus, the surface of the droplet represented the battle ground for evaporation and condensation processes.

The temperature of the thermocouple dropped until a quasi-equilibrium state was established. We discussed this process in Chap. 1 from another point of view: at the early stages of the investigation of evaporation we wondered how it was possible that the temperature of the evaporated liquid be lower than the temperature of the surrounding air. Here we treat such tiny matters as fluctuations.

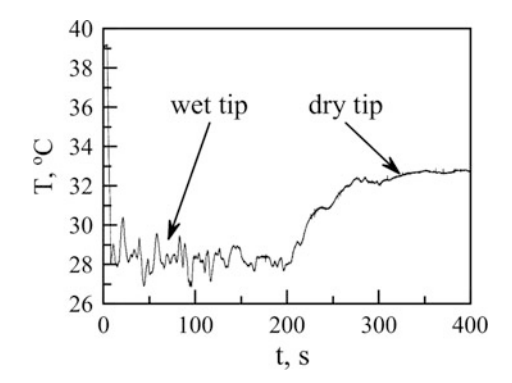
At a quasi-steady-state (we suppose that it is more correct to term this process in such a way) one could see oscillations in the temperature of the thermocouple (see Fig. 6.15). We propose several reasons for these oscillations:

- Oscillations of the cold wires in the thermocouple.
- Convection processes.
- Oscillations caused by condensation—evaporation processes.

The first of these reason may cause a temperature oscillations up to ~ 0.5 °C, but no higher. Both the first and the second reasons could be manifested in both a wet and dry thermocouple. However on dry tip we see (and not in every experiment) weak oscillation less than 1 °C. On the wet thermocouple we always observe oscillations by several degrees. Thus, as Sherlock Holmes taught us, we have to admit the last unfalsified version.

This last unfalsified version, considering the volume of our chamber was ~ 1 L, leads us to the estimation that was made above: the period of oscillation must be $\sim 1-10$ s, this value is significantly higher than the inertial time of the

Fig. 6.15 Temperature of a wet thermocouple over a liquid surface



thermocouple. We can see the corresponding frequencies on the experimental graph (Fig. 6.15).

However, we prefer to soften our conclusion. This is a very simple experiment, and many factors must be examined before a final conclusion be stated. It is more convenient to say that the hypothesis that has been proposed in previous sections does not contradict these experiments.

6.4.6 Fluctuations with Temperature

It is useful to understand how fluctuations in temperature, or of the work function, affect the evaporation flux:

$$j = n\bar{\nu}, \ n = n_0 \frac{1}{2\sqrt{\pi}} \Gamma\left(\frac{1}{2}, \frac{U}{T}\right).$$
 (6.4.16)

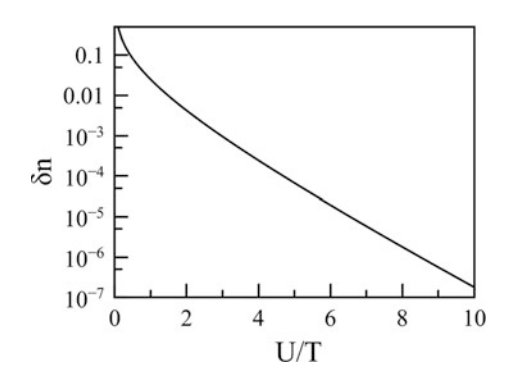
It is evident that small changes in the temperature of the surface do not significantly affect the average velocity \bar{v} or the number density of the liquid at the surface n_0 . However, if the temperature increases by a small value, how does it influence the total number of evaporated particles through the term containing the gamma function?

Usually, we have to deal with a situation where U/T > 1. In the case where argument of an incomplete gamma function is sufficiently large, we can represent the number density in a more suitable form as:

$$n \approx \frac{n_0}{2\sqrt{\pi}} \sqrt{\frac{T}{U}} \exp\left(-\frac{U}{T}\right).$$
 (6.4.17)

The difference between $\delta n = \Delta n/n_0$ in (6.4.16) and (6.4.15) is shown in Fig. 6.16. In simple terms, if U/T > 1 then this difference is practically negligible.

Fig. 6.16 The difference between exact (6.4.16) and approximation (6.4.17)



Thus, with (6.2.17) we can estimate the influence of temperature on the particle efflux. We have:

$$\frac{\mathrm{d}n}{\mathrm{d}T} = \frac{n_0}{2\sqrt{\pi}} \frac{U}{T^2} \left(\frac{1}{2} \left(\frac{T}{U} \right)^{3/2} + \left(\frac{T}{U} \right)^{1/2} \right) \exp\left(-\frac{U}{T} \right),\tag{6.4.18}$$

$$\frac{1}{n}\frac{dn}{dT} = \frac{U}{T^2}\left(1 + \frac{1}{2}\frac{T}{U}\right). \tag{6.4.19}$$

The dependence (6.4.18) is illustrated in Fig. 6.17 for different values of the work function U.

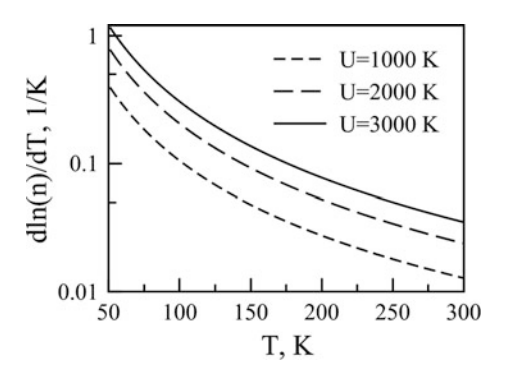
We see that at temperatures of ~ 100 K the variation of 1 K leads to a change of evaporation flux of the order of 10%. This fact helps us to understand the variations in the flux with time: because the evaporated particles remove a lot of energy (only high-energy particles can leave the liquid), the temperature of the surface decreases, and in Fig. 6.17 we can see the corresponding decrease in evaporation flux. Later, due to the heat flux from the bulk of the liquid, the temperature returns to its original level, and the process continues (see previous section).

The next important point is the variation in the pressure of the vapor emitted by the evaporating liquid. Quantitatively, this process can be described by the same dependence (6.4.19) and, in brief, one may conclude that this dependence is strong.

It is more interesting that we can recognize the Clapeyron-Clausius equation in (6.4.19). In the Clapeyron equation p = nT the main dependence of pressure on temperature is hidden in the function of the number density of molecules in a gas n(T) (6.4.16). The number density in a gas, in turn, is proportional to the number density of the evaporated particles. Thus, the pressure of the evaporated particles depends on the temperature of the liquid surface as:

$$\frac{1}{n}\frac{\mathrm{d}p}{\mathrm{d}T} \sim \frac{1}{n}\frac{\mathrm{d}n}{\mathrm{d}T}.$$
 (6.4.20)

Fig. 6.17 The responsivity of the number of evaporated particles to the temperature of the liquid surface



The right-hand side of (6.4.20) can be expressed with (6.4.19). We also may take into account that $T \ll 2U$, i.e., the last term in (6.4.19) can be ignored, so:

$$\frac{\mathrm{d}\ln p}{\mathrm{d}T} \sim \frac{U}{T^2}.\tag{6.4.21}$$

Because $U \sim \Delta H$ (the latent heat of vaporization, see Sect. 6.1.3), (6.4.21) is a kind of analog to the Clapeyron-Clausius equation.

In brief, we may note that dependence (6.4.21) arises not for the special function n(U,T) such as in (6.4.17). It is sufficient that $p \sim n(U/T)$ —the same scaling that led us to Trouton's rule earlier.

The strong temperature dependence of the pressure leads to some difficulties in numerical simulations. To determine some parameters (like the evaporation coefficient, for example) we have to calculate the pressure that corresponds to the temperature of the liquid surface. For sharp dependence p(T) the error will be large, and this error will be reflected in the error of the value of this parameter (e.g., the evaporation coefficient).

Thereby, evaporation into a vacuum becomes a special process which is "too pure" to simulate a real situation, when the evaporating liquid contacts with its vapor. However, of course, the investigation of pure evaporation helps us to understand the nature of this processes and, moreover, helps us to point out the details that must be considered in a liquid-vapor system: first of all, the role of U/T at the surface.

These nuances will be discussed in the next chapters.

6.5 The Non-linear Effect Within Evaporation: Hyperevaporation

In Chap. 5 we used U = const for binding energy. Actually, this is not correct. The binding energy of a given atom depends on many factors, so it is more accurate to consider the DF of U. In this chapter we discussed this DF and found this function as an analytical expression, but we did not touch upon another nuance. Is the binding energy an independent parameter? There is no doubt that the rate of evaporation depends on U, but is the reverse true—can binding energy be a function of the rate of evaporation?

Generally, the answer is affirmative. When an atom (or a molecule) leaves its place at the surface of a liquid, its neighbors acquire a lower binding energy. Thus, the probability of evaporation of such atoms—neighbors of the newly vacated atom—is higher. This means that one of them may leave the surface, producing a newly vacated site, etc. The evaporation in such a regime is a cascade process: a particle which has evaporated will lead to the evaporation of one of its neighbors. Considering fast relaxation in liquids, this process may be observed only a short time period after the evaporation of the first atom; thereby, this process may be looked at as the escape of a "molecule"—with a cluster of two or more atoms detaching from a liquid.

Let us estimate the result of lowering the binding energy described above. Denote U_N as the binding energy of an atom with N neighbors, consequently, the binding energy of atom with N-1 neighbors is U_{N-1} . Let $U_N=NU_1$, where U_1 is the binding energy to a single neighbor. Thus, the probability of leaving the surface is:

$$p(U) = \frac{1}{2\sqrt{\pi}} \Gamma\left(\frac{1}{2}, \frac{U}{T}\right). \tag{6.5.1}$$

After the escape of one neighbor this increases to:

$$\delta = \frac{p(U_{N-1})}{p(U_N)} = \frac{\Gamma\left(\frac{1}{2}, \frac{U_1(N-1)}{T}\right)}{\Gamma\left(\frac{1}{2}, \frac{U_1N}{T}\right)} \approx \exp\left(\frac{U_1}{T}\right). \tag{6.5.2}$$

This simplified approach does not take into account that an "escaped" particle "pulls out" its neighbor.

In Table 6.3 we present some values of δ for different U_1/T and N=6 [we use the absolute equality in (6.5.2)].

On the one hand, δ is rather significant. On the other hand, the probability p is low. Actually, this means that the effect of non-linearity is small, due to the low probability of evaporation for the given atom. Even when the probability increases—by an order of magnitude—its value is still too low. Most probably the configuration of surface atoms "would recreate" and any trace of the vacancy vanishes before one of the atoms nearby this vacancy leaves the surface.

This is good news because we can use our "linear" approach correctly; otherwise all the theory presented in this chapter would need to be adjusted. However, this optimistic conclusion is correct only for "typical" situations. For extremely high temperatures, when the ratio U_1/T is sufficiently small and probability $p(U_N) \sim 1$, we can expect the non-linear regime of hyperevaporation, described in this section. Anyway, such interesting effects cannot be neglected entirely. There may be exceptional conditions where such process may appear, and one of these special cases is 2D geometry.

The evaporation of two or more particles at once may be observed much better in a 2D system. In 2D geometry the number of bonds for an atom in a liquid is less than for 3D geometry; thus, as it follows from our consideration, the absence of a single bond exhibits itself more clearly: the relative weight of one bond is higher in a 2D system. Consequently, one can observe the detachment of several particles at once with much higher probability.

We can see an illustration of such a process in Fig. 6.18. Here we represent the flight of five atoms detached from the evaporation surface—an impressive sight.

 Table 6.3 Parameters of possible hyperevaporation

	$U_1/T=1$	$U_1/T=2$	$U_1/T = 3$
δ	3	8	22
$p(U_N)$	2.5×10^{-4}	5×10^{-7}	10^{-9}

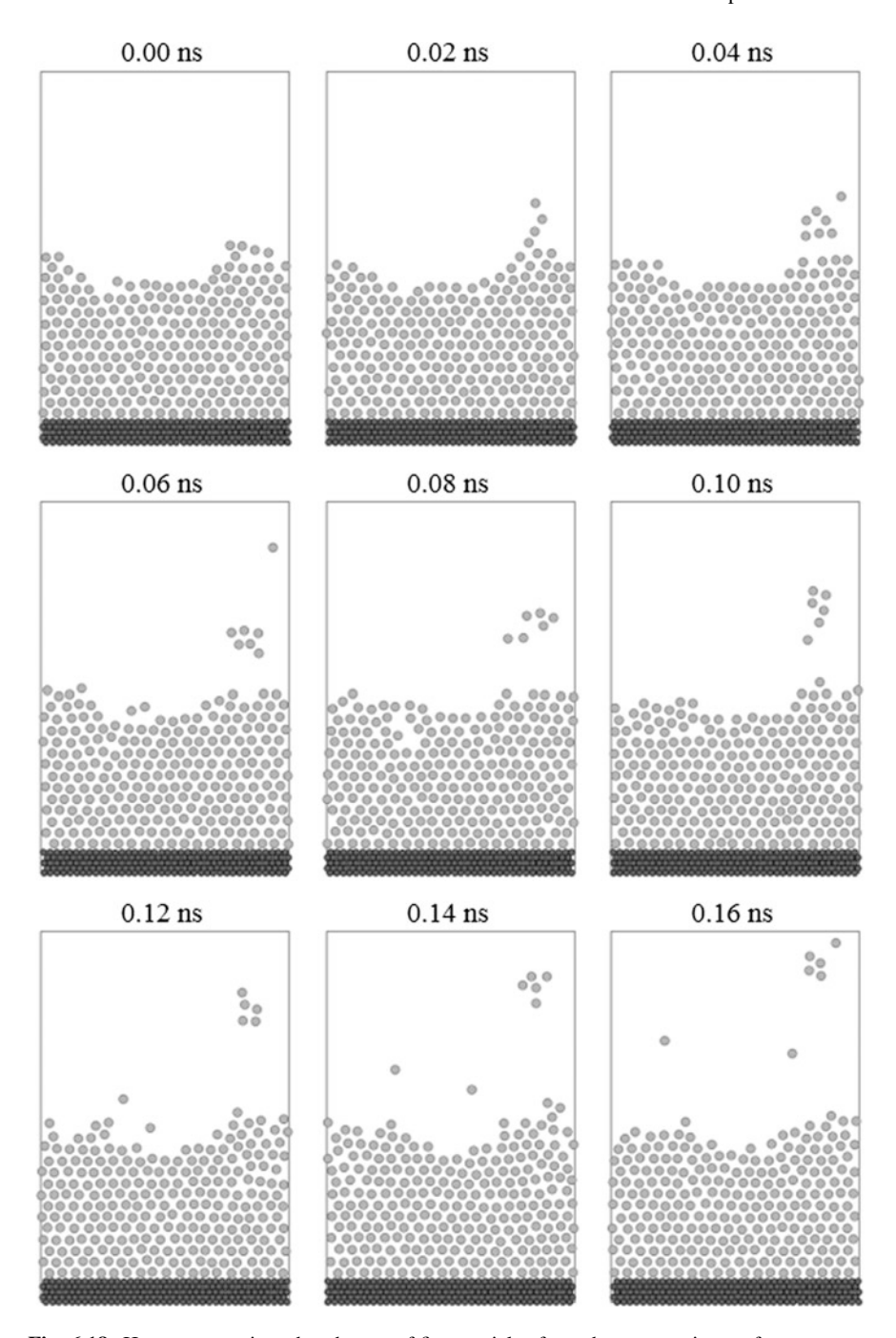


Fig. 6.18 Hyperevaporation: detachment of five particles from the evaporation surface

6.6 Conclusion 193

6.6 Conclusion

The work function of a surface atom is not a constant. There exists a potential energy DF:

$$g(u) = \int_{0}^{\infty} 2\sqrt{\frac{\varepsilon}{2\pi^{2}\theta^{2}T^{3}}} \exp\left(-\frac{\varepsilon}{T}\right) \exp\left(-\frac{(\varepsilon - u - l_{m})^{2}}{20^{2}}\right) d\varepsilon,$$

where ε is the kinetic energy of the particle; T is the temperature of the liquid (i.e., the mean potential energy of the particles); $l_m = \varepsilon_m - u_m$ is the Lagrangian (the difference between the average kinetic energy and the potential energy) and θ is the special parameter termed "fluctura." This DF was obtained for condensed media and, strictly, the area of its application is unclear.

Our numerical simulations for liquids in equilibrium confirm both the form of the DF of potential energy and the assumptions that led to this function: the potential energy of a particle and its kinetic energy are statistically independent parameters; the DF of the Lagrangian of the particle is a symmetrical function.

Parameter θ is the source of the problems which were not solved analytically in this chapter (and in this book as a whole). In equilibrium, the fluctura is equal to the temperature of a media, this fact follows from the definitions of terms "equilibrium" and "temperature" (as a measure of equilibrium fluctuations). However, we have no sufficient reason to state that $\theta=T$ everywhere, including in non-equilibrium systems (with temperature gradients, heat fluxes, etc.). Actually, we do not know much about θ , but we suppose that the theory presented in this chapter is strong enough to point out its problems.

We have no solid arguments to establish θ in a general case, and we cannot establish the form of the DF g_{ε} in a substance at the ideal gas limit.

Does the fluctura depend on the density of a media? At first glance, for an ideal gas —the gas of non-interacting particles, where $u \equiv 0$ —there must be $u_m = 0$ and $\theta = 0$. Thus, from this point of view, we see the limit $\lim_{T \to \infty} \theta(T) = 0$; and the dependence $\theta(T)$ is important in itself. From another point of view, this description is too sophisticated, because in a real ideal gas (the gas in a room, which obeys the Clapeyron equation, but consists of real molecules) for collided molecules the energy of interaction is non-zero; moreover, at the very moment of a collision this energy is huge. Additionally, to continue the argument at the beginning of this paragraph, it is more logical to demand the condition $D_u = 0$ instead of $\theta = 0$. Finally, we have to admit that we cannot give a full explanation of fluctura in a general case. It rather looks like all the methods to obtain a DF of potential energy are incorrect for an ideal gas, where the potential energy is equal to zero and, consequently, all the approaches based on the principle of least action lose their force.

We cannot point out the value of fluctura in a common case, but we have ideas about its measured value: in a wide layer of a liquid where the mean potential energy in a layer differs by Δu_m , the DF of potential energy may be represented

(exactly, approximated) by the DF g(u) but with the replacement $\theta \to \Theta$, where the measured fluctura (e.g., the value of Θ determined in numerical simulations) is:

$$\Theta^2 = \theta^2 + \frac{(\Delta u_m)^2}{12}.$$

Our calculations show that at the surface layer with temperature T the measured fluctura is $\Theta \sim 2T$, which corresponds to $\theta \sim T$. Can we conclude that $\theta = T$ always? No, because we still need more arguments to make such a common conclusion.

Thus, we obtained the DF of binding energy at the liquid surface and estimated the probability of evaporation, number density of evaporated particles, fluxes from the evaporation surface, etc.

The probability of detachment is different for particles with different potential energy; actually, the main part of the evaporation flux is determined by particles with low binding energy. To estimate this probability, one may use the old equation from Chap. 5: $w(U) = \frac{1}{2\sqrt{\pi}}\Gamma(\frac{1}{2},\frac{U}{T})$, however the value U here corresponds not to the average energy $\int_{-\infty}^{\infty} Ug(U) \mathrm{d}U$ but to the value that satisfies the condition $w(U) = \overline{w(U)}$. Thereby, the number of evaporated particles may be found with the total number density of particles at the liquid surface n_0 :

$$n = n_0 \overline{w(U)} = n_0 \int_{-\infty}^{\infty} w(U)g(U)dU.$$

If $g(U<0) \neq 0$, i.e., if we take into account particles with negative binding energy, then the probability of detachment is w(U<0)=1/2. Actually, the DF of potential energy at a surface differs from the DF in the bulk of a liquid: particles arrive at the surface with high binding energy, and they always have a choice—to decrease their binding energy or to leave the surface.

The number density at the liquid surface n_0 does not coincide with the number density in the bulk of the liquid. It is lower; we can estimate this quantity through the binding energy at the surface. Note that the accuracy of this estimation seems to be not much worse than the accuracy of numerical simulation: it is difficult to calculate n_0 in molecular dynamics simulations.

The fluxes from the evaporation surface may be expressed with results from Chap. 5: one can take the expressions for the fluxes and multiply them by the number density n. The mass and energy fluxes are:

$$J = \begin{cases} n\sqrt{\frac{\pi mT}{2}}, & q = \begin{cases} nT\sqrt{\frac{25\pi T}{8m}}, \\ n\sqrt{\frac{8m\Upsilon_z}{\pi}}. & q = \begin{cases} nT\sqrt{\frac{25\pi T}{8m}}, \\ n(\Upsilon_x + 2\Upsilon_z)\sqrt{\frac{8\Upsilon_z}{\pi m}}. \end{cases}$$

6.6 Conclusion 195

where the first expression for each flux corresponds to a flat evaporation surface, the second one to a strongly irregular surface and in the last case the parameters Υ_x and Υ_z are modules of the velocity DFs (see Chap. 5).

Simple estimations of the evaporation fluxes show very large values; the total flux on the interface is much less than the pure evaporation flux. Thus, the condensation flux plays a role too; then we go to conditions of equilibrium, but the DF of evaporated particles on velocities, so to say, has an unusual form. We have no expression for a condensation flux on an interface, but it is difficult to expect that this function has an analog form. In the case of different DFs all the balanced equations for fluxes and thermodynamic parameters (for pressure and temperature) cannot be satisfied at any instant; thus, one may expect fluctuations in all these parameters. At the equilibrium state, i.e., when the evaporation flux is compared to the condensation flux, we estimate the period—timescale—of such fluctuations; at ordinary external parameters this period is around 1 s. Note that fluctuations in an evaporated liquid are much faster; their timescale is ~ 1 ns or less.

All our approaches concern only a simple linear approximation: the evaporation flux does not affect itself. Usually, this approach is correct, but sometimes evaporated particles may leave a surface altogether: in this special regime we need a non-linear description of evaporation.

References

```
S.I. Anisimov, V.V. Zhakhovskii, JETP Lett. 57, 91 (1993)
```

- F. Duan et al., Phys. Rev. E 78, 041130 (2008)
- A. Einstein, Ann. Phys. 14, 351 (1904)
- G. Fang, C.A. Ward, Phys. Rev. E 59, 441 (1999)
- L.D. Landau, E.M. Lifshitz, *Mechanics* (Course of Theoretical Physics, volume 1) (Butterworth-Heinemann, Oxford, 1976)
- B. Lavenda, Statistical Physics: A Probabilistic Approach (Wiley, New York, 1991)
- E.N. Lorenz, J. Atmos. Sci. 20, 130 (1963)
- J. Loschmidt, Wien. Ber. 73, 128 (1876)
- D. Ruelle, F. Takens, Commun. Math. Phys. 20, 167 (1971)
- R.A. Swalin, Thermodynamics of Solids (Wiley, New York, 1972)
- L. Turner, Phys. Rev. E 54, 5822 (1996)

Recommended Literatures

- T. Alty, Lond. Edinb. Dublin Philos. Mag. J. Sci. Ser. 7(15), 82 (1933)
- A. Einstein, Ann. Phys. 17, 132 (1905)

Chapter 7 The Evaporation Coefficient



Probably, this is a unique situation in physics: for a quite defined physical parameter (almost of a mechanical nature, because a mass flux is a well-defined and well-understood physical quantity), with a simple substance such as water, in relatively clear experiments, the evaporation–condensation coefficient differs from experiment to experiment by about two or even three orders of magnitude. This is not, for instance, the vibrational temperature of hydroxyl in a non-equilibrium plasma: the proportional factor for a mass flux seems to be a certain and easily-measureable parameter. Alice measures a mass flux under known temperature and external pressure, then she divides the obtained value by the calculated Hertz flux and ... she obtains a number that differs, by a factor of five, from the value obtained by Bob in the laboratory next door. Why?

7.1 The Evaporation and Condensation Coefficients

7.1.1 Overview

Generally, these two quantities—the coefficients of evaporation and condensation—are surplus. For the complete theory of interfacial processes both coefficients must be corollaries but not independent external parameters.

Unfortunately, we still have no "complete theory" of surface processes. Historically, the Hertz-like correlations:

$$j \sim \frac{p}{\sqrt{2\pi mT}} \tag{7.1.1}$$

were used both for the evaporation and condensation fluxes, and these coefficients were introduced into the right-hand side of (7.1.1) to take into account the "non-ideality" of the processes.

It is easy to explain the meaning of the condensation coefficient: it is the fraction of the stuck particles relative to the overall number of particles that fall onto a surface. Assuming that the flux of the striking particles obeys the Hertz flux (actually—it does not, see below), one may see that this consideration leads us to the usual definition.

It is harder to explain the meaning of the evaporation coefficient. Usually it refers to the inequality of the number density of particles at the liquid surface and in the bulk vapor, but this interpretation is insufficient, because, of course, the number density *inside* a liquid is much higher than the number density inside a vapor. That is, the number density at the liquid surface means the "number density of particles in vapor phase near the liquid surface." That sounds better, but in this case we must explain what the pressure in (7.1.1) is. Why does this vapor, with a "reduced" number density of particles, produce an "unreduced" pressure p?

Another way to explain the meaning of the evaporation coefficient follows from the determination of the flux. According to this interpretation, the flux (7.1.1) represents a maximum flux that can be reached in an ideal case (exactly, which can never be reached). Actually, this explanation leaves an open question: what makes the flux non-ideal? What processes at the surface prevent the achievement of a maximum flux? From this group of explanations we may highlight the concept that the flux with $\alpha=1$ is the evaporation flux into a vacuum, i.e., the evaporation coefficient arises only at the point of contact of liquid and vapor.

We can also try to interpret the existence of the evaporation coefficient through the condensation coefficient. Since the condensation flux (defined by (7.1.1) with condensation coefficient <1) must be equal to the evaporation flux at the saturation parameters, then the evaporation flux must contain the same factor—the evaporation coefficient. From this point of view it is difficult to understand how the ability of the surface to attach particles from a gas is connected with the ability of the same surface to emit particles. As a variation, we may state (according to H. Hertz) that the evaporation flux is only a part α of the flux emitted from the surface; the other $(1-\alpha)$ fraction represents reflected molecules. From this consideration we again obtain the same form for the evaporation flux.

In fine, there always exists a last option: not to explain anything. The beginning of such non-explanation is: "The evaporation flux can be represented in a form $J^{\rm ev}=\alpha p_{\rm s}\sqrt{m/2\pi T_{\rm s}}$, where α is the evaporation coefficient ..." Such "positivism" has many advantages (besides which it leaves space for imagination), and we start the next section in this manner. We will return to the discussion about the problems concerning the meaning of the evaporation coefficient, but will do that later, in Sect. 7.3.

7.1.2 The Hertz-Knudsen Formula

The evaporation coefficient α and the condensation coefficient β play an important role in the theoretical description of processes at the interfacial surface. Both of them are determined as factors for mass fluxes:

$$j^{\text{ev}} = \alpha j^{\text{H}}, \quad j^{\text{cond}} = \beta j^{\text{H}}.$$
 (7.1.2)

Here j^H is a unidirectional mass flux in the equilibrium gas; according to the Hertz formula:

$$j^{\rm H} = \frac{1}{4} n_{\rm g} \bar{\nu} = \frac{1}{4} n_{\rm g} \sqrt{\frac{8T}{\pi m}},\tag{7.1.3}$$

where n_g is the number density in a gas (usually the ideal gas approach can be applied and $n_g = p/T$), m is the mass of an atom and \bar{v} is the thermal velocity. For the mass flux J = mj we have a similar equation, thus:

$$J^{\rm H} = p\sqrt{\frac{m}{2\pi T}}. (7.1.4)$$

We see that both α and β have been added to the gas flux as proportional factors. We can expect that the temperatures of liquid and gas are equal, with no problems hiding on this front. Indeed, the first approach would always be to use an equilibrium description; thereby, we may use the saturation number density $n_g = n_s$.

For the condensation coefficient, we can provide some reasons concerning its predictable value. If we use (7.1.2) for the condensation flux then the condensation coefficient has a sense of being the fraction of the atoms attached to the surface: when an atom hits the interface, it has a probability of becoming attached or being reflected. In old numerical simulations or analytical considerations there was a standard model of interaction between an atom and a wall: it might result in an absolutely elastic impact or something else.

However, in reality, an interaction between an atom and a continuous wall does not exist. It is always an interaction between atoms of vapor and atoms of liquid (or of solid), with there being a drastic change in their physical descriptions. Even in a solid the mean distance between two neighboring atoms is sufficiently large, and a "solid" represents a quite "porous" object for an incoming atom. Atoms of gas do not interact with a continuously solid wall but impact a rather hollowed structure of surface atoms and, after several (or many) collisions with this structure atoms may move back into a gas or stay attached to the condensed media for a long time. Per se, this refinement does not change the common situation concerning the condensation coefficient; this consideration will be continued in detail in Sect. 7.4. Thus, we expect almost all impacting atoms to attach rather than to be reflected.

We can formulate the expression for the total flux on the surface as:

$$J^{\text{tot}} = J^{\text{ev}} - J^{\text{cond}} = \sqrt{\frac{m}{2\pi}} \left(\alpha \frac{p_1}{\sqrt{T_1}} - \beta \frac{p_{\text{v}}}{\sqrt{T_{\text{v}}}} \right), \tag{7.1.5}$$

where indexes "l" and "v" denote liquid and vapor, correspondingly. This correlation is termed the Hertz–Knudsen equation, but usually this expression does not look exactly like (7.1.5).

First, the evaporation coefficient is usually conceived to be equal to the condensation coefficient (except for very rare considerations). The reason behind this is clear: at equilibrium conditions $p_1 = p_v$ and $T_1 = T_v$ and one can expect that $J^{\text{tot}} = 0$; consequently, we must have $\alpha = \beta$.

The next particularity of (7.1.5) consists in the assumption that pressure p_1 is the saturation pressure for temperature T_1 ; this leads to the following substitutions in (7.1.5) $p_1 \rightarrow p_s$ and $T_1 \rightarrow T_s$.

Finally, it is usually supposed that the temperature of the vapor is equal to the temperature of the liquid; thus, the total flux is determined only by the pressure difference in (7.1.5). Of course, as in other cases, this is only an assumption: in the next chapter we consider the "temperature jump" between the liquid and the vapor at the interface. After all these simplifications, instead of (7.1.5) we have:

$$J^{\text{tot}} = \alpha \sqrt{\frac{m}{2\pi T_{\text{s}}}} (p_{\text{s}} - p_{\text{v}}). \tag{7.1.6}$$

Again, we note that T_s here is only the temperature of the liquid; the corresponding pressure is $p_s(T_s)$.

With these refinements, (7.1.5) and (7.1.6) come to represent the fundaments for many experimental works devoted to the determination of the evaporation (condensation) coefficient. However, (7.1.5) needs some improvement in its part containing the condensation flux.

7.1.3 The Condensation Flux

The Hertz equation implies that the distribution function (DF) of velocities is Maxwellian. This assumption is correct when we consider, for example, the flux of molecules from air to the surface of a table, but we have different physical conditions at an interface. Ignoring evaporation, we would see that vapor molecules "vanish" at the liquid surface due to condensation. Thereby, the average velocity of the vapor is non-zero, i.e., the DF of the vapor cannot have the equilibrium Maxwellian form (Kucherov and Rikenglaz 1960a, b). In the presence of the evaporation flux, there may be a contrary occurrence: vapor moves away from the interface. Again, in this case the DF of particles would not be Maxwellian.

The easiest way to take into account the average velocity of the vapor V is to assume that the DF can be represented as for a stream:

$$f(v) = \sqrt{\frac{m}{2\pi T}} \exp\left(-\frac{m(v-V)^2}{2T}\right). \tag{7.1.7}$$

The flux for such a DF differs from the Hertz formula. We have:

$$j = n \int_{0}^{\infty} v f(v) dv = n \sqrt{\frac{m}{2\pi T}} \int_{0}^{\infty} v \exp\left(-\frac{m(v - V)^2}{2T}\right) dv.$$
 (7.1.8)

Integrating, we have:

$$j = n\sqrt{\frac{T}{2\pi m}}\Psi(\tilde{V}),\tag{7.1.9}$$

where quantity:

$$\Psi(\tilde{V}) = \exp(-\tilde{V}^2) + \tilde{V}\Gamma(\frac{1}{2}, \tilde{V}^2), \tag{7.1.10}$$

$$\tilde{V} = V \sqrt{\frac{m}{2T}}. (7.1.11)$$

Here $\tilde{V} > 0$ if the vapor moves toward the liquid surface (condensation) and $\tilde{V} < 0$ if the vapor moves away from the interface (evaporation).

For low values of average velocity $\tilde{V} \to 0$ and $\Psi(\tilde{V}) \to 1$ and (7.1.9) gives the regular Hertz equation. For any value of \tilde{V} , the expression for the total flux is (with the assumptions listed above):

$$J^{\text{tot}} = \alpha \sqrt{\frac{m}{2\pi T}} (p_{s} - \Psi(\tilde{V})p_{v}). \tag{7.1.12}$$

It is useful to understand what the "low average velocities" mean in this case. Function $\Psi(\tilde{V})$ is shown in Fig. 7.1. Note that the scale for the velocity V is $\sqrt{2T/m} \approx 10^2$ m/s for room temperatures of $T \sim 10^2$ K.

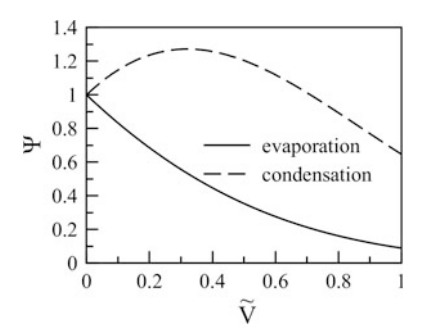
The average velocity V is not a free parameter, it is connected to the total mass flux J^{tot} at the interface:

$$\tilde{V} = -\frac{J^{\text{tot}}}{n\sqrt{2mT}},\tag{7.1.13}$$

where the "-" sign appears as a consequence of the user's choice: the "+" sign being used for the evaporation flux in (7.1.12) but also for the condensation flux in (7.1.7). Then, expanding into series we have:

$$\Psi(\tilde{V}) \approx 1 + \tilde{V}\sqrt{\pi} + \cdots, \tag{7.1.14}$$

Fig. 7.1 Function $\Psi(|\tilde{V}|)$ for evaporation [the "-" sign before the second term in (7.1.10)] and for the condensation [the "+" sign in (7.1.10)]



and combining (7.1.11) and (7.1.12) with the correlation for the total flux we have:

$$J^{\text{tot}} = \alpha \sqrt{\frac{m}{2\pi T}} \left[p_{\text{s}} - \left(1 - \frac{J^{\text{tot}}}{mn} \sqrt{\frac{m\pi}{2T}} \right) p_{\text{v}} \right]. \tag{7.1.15}$$

Finally, we use $p_v = nT$ again and get:

$$J^{\text{tot}} = \alpha \sqrt{\frac{m}{2\pi T}} (p_{\text{s}} - p_{\text{v}}) + \frac{\alpha}{2} J^{\text{tot}}, \qquad (7.1.16)$$

$$J^{\text{tot}} = \frac{2\alpha}{2 - \alpha} \sqrt{\frac{m}{2\pi T}} (p_{s} - p_{v}). \tag{7.1.17}$$

Equation (7.1.17) is sometimes referred to as the Hertz–Knudsen–Schrage formula. This correlation takes into account a relatively slow vapor flux at the interface: for both the vapor motion to the interface (condensation) and for the flux away from the liquid surface (evaporation). As shown in Fig. 7.1, this approximation—based on linearization (7.1.14)—is valid for:

$$|J^{\text{tot}}| \le 0.1 mn \sqrt{\frac{2T}{m}} \sim 0.1 p \sqrt{\frac{m}{T}},$$
 (7.1.18)

where we omit the factor $\sqrt{2}$, because (7.1.18) is only an estimation to one order of magnitude. Strictly, here $p=p_{\rm v}$, but it does not matter because it follows from (7.1.17) that at condition (7.1.18) $p_{\rm s} \sim p_{\rm v}$.

One may assume that (7.1.17) is better than (7.1.6) for three reasons:

- Expression (7.1.17) transients to (7.1.6) at $\alpha \to 0$, thereby, (7.1.6) is a particular case of (7.1.17).
- Expression (7.1.17) takes into account the factor that is ignored in correlation (7.1.6): the effect of the total non-zero flux on the DFs of gas particles.
- Expression (7.1.17) was obtained in a more complicated way.

Actually, the second reason is not that much more serious than reason three. Yes, the Hertz–Knudsen equation assumes that both DFs are Maxwellian (for the evaporated particles and for the particles in the condensation flux). This is a model, and it is very hard to verify it, especially for commensuration of the fluxes of evaporation and condensation.

However, correlation (7.1.17) is based on model assumptions too. First of all, there are no clear foundations for the DF in form of (7.1.7). This DF considers only one issue—a non-zero total flux; but there are infinite possibilities to compose non-symmetric DFs which can provide the desirable mass flux. Strictly, DF (7.1.7) may be used for an equilibrium flow—a steady flow with average velocity V where particles are thermalized at temperature T. The possibility of using (7.1.7) near the interface is questionable.

Besides this complication, we face the problem of discontinuity at the interface: DF (7.1.7) pretends to describe both branches of the DF (both for particles that move toward a liquid surface and for particles that move away from it), but for the runaway particles we must have the same DF at the evaporation surface (in the absence of an energy barrier, of course; see Chap. 5). It is evident that Maxwellian DF (MDF) used in (7.1.17) for the evaporation flux cannot coincide with DF (7.1.7) having $V \neq 0$.

7.1.4 A Sidestep: The Accommodation Coefficient

This coefficient shows how the temperature T'_{v} of a particle which has been absorbed having departed from vapor at temperature T_{v} differs from the temperature of the liquid (or solid) surface at temperature T_{i} :

$$\kappa = \frac{T_{\rm v}' - T_{\rm l}}{T_{\rm v} - T_{\rm l}}. (7.1.19)$$

Consequently, when a gas accepts the temperature of the liquid surface, after the sorbing–desorbing process, then $\kappa=0$; when the gas does not change its temperature after interaction with the condensed phase, then $\kappa=1$.

Sometimes, the accommodation coefficient plays a notable role in analytical considerations, but we assign it to our "sidestep" sections. When the temperature of desorbed particles differs from the temperature of the liquid, this means that an ensemble of the departed particles is not thermalized, and for this out-of-equilibrium group it is difficult to expect the MDF. In the case when $0 < \kappa < 1$ a much more complicated consideration is needed, where such a parameter as temperature cannot be used.

As for the case of an absolutely elastic reflection of particles, $\kappa = 1$, we have discussed this earlier. It is unlikely that this happen in a real situation.

7.2 The Experiment

7.2.1 How to Determine an Evaporation Coefficient

There are several methods which can be used to calculate an evaporation coefficient from experiment data. We mean here that after measurement of the total mass flux at the interface with known parameters p and T, various correlations can be used to define (to extract) the evaporation coefficient from this data.

In the presence of a condensation flux from the vapor at pressure p_v , in the earliest works (Alty 1933) the Hertz–Knudsen equation, in its simplest form, was used for the total flux on the interface (in this section we omit the index "tot" at J because here we do not consider the evaporation or condensation flux separately):

$$J = \alpha(p_{\rm s} - p_{\rm v})\sqrt{\frac{m}{2\pi T}}.\tag{7.2.1}$$

Thus, it is supposed here that both the evaporation flux and the condensation flux satisfies the Hertz formula with the condensation coefficient $\beta = \alpha$. There are no distinctions of temperature in the liquid and in the vapor, as discussed in the previous section.

The total mass flux J was determined experimentally, as in many successive works, by the weight method: $J = \Delta m/S\Delta t$, where Δm is the variation of liquid mass at time Δt on surface area S.

This method, based on (7.2.1), was also used in Delaney et al (1964) and Barnes (1978) and several others (see Table 7.1).

Another method has been applied in later works. The modified equation for the total mass flux was used (see Sect. 7.1.3):

$$J = \frac{2\alpha}{2 - \alpha} (p_{\rm s} - p_{\rm v}) \sqrt{\frac{m}{2\pi T}}.$$
 (7.2.2)

For some reason, this equation is supposed to be more precise than the Hertz–Knudsen formula. Here, as we see, there is no difference between the evaporation and the condensation coefficients. However, for example, in Bonacci et al. (1976) two kinds of coefficient α were measured: at conditions of total evaporation (i.e., for J>0), where the obtained value α was termed the "evaporation coefficient," and at the condition of condensation (J<0), where the "condensation coefficient" α was determined.

It is interesting to compare experimental results with methods based on (7.2.1) and (7.2.2). For small evaporation coefficients $\alpha \ll 1$ the data obtained with these two expressions is the same. But for a large α the discrepancy will be huge; for instance, assuming that the true value of $\alpha = 1$, the mass flux in (7.2.2) exceeds the mass flux in (7.2.1) by a factor of two. Anyway, the difference between the two

Table 7.1 The evaporation (condensation) coefficient of water

References	Model	α	Comments	
Alty and Nicoll (1931)	(7.2.1)	0.0156		
Alty (1931)	(7.2.1)	0.0083-0.0155		
Alty (1933)	(7.2.1)	0.04	The average value and actual values are within the range 0.0268–0.0584	
Barnes (1978)	(7.2.1)	0.0002	The apparent evaporation coefficient	
Bonacci et al. (1976)	(7.2.2)	0.55, 0.7–1 "with plausible corrections"	Used both for evaporation and condensation experiments	
Chodes et al. (1974)	(7.2.24)	0.033 ± 0.005		
Delaney et al. (1964)	(7.2.1)	$\begin{array}{c} 0.0415 \pm 0.0036 \\ 0.0265 \pm 0.0031 \end{array}$	For 0 °C For 43 °C	
Finkelstein and Tamir (1976)	(7.2.8)	From 0.006 ± 0.0003 to 0.060 ± 0.002	For condensation: $T_{\rm v} = 99 ^{\circ}{\rm C}$ $T_{\rm v} = 60 ^{\circ}{\rm C}$	
Hagen et al. (1989)	(7.2.24)	1.0 ~0.01	For condensation: Fresh drops Aged drops	
Hickman (1954)	(7.2.1)	0.243 (uncorrected) 0.424 (corrected)	Not less than 0.25 and probably approximates to unity	
Jamieson (1964)	See text	>0.305	Data for long residence times (α < 0.3) were ignored	
Li et al. (2001)	(7.2.1)	$ \begin{array}{c} 0.17 \pm 0.03 \\ 0.32 \pm 0.04 \end{array} $	At 280 K At 258 K	
Levine (1973)	(7.2.24)	1		
Maa (1967)	(7.2.3)	1	Uncorrected value (see text) where $\alpha' \approx 0.5 - 1$	
Mills and Seban (1967)	(7.2.2)	0.45–1		
Nabavian and Bromley (1963)	(7.2.2)	0.35–1		
Narusawa and Springer (1975)	(7.2.2)	0.038 0.17–0.19	Surface stagnant Surface replenished	
Shaw and Lamb (1999)	(7.2.24)	0.04-0.1	β and γ (7.1.19) were determined in common	
Sinnarwalla et al. (1975)	(7.2.24)	0.022-0.032	Condensation	
Smith et al. (2006)	(7.2.10)	0.62 ± 0.09		
Tamir and Hasson (1971)	(7.2.8)	0.18 0.23 0.11	Vacuum evaporation Vacuum condensation Pressure condensation	
Vietti and Fastook (1976)	(7.2.24)	0.1–1 0.036	For drops of ~2 μm size For larger drops	

(continued)

References	Model	α	Comments
Wakeshima and Takata (1963)	(7.2.24)	0.02	
Winkler et al. (2006)	(7.2.34)	0.8–1 0.4–1	250–270 K 270–290 K
Zientara et al. (2008)	(7.2.5)	0.13-0.18	Decreases with temperature according to the Arrhenius' law

Table 7.1 (continued)

methods cannot be responsible for the spread of experimental points of two orders of magnitude.

In some cases expression (7.2.1) was modified. In Offringa et al. (1983) the coefficient $\alpha\gamma$ was used instead of α in (7.2.1), where γ is the degree of the surface roughness. In this work a value $\alpha\gamma = 0.99 \pm 0.07$ was presented for transdiphenylethene, but the "clear" value of the evaporation coefficient (or the estimation of γ) was not calculated.

In Maa (1967) an attempt to obtain a "true" evaporation coefficient α from the measured value α' was realized. The "true" evaporation coefficient is the factor in (7.2.1), but with a different pressure and temperature:

$$J = \alpha (p_{\rm tr}(t) - p_{\rm v}(t)) \sqrt{\frac{m}{2\pi T_{\rm tr}(t)}},$$
(7.2.3)

where $p_{\rm tr}$ and $T_{\rm tr}$ is the pressure and the temperature at the interface. Here we emphasize that all parameters actually depend on time. Then, according to Maa (1967), another flux is determined in the real experiment: the value J' averaged over time interval Δt :

$$J' = \frac{1}{\Delta t} \int_{0}^{\Delta t} J dt. \tag{7.2.4}$$

Thus, the measured evaporation coefficient α' corresponds to the flux J', not to the true flux J. Under some assumptions, for a certain scheme of the experimental setup, the correlation between α and α' was obtained in Maa (1967).

An approach taking into account the temperature dependence of α was made by Zientara et al. (2008). For droplet evaporation in air the authors used correlation (7.2.1) for the mass flux on the surface of a small droplet; the evaporation coefficient was determined from the data on dR/dt—the rate of droplet diminishment. The effect of the temperature difference $\Delta T = T_a - T_R$ on the evaporation coefficient is:

$$\frac{\alpha}{\alpha(\Delta T = 0)} = \frac{\xi - \frac{\rho_{\nu}(T_a)}{\rho_{\nu}(T_R)}}{\xi - 1},\tag{7.2.5}$$

where ξ is humidity, T_a is the temperature of the droplet surface and T_R is the temperature of the reservoir (i.e., of the surrounding medium).

Evaporation coefficient can also be obtained through heat exchange measurements (Tamir and Hasson 1971). The heat transfer coefficient h on the interface can be expressed by (7.2.1) with different temperatures for phases, i.e., for a general case:

$$h = \frac{\Delta H}{T_{\rm s} - T_{\rm v}} \alpha \sqrt{\frac{m}{2\pi}} \left(\frac{p_{\rm s}}{\sqrt{T_{\rm s}}} - \frac{p_{\rm v}}{\sqrt{T_{\rm v}}} \right), \tag{7.2.6}$$

where ΔH is the enthalpy of vaporization. For high values of α , one can expect that $T_{\rm s} \approx T_{\rm v}$ and with the Clapeyron-Clausius equation in the form:

$$\Delta p \equiv p_{\rm s} - p_{\rm v} = (T_{\rm s} - T_{\rm v}) \frac{\Delta H}{\nu_{\rm s} T_{\rm s}},\tag{7.2.7}$$

 (v_s) is the specific volume of the vapor at saturation point) we have:

$$h \approx \alpha \sqrt{\frac{m}{2\pi}} \frac{(\Delta H)^2}{v_s T_s^{3/2}}.$$
 (7.2.8)

Then, α was determined from the correlation between the local Nusselt number $Nu_x = \frac{2sh}{\lambda}$ (s is the thickness of the liquid layer and λ is the thermal conductivity of the liquid) and the Graetz number $Gz = \frac{(2s)^2 \bar{u}}{x\alpha}$ (x is the distance from the origin and \bar{u} is the constant liquid velocity for no phase change):

$$\frac{Nu_x}{4} = \frac{Gz^{1/3}}{R},\tag{7.2.9}$$

which is obtained for small Gz, with the surface resistance parameter R that can be calculated from experimental data. Thus, the experimental dependence $Nu_x = f(Gz)$ was fitted by (7.2.8) with adjustment parameter α .

This method is rather original. Under many assumptions we obtain coefficient α through the heat exchange equations, the correctness of which is restricted not only by the usual allowance of the local equilibrium, etc., but also by the form of the equations themselves. Taking into account that usually errors of heat exchange experiments are high, it is difficult to expect great precision for the evaporation coefficient measured using such a method. Note that the initial problems (concerning correctness of the Hertz–Knudsen equation with $\alpha = \beta$) remain in this method too.

Another method where the evaporation coefficient can be determined with the heat balance equation has been applied in Smith et al. (2006). The main correlation is the equation of the heat balance of the evaporated droplet in a vacuum:

$$\frac{\mathrm{d}T}{\mathrm{d}t} = -JF \frac{\Delta H}{c_{p}M},\tag{7.2.10}$$

with J taken from (7.2.1), $F = 4\pi r_0^2$ is the surface area of the droplet, c_p is the isobaric heat capacity and $M = \frac{4}{3}\pi\delta^3\rho$ is the mass of the spherical shell of the liquid (with density ρ) of radius δ .

Thus, the heat flux on the surface of the evaporated droplet is supposed to be the mass flux multiplied by the equilibrium value of the enthalpy difference between two phases; this approach is widespread in heat transfer science.

In an experiment (Smith et al. 2006), the temperature dependence T(t) of the interface of the droplet was approximated by (7.2.10), with the unique free parameter α (from J) determined in this way. Actually, the "philosophy" of measuring the evaporation coefficient in Smith et al. (2006) is old: here the Hertz flux is interpreted as the theoretical maximum of the evaporation rate.

As we discussed above, in the literature the evaporation coefficient and the condensation coefficient are mixed. The condensation coefficient usually may be obtained from experiments for droplet growth; the mass balance for a droplet is:

$$\frac{\mathrm{d}M}{\mathrm{d}t} = -4\pi R^2 J,\tag{7.2.11}$$

where M and R are the mass and radius of a droplet, correspondingly. The "-" sign holds our agreement about the sign of the flux: plus for evaporation, minus for condensation. In a macroscopic (hydrodynamic) description one can define the total mass flux J as a diffusion flux, i.e.:

$$J = -D\frac{\partial \rho}{\partial r},\tag{7.2.12}$$

according to Fick's law (*D* is the diffusion coefficient and ρ is the density of a vapor surrounding our droplet). In a stationary case, $\operatorname{div} \vec{J} = 0$ and we see from:

$$\frac{1}{r^2} \frac{\partial (r^2 J)}{\partial r} = 0 \tag{7.2.13}$$

that $r^2J = \text{const}$ and that:

$$\rho = \rho_{\rm v} + (\rho_{\rm i} - \rho_{\rm v}) \frac{R}{r}, \tag{7.2.14}$$

where $\rho_{\rm v}=\rho(\infty)$ is the vapor density far from the droplet and $\rho_{\rm i}$ is the density of gas near the interface: $\rho=\rho(R)$.

Thus, with (7.2.14) we have for the diffusion flux (7.2.12):

$$J = D \frac{\rho_{\rm v} - \rho_{\rm i}}{R},\tag{7.2.15}$$

and for the so-called diffusion-controlled growth rate we have, with (7.2.11):

$$\frac{\mathrm{d}M}{\mathrm{d}t} = 4\pi DR(\rho_{\mathrm{v}} - \rho_{\mathrm{i}}),\tag{7.2.16}$$

Then, we may note that because of phase transitions the variation of droplet mass is connected to the variation of the amount of heat in the droplet. For this amount of heat Q we have:

$$\frac{\mathrm{d}Q}{\mathrm{d}t} = -4\pi R^2 q,\tag{7.2.17}$$

where the heat flux for a small droplet can be expressed only through heat conduction:

$$q = -\lambda \frac{\partial T}{\partial r},\tag{7.2.18}$$

where λ is the heat conductivity. Analogically, from $\operatorname{div} \vec{q} = 0$ we see the temperature distribution in the vapor phase and the heat balance at the droplet surface as:

$$T(r) = T_{\rm v} + (T_{\rm i} - T_{\rm v})\frac{R}{r},$$
 (7.2.19)

$$\frac{\mathrm{d}Q}{\mathrm{d}t} = 4\pi\lambda R(T_{\mathrm{v}} - T_{\mathrm{i}})\tag{7.2.20}$$

Thereby, (7.2.16) and (7.2.20) describe the growth of the liquid droplet in a vapor at density ρ_v and temperature T_v , with the droplet having a temperature T_s . Taking into account that the energy ΔH released due to condensation must be dissipated in vapor, we have the connection:

$$\Delta H \frac{\mathrm{d}M}{\mathrm{d}t} = -\frac{\mathrm{d}Q}{\mathrm{d}t}.\tag{7.2.21}$$

We can rewrite (7.2.16) as:

$$\frac{1}{\rho_{s}}\frac{dM}{dt} = 4\pi DR\left(\frac{\rho_{v}}{\rho_{s}} - \frac{\rho_{i}}{\rho_{s}}\right),\tag{7.2.22}$$

with the saturation density ρ_s . Then, we can use a simplified version of the Clapeyron-Clausius equation (far from the critical point, where the specific volume of vapor is much greater than the specific volume of a liquid, and the Clapeyron equation $p = \frac{\rho T}{m}$ can be correctly applied to the vapor phase) in the form:

$$\frac{\mathrm{d}p}{\mathrm{d}T} = \frac{pm\Delta H}{T_s^2},\tag{7.2.23}$$

where the latent heat ΔH is measured in K. The next step depends on the assumption concerning the variation of T. If $T_v \sim T_i \sim T_s$, then we can neglect the dependence of ΔH on T at this interval and from (7.2.23) we obtain:

$$\ln\left(\frac{p_{\rm i}}{p_{\rm s}}\right) \approx \frac{m\Delta H}{T_{\rm s}^2}(T_{\rm i} - T_{\rm s}),\tag{7.2.24}$$

$$\frac{p_{\rm i}}{p_{\rm s}} = \frac{\rho_{\rm i}}{\rho_{\rm s}} \approx 1 + \frac{m\Delta H}{T_{\rm s}^2} (T_{\rm i} - T_{\rm s}).$$
(7.2.25)

Substituting for $T_i - T_s$ the expressions (7.2.20) and (7.2.21):

$$T_{\rm i} - T_{\rm s} = \frac{\Delta H}{4\pi R^2} \frac{\mathrm{d}M}{\mathrm{d}t}.\tag{7.2.26}$$

Combining (7.2.22), (7.2.25) and (7.2.26) we have:

$$\frac{1}{\rho_{\rm s}} \frac{\mathrm{d}M}{\mathrm{d}t} = 4\pi DR \left(\frac{\rho_{\rm v}}{\rho_{\rm s}} - 1 - \frac{\Delta H^2 m}{4\pi R \lambda T_{\rm s}^2} \frac{\mathrm{d}M}{\mathrm{d}t} \right),\tag{7.2.27}$$

$$\frac{\mathrm{d}M}{\mathrm{d}t} = \frac{4\pi R \left(\frac{\rho_{\mathrm{v}}}{\rho_{\mathrm{s}}} - 1\right)}{\frac{1}{\rho_{\mathrm{v}}D} + \frac{m\Delta H^{2}}{\lambda T_{\mathrm{s}}^{2}}}.$$
(7.2.28)

Here $\rho_{\rm v}/\rho_{\rm s}$ is the saturation ratio. Equation (7.2.28) is usually referred to as the Maxwell equation. In Fukuta and Walter (1970) this equation was generalized in the form:

$$\frac{\mathrm{d}M}{\mathrm{d}t} = \frac{4\pi R \left(\frac{\rho_{\mathrm{v}}}{\rho_{\mathrm{s}}} - 1\right)}{\frac{1}{f_{\mathrm{s}\theta}\rho_{\mathrm{w}}D} + \frac{m\Delta H^{2}}{f_{\mathrm{s}\phi}\lambda T_{\mathrm{s}}^{2}}},\tag{7.2.29}$$

where $f_{3\alpha}$ and $f_{3\beta}$ are correction factors for temperature and vapor density differences, correspondingly; these factors depend on the condensation coefficient β and the accommodation coefficient γ and appear in corrected equations:

$$\frac{\mathrm{d}M}{\mathrm{d}t} = 4\pi DR f_{3\beta}(\rho_{\mathrm{v}} - \rho_{\mathrm{i}}),\tag{7.2.30}$$

$$\frac{\mathrm{d}Q}{\mathrm{d}t} = 4\pi\lambda R f_{3\gamma} (T_{\mathrm{v}} - T_{\mathrm{i}}). \tag{7.2.31}$$

Fukuta and Walker (1970) obtained that:

$$f_{3\beta} = \frac{R}{R + L_{\beta}}, \quad f_{3\gamma} = \frac{R}{R + L_{\gamma}},$$
 (7.2.32)

$$L_{\beta} = \frac{D}{\beta} \sqrt{\frac{2\pi m}{T_{\rm v}}}, \quad L_{\gamma} = \frac{\lambda \sqrt{2\pi m T_{\rm v}}}{\gamma P(C_{\rm v} + 1/2)}. \tag{7.2.33}$$

An equation of the same type was obtained by Langmuir, but under some assumptions: with $\beta = 1$ and without consideration of heat conduction.

In brief, the equations of Maxwell (7.2.28) and Fukuta and Walter (7.2.28) take many factors into account, including diffusion. In the case when we restrict our consideration to only diffusion, we may obtain the correlation for the mass flux on the surface of a droplet of radius R (Winkler et al. 2004):

$$J = \beta C \frac{4\pi R m D_{\infty} p}{T_{\infty}} \ln \left(\frac{1 - x_{\infty}}{1 - x_{R}} \right), \tag{7.2.34}$$

where x_{∞} and x_R are the vapor mole fraction far from the droplet and at its surface, correspondingly, p is the total pressure and C is a quantity that takes into account the temperature dependence of the diffusion coefficient D.

7.2.2 The Experimental Results

Considering that, at first glance, there are so many methods to obtain α experimentally, it is no wonder that the difference in results is large. Actually, the spread of values of α is wide, but the reason seems to be something other than the large set of methods for its determination.

In this section we present the evaporation coefficient only for water. Also, we present some values of the condensation coefficient for two cases: obtained using the methods in (7.2.1) or (7.2.2), at conditions of total condensation, and for comparison, derived using the method in (7.2.29) of Fukuta and Walter. Evidently, if there is no distinction between α and β in theory, then it is impossible to find this distinction in experiments, where the same parameter from (7.2.1) is referred to as the "evaporation coefficient" for J > 0 and termed as the "condensation coefficient" otherwise. We suppose that the uncertainty in the presented results of the evaporation (condensation) coefficient demonstrates the problem as a whole.

Table 7.1 features experimentally measured evaporation coefficients. We also provide a theoretical model that stands behind the treatments—we assume that this is an important factor; under the "theoretical model" we understand the equation in which the evaporation coefficient appears. We slightly generalize these approaches; for instance, we always refer to (7.2.29) even for cases when simplified variations

of this equation were used, e.g., for Wakeshima and Takata (1963). Also, for instance, in Li et al. (2001) the evaporation coefficient was extracted from the experimental data in a complicated way, but the basic equation used was the Knudsen correlation, thus, we refer to (7.2.1).

In the work by Bonacci et al. (1976) a dependence on time was observed (at time intervals ~ 1 s). In some works (see Table 7.1) temperature dependence has been examined, but, in the context of the spread of overall results, it is difficult to discuss such results in detail. In Marek and Straub (2001) the $\alpha-p$ diagram is presented; despite the huge spread one may see a certain trend: the evaporation coefficient tends to decrease with an increase in pressure. Specifically, low values of α were observed at any pressures while $\alpha \sim 1$ was obtained only for low pressures. As for the condensation coefficient, it is problematic to see any dependence from the field of points on the $\beta-p$ diagram presented in that review.

A rather interesting aspect is that some experimental works do not even contain any exact value of the evaporation coefficient in the form $\alpha=a\pm b$, where $b\ll a$. In several works α is presented only as an estimate to an order of magnitude. In some works the dispersion of α is large even for the same (or close) experimental conditions. In other works α differs by ten or more times for the same methods but at different special conditions: for instance, the evaporation coefficient varies with the size of droplets. As an example, it is an interesting fact that the value obtained in Hickman (1954) is referred to in Nabavian and Bromley (1963) as $\alpha=0.42$, while in Eames et al. (1997) this value is highlighted as $\alpha \geq 0.25$; in Mills and Seban (1967) $\alpha=1$ was obtained (after recalculation). The most interesting fact in this story is that all these references are indeed correct.

7.2.3 Explanations for Discrepancy (A Preliminary Round)

Of course, this strange situation—when a physical parameter varies by a few orders of magnitude—demands explanation. Usually, these interpretations do not concern the initial form of equations for evaporation coefficient determination. There is no doubt in these works that:

- the evaporation flux can be calculated by a Hertz-like formula, where α determines a difference between the real flux and the theoretical (maximum) flux—an unreachable maximum flux, as stated in some works (Knake and Stranskii 1959), i.e., the Hertz formula directly.
- thermodynamic parameters in this Hertz-like formula for evaporation flux (temperature and pressure) correspond to the saturation quantities of this liquid, i.e., in this formula the pressure $p = p_s(T)$ if the temperature of the liquid is T.
- the expression for the condensation flux has the same Hertzian form, but, generally, with parameters corresponding to the vapor, i.e., in common case $T_v \neq T_1$ and $p_v \neq p_s$.

- because of the two previous statements and the obvious fact that the total flux at saturation must be equal to zero, the condensation coefficient must be equal to the evaporation coefficient.
- last, but not least, the evaporation coefficient is an "external" physical property
 for the evaporation flux, it cannot be found directly from the same theory as the
 evaporation flux itself; this quantity must be accepted from the outer
 consideration.

Thus, from our point of view, the principal and most interesting reasons were banished from the analysis. We will argue four positions from the five in this list in the next two sections (except for the second statement about $p_s(T)$ for the evaporation flux). Setting these factors to one side, the only two sorts of explanation for the range of evaporation coefficient $\alpha \sim 10^{-3} \div 1$ are:

- Inaccuracy of experiments or of methods of calculations during the treatment of experimental data, e.g. in Jamieson (1964) the neglection of evaporation was mentioned in its discussion.
- Some "uncontrolled" factors.

The second group may be expanded as follows:

- The temperature of the water surface being lower than the estimated value (Hickman 1954; Barnes 1978).
- The orientation of water molecules (Alty and Nicoll 1931).
- The contamination of the water surface (Hickman and White 1971).
- The thermal resistance of the interface (Mills and Seban 1967).
- The convective heat exchange (Mozurkewich 1986).
- The presence of foreign non-condensing gases and diffusion (Pound 1972).

The temperature of the surface is an important parameter, of course, and sometimes it is difficult to understand at what point inside the liquid the temperature has been measured, especially considering the fact that the temperature of the surface notably differs from the temperature of the bulk of the liquid.

As for the effect of contamination, this in an old problem (Rideal 1924), and contradictory results can be found in the literature. One may intuitively assume that this influence must be strong; this conclusion corresponds, e.g., to experiments by Miles et al. (2016). On the other hand, for example, we can refer to a work (Barnes 1978) which was devoted to the determination of the "apparent" evaporation coefficient. To investigate the influence of the contamination of the water surface, Barnes covered the liquid surface with a monolayer of octadecanol. However, there was no resultant effect: the presence of the octadecanol film did not lower the measured evaporation coefficient.

The role of convection—diffusion processes that lead to different correlations for the fluxes on the interface also seems to be important (however, all these factors do), but we cannot imagine that these factors altogether can provide a difference of up to three orders of magnitude.

7.3 Calculation of the Evaporation Coefficient

7.3.1 Some Definitions

We should distinguish two kinds of fluxes here: a flux (of mass, energy, etc.) on an evaporation surface and a flux of evaporated atoms. The first one is the total flux: the difference between the evaporation and the condensation fluxes. Below we will assume that the total flux is represented by a "+" sign for the total evaporation condition and a "-" sign for the condensation.

The next important issue: we are interested in fluxes on the outskirts of the near-surface zone, where evaporated particles do not interact with the liquid surface (see Fig. 3.3). For this purpose, it is incorrect to consider fluxes in the liquid or near a surface (at distances ~ 1 nm), because the evaporation flux varies (diminishes) as the distance from the surface increases: large amounts of energy from molecules are spent to overcome forces originating from the liquid surface.

Then we have to define the term "evaporation coefficient," and this is not an easy task.

7.3.2 What Is the Evaporation Coefficient?

The DF of the evaporated particles has a non-Maxwellian shape (see Chap. 5). Thus, the evaporation flux does not have the Hertz form:

$$J^{\text{ev}} \neq \frac{mn\bar{\nu}}{4},\tag{7.3.1}$$

with thermal velocity $\bar{v} = \sqrt{8T/\pi m}$, because, first of all, the non-equilibrium flux has no such parameter as thermal velocity. Due to the non-symmetrical shape of the DF of velocities of evaporated particles, the expression for the mass flux has a non-Hertzian form, anyway, (see below) the factor $\sim \sqrt{T}$ (where T is the temperature of a liquid) arises for the mean velocity, and, consequently, we may write an expression in a form similar to (7.3.1):

$$J^{\text{ev}} = \alpha \frac{m n_{\text{s}} \bar{\nu}}{4}. \tag{7.3.2}$$

Thus, we express our evaporation flux as being proportional to the Hertzian flux at corresponding parameters. Two questions follow from the (7.3.2).

Why do we use such a strange representation? Historically, when the MDF was assumed to be correct for the DF of evaporated molecules, such a form as (7.3.2) looked logical, and parameter α described the distinction of real number density in a vapor phase at vicinity of a liquid n from the saturation value n_s in (7.3.2).

Honestly, we cannot explain this matter properly, because, from our point of view, it is impossible to do so: any consequent consideration based on the MDF must lead to $\alpha=1$, as we understand. Possibly, the references to the non-maximum rate of evaporation could be useful to understand the understandable. Actually, the meaning of the evaporation coefficient is plain and simple: it is the adjustment coefficient which must repair some problems concerning the question of agreement with experiments. Indeed, many parameters in physics have this meaning.

The second question to consider is: what are the "corresponding parameters?" These are parameters are the ones which satisfy the saturation state, i.e., the number density of particles in (7.3.2) must be chosen on the saturation curve: $n_s(T)$.

Thus, from the traditional position, the evaporation coefficient must be defined experimentally, or, at least, with additional theoretical methods.

However, if we are informed about the results of Chap. 5, then we understand that representation (7.3.2) leads to the determination of the evaporation coefficient almost immediately. No problems arise here in a sense of the discussion about a theoretically maximum flux, possibility of $\alpha = 1$, etc. With certain DFs (7.3.2) is a clear definition of the evaporation coefficient with a clear physical meaning of this value: we want (for some reason) to express the evaporation flux through the Hertz flux, then calculate the corresponding factor α from (7.3.2).

We may calculate α in two ways: with number density n obtained from the results of Chap. 6, or by constructing some correlations for n, connecting this quantity with vapor parameters.

Because the second way looks more sophisticated, we shall start with this approach.

7.3.3 Analytical Calculation

To calculate the evaporation coefficient, we must clearly understand its redundancy. As we stated above, we may calculate fluxes without such parameters as α . Thus, because we can find mass flux independently from expression (7.3.2), we may use (7.3.2) to define parameter α .

As it follows from Chap. 5, the evaporation flux is:

$$j^{\text{ev}} = n_{\text{L}}\bar{v} = n_{\text{L}}\sqrt{\frac{\pi T}{2m}}.$$
(7.3.3)

According to the consideration presented above, we have to find the number density $n_{\rm L}$ in (7.3.3), connecting it with the vapor pressure. The simplest way seems to replace the number density in (7.3.3) with a Clapeyron equation–like $n_{\rm L} = p/T$. However, this would be an erroneous move. Actually, for non-equilibrium state (with a non-MDF) the equation of state differs from the Clapeyron expression. Thus, to bind the pressure of the evaporated particles we must find the "equation of

state" for the evaporation flux, i.e., find the dependence $p = f(n_L, T)$ for the evaporation flux.

As it follows from statistical physics, pressure p that is exerted perpendicular to the surface of a liquid (i.e., in the direction of z axis) can be calculated through the DF as the moment of flux:

$$p = \overline{2mv^2} = n \int_{0}^{\infty} 2mv^2 f_z(v) dv.$$
 (7.3.4)

Here *n* (the number density of the particles) appears because all our DFs f(v) are normalized on unity. We must integrate (7.3.4) for all velocity components; (7.3.4) is written with regards to the normalized condition for DFs on all other projections of velocity: $\int_{-\infty}^{\infty} f(v_{x,y}) dv_{x,y} = 1$; in (7.3.4) we omit the index "z" for the velocity v.

For example, for the MDF we have from (7.3.4):

$$p = n_{\rm s}T,\tag{7.3.5}$$

that is, the Clapeyron equation. With (7.3.5), we are able to represent the Hertz flux, rewriting it in the form:

$$j^{\mathrm{H}} = \frac{p}{\sqrt{2\pi mT}}.\tag{7.3.6}$$

Evaporated atoms have a DF with a more "filled" high-energy tail, thus, the pressure of this flux is:

$$p = \int_{0}^{\infty} 2mn_{\rm L}v^2 \frac{mv}{T} e^{-\frac{mv^2}{T}} dv = 4n_{\rm L}T,$$
 (7.3.7)

As we see, our demanded "equation of state" differs from the usual correlation. Note, of course, that this is not an equation of state per se: pressures for directions x and y correspond to the Clapeyron equation.

Consequently, the flux from the evaporation surface can be expressed with $n_L = n_s/4$ as:

$$j^{\text{ev}} = n_{\text{L}} \sqrt{\frac{\pi T}{2m}} = \frac{\pi}{4} \frac{p}{\sqrt{2\pi mT}} = \frac{\pi}{4} j^{\text{H}}.$$
 (7.3.8)

Thus, if one demands that the pressure of evaporated particles must be equal to the pressure of the saturated vapor, then we obtain from (7.3.8) that the evaporation coefficient is:

$$\alpha = \frac{\pi}{4} \approx 0.785. \tag{7.3.9}$$

As we see, this number is very close to some experimental values for the evaporation coefficient (or, considering its history, to the most frequently measured value). Note that this value of α is also obtained in various numerical simulations, e.g., Zhakhovskii and Anisimov (1997), Tsuruta and Nagayama (2004) and Yasuoka et al. (1995).

For a DF for an irregular surface (see Chap. 5 for detail) we have by analogy:

$$p = 6n_{\rm L}\Upsilon_{\rm z},\tag{7.3.10}$$

$$\alpha = \frac{2}{3} \sqrt{\frac{T}{\Upsilon_z}}. (7.3.11)$$

We see from (7.3.10) that in a more general case the evaporation coefficient varies according to the parameter $\bar{\epsilon}$. As usual $\Upsilon_z < T$ (see Chap. 5) then $\alpha > 2/3$; for instance, for conditions of numerical simulations from Chap. 5, $T = 120 \, \text{K}$, $\Upsilon_z = 93 \, \text{K}$ and $\alpha \approx 0.76$, i.e., almost the same value.

However, someone may state that all our considerations are speculative ... the "equation of state" which is not, in fact, an equation of state, and so on. We have to calculate the evaporation coefficient in another way, under another assumption.

Another approach to calculate the evaporation coefficient may be based on the equality of heat fluxes. That is, the heat flux from the evaporation surface:

$$q^{\text{ev}} = n_{\text{L}} T \sqrt{\frac{25\pi T}{8m}},\tag{7.3.12}$$

and the heat flux from the vapor obtained with the MDF:

$$q = n_{\rm s}T\sqrt{\frac{2T}{\pi m}}. (7.3.13)$$

As we see, to satisfy both (7.3.11) and (7.3.12) with $q^{\text{ev}} = q$, there must be $n_{\text{L}} = \frac{0.8n_{\text{s}}}{\pi}$. Consequently, for the evaporation flux we have:

$$f^{\text{ev}} = n_{\text{L}}\bar{v} = \frac{0.8n_{\text{s}}}{\pi} \sqrt{\frac{\pi T}{2m}} = 0.8 \frac{p_{\text{s}}}{\sqrt{2\pi mT}}.$$
 (7.3.14)

Thus, we obtain (once again!) that the evaporation coefficient $\alpha = 0.8$. This result is not surprising, considering the fact that now $n_L = 0.255n_s$ instead of $n_L = 0.25n_s$ from the previous consideration.

Analogically, for an irregular surface one may obtain $\alpha = \frac{1}{1 + \Upsilon_z/4T}$, i.e., slightly larger than 4/5. For values $\Upsilon_z = 93 \text{ K}$ and T = 120 K we have $\alpha \approx 0.84$.

As we see from the analytical consideration $\alpha \approx 0.8 \pm 0.1$ regardless of the method applied. Let us see the results of numerical simulations next.

7.3.4 Numerical Calculations

It is not very hard to calculate the total mass flux from the evaporation surface. The problem is to associate this flux with the *corresponding* Hertz flux. We will compare our calculated flux with the Hertz flux (7.3.3) for $p = p_s(T)$ —the saturation pressure at the interface temperature T; saturation pressures were taken from the National Institute of Standards and Technology database.

As in previous chapters, in numerical calculations we consider the evaporation of liquid argon into a vacuum; results are presented in Table 7.2.

In the general case, the calculated value of the evaporation coefficient is close to values predicted for an absolutely flat evaporation surface and for a highly disturbed surface, for which DF (5.2.25) was obtained. Evidently, this situation is predictable considering the fact that these two DFs were obtained for two limiting cases; thus, one may expect that the true value of any quantity lays between these two limiting values α^{flat} and $\alpha^{\text{irregular}}$.

The final matter to discuss is to what degree the results for evaporation into a vacuum are adequate for real situations of evaporation into a gas? Evaporation into a vacuum is the limiting or the model case which allows us to consider the case of pure evaporation. This is not an adequate consideration, this is the consideration we need. Complicated situations, where the evaporation flux is affected by the condensation flux will be considered later.

7.3.5 The Evaporation Coefficient Is Unnecessary

The evaporation flux may be calculated without any hypothesis about the pressure on the evaporation surface, the value of the total heat flux (operations which were used above), etc.

From the results of Chap. 6, we see that the evaporation flux may be defined through the number density at the liquid surface n_0 and the binding energy of the atom on the surface U:

$$j^{\text{ev}} = n_0 \Gamma\left(\frac{1}{2}, \frac{U}{T}\right) \sqrt{\frac{T}{8m}}.$$
 (7.3.15)

If, for unknown reasons, someone needs the evaporation coefficient anyway, they may obtain it from (7.3.14) and (7.3.15):

Table 7.2 Evaporation coefficient from numerical simulations

T (K)	αnumerical	α ^{irregular}	$\alpha^{\rm flat}$
115	0.83	0.83	0.8
120	0.86	0.84	0.8

$$\alpha = \frac{\sqrt{\pi} n_0}{2 n_s} \Gamma\left(\frac{1}{2}, \frac{U}{T}\right),\tag{7.3.16}$$

where the ratio n_0/n_s is the ratio of the densities of the liquid and the vapor.

7.3.6 Condensation Coefficient Versus Stick Coefficient

Can we calculate the condensation coefficient as easily as the evaporation one? The answer depends on our definitions.

One of the definitions of the condensation coefficient is the ratio:

$$\beta = \frac{\text{number of molecules that stick to a liquid}}{\text{number of molecules that strike a liquid}}.$$
 (7.3.17)

However, actually, this value would differ from the factor in Hertz–Knudsen equation in cases when the condensation flux on the interface from the vapor phase does not obey the Hertz formula. Thus, the condensation coefficient and the quantity defined by relation (7.3.17) are different things.

This is an interesting point, deserving special consideration.

7.4 About the Condensation Coefficient

7.4.1 Two Types of Condensation Coefficient

Under the term "condensation flux" j^{cond} we mean the number of vapor particles attaching to a liquid surface per second per a square unit. This is a solid-state quantity in contrast to the condensation coefficient. As we discussed in the beginning of this chapter, the condensation coefficient may be defined in two different ways:

• As the striking coefficient—ratio of the surface flux j^{surf} to the Hertz flux $j^{\text{H}} = \frac{n\bar{v}_T}{4}$ at corresponding parameters, i.e., the condensation coefficient Mark I is:

$$\beta^{\rm I} = \frac{j^{\rm surf}}{j^{\rm H}}.\tag{7.4.1}$$

• As the sticking coefficient—the fraction of particles attached to the surface, i.e., if the flux from the vapor on the evaporation surface is j^{surf} then condensation coefficient Mark II is:

$$\beta^{\rm II} = \frac{j^{\rm cond}}{j^{\rm surf}}.$$
 (7.4.2)

• Thereby, the total condensation coefficient is:

$$\beta = \beta^{\mathrm{I}} \beta^{\mathrm{II}} = \frac{j^{\mathrm{cond}}}{j^{\mathrm{H}}}.$$
 (7.4.3)

The condensation coefficient β^{I} may also be redefined through the corrected flux in the style of Kucherov-Rickenglaz instead of j^{H} (i.e., with the shifted MDF for vapor particles; see Sect. 7.2), but, anyway, the logic behind both approaches is the same. Below we will strictly use expression (7.4.1) for β^{I} .

The two definitions of condensation coefficient, i.e., (7.4.2) and (7.4.3), are equivalent if and only if the surface flux is determined by the Hertz formula. Because a vapor phase is supposed to be an equilibrium state and the DF of vapor molecules is Maxwellian, then we may expect the Hertz formula for the flux on the surface. However, commonly, this is not the case. We may point out at least two reasons for the inequality $j^{\text{surf}} \neq j^{\text{H}}$.

The first reason for a non-Hertzian flux on an interface is the possible non-equilibrium state of vapor near a liquid surface. For instance, this non-equilibrium may be caused by the temperature difference between a liquid surface and a vapor.

The second reason is the interaction of the condensation flux with particles being evaporated from the liquid surface. Collisions between two fluxes lead—again, in the common case—to a suppressed condensation flux. One may expect that evaporated particles (which have higher velocities than Maxwellian-distributed particles) may repel the condensing atoms from the liquid surface. Thus, the condensation flux on the interface may be $j^{\text{surf}} < j^{\text{H}}$, and the diminishing of the measured condensation flux on the surface—relative to our expectations that $j^{\text{surf}} = j^{\text{H}}$ —is not caused by the sticking properties of the liquid surface, but induced by the decreasing vapor flux on the liquid surface.

It is difficult to describe this problem in the latter sense, but we may at least depict a description to estimate the influence of the evaporation flux on the flux of condensing particles.

7.4.2 A Sidestep: A Collision Map

As we discussed in Chap. 3, a differential equation is a questionable theoretical instrument for use on small scales. During a single collision, the velocity DF may undergo appreciable deviations, thus, one cannot expect the DF to have a continuous character on such scales.

Usually, it is assumed that any DF would be "thermalized" at scales much greater than the mean free path (MFP) l; i.e., after $\sim 10^1$ collisions any DF turns into a Maxwellian. Of course, one may find a smoothed DF with a kinetic equation anyway, but, usually, the next step after such solutions is the interpretation of the results obtained from them.

Let us try to avoid the use of differential equations using an old alternative way: maps. Assume that we have a velocity $\mathrm{DF}\,f(v)$ at x=0. Then we want to know this DF at x=L, where distance $L\!\sim\!l$, i.e., an order of magnitude of the MFP. Note that, e.g., L=0.5l satisfies this condition too: in this case some particles would also undergo collisions.

Thus, we want to construct a map Λ for a new DF: if the DF before a collision is $f_0(\nu)$ and after a single collision is $f_1(\nu)$, then:

$$f_1(v) \leftarrow \Lambda f_0(v). \tag{7.4.4}$$

Thereby, for n collisions we have DF in the form:

$$f_n(v) \leftarrow \Lambda^n f_0(v).$$
 (7.4.5)

Then, we have to enter the probability p_n of a particle extending the distance L with n collisions; i.e., the probability to pass all the way without any collision is p_0 , the probability to move through with one collision is p_1 , etc. Of course, there must be:

$$\sum_{n=0}^{\infty} p_n = 1. (7.4.6)$$

To construct the final form of the DF at distance L, we should remember the meaning of the DF: f(v)dv is simply the number of particles with velocity v. Thus, the total number of particles with velocity v can be found at distance L with:

$$f(v,L)dv = \sum_{n=0}^{\infty} p_n \Lambda^n f(v,0) dv.$$
 (7.4.7)

As for the probability to pass distance L with n collisions, the Poisson distribution seems to be a convenient function with a mean value $\lambda = L/l = Kn^{-1}$:

$$p_n = \frac{e^{-\lambda} \lambda^n}{n!}. (7.4.8)$$

Map Λ is the key of course. It may be represented in the style found in Chap. 3:

$$\Delta f = \int w(\Delta)f(v - \Delta)d\Delta, \qquad (7.4.9)$$

where $w(\Delta)$ is the probability of changing velocity v to Δ due to a collision. In turn, function $w(\Delta)$ may be represented with DFs of particles which have collided; note

that in the general case we may consider different DFs: f(v) for the particles of interest and F(V) for scattering particles; see also Chap. 3, where such constructions like (7.4.9) were discussed in detail. Below we give an example of the use of (7.4.9) for evaporation–condensation DFs.

Finally, we may note that one may expect that $\lim_{n\to\infty} \Lambda^n f$, or at least $\lim_{\lambda\to\infty} \sum_{n=0}^\infty p_n \Lambda^n f$ for any function f, tends to be a MDF; in this case it is necessary that the DF of scattering particles is F=f. We discuss the nature of the MDF in Chap. 2.

7.4.3 Estimation of the Role of an Evaporation Flux

Here we apply the consideration given in the previous section to estimate the influence of the evaporation flux on the condensation flux.

Let us consider the flux from a vapor with a DF $f_1(\nu)$ and the flux of the countermoving particles from the liquid surface, DF $f_2(\nu)$. We want to find the DF for vapor particles after collisions with the evaporation flux. To simplify, we will consider only a single projection of velocity—normal to the liquid surface. In this section we only illustrate how an evaporation flux distorts the condensation flux from the bulk of a vapor, rather than attempting to calculate the exact value of the condensation coefficient.

Assume that far from the evaporation surface the DF is Maxwellian:

$$f_1(v_1) = \underbrace{\sqrt{\frac{2m}{\pi T}}}_{A} \exp\left(-\frac{mv_1^2}{2T}\right).$$
 (7.4.10)

We normalize this function in a such manner that $\int_0^\infty f_1(v) dv = 1$. For evaporation particles, we will use the DF:

$$f_2(v_2) = \frac{mv_2}{T} \exp\left(-\frac{mv_2^2}{2T}\right).$$
 (7.4.11)

After a collision, using the probable density function $\omega(\theta)$ and a scattering angle θ in a center-mass coordinate system, the vapor particle obtains velocity:

$$v = (v_1 + v_2)\cos^2(\theta/2) - v_2. \tag{7.4.12}$$

We are interested in DF f(v), which may be found as:

$$f(v) = \int \int f_1(v_1) f_2(v_2) \omega(\theta) \frac{\mathrm{d}v_1}{\mathrm{d}v} \mathrm{d}\theta \mathrm{d}v_2. \tag{7.4.13}$$

Below we will use the solid-sphere potential of interaction with:

$$\omega(\theta) = \frac{\sin \theta}{2}.\tag{7.4.14}$$

After a collision, the flux on the liquid surface consists of two parts:

- Particles from the vapor which were scattered at angle $\varphi = \frac{\theta}{2} < \frac{\pi}{2}$ in a laboratory coordinate system.
- Particles from the liquid, that are returning to the liquid after a collision at angle $\varphi > \frac{\pi}{2}$.

Let us find the first part of the flux. We have:

$$f^{(1)}(v) = \int_{0}^{\infty} f_{2}(v_{2}) \left(\int_{0}^{\pi} f_{1} \left(\frac{v + v_{2}}{\cos^{2}(\theta/2)} - v_{2} \right) \frac{\sin \theta d\theta}{2 \cos^{2}(\theta/2)} \right) dv_{2}$$

$$= \frac{A}{2} \frac{\Gamma(1/2, z)}{\sqrt{z} + 2/\sqrt{\pi}},$$
(7.4.15)

where:

$$z = \frac{mv^2}{2T}. (7.4.16)$$

Thus, in this case only a fraction $\int_0^\infty f^{(1)}(v)dv = 0.38$ of the vapor molecules reach the liquid surface after a single collision. The DF for other particles, which were scattered back to the vapor, is:

$$f_{-}^{(1)}(v) = \int_{-v}^{\infty} f_2(v_2) \left[\int_{2\arccos\sqrt{\frac{v+v_2}{v_2}}}^{\pi} f_1\left(\frac{v+v_2}{\cos^2(\theta/2)} - v_2\right) \frac{\sin\theta d\theta}{2\cos^2(\theta/2)} \right] v_2$$

$$= \int_{-v}^{\infty} f_2(v_2) \left[\int_{-v}^{-1} 2f_1\left(\frac{v+v_2}{x^2} - v_2\right) \frac{dx}{x} dv_2. \right] (7.4.17)$$

The fraction of vapor particles that is reflected back to the bulk of a vapor after a collision is $\int_{-\infty}^{0} f_{-}^{(1)}(v_2) dv_2 = 0.62$. Thus, the flux from the liquid surface pushes back the vapor molecules: as we discussed above, evaporated particles have higher velocities and their flux is "stronger" than the condensation flux. For example, let the temperature of the liquid surface be 100 K, while the temperature of vapor is only 0.1 K (that is only an approximation of a limiting case of a super-cooled gas, a model of almost immobile particles). In such a case we have $\sim 2\%$ of the vapor

particles reaching the surface; the other 98% of very slow vapor particles are thrown back by the evaporated particles, akin to billiard balls.

However, as we remember, there also exists a second part of the flux—evaporated particles that have been scattered back to the liquid surface after collision. To obtain this flux, we replace the DFs in (7.4.14) as $f_1(v_1) \rightarrow f_2(v_1)$, $f_2(v_2) \rightarrow f_1(v_2)$ with functions (7.4.10) and (7.4.11); then we have to take into account that now the velocity after collision v has an opposite sign relative to the initial velocity v_1 . Finally, we have:

$$f^{(2)}(v) = 2A \int_{v}^{\infty} \exp\left(-\frac{mv_2^2}{2T}\right) \left(\int_{0}^{\sqrt{\frac{v_2-v}{v_2}}} \frac{m}{xT} f_2\left(\frac{v_2-v}{x^2}-v_2\right) dx\right) dv_2, \qquad (7.4.18)$$

where $x = \cos(\theta/2)$ and v > 0 is the velocity directed toward the liquid surface. Integrating, we have the same expression as (7.4.15), and the total DF $f_3(v) = f^{(1)}(v) + f^{(2)}(v)$ of the particles on the liquid surface is:

$$f_3\left(z = \frac{mv^2}{2T}\right) = \sqrt{\frac{2m}{\pi T}} \frac{\Gamma(1/2, z)}{\sqrt{z} + 2/\sqrt{\pi}}.$$
 (7.4.19)

Figure 7.2 shows a representation of the initial DF $f_1(v)$ in the bulk of the vapor along with the distorted function (7.4.19).

If we restrict our consideration to only function (7.4.19), i.e., assume that every vapor particle undergoes exactly one collision with evaporated particles (no more, no less), we may find for the ratio of fluxes, i.e., for a "type I" condensation coefficient:

$$\beta^{\rm I} = \frac{j^{\rm surf}}{j^{\rm H}} = \frac{\int_0^\infty v f_3(v) dv}{\int_0^\infty v f_1(v) dv} = \frac{1}{2}.$$
 (7.4.20)

It is interesting to apply the approach from the previous section, i.e., use the expressions in (7.4.15) and (7.4.19) as definitions of operator Λ (see Sect. 7.4.2). Of course, the flux of scattered particles cannot be described in 1D geometry, but, again, we can approximately calculate the DF after the second collision using (7.4.15) and (7.4.18) by replacing $f_1 \rightarrow f_3$ from (7.4.19). In this manner, the total DF may be represented by the expression:

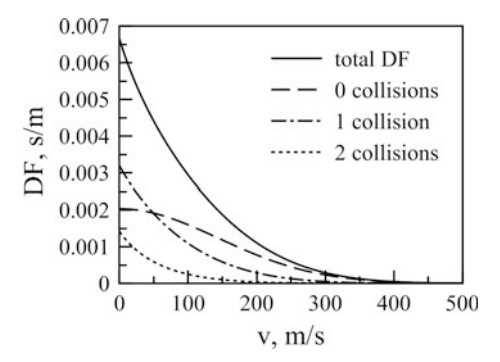
$$F(v) = p_0 F_0(v) + p_1 F_1(v) + p_2 F_2(v) + \cdots$$
 (7.4.21)

where each *i*th term describes the contribution of *i* collisions with probabilities p_i according to (7.4.8). Specifically, $F_0 = f_1$, $F_1 = f_3$ and F_2 must be calculated in the manner described in the previous paragraph.

Fig. 7.2 Distribution function at the surface both before and after one collision. DF, distribution function; MDF, Maxwellian distribution function

0.008 — MDF — after 1 collision 0.002 — 0 100 200 300 400 500 v, m/s

Fig. 7.3 Distribution function calculated from (7.4.20) and its components for Kn = 1. DF, distribution function



The DF (7.4.21) is represented in Fig. 7.3; as one can see, there are no qualitative differences from the DF in Fig. 7.2. However, for DF (7.4.21) we have a slightly larger condensation coefficient for $Kn \sim 1$, because a part of the condensation flux reaches the surface unimpeded (using function f_3 (7.4.20) we have just assumed that every particle in the vapor undergoes a collision). Specifically, for Kn = 1 (i.e., for L = 1) we have $\beta^I \approx 0.6$.

Possibly, it is not superfluous to depict that for our treatment—when we find the distortion of the condensation DF because of its interaction with the evaporation flux—the MFP l in the Knudsen number means "mean free path between two successive collisions with *evaporated particles*." For a weak evaporation flux, the effect of evaporated particles on the condensation flux would be negligible. For high evaporation conditions, we must take into account both collisions of vapor molecules with evaporated ones, and secondary "vapor molecule-vapor (scattered) molecule" interactions, etc. The only, and weak, excuse for such an approximate consideration of such a complex problem is the statement that such a complex problem is out of the scope of this book, evidently (because this is not a book about the "kinetics of condensation").

There more often path L is taken by a particle, the more collisions this particle undergoes. For a low Knudsen number, every vapor molecule has many collisions, thus, the DF (7.4.21) will be skewed to the ordinate axis, and the flux on the interface

will be significantly different from the Hertz flux of Maxwellian-distributed particles. In this case, one may expect that $\beta^I \ll 1$.

In fine, we should also note that for a cold evaporation surface (slow-moving evaporated particles) and hot vapor, the fast vapor molecules would "grab" evaporated molecules and return them to the liquid surface. In this case, the former condensation flux increases (because now it consists not only of the condensation flux itself but of the returning evaporated particles too). Depending on the experimental method, in this case the condensation coefficient $\beta > 1$ would be measured.

Let us briefly analyze these conditions. In an experiment, for "the total condensation conditions" (i.e., for the mass flux on the interface J < 0) the measured flux:

$$J = \beta \left(J^{\text{H,ev}} - J^{\text{H,cond}}\right),\tag{7.4.22}$$

where $J^{\rm H,\,ev}$ and $J^{\rm H,\,cond}$ are the Hertz fluxes at the interface. In the case when the evaporation flux is partially suppressed by the condensation flux, i.e., the evaporation flux is $J^{\rm H,\,ev}-\Delta J^{\rm H,\,ev}$ (because part of the flux $\Delta J^{\rm H,\,ev}$ returns to the surface), the form of the calculated (or measured) condensation coefficient β (7.4.22) would be different from the "true" value β' as:

$$\frac{1}{\beta} - \frac{1}{\beta'} = \frac{\Delta J^{\mathrm{H, ev}}}{J}.\tag{7.4.23}$$

7.4.4 A Sidestep: A Common Consideration

The problems of the evaporation/condensation coefficients may be discussed in common, without any certain DFs. This appears logical, because, as we see, we have some difficulties with certain DF for particles condensing on the liquid surface.

Let us consider a quasi-equilibrium DF in the form:

$$f(v) = Af\left(\frac{v^2}{T}\right),\tag{7.4.24}$$

where A is the normalizing factor. The simplest example of such a DF is the MDF $f \sim \exp(-mv^2/2T)$ or a shifted Maxwellian—a Maxwellian-like DF with a non-zero average velocity. Then, from the normalization condition $\int Af(v)dv = 1$ we have $A \sim 1/\sqrt{T}$. Consequently, for the flux we can obtain the correlation:

$$j = n \int vAf\left(\frac{v^2}{T}\right)dv = \left\{x = \frac{v^2}{T}; dv = \frac{1}{2}\sqrt{\frac{T}{x}}dx\right\} \sim \sqrt{T}n \underbrace{\int f(x)dx}_{0}, \quad (7.4.25)$$

where the last integral is represented as a constant. Again, for a quasi-equilibrium system it follows from the Clapeyron equation that n = p/T, and that the flux from the vapor to the interface is:

$$j^{\text{cond}} = C \frac{p}{\sqrt{T}} = \frac{\beta^{\text{I}} \beta^{\text{II}} p}{\sqrt{2\pi mT}}.$$
 (7.4.26)

In other words, when the temperature exists as a measure of the kinetic energy of particles, the flux must take the form of (7.4.26). Expression (7.4.26) could be obtained even more easily based on dimension reasons: if we can operate with such parameters as pressure and temperature, then we must have (7.4.26).

In (7.4.26) the quantity β^{I} is the parameter defining the distinction of the condensation flux from the Hertz expression, β^{II} is a sticking coefficient.

As discussed above, for an evaporation flux we have a relation in the same form. Combining the expressions for evaporation and condensation fluxes in one expression for the total flux, we obtain the Hertz–Knudsen formula:

$$j^{\text{tot}} = \frac{\alpha p}{\sqrt{2\pi mT}} - \frac{\beta^{\text{I}} \beta^{\text{II}} p}{\sqrt{2\pi mT}}.$$
 (7.4.27)

Actually, we have made an assumption in this consideration—about the equilibrium-like DF (7.4.27) in the vicinity of the interface: indeed, in common the case, a non-equilibrium state cannot be described by such a parameter as temperature. In the case of a strongly non-equilibrium state, one may replace T in the second term of the right-hand side of (7.4.27) with the measure of kinetic energy $\bar{\epsilon}$, this is an absolutely essential move. Also, pressure p, in the common case, must be calculated as described in the beginning of Sect. 7.2.

The sticking coefficient β^{II} may be found very easily in comparison to the mysterious parameter β^{I} .

7.4.5 The Sticking Coefficient

As we see from the previous section, the condensation coefficient can be defined as the fraction of the adsorbed particles on the liquid surface, i.e., as the sticking coefficient. We also defined it above as the condensation coefficient.

It is difficult to determine this experimentally, but easy to calculate this ratio in numerical simulations. In comparison with other calculations presented in this book, this a relatively simple task. The only requirement is "purity" of the numerical experiment: we need to exclude interference from condensation and evaporation fluxes. The easiest way to suppress the evaporation process is by introducing a low-temperature condition; thus, we may expect that the evaporation flux would be weak.

Let us consider a liquid (as usual for our calculations we chose argon) at a sufficiently low temperature. We will not consider an interaction between the vapor phase and the liquid phase; we will "throw" atoms from a vacuum (yes, remember what we wrote about condensation from a vacuum) onto a liquid surface. In such a manner, we can easily observe the fate of any particle impacting the liquid surface. It is a clear method: we can determine atom energy (i.e., velocity) and then construct a dependence of the condensation coefficient on this energy (velocity).

However, our numerical experiment did not let us define any function of the condensation coefficient, because all the atoms that were dropped on the liquid surface were attached. These particles draw different trajectories (see Fig. 7.4), but all these trajectories contain their longest part inside the liquid. Actually, this fact was predictable: in previous chapters, we discussed the difference between a solid wall (a model construction) and a real surface. The local area of a liquid surface consists of a few atoms and wide holes between them, these holes are large enough to accept a new guest atom without any problem.

It is possible, of course, that an atom from the vapor would strike an atom from the surface directly, thus, after such a collision the impacting particle can be reflected. Such cases decrease the value of the sticking coefficient, but the probability of such processes is very low. Indeed, in our calculations we saw that all 22 particles became attached; in simulations by Kryukov and Levashov (2016) we find

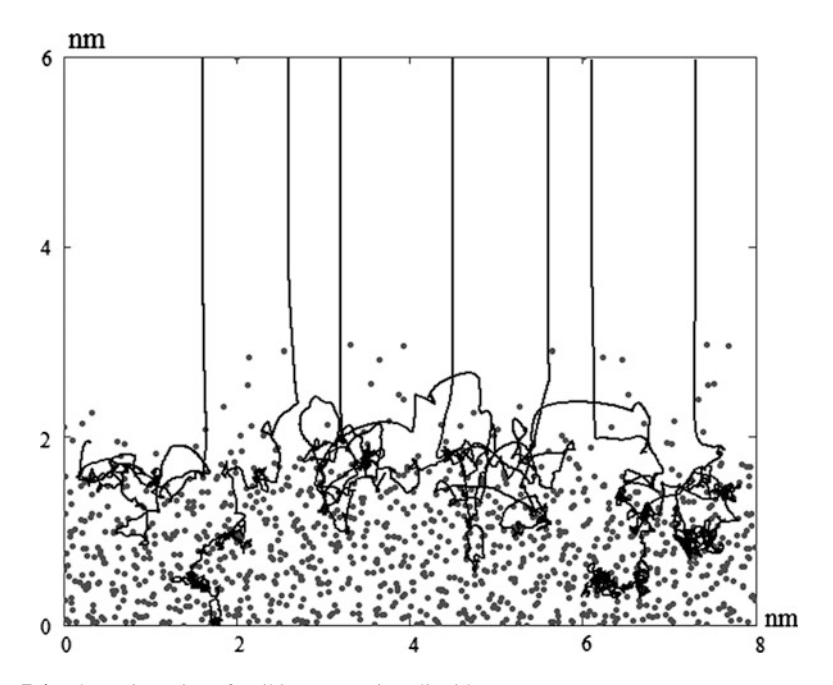


Fig. 7.4 The trajectories of striking atoms in a liquid

similar results: the value of the condensation coefficient is about 0.98. In recent work by Iskrenova and Patnaik (2017) a result of $\beta \approx 0.93 - 0.96$ was obtained.

Thus, we may conclude that $\beta^{II} \approx 1$, distinct from β^{I} which has, generally, a badly predicted value.

7.4.6 Experimental Values for Evaporation and Condensation Coefficients

In this section we try to explain how values of the evaporation coefficients differ in their magnitudes.

First, we admit that some explanations from Sect. 7.2 look reasonable: indeed, there are many uncontrolled parameters during the evaporation process. However, we also want to point out that there exists a deeper problem: a problem of the definition of the evaporation and condensation coefficients themselves.

As follows from considerations made in this section, the meanings of evaporation and condensation coefficients are unclear. The vapor flux on the liquid surface depends on the evaporation process, and vice versa, thus, the expression for the total mass flux is:

$$J^{\text{tot}} = J^{\text{ev}}(J^{\text{cond}}) - J^{\text{cond}}(J^{\text{ev}}). \tag{7.4.28}$$

By this formulation we mean that in the general case, when both fluxes are presented and are commensurable, the total mass flux on the interface is determined by a function $f(J^{\text{ev}}, J^{\text{cond}})$. It is almost impossible to extract the quantities α (evaporation coefficient) and β (condensation coefficient) from the measured value J^{tot} , especially considering the fact that the condensation flux is defined by two condensation coefficients:

$$J^{\text{tot}} = \beta^{\text{I}} \beta^{\text{II}} J^{\text{H}}. \tag{7.4.29}$$

Thus, we are faced with the task of determining three coefficients α , $\beta^{\rm I}$ and $\beta^{\rm II}$ from the single measured quantity $J^{\rm tot}$ and, evidently, it seems to be a rather impossible problem. Note that we do not see any physical reason for the equality $\alpha = \beta^{\rm I}$, $\beta^{\rm II}$, because all three parameters have a different meaning, as well as the fact that there appears to be no cause for the equalities $\alpha = \beta^{\rm II}$ at $\beta^{\rm I} = 1$.

Evaporation and condensation coefficients can only be determined for the clearest of cases of evaporation (when condensation is negligible) or condensation (neglecting evaporation, in this case $\beta=\beta^{\rm II}$). If we consider option #1, then we expect to find the evaporation coefficient $\alpha\approx 0.8$. For option #2, the expected value for the sticking coefficient is $\beta\approx 1$. In all other cases, when $J^{\rm ev}$ and $J^{\rm cond}$ are comparable, any value of the coefficient γ , which portrays an illusory coefficient $\alpha=\beta^{\rm II}$ at an illusory condition $\beta^{\rm I}=1$, will be obtained. Because of incomparable fluxes $J^{\rm ev}\gg J^{\rm tot}$ at the interface, we expect $\gamma\ll 1$ to be measured in such experiments.

7.5 Conclusion

The evaporation coefficient and its condensation analog are delicate things.

The evaporation coefficient α establishes a connection between the real mass flux from the interface and the Hertz expression with corresponding parameters: the temperature of the liquid (specifically, of the liquid surface) and with the mass (number) density or the pressure. Traditionally, pressure is always used, and its value corresponds to T, i.e., $p = p_s(T)$.

We should distinguish the condensation coefficient and the sticking coefficient from one another. Nowadays, they are different parameters, despite the definitions. The sticking coefficient is close to unity, while the condensation coefficient in its common sense is a mysterious quantity. Initially, the condensation coefficient represents the fraction of the sticking particles of the incoming flux, but this incoming flux must be defined correctly. The Hertz formula can be applied to a solid (non-evaporating) surface at equilibrium conditions, where the DF of the gas atoms is undisturbed.

However, we have another situation at the "liquid-vapor" interface. In a similar manner to flak artillery, the evaporation flux opposes part of the condensation flux. Evaporated particles distort the DF of vapor atoms, and the DF of the impacting particles is no longer Maxwellian. In this case the condensation coefficient obtains dual sense: the sticking coefficient β^{II} is unequal to the ratio of the condensation flux to the Hertz flux, which is now equal to the product $\beta^{I}\beta^{II}$, where parameter β^{I} defines deviations from the Hertz formula. We emphasize that β^{I} is not a constant: it depends on the evaporation flux and, more commonly, on conditions near the interface.

Under these considerations, the total flux on the interfacial surface may be represented in the form:

$$j^{\text{tot}} = \frac{\alpha p}{\sqrt{2\pi mT}} - \frac{\beta^{\text{I}} \beta^{\text{II}} p}{\sqrt{2\pi mT}}.$$

Strictly speaking, the second term does not matter much, because the dependence $\beta^{\rm I}(p,T)$ is stronger than the factor p/\sqrt{T} extracted from this term.

Thus, in experiments, the quantity j^{tot} can be measured (comparatively) easily using the weight method, for example. However, the unknown form of the right-hand side of the expression presented above forcefully obstructs any attempt to determine the evaporation and condensation coefficients. We cannot predict with any certain result β^{I} (except with estimations), thus, we cannot predict results obtained in certain treatments. However, we may predict that the range of the "artificial" (or "apparent", if we use existing terminology) coefficients will be wide.

However, within this chapter we present some certain results for the evaporation coefficient and—considering known relationships—for the condensation coefficient too.

7.5 Conclusion 231

With the DF function from Chap. 5, we find the value of the evaporation coefficient. With any method used the value obtained is always $\alpha \sim 0.8$ for any kind of evaporation surface (see Chap. 5).

In addition, in this chapter we calculated the sticking coefficient, i.e., $\beta^{II} \approx 1$. This result is not surprising, because, as we understand it, a liquid is always ready to accept atoms from a vapor. Both results—for α and β^{II} —were obtained earlier in numerical simulations.

However, we cannot determine β^{I} . With ponderous consideration we only estimate that the interaction with the evaporation flux strongly changes the DF of the condensing vapor atoms. Even a single collision between a vapor atom and evaporated atom leads to a noticeable decrease in parameter β^{I} .

Finally, we may conclude (just like a student defending their thesis) that further research is needed.

References

```
T. Alty, Proc. R. Soc. Lond. Ser. A 131, 554 (1931)
```

T. Alty, F.N. Nicoll, Can. J. Res. 4, 547 (1931)

T. Alty, Lond. Edinb. Dublin Philos. Mag. J. Sci. Ser. 7(15), 82 (1933)

G.T. Barnes, J. Colloid Interface Sci. 65, 566 (1978)

J.C. Bonacci et al., Chem. Eng. Sci. 31, 609 (1976)

N. Chodes et al., J. Atmos. Sci. 31, 1352 (1974)

L.J. Delaney et al., Chem. Eng. Sci. 19, 105 (1964)

I.W. Eames et al., Int. J. Heat Mass Transfer 40, 2963 (1997)

Y. Finkelstein, A. Tamir, Chem. Eng. J. 12, 199 (1976)

N. Fukuta, L.A. Walter, J. Atm. Sci. 27, 1160 (1970)

D.E. Hagen et al., J. Atmos. Sci. 46, 803 (1989)

K.C.D. Hickman, Ind. Eng. Chem. 46, 1442 (1954)

K.C.D. Hickman, I. White, Science 172, 718 (1971)

E.K. Iskrenova, S.S. Patnaik, Int. J. Heat Mass Transf. 115, 474 (2017)

D.T. Jamieson, Nature 202, 583 (1964)

O. Knake, I.N. Stranskii, Phys. Usp. 68, 261 (1959)

R.Y. Kucherov, L.E. Rikenglaz, Sov. Phys. JETP 37, 88 (1960a)

R.Y. Kucherov, L.E. Rikenglaz, Dokl. Akad. Nauk SSSR 133, 1130 (1960b)

A.P. Kryukov, VYu. Levashov, Heat Mass Transf. 52, 1393 (2016)

N.E. Levine, J. Geophys. Res. 78, 6266 (1973)

Y.Q. Li et al., J. Phys. Chem. A 105, 10627 (2001)

J.R. Maa, Ind. Eng. Chem. Fundam. 6, 504 (1967)

R. Marek, J. Straub, Int. J. Heat Mass Transfer 44, 39 (2001)

R.E.H. Miles et al., Phys. Chem. Chem. Phys. 18, 19847 (2016)

A.F. Mills, R.A. Seban, Int. J. Heat Mass Transf. 10, 1815 (1967)

M. Mozurkewich, Aerosol Sci. Tech. 5, 223 (1986)

K. Nabavian, L.A. Bromley, Chem. Eng. Sci. 18, 651 (1963)

U. Narusawa, G.S. Springer, J. Colloid Interface Sci. 50, 392 (1975)

J.C.A. Offringa et al., J. Chem. Thermodyn. 15, 681 (1983)

G.M. Pound, J. Phys, Chem. Ref. Data 1, 135 (1972)

E.K. Rideal, J. Phys. Chem. 38, 1585 (1924)

R.A. Shaw, D. Lamb, J. Chem. Phys. 111, 10659 (1999)

A.M. Sinnarwalla et al., J. Atmos. Sci. 32, 592 (1975)

J.D. Smith et al., J. Am. Chem. Soc. 128, 12892 (2006)

A. Tamir, D. Hasson, Chem. Eng. J. 2, 200 (1971)

T. Tsuruta, G. Nagayama, J. Phys. Chem. B 108, 1736 (2004)

M.A. Vietti, J.L. Fastook, J. Chem. Phys. 65, 174 (1976)

H. Wakeshima, K. Takata, Jpn. J. Appl. Phys. 2, 792 (1963)

P.M. Winkler et al., Phys. Rev. Lett. 93, 075701 (2004)

P.M. Winkler et al., J. Geophys. Res. 111, D19202 (2006)

K. Yasuoka, M. Matsumoto, Y. Kataoka, J. Mol. Liq 65-66, 329 (1995)

V.V. Zhakhovskii, S.I. Anisimov, J. Exp. Theor. Phys. 84, 734 (1997)

M. Zientara et al., J. Phys. Chem. A 112, 5152 (2008)

Recommended Literatures

T. Alty, Proc. R. Soc. Lond. Ser. A 149, 104 (1935)

M.A. Bellucci, B.L. Trout, J. Chem. Phys. 140, 156101 (2014)

K.S. Birdi et al., J. Phys. Chem. 93, 3702 (1989)

P.R. Chakraborty et al., Phys. Lett. A 381, 413 (2017)

E.J. Davies et al., Ind. Eng. Chem. Fundam. 14, 27 (1975)

P. Davidovitz et al., Geophys. Res. Lett. 31, L22111 (2004)

H.A. Duguid, J.F. Stampfer, J. Atmos. Sci. 28, 1233 (1971)

J.P. Garnier, Atmos. Res. 21, 41 (1987)

D.N. Gerasimov, E.I. Yurin, High Temp. 53, 502 (2015)

R. Goldstein, J. Chem. Phys. 40, 2793 (1964)

J.P. Gollub, J. Chem. Phys. 61, 2139 (1974)

J.M. Langridge et al., Geophys. Res. Lett. 43, 6650 (2016)

H. Mendelson, S. Yerazunis, AIChE J. 11, 834 (1965)

E.M. Mortensen, H. Eyring, J. Chem. Phys. 64, 846 (1960)

D.W. Tanner et al., Int. J. Heat Mass Transf. 8, 419 (1965)

J. Voigtlander et al., J. Geophys. Res. 112, D20208 (2007)

Chapter 8 Temperature Jump on the Evaporation Surface



We always expect the character of physical quantities to be continuous. For example, when we formulate a problem of heat transfer between two contacted bodies we put the temperatures of both bodies at the contact point as the same value—the so-called contact temperature.

This approach is generally incorrect for contact between two condensed matter bodies as well as being incorrect for more standard solid-gas or liquid-vapor contacts. At the contact point the temperature between two contacted phases differs. Starting in the late nineteenth century there were many works, both theoretical and experimental in approach, that tried to establish correlations between this temperature difference at an interface, along with other physical parameters.

In Sect. 8.1 we give an overall description of the theoretical expectations. In Sect. 8.2 we discuss the results of some experimental investigations of this phenomenon, which drastically differ from theoretical results. In fine, in Sect. 8.3 we give explanations for experimental data without corrupting the kinetic theory of gases.

8.1 Out of Equilibrium: The Difference Between the Temperature of a Liquid and of a Vapor

8.1.1 Non-equilibrium Kinetics

As was mentioned in Chap. 1, temperature T is the main thermodynamics parameter: in equilibrium all parts of a system have the same temperature T = const. However, evaporation is not an equilibrium process and one can expect that the temperature between two contacting phases can be different.

At first, we must explain what the "contacting phases" are. The macroscopic phase is a continuous medium; its kinetic properties (like viscosity, thermal

conductivity, etc.) may be subject to a physical description only under conditions of continuity. The macroscopic spatial scale L, must be much larger than the mean free path (MFP, l) of the molecules. Thus, if we introduce a Knudsen number:

$$Kn = \frac{l}{L}, \tag{8.1.1}$$

the condition for a continuous medium is $Kn \ll 1$. For $Kn \gg 1$, we have a so-called free molecular flow: particles move without collisions along a distance L. In both limiting cases (both on small scales and large scales) we have proper physical descriptions; for $Kn \ll 1$ this physical description collapses to the Navier-Stokes equations. The spatial scale corresponding to $Kn \sim 1$ is very inconvenient: rare collisions affect the flow here, but we cannot average these collisions on a sufficiently large scale and describe the whole medium as in continuum.

Thus, a medium is a continuous medium only at scales of $Kn \ll 1$. As for a liquid, the MFP there is approximately the mean inter-particle distance, so any volume of liquid that has a sufficient number of molecules to require the introduction of the parameter density can be considered a continuous medium (here are some remarks in terms of thermodynamics: we at least need locally defined properties of a medium, such as temperature and pressure; in any case, a large volume may be considered as a "continuous medium;" see Sect. 9.3). However, a gas is not so "continuous." The MFP of a molecule can be estimated as:

$$l \approx \frac{1}{n\sigma},\tag{8.1.2}$$

where the cross section of collisions is $\sigma \sim d^2$ (d is the diameter of a molecule) and the number density can be expressed through the Clapeyron equation n=p/T. Thus, for vapor at pressure p the MFP $l \sim T/(pd^2)$; for molecules with diameters of a few angstroms (further we will use 0.5 nm for consistency and precision) and temperatures of $\sim 10^2$ K we have an estimation for the MFP:

$$l \sim \frac{10^{-2}}{p[\text{Pa}]}, [\text{m}].$$
 (8.1.3)

We omit all the ~ 1 multipliers here, thus, the (8.1.3) is only an estimate to one order of magnitude. For example, for low pressures $\sim 10^3$ Pa we see that the MFP ~ 10 µm; for high pressures $\sim 10^6$ Pa we have a MFP ~ 10 nm.

Thus, a gas is not in continuum at scales approximating to the MFP. Particularly, a gas in not a continuum at distances approximating to the MFP from the liquid surface. For instance, on that spatial scale the distribution function (DF) of evaporated particles conserves its non-equilibrium form.

In other words, vapor in a continuous phase "begins at a distance" of ~ 10 MFPs from the liquid surface; here, the number 10 (which is equal to the number of fingers on two hands—the source of magic is finally identified here) reflects our representation of the term "a lot." Of course, the actual multiplier at the MFP represents the number of collisions which is sufficient to establish a stationary, uniform (or even equilibrium) DF.

On scales with $Kn \sim 1$ (inside the so-called Knudsen layer), at non-equilibrium conditions, vapor does not even have such a parameter as temperature. The DF of molecules and, thereby, the mean kinetic energy of molecules too, varies significantly from collision to collision; here it is impossible to provide any averaging to smooth the DF and quantities derived from it.

To obtain the expression for fluxes close to the evaporation surface, one needs to know the DF of velocity for vapor molecules near the evaporation surface.

The problem of determination of mass and energy fluxes in the Knudsen layer (see Sect. 3.7) may be solved using different formulations. One of these possible formulations is the problem of re-condensation: a gas flow between two parallel liquid layers with evaporation/condensation boundary conditions at the layers. The solution to this problem—functions for fluxes $j(\Delta p, \Delta T)$ and $q(\Delta p, \Delta T)$, i.e., functions of the temperature and of the pressure differences. The key problem is the DF in the gas layer.

Here we will follow the work of Labuncov (1966). Let us represent the velocity of a molecule as the sum of the mean (macroscopic) velocity \vec{u} and the chaotic component of velocity \vec{c} :

$$\vec{v} = \vec{c} + \vec{u}. \tag{8.1.4}$$

Thus, we represent all the fluxes—both from and to the evaporation surface—with two quasi-Maxwellian distribution functions (MDF) denoted as "a" and "b"; each DF has its own module (the mean kinetic energy $\varepsilon_{a,b}$) and normalizing factor:

$$F_{a}(v) = \frac{n_{a}}{(\sqrt{\pi}\varepsilon_{a})^{3}} \exp\left(-\frac{(v_{z} - u_{a})^{2} + v_{x}^{2} + v_{y}^{2}}{\varepsilon_{a}^{2}}\right), \quad v_{z} > 0,$$
 (8.1.5)

$$F_b(v) = \frac{n_b}{(\sqrt{\pi \varepsilon_b})^3} \exp\left(-\frac{(v_z - u_b)^2 + v_x^2 + v_y^2}{\varepsilon_b^2}\right), \quad v_z < 0.$$
 (8.1.6)

Thus, six constants must be obtained: $n_a, n_b, \varepsilon_a, \varepsilon_b, u_a, u_b$ —number density of particles, mean kinetic energy (analog of temperature) and velocities of two streams (from and at the interface). These parameters can be found from the kinetic equation having the form:

$$\frac{\mathrm{d}}{\mathrm{d}z} \int v_z \varphi_k(v) F(v) \mathrm{d}v = I(\varphi_k(v)), \tag{8.1.7}$$

where $I(\varphi_k)$ is the collision integral for functions φ_k that can be constructed for the moments of velocities. Here, the integral is:

$$\int v_z \varphi_k(v) F(v) dv = \int_0^\infty \int_{-\infty}^\infty \int_{-\infty}^\infty v_z \varphi_k(v) F_a(v) dv_x dv_y dv_z$$

$$+ \int_0^\infty \int_0^\infty \int_0^\infty v_z \varphi_k(v) F_b(v) dv_x dv_y dv_z$$
(8.1.8)

Here we use the functions which were chosen in Labuncov (1966):

$$\varphi_1 = 1$$
, $\varphi_2 = v_z$, $\varphi_3 = \frac{v^2}{2}$, $\varphi_4 = v_z^2$, $\varphi_5 = \frac{v_z v^2}{2}$, $\varphi_6 = \frac{v_z^2}{2}$. (8.1.9)

For the first three momentums $I(\varphi_{1,2,3}(v)) = 0$. For Maxwellian molecules (molecules with an interaction potential $\varphi(r) \sim r^{-4}$) one may represent:

$$I(v_z^2) = \frac{1}{9} \frac{m}{\eta} I(c^2) \left(I(c^2) - 3I(c_z^2) \right), \tag{8.1.10}$$

$$I\left(\frac{v_z v^2}{2}\right) = -\frac{1}{9} \frac{m}{\eta} I(c^2) I(c_z c^2) + u I_c(v_z^2), \tag{8.1.11}$$

$$I\left(\frac{v_z^2}{2}\right) = \frac{1}{6} \frac{m}{\eta} I(c^2) \left(I(c_z c^2) - 3I(c_z^3)\right) + 3uI(v_z^2), \tag{8.1.12}$$

where m, as usual, is the mass of the molecule and η is the dynamic viscosity of the vapor. The equations presented above, in principal, can be applied to various problems in which the DF in the Knudsen layer is needed; below we use it for the problem of re-condensation: gas evaporates from the liquid surface A and condenses on liquid surface B.

To solve system (8.1.7) with (8.1.10–8.1.12) we need boundary conditions. Let us consider a layer between planes A and B with known temperatures $T_A > T_B$ (under the condition $(T_A - T_B)/T_{A,B} \ll 1$); each plane corresponds to a liquid with a certain condensation coefficient β , i.e., fraction β is absorbed and fraction $(1 - \beta)$ is reflected (under diffusive or mirror conditions).

We omit the method of the solution of that system; in Labuncov (1966) various functions for various cases were obtained. For small Knudsen numbers and diffusive types of reflections we have simple equations for a continuous media:

$$j = k(\beta) \frac{\Delta p}{\sqrt{2\pi T}}, \quad q = jC_p T, \quad k(\beta) \approx \frac{\beta}{1 - 0.4\beta}.$$
 (8.1.13)

For high Knudsen numbers and mirror conditions for reflected molecules we have the following expressions for the fluxes:

$$j = \frac{2\beta}{2 - \beta} \frac{\Delta p}{\sqrt{2\pi mT}} \left(1 - \frac{1}{2} \frac{\Delta T}{\Delta p} \frac{p}{T} \right), \tag{8.1.14}$$

$$q = \frac{2\beta}{2-\beta} \sqrt{\frac{2T}{\pi m}} \Delta p \left(1 + \frac{1}{2} \frac{\Delta T}{\Delta p} \frac{p}{T} \right). \tag{8.1.15}$$

As we can see, we represent here the fluxes from the finite differences of the pressure and temperature of the liquid layers. One may find from (8.1.14) and (8.1.15) the expressions for Δp and ΔT to calculate these quantities with known mass and energy fluxes.

The problems of discontinuities on the liquid surface were considered in Albertoni et al. (1963) and Bassanini et al. (1967); more directly, the problem of the temperature jump on the evaporation surface was considered in Pao (1971) and using methods of irreversible thermodynamics in Cipolla et al. (1974). Actually, it is difficult to point out the single milestone work that determined the required temperature jump. This problem was solved step-by-step over a decade from the mid-1960s to the mid-1970s.

Using a modern approach, the temperature discontinuity between the vapor and the liquid phases can be expressed as:

$$\frac{T_{\rm V} - T_{\rm L}}{T_{\rm I}} = -C_1 q - C_2 J,\tag{8.1.16}$$

with $C_1=1.03\sqrt{\frac{m}{2T_{\rm L}}\frac{1}{p_s}}$ and $C_2=0.45\frac{1}{\sqrt{2mT_{\rm L}}}\frac{T_{\rm L}}{p_s}$. For instance, in the absence of a heat flux for water at $J\sim 1\frac{\rm g}{\rm m^2s}$, $T_{\rm L}=283~{\rm K}$ and, consequently, $p_s\approx 1.2\times 10^3~{\rm Pa}$, we have $T_{\rm V}-T_{\rm L}\sim -0.03~{\rm K}$.

We provide some explanations for correlation (8.1.16) in Sect. 8.1.3.

The temperature jumps predicted by (8.1.16) are very small, usually they are much less than 1 K. It is very difficult to measure such small temperature differences, especially considering the fact that these measurements must be done near the evaporated liquid surface (at distances of less than 1 mm). Some scientists were certain that it was impossible to determine such a small temperature discontinuity on such a small spatial scale experimentally, however, such experiments were performed with surprising results, see Sect. 8.2. However, before we examine such experimental data, we should discuss some overall problems with the temperature jump.

8.1.2 Some History of the Temperature Jump

The general concept about an inequality of temperatures between two contacted phases developed at the dawn of the theory of kinetics. Possibly, the earliest work

devoted to the temperature discontinuity is by Kundt and Warburg (1875). At the transition between the nineteenth and twentieth centuries, the temperature jump between the solid phase and the gas phase was considered in by Gregory (1936):

$$\Delta T = -v \frac{\mathrm{d}T}{\mathrm{d}n},\tag{8.1.17}$$

where ΔT is the temperature difference between the heated solid and the gas and $\frac{dT}{dn}$ is the temperature gradient in the gas near the surface in a normal direction. Quantity v was the object of investigation; in early works it was established that $v \sim 1/p$ or $v \sim l$ (mean free path).

Later, the first theory of the temperature jump at a "solid-gas" interface was provided by Smoluchowski in 1911; Smoluchowski obtained his results partly as a consequence of the work by Maxwell (1879), who introduced a method to solve a kinetic problem for a Knudsen layer. Note that the term "Knudsen layer" itself appeared in physics much later than Maxwell published that work: at that time Martin Knudsen was only 8 years old.

Smoluchowski found that (in simplified form provided by Gregory):

$$v = \frac{15}{2\pi} \frac{2 - \beta}{2\beta} l. \tag{8.1.18}$$

The temperature jump in the form of (8.1.17) was widely used in the mid-twentieth century, for example, in experiments for the determination of the thermal conductivity of gases at low pressure (earlier in that century the coefficient ν was derived from the same experiments) (see, e.g., Makhrov 1977a, b).

Then, in 1960s–1970s the modern life of the temperature discontinuity in the Knudsen layer near the evaporation surface began.

8.1.3 Discontinuity of Parameters: A Brief Overview

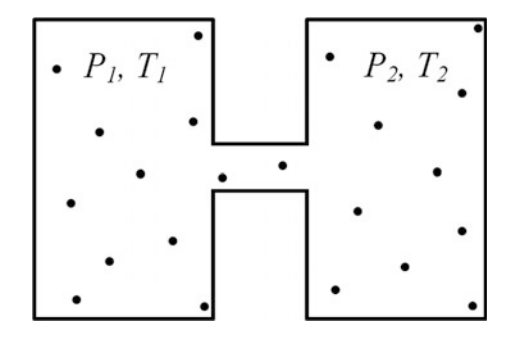
There is no exceptional magic accounting for jumps in physical parameters. Natura diligit vacuum, and finite differences of physical quantities are common things.

For instance, let us consider two large vessels containing gas at different temperatures and pressures (see Fig. 8.1). The vessels are connected with a sufficiently short tube: the Knudsen number here is $Kn \gg 1$; thus, molecules of gas can travel from one vessel to another without any collisions; arriving molecules can interact with their new neighbors only in the receiving vessel.

The flux from each vessel connected to the tube is:

$$j_{1,2} = \frac{p_{1,2}}{\sqrt{2\pi m T_{1,2}}}. (8.1.19)$$

Fig. 8.1 The Knudsen effect



In equilibrium state, flux $j_1 = j_2$, and we have:

$$\frac{p_1}{\sqrt{T_1}} = \frac{p_2}{\sqrt{T_2}}. (8.1.20)$$

This is a so-called Knudsen effect. Thus, for instance, at unequal pressures we have some sort of a temperature jump in such a system.

The Knudsen effect is the key to understand the physics of the temperature jump. For a non-equilibrium state, but one which is in the vicinity of equilibrium, the scale of the velocity is the thermal velocity $\sim \sqrt{T/m}$. Thus, the flux is $\sim n\sqrt{T/m} \sim p/\sqrt{mT}$, leading to the following expression for the total flux at the interface:

$$j = \frac{C_1 p_1}{\sqrt{2\pi m T_1}} - \frac{C_2 p_2}{\sqrt{2\pi m T_2}}. (8.1.21)$$

Constants C_1 and C_2 are close to one another, moreover, one can expect that in the case of full equilibrium $p_1 = p_2 = p_0$, $T_1 = T_2 = T_0$ and, since the total zero flux is expected, $C_1 = C_2$. We may slightly generalize this consideration, assuming that quantities $C_{1,2}$ are not constants and may depend on parameters of the non-equilibrium state, i.e., only at the equilibrium state does $C_1 = C_2$; for near-equilibrium states we may only have $C_1 \sim C_2$.

For a weak non-equilibrium—when pressures and temperatures in both phases almost coincide: $p_1 \sim p_2$ and $T_1 \sim T_2$ —one can expand the expression for flux (8.1.21) into a series both for p and T. Supposing that $C_1 = C_2 = C$, we obtain an equation for the total flux in the form:

$$j = \frac{C\Delta p}{\sqrt{2\pi mT_0}} - \frac{p_0}{T_0} \frac{C\Delta T}{\sqrt{8\pi mT_0}}.$$
(8.1.22)

This equation coincides with (8.1.14) at $C = \frac{2\beta}{2-\beta}$.

The meaning of (8.1.22) is clear: the total flux is caused by temperature or pressure differences. However, we can reverse this consideration: for a non-zero

total flux a difference in pressures or temperatures must exist. Actually, we doubt that these explanations are equivalent in their nature, because it seems to us that in the second case the cause and the effect has switched place.

In the most general case, we may compose a similar equation for the heat flux, obtaining a system of equations of the form:

$$\begin{cases} j = c_j^p \Delta p + c_j^T \Delta T; \\ q = c_p^p \Delta p + c_a^T \Delta T. \end{cases}$$
 (8.1.23)

We can then solve this system to find the jumps in temperature and pressure:

$$\begin{cases} \Delta T = c_T^j j + c_T^q q; \\ \Delta p = c_p^j j + c_p^q q. \end{cases}$$
 (8.1.24)

According to (8.1.24), one may calculate the temperature (and the pressure) difference through the fluxes. We may note, repeating ourselves here, that actually (8.1.23) describes the cause–effect relationships.

As we see, the principle that lays behind the existence of these jumps is clear. The kinetic theory of gases only defines coefficients $c_{p,T}^{j,q}$ for (8.1.24); this is its role. Note that the same kind of system could be obtained for any fluxes, not exclusively for a flux of form $j \sim p/\sqrt{T}$. For this to happen, all that is needed is: (1) the definition for parameters p and T and (2) the ability to represent fluxes in series for these parameters.

In some works, differences Δp and ΔT are connected with the Clapeyron-Clausius equation:

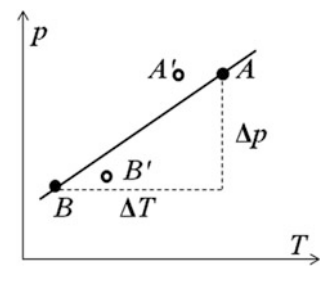
$$\frac{\Delta p}{\Delta T} = \frac{r}{T\Delta v}.\tag{8.1.25}$$

However, this approach is correct only for a limited number of cases, when parameters at both sides of the Knudsen layer correspond to the thermal equilibrium state. In the common case (see Fig. 8.2, where the saturation curve in p–T coordinates is presented) the differences in values of p and T for two arbitrary points A' and B', of course, have nothing in common with the differences along the saturation curve.

8.2 Confusing Experiments

We have seen that kinetic theory predicts a temperature jump between liquid and gaseous phases. This jump is comparatively small and it is difficult to discover experimentally. Even in the late twentieth century this temperature jump sometimes was described as "unmeasured," but recently the temperature difference was explored with stunning results: experimental values being a magnitude of order

Fig. 8.2 Points A' and B' do not sit on the saturation curve. Thus, $\frac{\Delta p(A'B')}{\Delta T(A'B')}$ cannot be determined with Clapeyron–Clausius equation



larger and having an opposite sign. While theory predicts both "+" and "–" for $\Delta T = T_{\rm V} - T_{\rm L}$, almost all experiments show $\Delta T > 0$. In some experiments ΔT exceeds 10 K.

This discrepancy is the source of far-reaching conclusions. In some works, kinetic theory was doubted with new theories being proposed; here we should mention SRT—statistical rate theory (Ward and Fang 1999). We will not enter into this battle by providing a new theory or defending an old one. Our explanation of the measured temperature jump follows from our previous consideration (especially from Chap. 5). We present these results in the next section.

Here we must treat these experimental results with care.

8.2.1 Experimental Temperature Jump: An Overview

Measuring a temperature jump is a delicate experimental procedure, which demands a unique experimental technique and skills. The area of the effect is narrow, and standard measurement error can negate any results: usually, the error of the thermocouple (TC) measurement is ~ 0.1 K, i.e., the same order of magnitude as the predicted temperature jump. Of course, it is impossible to determine such an effect with rough experimental equipment.

However, there still exists one serious aspect of the problem that must be considered here, before Sect. 8.3. Initially, from the early works of Knudsen and Smolukhovskii, the temperature jump was interpreted as the temperature difference between two contacting phases (here it does not matter whether they are solid-gas or liquid-vapor contacts). To determine the temperature difference, first we have to define the temperatures of the contacting phases; and, so to speak, the existence of temperature itself must be an essential point of this definition. We mean that temperature can be defined only for continuous media; in the general case, this parameter cannot be entered into the kinetic description for a non-equilibrium phase or used for extremely small spatial scales. Thus, strictly speaking, the temperature jump may be defined as follows:

• The temperature of the liquid at the surface is T_L ; this temperature must be determined in a near-surface layer of thickness that is wider than the "continuous scale"; there is no problem for such a condensed phase as liquid.

- The temperature of the vapor phase must be defined in the same way, but here the requirement for a sufficient thickness of the vapor phase leads to serious problems: we have to define $T_{\rm V}$ near the liquid surface in a layer that is wider than ~ 10 MFPs; also the DF of atoms in this layer must correspond to the MDF.
- If both T_L and T_V exist then we may define $\Delta T = T_V T_L$.

However, what should we do in the case of problems with T_V ?

We may depict at least two sorts of problems concerning vapor temperature: (1) it may not exist or (2) this parameter may be defined only with insufficient accuracy making it inappropriate for further analysis of a temperature jump.

Let us look at the problem from another viewpoint. We figured out that the vapor layer must be thick, so let us define the vapor temperature on a scale of ~ 1 cm (while the MFP, for instance, is $\sim 10~\mu m$) close to the liquid surface. With this method we obtain temperatures determined by averaging too large a volume; if the temperature difference works on scales of $\sim 1~mm$ (i.e., the temperature varies only at a distance of $\sim 1~mm$ from the interface), then after averaging at a scale of $\sim 1~cm$ we would have nothing—we would simply the temperature of the bulk of the vapor. Evidently, the temperature jump in this case has nothing in common with the temperature jump that was predicted by the kinetic theory of gases (KTG).

Thus, the temperature of the vapor must be determined on intermediate scales: not too small, not too large. This is the worst situation that can be imagined. There is always the risk of moving into one of these two extremes of scale.

8.2.2 Some Experiments and Experimental Data

As an example of experimental technique, we describe here the experimental procedure used in Badam et al. (2007).

Distilled and deionized water evaporates from a rectangular base through a channel (see Fig. 8.3). The height of the meniscus—i.e., the evaporation surface—was maintained ~ 1 mm above the mouth of the channel. The temperature of both the liquid and the vapor was measured by a U-shaped TC: the ratio of the length of the horizontal wire (~ 3 mm) to its diameter (~ 25 μ m) was large enough to neglect thermal conduction fluxes along the wire (as is stated in the work). Radiation fluxes were also negligible compared to the heat fluxes from the vapor. The TC was mounted at the centerline of the channel and could be moved up and down. Temperature was measured at two points in the vapor (distance $10~\mu$ m) near the liquid surface and at two points in the liquid (distance $20~\mu$ m); the distance between the vapor measurement point and the liquid measurement point was $50~\mu$ m.

An interesting part of the experimental setup of Badam et al. (2007) was the heating element mounted at ~ 3 mm above the interface. This heater provided a significant heat flux from the vapor onto the liquid surface, and, consequently,

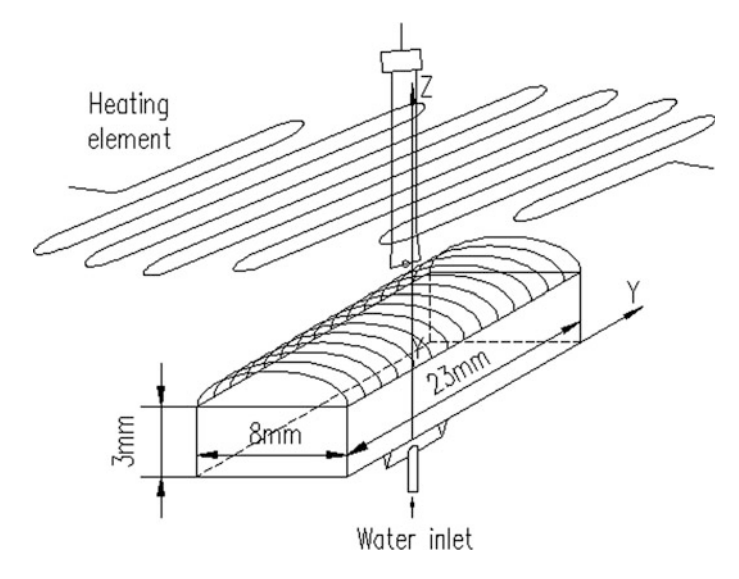


Fig. 8.3 Experimental setup used by Badam et al. (2007)

allowed a comparison between the measured temperature jump and the value predicted by the KTG.

The experimental results of Badam et al. (2007) are presented in Table 8.1 (full data set can be found in the original paper). As one can see, the measured values of the temperature jump are much higher than those predicted by the KTG: while the theory predicts $\Delta T = T_{\rm V} - T_{\rm L} \sim 0.1$ K, the experiment gives $\Delta T \sim 1-10$ K.

Besides the values of temperature difference, the dependence of ΔT on the pressure of the vapor p is particularly noteworthy. As one can see, ΔT decreases with an increase of p.

The same result for temperature discontinuity was obtained earlier by Fang and Ward (1999); see Table 8.2. With the same accurate technique, values for a temperature jump of 1–8 K were obtained. Again, the temperature measured in the vapor phase exceeded the temperature of the liquid.

8.2.3 The Temperature of the Interface

Actually, the temperature of the heating element in Badam et al. (2007) weakly influences the temperature of the surface of the liquid. Let us analyze the experimental data set: for vapor at ~ 560 Pa pressure the temperature of the liquid in all data sets varies from -0.77 °C (with the temperature of the heater being 80 °C) to -1.1 °C (for conditions without additional heating). At ~ 300 Pa the temperature of the liquid was -9.6 °C (with a spread ~ 0.1 °C).

Heating temperature (°C)	Evaporation flux [g/(m ² s)]	Pressure in vapor (Pa)	Experimental ΔT (°C)	KTG Δ <i>T</i> (°C)
30	0.578	736.0	3.99	0.15
30	0.607	569.5	3.84	0.17
30	0.636	483.0	4.22	0.20
30	0.687	391.2	4.76	0.26
30	0.737	295.2	5.50	0.33
30	0.768	240.3	5.76	0.43
50	0.766	847.9	6.25	0.24
50	0.781	743.0	6.71	0.27
50	0.836	572.4	7.29	0.36
50	0.904	391.4	8.80	0.51
50	0.970	288.5	9.69	0.68
50	1.01	236.0	10.25	0.84
70	0.882	966.8	4.10	0.30
70	0.922	850.5	8.62	0.33
70	0.958	747.0	9.52	0.38
70	1.02	573.1	10.47	0.50
70	1.09	389.2	11.51	0.72
70	1.13	290.7	12.81	0.95
70	1.18	215.6	14.63	1.26

Table 8.1 Experimental data obtained by Badam et al. (2007)

KTG Kinetic theory of gases

Thus, the role of the heater is the creation of a weak additional heat flux; the temperature of the liquid surface obeys the deep, inner dependencies of the evaporation–condensation processes and cannot be significantly disturbed by such insignificant fines as the heat flux.

Note that the temperature difference in these experiments differed significantly for different heater temperatures: for ~ 560 Pa $\Delta T = 1.8 - 11.6$ K while for ~ 300 Pa $\Delta T = 2.8 - 14.4$ K.

Thereby, one may conclude that ΔT does not depend on the temperature of the liquid and on the pressure of the gas explicitly: for almost identical $T_{\rm L}$ and p the temperature jump differs by an order of magnitude. In other words, the measured value of the temperature of the vapor $T_{\rm V}$ near the liquid surface does not depend on $T_{\rm L}$ and p, or, specifically, it does not depend on $T_{\rm L}(p)$.

Considering the fact that the evaporation flux is determined exactly by this parameter, it is interesting to check whether the temperature jump depends on the evaporation mass flux or not. Is it possible that the temperature of the vapor is determined only by the temperature of the heating element? Indeed, the larger the temperature of the heater—the higher the temperature of the gas. There are no contradictions in this statement, and the evaporation process is out of the game. Or is it?

Evaporation rate (µl/h)	Evaporation flux [g/(m ² s)]	Pressure in the vapor (Pa)	TC position (MFP)	Experimental ΔT (°C)
70	0.2799	596.0	2.2	3.5
75	0.2544	493.3	3.7	3.7
85	0.3049	426.6	1.6	4.2
90	0.4166	413.3	1.7	4.2
100	0.3703	310.6	1.8	5.1
100	0.3480	342.6	4.7	5.3
100	0.3971	333.3	1.3	6.2
110	0.4081	269.3	2.7	6.3
110	0.4347	277.3	1.6	6.1
120	0.4097	264.0	1.4	6.2
120	0.4860	269.3	1.3	6.5
130	0.4166	245.3	2.0	6.0
140	0.4938	233.3	1.9	7.4
150	0.5086	213.3	2.2	7.5
160	0.5386	194.7	1.2	8.0

Table 8.2 Experimental data obtained by Fang and Ward (1999)

MFP Mean free path

8.2.4 Correlation with the Mass Flux

The correlation between the temperature jump and the total flux on the evaporation surface is shown in Fig. 8.4a (taken from Badam et al. 2007) and Fig. 8.4b (taken from Fang and Ward 1999).

On these graphs all the experimental points are plotted: for all pressures, for all heating modes. As one can see from these figures, a good linear dependence may approximate these data sets:

$$\Delta T = C_1 + C_2 J^{\text{tot}}, \tag{8.2.1}$$

where coefficients for Badam et al. (2007) are: $C_1 \approx -9 \text{ K}$, $C_2 \approx 19 \text{ K m}^2 \text{ s/g}$; and for Fang and Ward (1999): $C_1 \approx -0.5 \text{ K}$, $C_2 \approx 15 \text{ K m}^2 \text{ s/g}$.

Thus, the temperature difference, generally, has a function of the linear dependence of the total mass flux on the evaporation surface, as almost predicted by the KTG, but with a sharper slope and with $C_1 \neq 0$; however, for the second data set this constant is nearly equal to zero.

Note that the total flux is defined as:

$$J^{\text{tot}} = J^{\text{ev}} - J^{\text{cond}}, \tag{8.2.2}$$

and, for example, the condensation flux for the MDF of vapor atoms is:

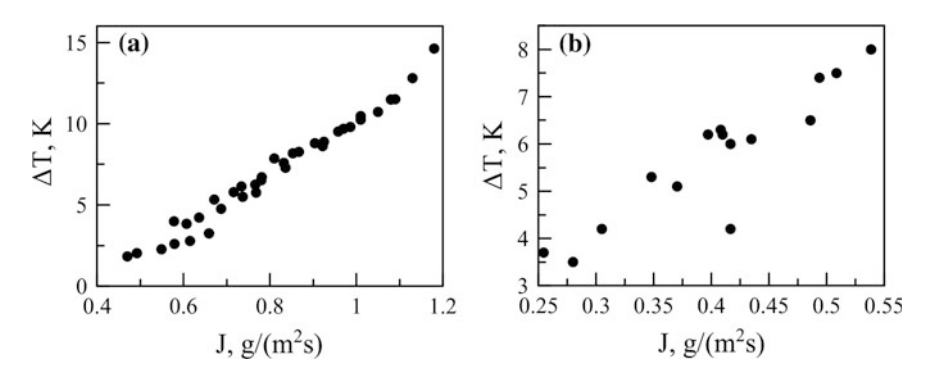


Fig. 8.4 Temperature jump as a function of the mass flux. a Taken from Badam et al. (2007). b Taken from Fang and Ward (1999)

$$J^{\text{cond}} = p \sqrt{\frac{m}{2\pi T_{\text{V}}}}. (8.2.3)$$

Consequently, if we suppose that the evaporation flux is a constant $J^{\text{ev}} = f(T_{\text{L}}) = \text{const}$ (because, as we stated above, $T_{\text{L}} = \text{const}$), then the increase in the total flux on the evaporation surface is determined only by the decrease in the condensation flux on the liquid surface. Since the deviations of the vapor temperature are small (~ 10 K compared with $T_0 \sim 273$ K), we may expand (8.2.3) into a series in the vicinity of T_0 , finding that:

$$J^{\text{tot}} = J^{\text{ev}} - p\sqrt{\frac{m}{2\pi T_0}} + \frac{p}{2T_0}\sqrt{\frac{m}{2\pi T_0}}(T_V - T_0). \tag{8.2.4}$$

From this equation we may:

- Identify constant C_1 from (8.3.1); we will not even represent this expression here because it is hard to extract useable information from it.
- Estimate constant C_2 from expression (8.3.1); this is a much more interesting move:

$$C_2 = \frac{\partial T_{\rm V}}{\partial J^{\rm tot}} = \frac{2T_0}{p} \sqrt{\frac{2\pi T_0}{m}}.$$
 (8.2.5)

For instance, for pressure $p = 300 \,\text{Pa}$ and temperature $T_0 = 273 \,\text{K}$ we have (for water) $C_2 = 1.6 \,\text{K} \,\text{m}^2 \,\text{s/g}$, i.e., constant C_2 is smaller than the constant C_2 obtained from the experimental data (see above) by an order of magnitude. As icing on the cake, note that constant (8.2.5) is not really a constant—it is a function of the vapor pressure, while the experimental value of C_2 was obtained at various pressures.

Thus, our blitzkrieg fails—we cannot explain the experimental data in such manner. The total flux on the evaporation surface cannot be explained by condensation flux variations due to variation in the vapor temperature near the evaporation surface. We see that $\partial T_{\rm V}/\partial J^{\rm tot}$ is too small, consequently, the derivation $\partial J^{\rm tot}/\partial T_{\rm V}$ is too large (we discussed this matter in Chap. 6) to explain the experiment results.

We have to admit that:

- At various regimes with different heater temperatures, the total flux on the evaporation surface is determined not only by the condensation flux, but also by the evaporation flux itself, despite the fact that the temperature of the liquid surface and the pressure of the gas stays the same.
- The temperature jump at the evaporation surface cannot be explained only by variations in the vapor temperature caused by variations in the heater temperature.

Both problems are confusing. We may also note that it follows from the first problem that the evaporation flux is somehow directly connected to the process of condensation: the temperature of the liquid surface remains the same, but under a condensation flux atoms of liquid evaporate "more willingly." As for the second problem, we mention again that the KTG cannot explain temperature jumps this big. Double trouble!

8.2.5 The First Step of a Thousand-Mile Journey

The experiments that were discussed in this section are very subtle. Instead of the temperature of the bulk of the vapor at the vicinity of the liquid surface, the temperature inside the Knudsen layer was measured both in Badam et al. (2007) and Fang and Ward (1999).

Strictly speaking, this is a new problem in respect to the problem that was solved in the KTG. However, does this remark change anything concerning the problem itself? If we care about the KTG, we may refer to the nuance that was stated above in this section and feel at ease.

But we do not.

The experiments discussed in this section raise a couple of serious problems concerning evaporation, and these problems must be solved. Any experiment needs be explained, especially in the case of such delicate and accurate experiments.

In the next section we provide explanations for the temperature differences observed in these experiments. However, considering all the circumstances, we will refer to this quantity as a "measured temperature jump."

8.3 Measured Temperature Jump

Two matters are important here: (1) the problem of the measured temperature difference between the liquid phase and the gaseous phase; (2) the fact that a non-equilibrium DF (with a rich, high-energy tail relative to the MDF) must be manifesting clearly at short distances from the evaporation surface.

As we have seen form the previous section, mysterious experimental results break all expectations about the KTG: in a few words, the measured temperature difference between the liquid and the gaseous phase has nothing in common with the predictions of the KTG. Does this mean that kinetic theory is compromised and we need some new theoretical description? Or, is it possible that KTG predicts adequately but we poorly understand the properties of the evaporation process?

We think that the second choice is correct. Experimental results presented in the previous section confirm the main conclusion of Chap. 5: a non-equilibrium DF of atoms, after evaporation, "bears" higher energy. That is one reason why objects near the evaporation surface are always overheated. For instance, one such object may be the TC: its tip may be overheated if placed at a distance of about one MFP from the evaporated atoms in a surrounding gas.

8.3.1 Which Is Stronger: The Equilibrium or Non-equilibrium Distribution Function?

Everybody knows that a whale is stronger than an elephant. What about DFs? A MDF for a 1D case:

$$f_x^M(v) = \sqrt{\frac{m}{2\pi T}} \exp\left(-\frac{mv^2}{2T}\right),\tag{8.3.1}$$

provides a mean kinetic energy:

$$\bar{\varepsilon}_x^M = \int_{-\infty}^{\infty} \frac{mv^2}{2} f(v) dv = \frac{T}{2}, \qquad (8.3.2)$$

while the mass and energy fluxes are:

$$j^{M} = n \int_{0}^{\infty} v f^{M}(v) dv = \frac{1}{4} n \bar{v}_{T} = n \sqrt{\frac{T}{2\pi m}},$$
 (8.3.3)

$$q_x^M = n \int_0^\infty v \frac{mv^2}{2} f^M(v) dv = nT \sqrt{\frac{T}{2\pi m}},$$
 (8.3.4)

where the thermal velocity is:

$$\bar{v}_T = \sqrt{\frac{8T}{\pi m}}. (8.3.5)$$

Correlation (8.3.3) is also referred to as the Hertz formula. Here n is the number density of particles (atoms or molecules) of the medium; we factor it out from the DF, which is normalized on unity: $\int_{-\infty}^{\infty} f^{M}(v) dv = 1$. Note that, of course:

$$\int_{-\infty}^{\infty} v f^{M}(v) dv = 0 \quad \text{and} \quad \int_{-\infty}^{\infty} v \frac{mv^{2}}{2} f^{M}(v) dv = 0, \tag{8.3.6}$$

because a symmetrical MDF does not "transfer" any flux: the absence of fluxes is a necessary property of equilibrium and the MDF describes an equilibrium state.

In a 3D case, where the DF is the multiplication:

$$f^{M}(v) = f^{M}(v_{x})f^{M}(v_{y})f^{M}(v_{z})$$
(8.3.7)

of three functions of the kind found in (8.3.1), the total kinetic energy is:

$$\bar{\varepsilon} = \frac{3}{2}T,\tag{8.3.8}$$

and total energy flux may be obtained for $v^2 = v_x^2 + v_y^2 + v_z^2$:

$$q = n \int_{-\infty}^{\infty} \int_{-\infty}^{\infty} \int_{0}^{\infty} \frac{mv^2}{2} v_x f^M(v_x) f^M(v_y) f^M(v_z) dv_x dv_y dv_z = nT \sqrt{\frac{2T}{\pi m}}.$$
 (8.3.9)

The mass flux in the 3D case is still determined by the Hertz formula (8.3.3), because $\int_{-\infty}^{\infty} \int_{-\infty}^{\infty} f^M(v_y) f^M(v_z) dv_y dv_z = 1$, and we have the 1D integral again.

Evaporation in the simplest case of a flat surface DF:

$$f(v) = \frac{mv}{T} \exp\left(-\frac{mv^2}{2T}\right),\tag{8.3.10}$$

gives for mean energy and fluxes:

$$\bar{\varepsilon} = T, \quad j = n\sqrt{\frac{\pi T}{2m}}, \quad q = nT\sqrt{\frac{9\pi T}{8m}}.$$
 (8.3.11)

For the 3D case, as discussed in Chap. 5, the DFs of tangential velocities are Maxwellian, so, the mean energy:

$$\bar{\varepsilon} = 2T. \tag{8.3.12}$$

We calculate fluxes for 3D geometry later. We may emphasize that the temperature T in (8.3.9) is the temperature of the liquid, not the temperature of evaporated atoms: their non-equilibrium DF does not contain such a parameter as temperature.

Then, we may conclude that the evaporation flux bears a higher energy than the equilibrium flux. Of course, the DF becomes Maxwellian far from the evaporation surface due to collisions with atoms of gas. However, at the very edge of the interfacial boundary, where DF (8.3.4) is undistorted, there must exist clear evidence of this non-equilibrium DF. Objects placed close to the evaporation surface receive a high-energy flux of evaporated atoms, and, generally, reach higher temperatures than in the bulk of gas. We would like to emphasize that even for equal liquid and gas temperatures an object gains temperature $T_0 > T$.

8.3.2 What Is a Thermocouple

A TC is the most widely used temperature meter for technical applications. It consists of two separate wires (made of different metals); the melted contacts (tips) of these wires have different temperatures T_{hot} and T_{cold} . Due to the Zeebeck effect, the emf Ξ in such a circuit is:

$$\Xi = \vartheta(T_{\text{hot}} - T_{\text{cold}}), \tag{8.3.13}$$

where ϑ is the Zeebeck coefficient; this parameter depends on the materials (metals wires) that are used in the TC.

Thus, the temperature of the hot tip of the thermocouple may be determined with:

- The known Zeebeck coefficient.
- The specific temperature of the cold tip T_{cold}; usually this temperature is created by inserting a cold tip of a TC into a medium with a well-defined temperature: an old fashioned way is to position it in melting ice (i.e., one may expect that T_{cold} = 0 °C); today modern devices are used (so-called "zero-point devices": special thermostats).
- The measured emf Ξ .

The temperature $T_{\rm hot}$ can be determined in this manner. As for the accuracy of the TC measurement, all three parameters mentioned above make their contribution to the total error. Usually, deviations of $T_{\rm cold}$ from the required value (caused by fluctuations or by more prosaic reasons such as heating from fully melted ice—i.e., water—in a Dewar vessel, when the experimenter falls asleep!) play a restrictive role. For good experimentation, the error of $T_{\rm hot}$ is ~ 0.1 K; however, sometimes special tricks (such as using a differential TC) are used to decrease this error by an order of magnitude.

However, there is a delicate question here: why are we sure that the temperature of the TC—i.e., the temperature of the juncture of two wires—has the same temperature as the medium surrounding this TC? Actually, we are not interested in the temperature of the hot tip, the temperature of the external substance is what we are looking for. As for the accuracy of the measurement: we also have to know the discrepancy between the read-out of $T_{\rm hot}$ and the true value of the temperature of the medium, not the discrepancy between the read-out and the true value of the TC temperature.

To be sure that $T_{\rm hot} = T_{\rm medium}$, one needs to provide a "perfect" heat transfer between the TC and the medium where the TC junction is placed: in stationary cases, the heat that the TC collects from the medium must be equal to the heat that the TC gives back to the medium; only in this case one may declare an equilibrium state. If, for example, the TC takes heat from the gas and transfer this heat through its wires somewhere else, then the real temperature of the medium is undetermined. Thus, strictly speaking, for measurements to be correct, a TC's wires must be laid along isotherms; only in this case is the conductive heat flux equal to zero. In real experiments, however, sometimes it is difficult to determine an isotherm position; in such cases the estimation of the additional heat flux (along the wires) is necessary (but, rarely provided).

It is easy to organize incorrect measurements with a TC. Let us, for example, irradiate the TC's tip (which means that the incoming heat flux would be determined by the thermal radiation). The outcoming flux from the tip would be the sum of all possible types: of conductance (through the wires), of convection (into the surrounding gas) and of radiation (this part is usually negligible, see the next section).

There are many works dedicated to the correct processes used for measuring with a TC (Mingchun 1997; Jones 2004; Roberts et al. 2011; Hindasageri et al. 2013; Fu and Luo 2013; and especially Kazemi et al. 2017, which is devoted to experiments by Fang and Ward 1999). However, we are faced with a slightly different problem: what is the temperature of a TC in a gas that has no temperature?

8.3.3 What Does a Thermocouple Measure?

As depicted in previous sections, it is not superfluous to discuss this question. In a previous section we discussed how a TC measures temperature. However, how can we explain that the temperature of a TC is equal to the temperature of the surrounding medium? In addition, and perhaps the main question, what is the temperature of a TC in a non-equilibrium media, where temperature does not exist?

Atoms of gas (or of a liquid—if a TC is placed into a liquid) bombard the TC surface. Reflection of atoms from the TC surface is not absolutely elastic and the reflected flux is in equilibrium with the TC temperature: in the case when atoms of gas do not react with atoms of the TC we may expect that the work function U of an atom detached from a TC is equal to zero. For the short-range potential of a "gas

atom-TC atom" interaction, we expect many collisions of adsorbed atoms of gas with atoms of the TC surface, and "thermalization" is expected as a result of these collisions. Atoms of gas detached from the metallic TC surface have a Maxwellian distribution with the temperature of the TC.

Strictly speaking, the scheme described above is only a simplified assumption. The main feature of this approach is the renunciation of analysis of the "atom-surface" collisions; we consider "atom-atom" interaction, for which the opportunity of absorbance is clear (see Chap. 7).

Finally, we conclude that when a TC contacts with an equilibrium gas with temperature T, it takes the temperature of the gas: $T_{TC} = T$. However, what happens when the gas around the TC is out of equilibrium? For instance, when the DF of gas atoms is (8.3.4), parameter T is not even the "temperature of gas": for a non-equilibrium state, the parameter "temperature" does not have any sense. It is obvious that in any external conditions a TC would obtain a certain temperature, but in non-equilibrium media the value of this temperature is not a trivial parameter.

Here we calculate the temperature of the TC under the following assumptions:

- 1. The TC has uniform temperature: any part of the TC has the same temperature.
- 2. The DF of detached atoms is Maxwellian.
- There is an equilibrium between the gas and the TC: total mass and energy fluxes on the TC are absent, that is, the fluxes from the gas phase onto the TC surface are equal to the fluxes of atoms detached from the TC.
- 4. We neglect any radiation losses. For the TC at high temperatures this is a rather bold assumption, but here (and everywhere in this book) we have to deal only with intermediate temperatures.

All these assumptions will be discussed further, especially in Sect. 8.3.8. First, we want to estimate the temperature of the TC placed in a non-equilibrium gas.

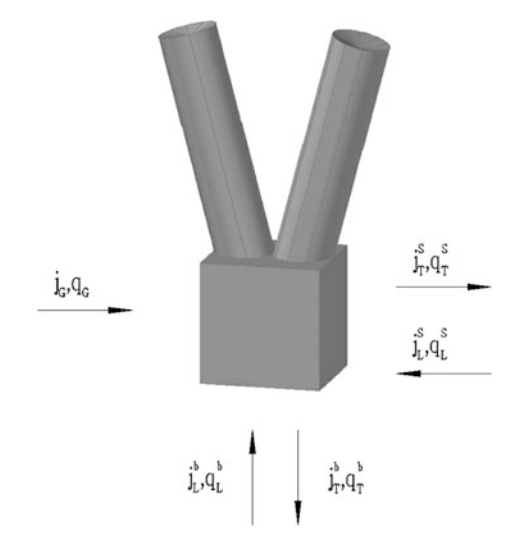
8.3.4 Temperature of the Thermocouple

Actually, here we return to the original works of Smoluchowski and Maxwell. The main distinction of our consideration from the previous attempts is that we tend to find the temperature of the thermocouple in a gas that has no temperature of its own. To find the TC temperature, we will consider the fluxes on/from the TC surface (see Fig. 8.5). Temperature will be found from the balanced equations written for the TC.

Further, we will use a model of a cubic TC (see Fig. 8.5), i.e., the junction of the wires has a cubic form. This is the simplest model that lets us obtain a solution to our problem, because in this case we can calculate fluxes separately for each cubic surface. By the way, we have never seen a cubic TC, of course.

At first, we consider a TC placed in the vicinity of the evaporation surface in a vacuum. This means that there are not any additional fluxes on the TC surface,

Fig. 8.5 The thermocouple and fluxes on its surfaces: from the gas (index "G"), from the evaporated liquid (index "L") and from the thermocouple itself (index "T")



except for the fluxes from the evaporation surface. This model explains all the basic principles of our solution to the problem and, moreover, gives an answer to the limiting case that will be correct for a more complicated problem.

We can formally write the flux from the TC as:

$$j_{\text{TC}}^{M} = \frac{1}{4} n_{\text{TC}} \sqrt{\frac{8T_{\text{TC}}}{\pi m}}.$$
 (8.3.14)

Here n_{TC} is the corresponding number density of adatoms (adsorbed atoms of gas at the TC surface). The mass flux (8.3.14) is obtained from the MDF.

Analogically, the energy flux is:

$$q_{\text{TC}}^{M} = n_{\text{TC}} \underbrace{T_{\text{TC}} \sqrt{\frac{2T_{\text{TC}}}{\pi m}}}_{\tilde{q}_{\text{TC}}^{M}} = n_{\text{TC}} \tilde{q}_{\text{TC}}^{M}. \tag{8.3.15}$$

If our special cubic TC collects atoms only via its underside, the fluxes on the TC surface from the evaporation surface are:

$$j_{\rm L}^b = \overline{n_{\rm L} v_z} = n_{\rm L} \sqrt{\frac{\pi T_{\rm L}}{2m}}.$$
 (8.3.16)

$$q_{\rm L}^b \equiv \overline{n_{\rm L} \frac{mv^2}{2} v_z}.$$
 (8.3.17)

The last flux must be calculated accurately. We have:

$$q_{\rm L}^b = n_{\rm L} \int_0^\infty \int_0^\infty \int_0^\infty \left(\frac{mv_x^2}{2} + \frac{mv_y^2}{2} + \frac{mv_z^2}{2} \right) v_z f(v_x) f(v_y) f(v_z) dv_x dv_y dv_z, \quad (8.3.18)$$

where the DFs $f(v_x)$ and $f(v_y)$ are Maxwellian and $f(v_z)$ is (8.3.4). Thus:

$$\frac{\overline{mv_{x,y}^2}}{2}v_z = \frac{T_L}{2}\bar{v}_z = \frac{T_L}{2}\sqrt{\frac{\pi T_L}{2m}},$$
(8.3.19)

$$\frac{\overline{mv_z^2}}{2}v_z = 3T_L\sqrt{\frac{\pi T_L}{8m}},\tag{8.3.20}$$

$$q_{\rm L}^b = n_{\rm L} T_{\rm L} \sqrt{\frac{25\pi T_{\rm L}}{8m}}. (8.3.21)$$

In equilibrium there must be:

$$q_{\text{TC}}^M = q_{\text{L}}^b, \quad j_{\text{TC}}^M = j_{\text{L}}^b.$$
 (8.3.22)

From (8.3.14) we see that (8.3.14) is equal to (8.3.16) and (8.3.15) is equal to (8.3.21). We get:

$$n_{\rm TC} = n_{\rm L} \pi \sqrt{\frac{T_{\rm L}}{T}},\tag{8.3.23}$$

$$T_{\rm TC} = 1.25T_{\rm L}.$$
 (8.3.24)

Thus, in the simplest consideration we obtain a huge increase in temperature. However, the TC collects fluxes not only via its underside: the faces of its sides collect and emit fluxes too. Can this possibly change the result (8.3.16)?

For each of the four faces of the cubic TC the fluxes from the evaporation surface are:

$$j_{\rm L}^{\rm s} = \frac{1}{4} n_{\rm L} \bar{v}_{{\rm x},{\rm y}} = n_{\rm L} \sqrt{\frac{T_{\rm L}}{2\pi m}},$$
 (8.3.25)

and because the DF of velocities v_x and v_y are Maxwellian:

$$q_{\rm L}^{\rm s} = \overline{n_{\rm L} \left(\frac{m v_{\rm x}^2}{2} + \frac{m v_{\rm y}^2}{2} + \frac{m v_{\rm z}^2}{2} \right) v_{\rm x,y}}.$$
 (8.3.26)

Again:

$$\frac{\overline{mv_x^2}}{2}v_x = n_{\rm L}T_{\rm L}\sqrt{\frac{T_{\rm L}}{2\pi m}},\tag{8.3.27}$$

$$\frac{\overline{mv_y^2}}{2}v_x = n_{\rm L}T_{\rm L}\sqrt{\frac{T_{\rm L}}{8\pi m}},\tag{8.3.28}$$

$$\frac{\overline{mv_z^2}}{2}v_x = n_{\rm L}T_{\rm L}\sqrt{\frac{T_{\rm L}}{2\pi m}},\tag{8.3.29}$$

and, consequently:

$$q_{\rm L}^{\rm s} = n_{\rm L} T_{\rm L} \sqrt{\frac{25T_{\rm L}}{8\pi m}}.$$
 (8.3.30)

For this situation, the upper face of the TC is empty: there are no incoming or emitted fluxes, while for the side faces we have a balance of the mass fluxes:

$$n_{\text{TC}}^s \sqrt{\frac{T_{\text{TC}}}{2\pi m}} \equiv j_{\text{TC}}^s = j_{\text{L}}^s \equiv n_{\text{L}} \sqrt{\frac{T_{\text{L}}}{2\pi m}},$$
 (8.3.31)

$$n_{\text{TC}}^{s} = n_{\text{L}} \sqrt{\frac{T_{\text{L}}}{T_{\text{TC}}}}.$$
 (8.3.32)

For the underside, (8.3.23) is correct for the number density of adsorbed atoms n_{TC}^b . Finally, the balanced equation for the energy flux is:

$$4q_{\rm L}^s + q_{\rm L}^b = 4q_{\rm TC}^s + q_{\rm TC}^b = (4n_{\rm TC}^s + n_{\rm TC}^b)\tilde{q}_{\rm TC}^M, \tag{8.3.33}$$

where were \tilde{q}_{TC}^{M} is defined in (8.3.15). From (8.3.33) we see that still:

$$T_{\rm TC} = 1.25T_{\rm L}.$$
 (8.3.34)

Thus, the temperature of the TC in a vacuum is 25% higher than the temperature of the liquid. There is no thermodynamic problem here, since the evaporating system is in non-equilibrium; it would be an error to expect equality of temperatures in (8.3.34).

Now we take a gas into account—a gaseous phase that does not originate from a liquid phase; it may be a vapor at its own temperature (similar to the experiments described in previous section). Suppose that this vapor is in equilibrium and its temperature is T_G .

Additional fluxes from the gas to any face of the cubic thermocouple are:

$$j_{\rm G} = n_{\rm G} \sqrt{\frac{T_{\rm G}}{2\pi m}},$$
 (8.3.35)

$$q_{\rm G} = n_{\rm G} T_{\rm G} \sqrt{\frac{2T_{\rm G}}{\pi m}}.$$
 (8.3.36)

As previously, we demand the balance of the mass fluxes at any face of the TC and the total zero energy flux, i.e.:

$$j_{\text{TC}}^b = j_{\text{L}}^b + j_{\text{G}}, \quad j_{\text{TC}}^s = j_{\text{L}}^s + j_{\text{G}},$$
 (8.3.37)

$$(n_{\rm TC}^b + 4n_{\rm TC}^s)\tilde{q}_{\rm TC}^M = q_{\rm L}^b + 4q_{\rm L}^s + 5q_{\rm G}. \tag{8.3.38}$$

Here we consider a TC depicted in Fig. 8.5: the upper face does not "measure" temperature. Otherwise, we must add a term with n_{TC}^u to left-hand side of (8.3.38) and replace 5 with 6 on the right-hand side of this equation.

From (8.3.37) we have:

$$n_{\text{TC}}^b = n_{\text{L}} \pi \sqrt{\frac{T_{\text{L}}}{T_{\text{TC}}}} + n_{\text{G}} \sqrt{\frac{T_{\text{G}}}{T_{\text{TC}}}},$$
 (8.3.39)

$$n_{\text{TC}}^{s} = n_{\text{L}} \sqrt{\frac{T_{\text{L}}}{T_{\text{TC}}}} + n_{\text{G}} \sqrt{\frac{T_{\text{G}}}{T_{\text{TC}}}}.$$
 (8.3.40)

Combining (8.3.31) and (8.3.32) with (8.3.30), we obtain:

$$T_{\rm TC} = \frac{20\chi T_{\rm G}\sqrt{T_{\rm G}} + 5(\pi + 4)T_{\rm L}\sqrt{T_{\rm L}}}{20\chi\sqrt{T_{\rm G}} + 4(\pi + 4)\sqrt{T_{\rm L}}},$$
(8.3.41)

where $\chi = \frac{n_G}{n_L}$; this ratio demonstrates the role of the buffering gas in the heat transfer on the TC surface. To take the upper face into account we must replace 20 with 24 here.

We see from (8.3.33) that if the evaporation is negligible, $\chi \to \infty$ and $T_{\rm TC} \to T_{\rm G}$. In the absence of gas $\chi = 0$ and $T_{\rm TC} = 1.25 T_{\rm L}$, as in (8.3.26).

The most interesting result that follows from (8.3.33) is that even in the case of equal temperatures $T_G = T_L$, the indication of the TC:

$$T_{\rm TC} = T_{\rm L} \frac{20\chi + 5(\pi + 4)}{20\chi + 4(\pi + 4)},\tag{8.3.42}$$

does not coincide with the temperature of both phases. This is the first difficulty that stands in the way of the experimental determination of the temperature jump between a liquid and its vapor.

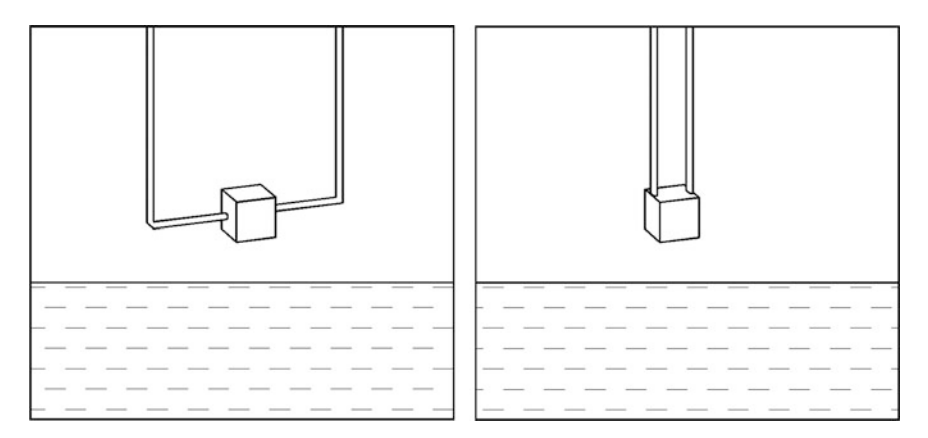


Fig. 8.6 Various schemes of a cubic thermocouple

The second difficulty is the necessity to calculate parameter χ with accuracy that, at least, does not eliminate the evaluation of T_{TC} ; it is a hard task when the expected temperature difference is ~ 0.1 K, while the temperature of a liquid is of the order of $\sim 10^2$ K.

The third difficulty is the form of the TC tip. The cubic thermocouple was a model that allowed us to find an estimation of the temperature, and nothing more. Even for a cubic junction, one may suggest different geometric schemes (see Fig. 8.6). Thus, the numerical coefficients in (8.3.42) vary for different geometric schemes; below, in the calculation section, we combine all these difficulties into a single parameter.

8.3.5 Additional Fluxes

The theory (or, specifically, consideration) described above might need some improvements. We take into account only the equilibrium flux on the TC surface in a gas: the one-directional part of the zero total flux. This assumption is correct only for full equilibrium, in absence of the non-zero total flux. However, usually this zero total heat flux is present in experiments. One question which arises is what is the exact amount of flux that taken into account?

The energy flux (8.3.15) can be rewritten through thermal velocity \bar{v}_T as:

$$q = \frac{p\bar{\nu}_T}{2}.\tag{8.3.43}$$

Thus, for thermal velocities of $\sim 10^2$ m/s and pressures of $\sim 10^{2-3}$ Pa we have $q \sim 10^{4-5}$ W/m². Thus, strictly, the $\sim 10^{2-3}$ W/m² heat flux measured in some

experiments may be considered only as a correction to the whole energy flux on a TC surface. However, this correction should be done in the common case.

In the balanced equation of mass and energy fluxes on the TC surface we must add the terms of the total fluxes, i.e.:

$$j_{TC} = j_L + j_G + \overline{j_G},$$
 (8.3.44)

$$q_{\rm TC} = q_{\rm L} + q_{\rm G} + \overline{q_{\rm G}}.\tag{8.3.45}$$

where $\overline{j_G}$ and $\overline{q_G}$ are the total fluxes brought into consideration. Thus, we should introduce the additional term $4\overline{j_G}/\overline{v_T}$ to (8.3.41) (for the bottom or the upper face of a TC) and, correspondingly, for a 6-faced TC tip we have:

$$T_{\text{TC}} = \frac{24\gamma T_{\text{G}}\sqrt{T_{\text{G}}} + 5(\pi + 4)T_{\text{L}}\sqrt{T_{\text{L}}} + \tilde{q}}{24\gamma\sqrt{T_{\text{G}}} + 4(\pi + 4)\sqrt{T_{\text{L}}} + \tilde{i}},$$
(8.3.46)

with
$$\tilde{j} = \overline{j_{\rm G}} \frac{\sqrt{2\pi m}}{n_{\rm L}}$$
 and $\tilde{q} = \overline{q_{\rm G}} \frac{\sqrt{2\pi m}}{4n_{\rm L}}$.

Equation (8.3.46) defines the temperature of the TC at external fluxes. It still assumes that the DF of atoms in a gas is Maxwellian and the DF of the evaporated atoms is function (5.2.14) for the plane surface in Chap. 5. Both assumptions, of course, are only assumptions. When the TC is placed far from the interface (at a distance of ~ 1 MFP or farther), the DF of evaporated atoms is disturbed and fluxes that were calculated so accurately become incorrect. In addition, because of collisions of gas atoms with evaporated atoms, the temperature of the vapor near the interface will increase with the distance from the liquid surface. All these nuances will be considered in the final section of this chapter.

8.3.6 A Sidestep: Thermal Radiation

Let us consider a TC over a surface of a liquid in the absence of evaporation or any media around it. Here we cannot neglect radiation because it is all that we have. The TC takes its temperature from equilibrium conditions, when the radiation flux from the TC is equal to the absorption flux.

The flux from the liquid surface to the TC is:

$$Q^{\rm in} = \underbrace{\alpha_{TC}^{(1)}}_{\text{absorption}} \cdot \underbrace{\varepsilon_{\rm L} \sigma k^{-4} T_{\rm L}^{4} F_{\rm L}}_{\text{emitted}} \cdot \underbrace{\varphi_{\rm L} - {\rm TC}}_{\text{angle}}, \tag{8.3.47}$$

where $\alpha_{TC}^{(1)}$ is the absorption coefficient of the TC corresponding to the spectral range of the thermal radiation of the liquid T_L ; ε_L and F_L are the radiation coefficient and the area of the liquid surface, correspondingly; the Stephen-Boltzmann constant is $\sigma =$

 $5.67 \times 10^{-8} \, \text{W/m}^2 \, \text{K}^4$ and also we have to use here the Boltzmann constant $k = 1.38 \times 10^{-23} \, \text{J/K}$ because of the accepted dimension of the temperature (Sect. 1.1.2). The radiation flux from the TC is:

$$Q^{\text{out}} = \varepsilon_{\text{TC}}^{(2)} \sigma k^{-4} T_{\text{TC}}^4 F_{\text{TC}}, \qquad (8.3.48)$$

where $\varepsilon_{\text{TC}}^{(2)}$ is the radiation coefficient of the TC at the range of wavelengths corresponding to the temperature of the TC itself T_{TC} ; and F_{TC} is the area of the TC. For Kirchhoff's law there should be:

$$\alpha_{\text{TC}}^{(1)} = \varepsilon_{\text{TC}}^{(1)} \approx \varepsilon_{\text{TC}}^{(2)}, \tag{8.3.49}$$

that is, (a) the absorption coefficient is equal to the radiation coefficient at the same spectral range and (b) we suppose that the temperatures of the TC and of the liquid are close.

The angle factor is:

$$\varphi_{\rm L} - TC = \varphi_{\rm TC} - L \frac{F_{\rm TC}}{F_{\rm I}}, \qquad (8.3.50)$$

according to the rule of reciprocity. Supposing that the TC is very close to the liquid, i.e., the radiation from five of the six sides of our cubic TC reaches the liquid, we have $\phi_{TC} - L = 5/6$; if we want to consider a TC "without an upper face," as in the previous section, $\phi_{TC} - L = 1$. Consequently, the temperature of the TC is:

$$T_{\rm TC} = T_{\rm L} \sqrt{4\varepsilon_{\rm L}},\tag{8.3.51}$$

or is the same equation but with a factor of "5/6" under the square root.

Of course, the square root of the 4th order here is close to 1. However, strictly speaking, the second factor in (8.3.51) is slightly less than unity, in this case, the temperature of the TC is slightly less than the temperature of the liquid. For example, if $\varepsilon_{\rm L}=0.5$ then $T_{\rm TC}=0.84T_{\rm L}$; for $\varepsilon_{\rm L}=0.9$ we have $T_{\rm TC}=0.97T_{\rm L}$. Thus, we see that the temperature of the TC may differ by a few percent from the temperature of the liquid; consequently, radiation may be an important factor in the general case. Let us estimate the role of radiation in the total heat balance.

Let us compare the radiation flux on the TC surface (at one of its faces):

$$q^{\text{rad}} = \varepsilon_{\text{L}} \sigma k^{-4} T_{\text{TC}}^4, \tag{8.3.52}$$

and the heat flux from the equilibrium gas:

$$q^{\rm gas} = n_{\rm G} T_{\rm G} \sqrt{\frac{2T_{\rm G}}{\pi m}}.$$
 (8.3.53)

In order not overcomplicate the problem, we put $T_{TC} = T_L = T$ and $\varepsilon_L = 1$. Then, for $n_G = p/T$ we get the expression for the pressure that is needed to compensate the radiation flux:

$$p \sim \frac{\sigma T^{7/2}}{k^4} \sqrt{\frac{\pi m}{2}}.$$
 (8.3.54)

For example, for argon at a temperature of 100 K the "critical" pressure $p \sim 0.1\,\mathrm{Pa}$, for water at 273 K the pressure is $p \sim 1\,\mathrm{Pa}$. This means that at gas pressures of $\sim 100\,\mathrm{Pa}$ (for instance, as in experiments discussed in Sect. 8.2), the role of thermal radiation from the TC is negligible.

8.3.7 Comparison with Experimental Results

Here we apply our ideas to a real situation: we will analyze experimental data which raised the problem of an "anomalous" temperature jump at an interface (Fang and Ward 1999; Badam et al. 2007). In brief, we suppose that the temperature jump measured in these experiments is not a real temperature difference between a vapor phase and a liquid phase. In fact, the measured temperature jump is the difference between the temperature of the TC's tip and that of the liquid. The temperature of the TC is not the temperature of the vapor in the general case: at the vicinity of an evaporation surface the gaseous phase is out of equilibrium due to evaporated atoms and their non-equilibrium DF. Gas even has no such parameter as "temperature." In other words, we suppose that $T_{\rm G} \approx T_{\rm L}$; in the final section we discuss the limitations of this approach.

In accordance with previous remarks, in order to calculate the temperature jump, we will use (8.3.34), but in a slightly changed form. We will take into account that the number density of evaporated atoms is:

$$n_L \sim \Gamma\left(\frac{1}{2}, \frac{U}{T_L}\right)$$
 (8.3.55)

By reference to Chaps. 5 and 6, we assume that the temperature of vapor is equal to the temperature of liquid, then, we may use (8.3.42) instead of a more common correlation (8.3.41). Applying the Clapeyron equation for $n_{\rm G} = \frac{p}{kT_{\rm G}}$, we obtain for $\Delta T = T_{\rm TC} - T_{\rm L}$:

$$\Delta T = \frac{T_{\rm L}}{\frac{P}{p_0 \Gamma(0.5, U/T_{\rm L})} + 4} \tag{8.3.56}$$

Here parameter p_0 includes an uncertainty regarding the geometry of the TC's tip. As follows from the previous consideration, actually, $p_0 \sim T_L$, but further we

Fig. 8.7 Pressure dependence

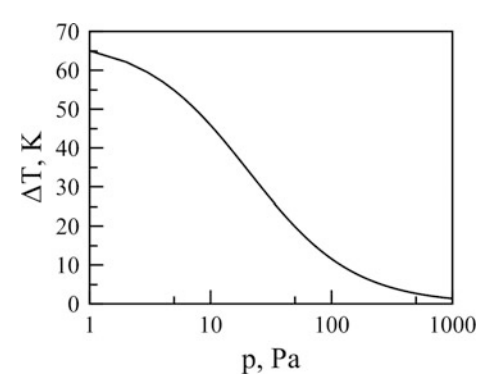
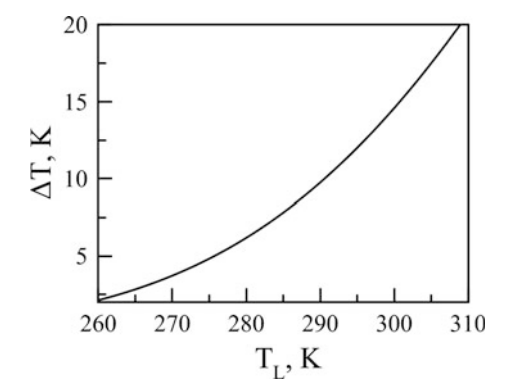


Fig. 8.8 Temperature dependence



neglect this dependence because usually the temperature interval for one experimental data set is quite narrow, for example, it could be water at temperatures of 270–280 K. Note that we cannot neglect this temperature dependence in the gamma-function because of the strong dependence on T_L .

Expression (8.3.56) is the simplest correlation for a measured temperature jump. We do not pretend to describe all the experimental data perfectly; we only provide some theoretical estimations for the experimental data presented in the previous section. At first, we analyze the behavior of the temperature jump (8.3.56) as a function of two basic parameters—the pressure and temperature of the liquid.

The dependence of the temperature jump (8.3.56) on the pressure (for $T_{\rm L}=273~{\rm K}$) and temperature of the liquid surface (for $p=300~{\rm Pa}$) is shown in Figs. 8.7 and 8.8, correspondingly. These are common dependencies for illustration, because to compare our results with experimental data (see previous section) we have to consider both dependencies—on p and on $T_{\rm L}$ —for certain experiment conditions. However, first, we need to determine all the free parameters in (8.3.56).

We have two parameters in (8.3.56) that must be defined: p_0 and U. Strictly speaking, both of them vary from experiment to experiment: even the work function U may depend on external conditions, as follows from Chap. 6. However, we hold

constant the analytically calculated parameter U and try to fit the experimental results of Badam et al. (2007) and Fang and Ward (1999) by changing p_0 .

Let us try to analytically calculate the work function U. As was discussed in Chap. 6, to use the probability of detachment in the form $w = \frac{1}{2\sqrt{\pi}}\Gamma(\frac{1}{2},\frac{U}{T})$, we have to insert into this function the mean value of U calculated using a special method (briefly, we must average w on all binding energies with the DF g(U) from Chap. 6). Next, we put the average value of the work function $U_m = \Delta H$, i.e., the latent heat of vaporization per particle. From the National Institute of Standards and Technology database we find that for water at temperature ~ 0 °C the value $\Delta H = 5400$ K. Thus, the mean value $\langle U \rangle = 3700$ K will be used as the work function in the expression for w (for T = 273 K, $\tilde{U}_m = 20$ and $\langle \tilde{U} \rangle = 13.7$, see Chap. 6).

It is very difficult to predict a precise value for p_0 analytically, because, among other problems, it depends on the distance from the TC to the interface—and it is rather complicated to predict this dependence on such an uncomfortable spatial scale. Nonetheless, we may estimate the value of p_0 , at least to an order of magnitude. According to our consideration:

$$p_0 \sim \frac{n_L T}{2\sqrt{\pi}}.\tag{8.3.57}$$

Taking $n_L = n_L^0 w$ and number density n_L^0 in the bulk of the liquid from the reference data, we have $n_L^0 \sim 3 \times 10^{28} \, \mathrm{m}^{-3}$ and $p_0 \sim 4 \times 10^7 \, \mathrm{Pa}$. Thereby, all that we can predict is the more or less certain value for the work function of the liquid, and estimate to an order of magnitude the parameter p_0 .

Comparing our calculations to the experimental data set of Badam et al. (2007), without heating, we obtain $p_0 = 1.5 \times 10^7$ Pa. This value will be used later for all calculations in these experiments, i.e., for experiments when the heater was turned on.

To take into account the heat flux from the heater, we must redefine the temperature of the liquid. Suppose, that any vapor particle that hits a liquid surface excites the atoms of the liquid (we do not mean electronic excitation, of course; the atom of the vapor transfers its energy to the atoms of the liquid). Assuming that this excitation is comparatively small, we may try to describe this additional energy with the effective temperature $\mu T_{\rm L}$ with factor $\mu \geq 1$. We emphasize that the temperature of the liquid surface is still $T_{\rm L}$; the multiplier μ describes the short time increase of the local mean kinetic energy. We further discuss this process for a common case in Sect. 9.4.

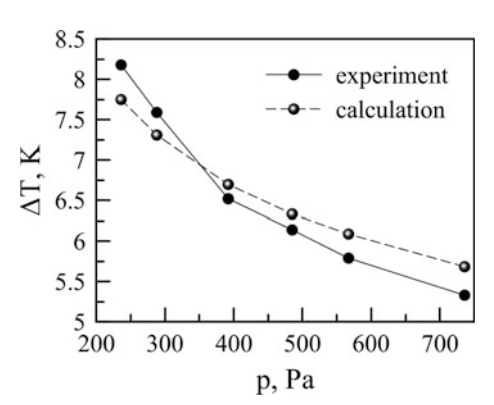
Thus, we will calculate the temperature jump with (8.3.56), holding $U = 3700 \, \mathrm{K}$ and $p_0 = 1.5 \times 10^7 \, \mathrm{Pa}$, but varying the parameter μ from one heating regime to another, i.e., for the each temperature of the heater we will have a separate parameter μ .

As we see from Table 8.3, we can achieve sufficient agreement with the experiment. Note that the dependence on the temperature of the liquid surface (through the gamma-function) is crucial; this function determines the shape of the

Table 8.3 Comparison between calculations and experimental results (Badam 2007)

p (Pa)	$\Delta T_{\rm exp}$	$\Delta T_{ m calc}$	p (Pa)	$\Delta T_{\rm exp}$	$\Delta T_{ m calc}$
	(K)	(K)		(K)	(K)
No heating, $\mu = 1.0$			$T_{\text{heating}} = 30 ^{\circ}\text{C}, \mu = 1.05$		
561.0	1.83	2.29	736.0	3.99	4.04
490.0	2.03	2.36	569.5	3.84	4.31
389.1	2.27	2.49	483.0	4.22	4.49
336.5	2.60	2.58	391.2	4.76	4.73
292.4	2.78	2.68	295.2	5.50	5.12
245.3	3.25	2.82	240.3	5.76	5.48
$T_{\text{heating}} = 40 ^{\circ}\text{C}, \mu = 1.08$			$T_{\text{heating}} = 50 ^{\circ}\text{C}, \mu = 1.10$		
736.0	5.33	5.68	847.9	6.25	6.78
567.0	5.79	6.09	743.0	6.71	7.02
485.0	6.14	6.33	572.4	7.29	7.50
392.3	6.52	6.70	391.4	8.80	8.29
288.5	7.59	7.31	288.5	9.69	9.05
236.6	8.18	7.75	236.0	10.25	9.59
$T_{\text{heating}} = 60 ^{\circ}\text{C}, \mu = 1.115$			$T_{\text{heating}} = 70 ^{\circ}\text{C}, \mu = 1.13$		
866.0	7.86	7.86	850.5	8.62	9.12
743.9	8.27	8.17	747.0	9.52	9.42
569.2	8.89	8.78	573.1	10.47	10.09
386.3	9.80	9.81	389.2	11.51	11.24
291.7	10.73	10.64	290.7	12.81	12.22
235.5	11.49	11.28	215.6	14.63	13.40

Fig. 8.9 Badam et al. (2007), 40 °C



curves $\Delta T = f(T_L)$ presented in Figs. 8.9 and 8.10 (we show two curves from Table 8.3 graphically).

We think that the agreement is acceptable; it is important not to overestimate the degree of matching from Fig. 8.10: the model that is presented in (8.3.56) is too rough to obtain such a perfect agreement with experiments. Sometimes the agreement is only a coincidence.

Fig. 8.10 Badam et al. (2007), 60 °C

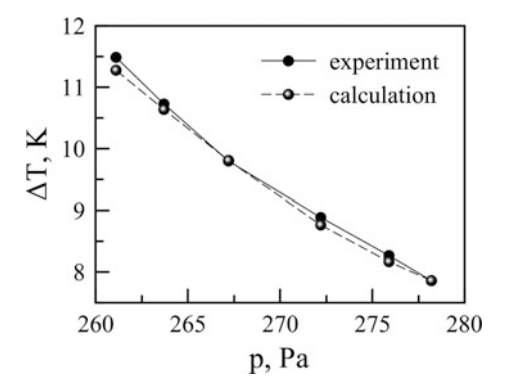


Fig. 8.11 Fang and Ward (1999) with different T_L

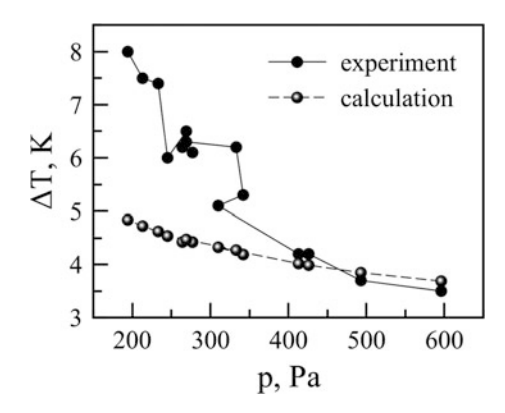
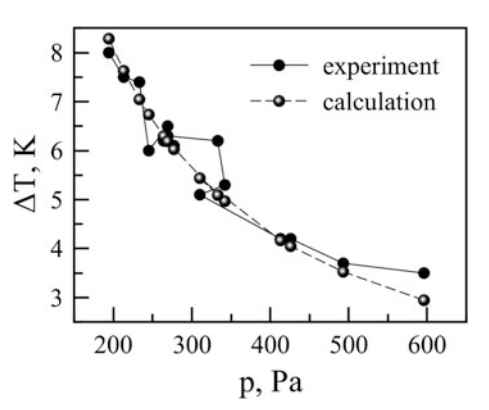


Fig. 8.12 Fang and Ward (1999) with $T_L = \text{const}$



Next we compare correlation (8.3.56) with data from Fang and Ward (1999). We hold U = 3700 K and set $p_0 = 2.5 \times 10^7$ Pa; the results are presented in Fig. 8.11. In Fig. 8.10 we see an agreement with the experimental results at high pressures, however, at low pressures (below 400 Pa) distinctions are sharp. It is worth noting that this experimental data set represents miscellaneous experimental points obtained in various modes, for different positions of the TC over the interface (in

the vapor) and inside the liquid. Considering the fact that the slope of theoretical correlation strongly depends on the temperature of the liquid, we can easily avoid any inconvenience by calculating ΔT with constant $T_{\rm L}=265$ K, corresponding to the average temperature of the liquid in these experiments; see Fig. 8.12 (with $p_0=3.1\times10^7$ Pa). One may see a much better matching for all the ranges of pressure.

Summarizing all the results of our calculations, we assume that we can fit experimental data with correlation (8.3.56) with parameters that follow from the theory presented in Chap. 6 (the work function U) or in agreement with them (the parameter p_0). The spread of ± 0.5 K (or less) is explained by the factors discussed in the next section.

The main result of these calculations is the true state of the temperature difference between the TC tip and the liquid. As we see, the amplitude of the measured temperature difference at the interface is ~ 10 K: actually, this is almost all that we need to know about this value ... almost!

8.3.8 What Features Should Be Brought into Account

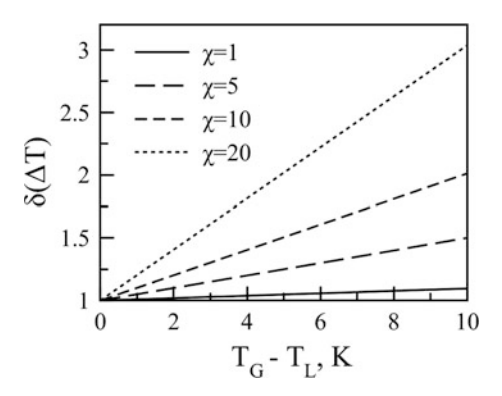
First, we enumerate the factors that were omitted in our approach:

- The temperature of the gas is not equal to the temperature of the liquid.
- The temperature of the gas increases with the distance from the surface once larger than one MFP.
- Fluxes from the evaporation surface decrease at the same distances as mentioned in the previous point.
- The energetic characteristic of vapor that was called "temperature" is really not a temperature, because the DF of the vapor molecules on velocities is not Maxwellian.
- The geometry of the TC is undefined.

Considering all these factors together, one may wonder how the theory that discounts such features may predict anything. For self-defense purposes, again, we should mention that we did not pretend to fit the experimental data, and the most encouraging result following on from our estimations is the matching of the temperature jump, for the theoretically calculated work function with the number density at the surface (i.e., the parameter p_0), to the predicted order of magnitude.

Let us address the concerns for those who believe that with the single adjustment constant we can describe an elephant as a large mouse and enforce him to wag the tail if we add one free parameter more (we are talking about p_0 , for sure). For example, if the work function is chosen for thousands of degrees less—at 2700 K—in order to fit experimental data, then pressure $p_0 \sim 10^5$ Pa should be used in the calculations. This value is absolutely contradictory to all the theory (which was mostly described in Chap. 6); it is impossible to explain the value of such an order

Fig. 8.13 Temperature jump for $T_G \neq T_L$



of magnitude. Thus, the results of our calculations are in agreement with themselves, something which is not coincidental.

To treat the effect of the inequality of temperatures $T_G \neq T_L$ we must return to the more common equation:

$$\Delta T = \frac{\frac{20\chi}{\pi + 4} \sqrt{\frac{T_{G}}{T_{L}}} [T_{G} - T_{L}] + 5T_{L}}{\frac{20\chi}{\pi + 4} \sqrt{\frac{T_{G}}{T_{L}}} + 4}.$$
 (8.3.58)

Thus, the temperature jump that is measured by the TC in a gas with temperature $T_G \neq T_L$ differs from the simplest estimation (8.3.56) (of course), as well as from the temperature difference $T_G - T_L$. The result also depends on parameter χ , that shows the relative role of the vapor phase in establishing the TC temperature. In Fig. 8.13 we show the ratio:

$$\delta(\Delta T) = \frac{\Delta T}{\Delta T_{T_G = T_L}},\tag{8.3.59}$$

that is, the ratio of the measured temperature jump calculated with (8.3.58) and (8.3.42). The temperature of the liquid is $T_L = 273 \text{ K}$ for $\chi = 1 - 20$; note that in our previous calculations $\chi \sim 10$.

Thus, one may see how the gas temperature affects the measured temperature jump. For instance, if $T_{\rm G}-T_{\rm L}=1\,\rm K$ then ΔT is 20% higher than in the case of $T_{\rm G}=T_{\rm L}$ (for $\chi=20$). This influence is appreciable, from the other hand, we see that the order of the temperature jump stays the same for $T_{\rm G}-T_{\rm L}\sim 1\,\rm K$. Concluding, we may note that this factor, possibly, deserves to be taken into account, but there is no way to do it in the absence of an independent method to determine $T_{\rm G}$, especially with to an accuracy of $\sim 0.1\,\rm K$.

The temperature of the vapor, generally, must have a tendency to increase with the distance L from the interface for L > MFP. When collisions take place, the heat flux from the evaporation surface transfers energy to the vapor; then, one may

expect an increase in temperature. However, it should be remembered that vapor near the liquid surface exchanges its energy not only with the interface, but also with the bulk of the vapor. Parameters of the vapor at infinity also determine the dependence $T_G(L)$; this simple answer deserves attention too. For example, in some experiments (Badam et al. 2007) the use of a heater in front of the evaporation surface is the evident reason for a temperature rise.

As for the effect of the non-Maxwellian distribution of vapor particles, it is difficult to provide any estimation without this non-MDF. We may expect that the difference with our approach would not be enormous. Consequently, our "temperature of gas" is not exactly a temperature, but a sort of a measure of the mean kinetic energy of the vapor molecules. Theoretically, this is represents a significant difficulty, but, practically, there is no a difference between $T_{\rm G}$ and some other parameter $\overline{\varepsilon_{\rm G}}$.

An interesting consideration to be had is the behavior of the measured temperature jump with the distance from the evaporation surface (we mean for distances larger than 1 MFP). From one point of view, the fluxes from the interface attenuate because of the interaction with molecules of vapor; thus, one may expect that the heat flux from the evaporation surface onto a TC surface would decrease as well as the measured temperature jump. From another point of view, as discussed above, in these collisions the evaporated molecules transmit their energy to the gas molecules, thus, it is difficult to say whether the energy flux on a TC would decrease or increase. Moreover, we can easily propose a model according to which the heat flux from the evaporation surface, onto the surface of the TC tip, would increase even more due to collisions of molecules from the interface.

Let us imagine two particles: one moves toward the z axis, i.e., $v_{1z} > 0$, and the other in the plane z = const., i.e., $v_{2z} = 0$. Before the collision these particles had energy $mv_1^2/2$ and $mv_2^2/2$, correspondingly. After the collision there must be:

$$v_{1z} = v'_{1z} + v'_{2z}, (8.3.60)$$

$$\frac{mv_1^2}{2} + \frac{mv_2^2}{2} = \frac{mv_1'^2}{2} + \frac{mv_2'^2}{2}.$$
 (8.3.61)

We are not interested in other projections of velocity $v_{x,y}$. Thus, before the collision the "energy flux" from the single molecule is:

$$q = v_{1z} \frac{mv_1^2}{2},\tag{8.3.62}$$

and after collision this flux—now from both particles—is:

$$q' = v'_{1z} \frac{mv_1'^2}{2} + v'_{2z} \frac{mv_2'^2}{2}.$$
 (8.3.63)

Here $v'_{2z} = v_{1z} - v'_{1z}$. In the case of 1D motion, when $v_{iz} = v_i$, we have from these conditions that after the collision $v'_2 = v_1$, $v'_1 = 0$ and q' = q. However, in the 3D case, actually, the kinetic energy of particle number 2 is arbitrary. Thus, it is possible that q' > q.

In other words, the flux of particle number 1 (axial) captures the flux of particle number 2 (coplanar), and the total energy flux in the direction of the z axis increases.

We suppose that now the application of this model is clear. The energy flux on the TC surface may be magnified because of collisions between the vapor molecules and the evaporated ones with respect to the pure energy flux of molecules from the evaporation surface. Does this mean that the temperature of the TC would increase? Actually, the temperature of the TC is determined by the ratio q/j, not by the energy flux q itself; in other words, the temperature is determined by the velocity DF of molecules in the flux. Collisions kill the high-energy tail of the DF of evaporated particles, but they increase the energy of the vapor fluxes (i.e., T_G or $\overline{\epsilon_G}$). Thereby, there are two opposite tendencies for dependence $\Delta T(L)$; at least, in experiments (Fang and Ward 1999) the measured difference ΔT increased with L.

Last, but not least, is the question concerning the matter of the geometry of the TC. In strong non-equilibrium conditions, such as those in the vicinity of the evaporation surface, the TC obtains heat fluxes from various directions: both by its tip, placed in front of the interface, and its wires, located in the surrounding gas that has a strictly non-uniform temperature distribution (especially in cases when a heater with a temperature of tens of degrees higher than the temperature of an interface is placed in the vicinity of the TC).

8.4 Conclusion

The temperature jump between the evaporating liquid and the vapor is a delicate matter. Rough experiments cannot determine such a subtle parameter: if one tries to measure the temperature of the vapor with a standard TC, with a large tip (~ 1 mm, like domestic TCs), then we may predict that one would find out nothing from the experiment. Much subtler equipment is needed.

However, a TC too small is not suitable either. If a TC with a tip of $\sim 10~\mu m$ is placed in the vapor near the evaporation surface (i.e., $\sim 1~MFP$ from the liquid), then the result of such an experiment becomes very interesting from various viewpoints. However, one problem remains: the temperature jump at the interface that is predicted by the KTG. We honestly see no problem with this; it is the problem of the *measured* temperature jump which is far more interesting.

We should distinguish temperature and the measure of an average kinetic energy of molecules in a common manner. These are different things. A TC placed in a substance always gives some readout, but, possibly, this readout has nothing in common with the temperature of the media. Here we do not consider such examples as the temperature of the TC with radiation conditions; we mean that sometimes

8.4 Conclusion 269

temperature may not exist as a physical parameter (while a TC always gives some sort of readout).

As was shown in Chap. 5, the DF of evaporated particles is non-Maxwellian. The parameter T that is identified in this DF of the normal projection of velocity:

$$f(v) = \frac{mv}{T} \exp\left(-\frac{mv^2}{2T}\right),\,$$

is the temperature of the liquid, not the temperature of the vapor. This DF is in non-equilibrium, and, for example, the mean kinetic energy of a particle is 2T (instead of 1.5T as in the equilibrium Maxwellian function). Thereby, the gaseous phase near the interface (at a distance approximately equal to the MFP) is a kind of a mixture: here molecules from the evaporated surface are adjoined with molecules from the vapor. In the vicinity of the evaporation surface, this non-equilibrium cocktail has no such parameter as temperature.

In the presence of the non-equilibrium flux from the evaporation surface the TC takes, of course, some temperature T_{TC} : in the absence of a vapor, a metallic tip has a real temperature. Thus, actually, in experiments one measures the temperature difference between the TC in a vapor and the temperature of the liquid:

$$\Delta T = T_{\rm TC} - T_{\rm L}$$

instead of the difference $T_{\rm V}-T_{\rm L}$. We believe that a TC in a liquid takes the temperature of that liquid. Note that a TC in front of the evaporation surface would read some temperature even in a vacuum; moreover, in this case its temperature would be a maximum (neglecting thermal radiation).

We established a correlation between the temperature of a TC and the parameters of the flux from the evaporation surface and from the surrounding gas (or vapor); however, this expression contained vapor temperature $T_{\rm G}$ as an external parameter. We could not extract this temperature from the experimental data, thus, we simply put $T_{\rm G} = T_{\rm L}$, assuming that the difference between them must be small.

To compare the results of our calculations with the experimental data, we used formulae from Chap. 6: we calculated the work function directly and estimated the number density of the evaporated particles according to the approach presented in that chapter. The agreement between theory and experimental data is quite good, but we do not overestimate this. Actually, it is enough for us that we can predict, to within an order of magnitude, the temperature discontinuities (between the liquid and the TC) and the dependence of ΔT on the pressure of the vapor. Note that our formula allows a limiting transition for the case of the absence of evaporation: for this case, the TC temperature is equal to the temperature of the gas: $T_{\rm TC} = T_{\rm G}$.

However, our theory contains a special feature: according to our model, the condensation of the vapor stimulates the evaporation process. In the last section of the last chapter we will return to this approach and discuss it in further detail.

References

- S. Albertoni, C. Cercignani, L. Gotusso, Phys. Fluids 6, 993 (1963)
- V.K. Badam et al., Exp. Thermal Fluid Sci. 32, 276 (2007)
- P. Bassanini, C. Cercignani, C.D. Pagani, Int. J. Heat Mass Transf. 10, 447 (1967)
- J.W. Cipolla, H. Lang, S.K. Loyalka, J. Chem. Phys. 61, 69 (1974)
- G. Fang, C.A. Ward, Phys. Rev. E 59, 417 (1999)
- X. Fu, X. Luo, Int. J. Heat Mass Transf. 65, 199 (2013)
- H.S. Gregory, Lond. Edinb. Dublin Philos. Mag. J. Sci. Ser. 7(22), 257 (1936)
- V. Hindasageri, R.P. Vedula, S.V. Prabhu, Rev. Sci. Instrum. 84, 024902 (2013)
- J.C. Jones, Int. J. Eng. Perform. Based Fire Codes 6, 5 (2004)
- M.A. Kazemi, D.S. Nobes, J.A.W. Elliot, Langmuir 33, 7169 (2017)
- A. Kundt, E. Warburg, Ann. der Phys. und Chem. 156, 177 (1875)
- V.V. Makhrov, High Temp. 15, 453 (1977a)
- V.V. Makhrov, High Temp. 15, 1012 (1977b)
- J.C. Maxwell, Philos. Trans. R. Soc. Lond. 170, 233 (1879)
- L. Mingchun, J. Fire Sci. 15, 443 (1997)
- Y.-P. Pao, Phys. Fluids **14**, 1340 (1971)
- I.L. Roberts, J.E.R. Coney, B.M. Gibbs, Appl. Therm. Eng. 31, 2262 (2011)
- M. Smoluchowski, Ann. Phys. 340, 983 (1911)
- C.A. Ward, G. Fang, Phys. Rev. E 59, 429 (1999)

Recommended Literatures

- M. Bond, H. Struchtrup, Phys. Rev. E 70, 061605 (2004)
- C. Cercignani, W. Fiszdon, A. Frezzotti, Phys. Fluids 28, 3237 (1985)
- E.Y. Gatapova et al., Int. J. Heat Mass Transf. 83, 235 (2015)
- E.Y. Gatapova et al., Int. J. Heat Mass Transf. 104, 800 (2017)
- R. Holyst et al., Rep. Prog. Phys. **76**, 034601 (2013)
- D.A. Labuncov, High Temp. 5, 549 (1967)
- M. Luo, J. Fire Sci. 15, 443 (1997)
- P. Rahimi, C.A. Ward, Int. J. Thermodyn. 8, 1 (2005)
- C.A. Ward, D. Stanga, Phys. Rev. E 64, 051509 (2001)

Chapter 9 Evaporation in the Processes of Boiling and Cavitation



The most evident application for the physics of evaporation is the regular "liquid-vapor" phase transition, i.e., boiling. Various types of boiling may be considered with the approach developed in previous chapters. Evidently, boiling is a convenient object for the application of the evaporation technique.

The cavitation process—the formation of gaseous cavities in a cold liquid—may also be considered interesting.

9.1 Nucleate Boiling

9.1.1 The Boiling Curve

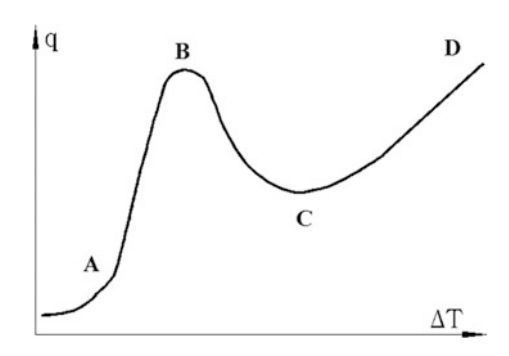
Here we will consider the boiling processes with a $q - \Delta T$ diagram, where q is the heat flux on the solid surface overheated at temperature $\Delta T = T_w - T_s$, relative to the saturation temperature. Such a curve—the so-called Nukiyama curve—is presented in Fig. 9.1.

The boiling curve has three distinct zones corresponding to three types of boiling:

- Nucleate boiling (A–B in Fig. 9.1); at these parameters boiling is the formation of bubbles on a solid wall.
- Transient boiling (B–C in Fig. 9.1); this is an unstable type for experimental condition q = const; this type is a mix between nucleate boiling and film boiling.
- Film boiling (C–D in Fig. 9.1); a thin film of vapor separates the solid wall from the liquid, this type of boiling is pure evaporation from a liquid surface.

Usually, in domestic conditions, we have all seen nucleate boiling. Film boiling may be observed when we put a very hot object into a liquid volume. To observe

Fig. 9.1 The boiling curve: AB represents nucleate boiling, BC represents transient boiling and CD represents film boiling



and identify transient boiling, one needs to learn about it first. An example of transient boiling may be observed during the cooling of the pan in the water.

9.1.2 A Sidestep: The Mathematics of the Boiling Curve

Formally, the boiling curve represents a bifurcation diagram with two points of saddle-node bifurcations: at point B (Fig. 9.1; from nucleate boiling to film boiling) and at point C (Fig. 9.1; reverse transition).

Thereby, we can use some formalistic reasons to describe boiling at the bifurcation point by non-stationary equations; for example, at the vicinity of point B with dimensionless variables for the flux and temperature there must be:

$$\frac{\mathrm{d}\tilde{T}}{\mathrm{d}t} = \tilde{T}^2 - \tilde{q} \tag{9.1.1}$$

for $\tilde{T} = \Delta T - \Delta T_{\rm cr}$ and $\tilde{q} = q_{\rm cr} - q$ with parameters at the critical point of the bifurcation diagram $\Delta T_{\rm cr}$ and $q_{\rm cr}$. Equation (9.1.1) is the normal form of the saddle-node bifurcation; from (9.1.1) it follows that the stationary solution at the vicinity of the critical point is:

$$\tilde{T} = \pm \sqrt{q_{\rm cr} - q},\tag{9.1.2}$$

that is, there are no solutions if $q > q_{cr}$, and two solutions in the opposite case. Stability analysis shows that the perturbation of temperature depends on time as:

$$\delta \tilde{T} = \delta \tilde{T}_0 \exp(2\tilde{T}t), \tag{9.1.3}$$

where \tilde{T} in the exponent is defined by (9.1.2), and therefore only the "-" sign in (9.1.2) corresponds to the stable solution (for the temperature on the branch of nucleate boiling) while the "+" sign in (9.1.2) gives an unstable result—transient boiling.

This simple consideration based on elementary bifurcation theory gives an example of how mathematics opens a doorway between theory and physics. According to these considerations we see that there should be a non-stationary theory of boiling which should predict dependence (9.1.2), i.e., correlation $q = q_{\rm cr} - (\tilde{T} - \tilde{T}_{\rm cr})^2$ in the vicinity of point B (Fig. 9.1).

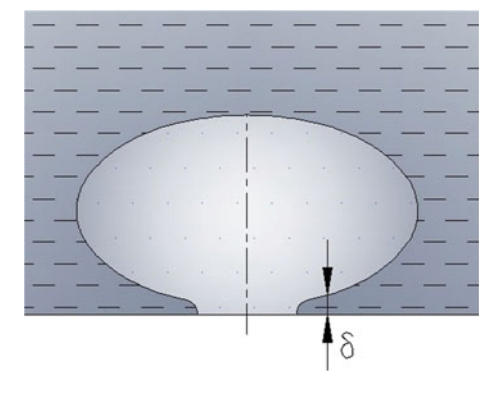
This represents a mathematical approach; however, physics is not in a hurry to walk through this mathematical doorway. From a physicist's point of view, the first statement that needs to be proven is the fact that function $q(\Delta T)$ even exists. This assumption will be considered later in this chapter; initially, we have to consider the basic physical matters of nucleate boiling.

9.1.3 The Physics of Nucleate Boiling

Nucleate boiling is the growth of vapor bubbles on a heated surface. These bubbles grow because of the evaporation on their walls: in the vicinity of a hot wall, the heated liquid has a temperature sufficiently high for intense evaporation. The interesting question is: where is the main front of evaporation in nucleate boiling—under the bubble, in the direction of the solid wall, or at the "bubble – bulk of the liquid" interface? At first glance, heat is conducted from the solid surface, thus, we may expect the evaporation front to be there. Another view is that there is no liquid below the bubble on the solid wall, therefore, there is nothing to evaporate below the bubble.

However, the last statement is wrong. According to old theories and modern investigations (for instance, Labuncov 1963; Gao et al. 2012; Chen and Utaka 2015), the growing bubble lays on a thin liquid microlayer, with the main role in the process of the nucleate boiling belonging to the evaporation of this microlayer (see Fig. 9.2).

Fig. 9.2 The bubble and its microlayer



This microlayer is very thin: its width δ is ~ 10 µm. The heat flux is supplied from the solid surface through this microlayer by heat conductance q^c , and is mainly spent on evaporation q^{ev} at the liquid-vapor interface; a small part of the heat is withdrawn into the bubble by free convection and heat conductance. Neglecting this heat flux, we may equate:

$$q^{\rm c} \equiv \frac{\lambda \Delta T}{\delta} = q^{\rm e},\tag{9.1.4}$$

where $\Delta T = T_{\rm w} - T$ is the temperature difference between the wall and the interface and $q^{\rm e} = n_0 T \sqrt{\frac{T}{2\pi m}} {\rm e}^{-U/T} \left(2 + \frac{U}{T}\right)$ is the heat flux directly on the evaporation surface. The heat flux $q^{\rm e}$ differs from the evaporation heat flux in the vapor $q^{\rm ev} = n^{\rm ev} T \sqrt{\frac{25\pi T}{8m}}$: the first flux is determined on the liquid surface while the second is the energy flux of particles, each of which lose energy U during the process of detachment.

We have based our logic on the fact that heat is conducted to the bubble *from* the heated wall. However, in actuality, that depends on certain conditions. If the liquid is cold (subcooled below saturation temperature), then the mechanism of microlayer evaporation is the only way for the bubble to grow; moreover, in this case the upper side of the vapor (of the cold liquid) is the condensation surface.

In an opposite case, if the liquid is sufficiently hot, then the heat may be conducted to the bubble surface from any direction: both from the solid surface and from the hot liquid. To better understand the combination of these two processes, we should note that:

- The liquid evaporates at any temperature.
- The rate of evaporation strongly depends on the temperature of the interface.
- The evaporation flux is higher than the condensation flux only for a sufficiently hot liquid surface.

In other words, the assumption that the bubble surface is always the isotherm of the saturation temperature T_s is only a brave, simplified assumption. This approach is useful for theoretical estimations, but we would not be surprised if the result of such an estimation would differ from experimental results by an order of magnitude (due to the sharp dependence $q^{ev}(T)$ on the evaporation surface, i.e., on the bubble wall).

For evaporation of the liquid microlayer, the static picture of (9.1.4) is incomplete. Usually, the flow of the liquid in this microlayer is considered; see, for example, Cooper and Lloyd (1969). However, in a real case, this is not a flow on the plane surface: usually, the scale of the roughness is not less than $\sim 1~\mu m$, i.e., it is comparable with the depth of the liquid. On such scales, the movement of liquid tongues rather represents an infiltration of the liquid in a disordered media, not the axisymmetric flow of a liquid from the periphery of the bubble toward the dry spot in the center of it. Indeed, the replenishment of the microlayer represents a difficult problem in the grand scheme.

Let us estimate the time for full evaporation of the liquid microlayer and the corresponding bubble radius. Mass loses of the liquid (see Chap. 1) may be estimated with the heat flux from the heated wall q^c and the latent heat of vaporization $h_{\rm LG}$:

$$J = \frac{q^{c}}{h_{\rm LG}}.\tag{9.1.5}$$

The mass flux for J, corresponding to the heat flux $\sim 10^2$ kW/m² in water (where the enthalpy of vaporization is $\sim 2 \times 10^6$ J/kg), is ~ 0.1 kg/m² s (we omit the 2, of course). This means that a layer of diameter ~ 1 mm (i.e., under a bubble of the same radius) with an average height of 10 μ m (i.e., a liquid mass $\sim 10^{-8}$ kg) would evaporate in ~ 0.1 s. The bubble radius corresponding to such an evaporated liquid mass at a pressure of $\sim 10^5$ Pa is ~ 1 mm; thus, this consideration is consistent.

The next point to consider for the heat transfer during nucleate boiling may be the determination of the heat transfer coefficient. Instead of this, we consider discarding such an item completely.

9.1.4 A Sidestep: The Heat Transfer Coefficient

Traditionally, in heat transfer science the main parameter is the heat transfer coefficient (HTC): the ratio of the heat flux q and the temperature difference between the wall and the liquid:

$$\alpha = \frac{q}{\Lambda T}.\tag{9.1.6}$$

For the phase transitions, $\Delta T = T_{\rm w} - T_{\rm s}$ is the difference between the temperature of the wall and the saturation temperature. Actually, the main (and, possibly, the last) convenience of representation (9.1.6) is its simplicity. However, this representation may seem strange to any person who knows the principles of general physics but has never studied heat transfers.

Note that the approach of (9.1.6) (among many others) was criticized in the very original book of E. F. Adiutori *The New Heat Transfer*. Despite the fact that we share almost no convictions of the author (for instance, in our book we obtain some results based on dimension theory, while the book by Adiutori is checkered with headings like "The method of dimensions is awful"; we believe that the Stefan-Boltzmann law, as a consequence of Plank's law, is a fundamental principle of physics, while Adiutori states that this law will be canceled in twenty first century; many, many others statements from *The New Heat Transfer* urge us to prefer the old heat transfer), we may note that such an unorthodox approach is undoubtedly interesting—under critical consideration, of course.

Here we provide statements based only on common physical and mathematical reasoning. We do not deny that for many problems the HTC provides adequate results, but sometimes the HTC approach seems to be the source of problems.

At first glance, correlation (9.1.6) reflects only our wishes: we may interpret any physical quantity in any way. For example, we may introduce a new HTC quantity according to (9.1.6): after any experiment, where the heat flux and the temperatures of the wall and of the liquid were measured, one may represent results in a form of the ratio of (9.1.6).

However, heat transfer science is constructed in such a way that it tries to find the universal correlation for the HTC (or its dimensionless analog—the Nusselt number) with other parameters \vec{x} for a certain class of problems (turbulent flow in a pipe, laminar wrapping of a plate, pool boiling, etc.). Then, this universal function $\alpha(\vec{x})$ may be used for this class of problems in order to calculate the heat flux for the given temperature head ΔT : $q = \alpha(\vec{x})\Delta T$.

However, to use correlation (9.1.6) we have to be assured, at least in terms of two common principles:

- That the representation of (9.1.6) may be designed correctly for the first degree of quantity ΔT .
- That the HTC is stable for small deviations in the determining parameters \vec{x} .

For example, let us consider the radiation heat transfer of the surface with temperature T inside a large chamber (with a much larger surface area) with temperature T_0 . Let us suppose that we do not know that in the case of absence of self-irradiation on the surface, the heat flux on it is determined by:

$$q = \sigma \varepsilon(T) \left(T^4 - T_0^4 \right), \tag{9.1.7}$$

where $\varepsilon(T)$ is the total emissivity of the surface.

Then, one tries to find an answer in the form $q = \alpha(T - T_0)$, where the HTC must be obtained experimentally by approximation of an experimental data set for $q(T, T_0)$. Evidently, we know the answer: for this problem, the HTC is:

$$\alpha = \sigma \varepsilon(T)(T + T_0)(T^2 + T_0^2). \tag{9.1.8}$$

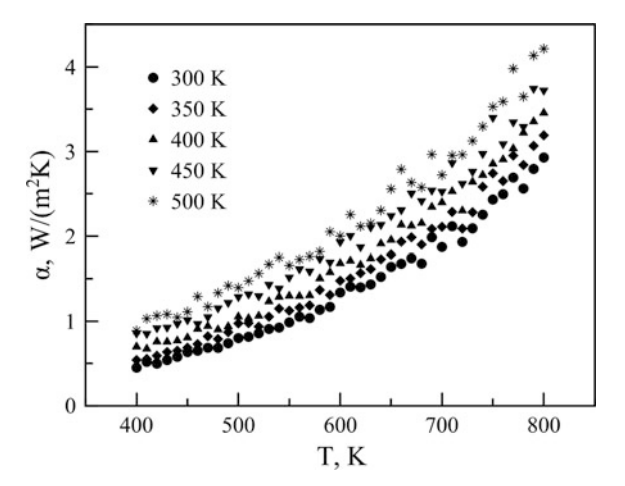
However, this correlation must be extracted from the experimental data set. Let us try to perform this operation, obtaining this "experimental" set from (9.1.8) and representing data in a manner acceptable to heat transfer science.

Assume that this data set is obtained by various scientific groups at different chamber temperatures, with each group representing their results in a form of $\alpha(T)$ or even $\alpha(T-T_0)$. Thus, all that we see is the HTC; we have no direct access to the set of heat fluxes [from which we may guess dependence (9.1.8)]. The material of our surface is aluminum with:

$$\varepsilon(T) = 0.05 + 4.8 \times 10^{-5} (T[K] - 400), \ 400 \le T \le 900.$$
 (9.1.9)

The imaginary reference data $\alpha(T)$ is presented in Fig. 9.3; for plausibility, we add a 5% "experimental" error to our data. We see a wide spread of experimental

Fig. 9.3 "Experimental" data set for radiation heat transfer coefficient

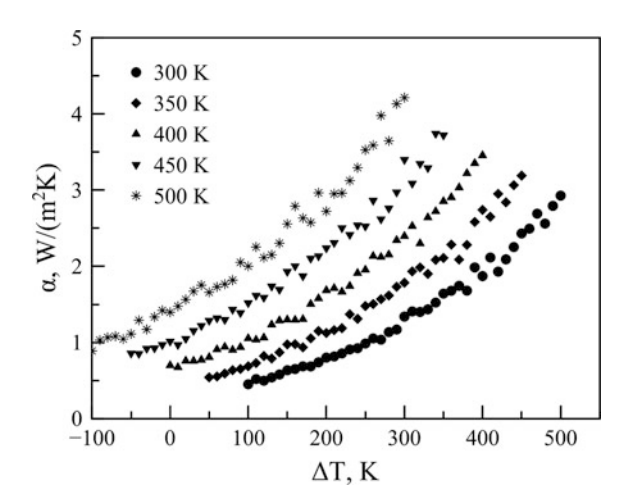


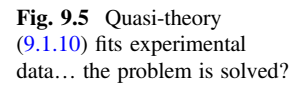
points. Possibly, one may decide to represent these data points applying the "physical sense": for many reasons, the HTC may depend on the temperature difference $\Delta T = T - T_0$ itself; for instance, the main dependence may be in the form $q = \alpha'(\Delta T)^n$. However, the representation $\alpha(\Delta T)$ is even worse (see Fig. 9.4) than function $\alpha(T)$; actually, this fact may have been evident earlier from the trend in Fig. 9.3.

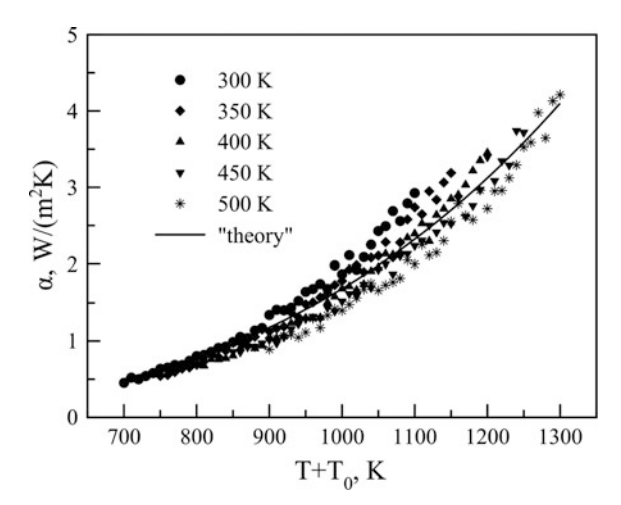
Another approach for the argument of function $\alpha(?)$ may be described in Figs. 9.3 and 9.4. A crazy idea: for unknown, elusive reasons, let us assume that the HTC depends on the sum $T+T_0$; the corresponding function $\alpha(T+T_0)$ is shown in Fig. 9.5.

At first glance, the agreement in Fig. 9.5 seems much better than for the representation $\alpha(T)$ (mainly, since it is visual). Thus, one may try to describe the

Fig. 9.4 Another representation of the data set in Fig. 9.3







experimental data with a simple correlation which is useful for practical applications:

$$\alpha = A(T + T_0)^n, (9.1.10)$$

with experimental constants $A = 1.06 \times 10^{-10}$ and n = 3.4. The discrepancy between theory (9.1.10) and the experiment data is ~20%—not the worst agreement for such a complicated process as heat transfer. No doubt, in time, some physics will be assigned to correlations of the kind similar to (9.1.8).

As for the stability of the results obtained for the HTC, note that we omitted the main experimental difficulty for experiments of such type: the total emissivity strongly depends on surface conditions. Correlation (9.1.9) is suitable for a clean, polished surface. The roughness, the grime, the oxide films, etc., are all factors which change the emissivity by tens of percent, or in some cases by several times. Thus, the real experimental set would have a much wider spread than is shown in Fig. 9.3 and, consequently, the analysis of this data would be much more interesting.

We suppose that it is almost impossible to see the common form of correlation (9.1.8) in the experimental data set in Fig. 9.3. The only way to obtain such formulae as (9.1.7) and (9.1.8) is a process named "theory first." The radiation heat transfer has an element of scientific luck because of the short lifetime of interpolative correlations for the heat flux in form of:

$$q(\lambda, T) = aT^{5-\mu}\lambda^{-\mu}\exp\left(-\frac{b}{\lambda T}\right),\tag{9.1.11}$$

where a and b are constants and μ is an adjustment parameter. For example, $\mu = 5$ gives Wien's law, $\mu = 4$ and b = 0 provides the Rayleigh–Jeans formula and $\mu = 4.5$ corresponds to the Thiesen correlation (the geometric mean between the

Rayleigh correlation and Wien's formula), etc. Planck's law finished the discussion almost in a cradle.

9.1.5 Back to Boiling and Evaporation

As we understand, the heat flux expenditure on the bubble surface is determined by the temperature of the surface rather than by the temperature difference between the wall and the solid surface. Moreover, the temperature of the bubble surface may differ from the saturation temperature; thus, it is difficult to expect that the defining parameter for nucleate boiling is $\Delta T = T_{\rm w} - T_{\rm s}$. According to Sect. 9.1.4, it would be abnormal if we could extract a certain universal correlation for the heat transfer coefficient in such conditions.

However, we have to try to represent at least the heat flux on the solid wall through the temperature of the bubble surface.

Both the heat flux and the mass one have strong dependence on the temperature of the liquid at the bubble surface. This temperature variates with time during evaporation: it tends to decrease because of the evaporation and tends to increase due to the heat conducted from the hot wall.

The main dependence on the surface temperature is expressed through the number of evaporated particles:

$$n \sim \Gamma\left(\frac{1}{2}, \frac{U}{T}\right) \sim \sqrt{\frac{T}{U}} \exp\left(-\frac{U}{T}\right).$$
 (9.1.12)

Multiplying (9.1.12) by $T\sqrt{T}$ (for the evaporation heat flux), we obtain the temperature dependence for the heat flux in the form:

$$q^{\text{ev}} \sim AT^2 \exp(-U/T).$$
 (9.1.13)

It is noteworthy that (9.1.13) is similar to the Richardson-Dushman correlation for thermionic emission. Again, we should note that here T is the temperature of the bubble wall; generally, $T \neq T_s$.

We should remember what (9.1.13) means. The heat flux q is not the heat flux on the solid wall; correlation (9.1.13) determines only the heat flux on the surface of the bubble. Suppose that the bubble is a sphere of radius R(t) at instant t; of course, it is not a sphere (it is rather a hemisphere), but we may correct this circumstance with an adjustment factor later. Then, the total heat spent for a single bubble during its growth time τ is:

$$Q_1 = \int_{0}^{\tau} 4\pi R^2(t) q^{\text{ev}} dt.$$
 (9.1.14)

If there are v bubbles formed and detached per unit time per unit area of the heated wall, then the average heat flux on the wall is $q_{\rm w}=vQ_1$. Taking into account the fact that usually at a given moment of time the major part of the solid surface is free from bubbles, we must conclude that local evaporation fluxes are much higher than the average value $q_{\rm w}$. This circumstance will be important later on in the chapter.

9.2 Film Boiling

9.2.1 Common Description

Film boiling takes place at the very high temperatures of a solid wall. For water, the corresponding ΔT is so high that surface burnout can be expected. In many experiments, the moment of transfer from nucleate boiling to film boiling is detected by burnout of a heating wire.

During film boiling (when the surface is able to withstand this type of boiling), the solid surface contacts only with the vapor phase: a thin vapor layer of width ~ 1 mm or less. The heat from the solid wall transfers to the liquid through this vapor layer. Such a heat flux (heat conductance plus free convection in vapor) cannot be very large—that is the reason for burnout at the moment of "nucleate boiling—film boiling" transition.

Anyway, the heat flux is non-zero and the liquid at the interface is hot, thus, intensive evaporation on the liquid surface takes place. Let us imagine a hot body (wire, sphere, etc.) submerged in liquid at the conditions required for film boiling. Due to evaporation of the liquid from the interface, vapor pressure in the film will increase, thus, we can expect that at some moment vapor pressure would become so high that liquid will be thrown from the solid surface (or in the opposite case: the solid will be thrown from the liquid).

However, this consideration is wrong. The vapor film can "discharge" itself, emitting bubbles into the bulk of the liquid; this mechanism prevents high pressures in the vapor layer. The mechanism, according to which gaseous bubbles may penetrate the interface to the liquid, is very interesting; the key word here being "instability."

9.2.2 The Rayleigh-Taylor Instability

We have not provide a detailed consideration of this type of instability here because we are only interested in the final result, which can be obtained easily with a simplified approach; common analysis can be found in many books devoted to such topics. 9.2 Film Boiling 281

Let us consider two separate phases with densities ρ_1 and $\rho_2 > \rho_1$; phase #1 is placed under phase #2. Thus, our common intuition suspects an instability in such a configuration: try to imagine a glass with a gas (air) at the bottom and with water over this gas. What forces, at least theoretically, may keep this configuration? Heavy liquid tends to move downward, however, when the interface bends toward the gas phase, the capillary forces try to prevent further bending. Thus, we have a duel between gravity and surface tension. Despite the fact that we can predict the winner immediately (if we only remember the Laplace formula for the pressure jump; see Sect. 1.2), we will obtain the answer in several steps.

First, we have to write the equation of the boundary of these two phases z(x), where z is the normal coordinate and x is the coordinate along the interface.

Assuming hydrostatic law for the pressures in both phases, we have:

$$p_1(z) = p_1^0 - \rho_1 gz, \ p_2 = p_2^0 - \rho_2 gz.$$
 (9.2.1)

Then, in equilibrium, the difference in pressures between the two phases must be balanced with the capillary force $\sigma\zeta$ (σ is the surface tension and ζ is the curvature), thus:

$$p_1^0 - \rho_1 gz + \sigma \frac{z''}{(1 + z'^2)^{3/2}} = p_2^0 - \rho_2 gz,$$
 (9.2.2)

where $z' = \mathrm{d}z/\mathrm{d}x$. For instance, neglecting gravity, we may obtain the usual expression for the Laplace jump of the curve $z^2 + x^2 = R^2$, when $\zeta = \pm \frac{1}{R}$:

$$p_1^0 = p_2^0 \pm \frac{\sigma}{R},\tag{9.2.3}$$

where the "+" sign corresponds to the surface deflected toward phase #2 (for equation $z = \sqrt{R^2 - x^2}$), and vice versa. Actually, this expression is not a usual Laplace formula because for our flat geometry we missed the multiplier 2 in the second term of the right-hand side of (9.2.3), which appears for spherical geometry.

For our problem, it is logical to assume the condition $p_1^0 = p_2^0$ for the flat surface, where $z(x) \equiv 0$. Then, we assume that:

- The interfacial disturbances have sinusoidal form, i.e., $z = A\sin kx$.
- The amplitude A is small, so we may neglect the term z^{2} in (9.2.2).

This way, we have from (9.2.2) that equilibrium takes place when:

$$g\Delta\rho = k^2\sigma,\tag{9.2.4}$$

where $\Delta \rho = \rho_2 - \rho_1 > 0$.

Thus, gravity forces may be dominated by the surface tension only for a sufficiently short-wave disturbance (i.e., for sufficiently large k; in this case the

right-hand side of (9.2.3) is greater than the left-hand part). In the opposite case, if the wavelength exceeds the critical value:

$$\lambda = 2\pi \sqrt{\frac{\sigma}{g\Delta\rho}},\tag{9.2.5}$$

the system becomes unstable, because the capillary forces can no longer equal the mass forces: in regions where z < 0, heavier liquids tends to move down, while for z > 0, lighter liquid tends to move up.

Indeed, the results were predicted at the very beginning: we know that the surface tension forces are stronger for high curvatures (small radiuses), thus, long-wave deflections from the surface cannot be balanced by capillary forces.

For film boiling, the Rayleigh-Taylor instability means—visibly—that vapor cavities penetrate into the liquid, forming pop-up bubbles. However, all these consideration have no allusion to boiling or evaporation processes: we considered two separate phases in the absence of phase transitions. However, how does evaporation affect instability?

9.2.3 Evaporation and Instability

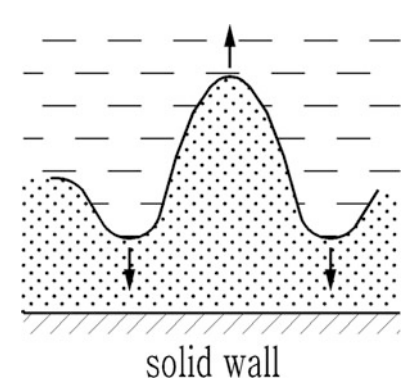
Another popular demonstration of the Rayleigh–Taylor instability is moving a glass with water upside down with an acceleration a > g. In this case, the result is an acceleration (a - g) < 0, and again we obtain the situation where a "heavy liquid sits over a light one." In this situation our "over" has the opposite sign, according to the direction of the total acceleration. Thus, in the glass accelerated toward the Earth one may observe waves on the water surface (because of the Rayleigh–Taylor instability).

This simple experiment may be applied to the instability of the evaporation surface. For intensive evaporation, two forces push the liquid away from the solid wall: the increasing pressure and the reactive forces that act on the evaporation surface. Both these factors may cause instability, for instance, if the liquid tries to jump off the wall (i.e., starts to move with an acceleration), then the Rayleigh–Taylor instability leads to a large disturbance of the interface, vapor bubbles enter the liquid, and, as a result, pressure inside the film decreases, and the interface goes back.

In addition, we may propose a more complicated scheme for the effect of evaporation on instability. When the vapor phase moves into the liquid (see Fig. 9.6), the amount of vapor in this cavern increases because of the increase of the evaporation surface area. Thus, the surface development gains the pressure that fosters surface development, etc. We cannot describe this process simply by replacing $p_1^0 \rightarrow p_1(z)$ in (9.2.2), because pressure equalizes with the speed of sound, and we need to decide what timescale is used in (9.2.2); this time must be connected

9.2 Film Boiling 283

Fig. 9.6 Instability of the vapor film



with the characteristic time of instability development, however, linear stability theory cannot provide a value for this quantity. Physics becomes much more complicated, thus, here we have to restrict our consideration to qualitative analysis.

In the general case, the flow of the vapor in the film may affect instability too; however, we will not consider such complicated schemes here. Note also that the instability of the interface under conditions of a phase transition was discussed in Sinkevich (2008).

9.3 Transient Boiling

9.3.1 Common Description

Transient boiling is an unstable type with condition q = const. for a heat flux on a solid wall, i.e., at a certain heat flux. However, when boiling is determined by the wall temperature (which is usually described by $\Delta T = T_{\rm w} - T_{\rm s}$, i.e., the difference between the temperature of the wall and the saturation temperature), it can be observed experimentally. For example, you can see this process in domestic conditions, e.g., plunging a hot pot into cold water.

Transient boiling is unstable. Liquid moves to an overheated surface, boils and jumps away. Vapor bubbles form large agglomerates near the solid surface; such groups of bubbles lay on the so-called macrolayer (in opposition to the microlayer which exists under a single growing bubble).

The non-stationarity of transient boiling leads to some interesting effects. In several works (for instance, Hsu et al. 2015; Yagov et al. 2015) it was described as a type of boiling with a high cooling rate for a solid wall; the heat flux being comparable to that for nucleate boiling despite the fact that the temperature of the wall exceeds the critical temperature of the liquid. Questions that will be discussed in this section are: what is the maximum heat flux that can be diverted from the solid wall and what are the conditions required for the existence of this flux.

9.3.2 Maximum Heat Flux on a Solid Surface

At the first glance, a heat flux of any intensity can be transferred from a solid wall through a liquid. Indeed, the heat flux in a liquid at a solid surface is:

$$q = -\lambda \frac{\mathrm{d}T}{\mathrm{d}n} = \lambda \frac{\Delta T}{\delta},\tag{9.3.1}$$

where we introduce the scale δ for the temperature difference ΔT at the surface, for future consideration. Thus, since the gradient of temperature can be as large as we can imagine—or, with the finite difference approach of (9.3.1), ΔT at the given scale δ can accept any value—one may expect that the heat flux in the liquid can be as large as we want.

Of course, as always, our imagination and desires are restricted by nature.

Due to the temperature distribution in liquid, different layers of liquid have different tensions, i.e., the strength gradient in a liquid in the normal direction (away from the solid wall), that is:

$$\frac{\partial \sigma}{\partial n} = \left(\frac{\partial \sigma}{\partial T}\right)_{Y} \frac{\partial T}{\partial n},\tag{9.3.2}$$

where X denotes the corresponding process: it can be an isochoric process, or a process along the saturation curve, etc.

The stress caused by this temperature gradient can be rather high. For instance, in the simplest case we may put $\sigma=p$, and for water at isochoric conditions $(\frac{\partial p}{\partial T})_V \sim 10^6$ Pa/K. Of course, this value is somewhat of a maximum estimation, and for the process at saturation parameters we have a much smaller derivation $(\frac{\partial p}{\partial T})_{\rm sat} \sim 10^2$ Pa/K. On the other hand, the condition V= const looks logical for the heat transfer inside a liquid over short periods of time.

Anyway, we see the clear mechanism that restricts the maximum value of the temperature gradient and, consequently, the maximum value of the heat flux. In the vicinity of a heated wall, one may expect a high value for the temperature gradient to cause thermal stress inside a liquid. In the case when the thermal stress is enough to overcome all the forces that hold a liquid close to a solid surface, the liquid will "jump away" from the wall. The forces which need to be overcome are:

- External pressure.
- Binding forces between the liquid and the wall, or—in the case when the "liquid-wall" binding energy is higher than that of "liquid-liquid"—forces between the atoms of the liquid.

Moreover, at high temperatures of the wall we may expect that the kinetic energy of atoms of liquid near the solid surface is high, thus, the total energy of many particles is positive. Thereby, a kind of "partial phase transition" close to the wall may be expected, i.e., the "liquid-wall" binding energy is weakened and the second type of forces can be neglected. In the limiting case, one can imagine vapor on the solid surface that attempts to push out the liquid; however, for wall temperatures which are higher than the critical temperature of the liquid, this simplification is incorrect.

The maximum heat flux on the surface can be estimated with (9.3.1) and (9.3.2). Expressing the maximum temperature difference from (9.3.2) as $\Delta T_{\text{max}} = \sigma_{\text{max}} (\partial T/\partial \sigma)_X$, and substituting this in (9.3.1), we have:

$$q_{\text{max}} = \frac{\lambda \sigma_{\text{max}}}{\delta} \left(\frac{\partial T}{\partial \sigma} \right)_{\text{v}}.$$
 (9.3.3)

For instance, neglecting the binding energy as it was discussed above, and estimating the derivate (in the absence of a better choice) $\left(\frac{\partial T}{\partial \sigma}\right)_X \sim \left(\frac{\partial T}{\partial p}\right)_V \sim 10^{-6} \frac{\text{K}}{\text{Pa}}$, with atmospheric pressure $\sigma_{\text{max}} \sim 10^5 \text{Pa}$, $\lambda \sim 1 \, \text{W}/(\text{m} \cdot \text{K})$ and $\delta \sim 10 \, \text{nm}$ (the most difficult parameter for estimation; this value corresponds to our assumptions taken from Sect. 9.3.8), we obtain $q_{\text{max}} \sim 10^7 \, \text{W/m}^2$.

However, the account of the binding energy between the liquid and the wall may enlarge this estimation by an order or a two of magnitude.

Some people may assume that because these heat fluxes are abnormally huge, they can never be observed in nature (or in experiments). However, the mechanism described above can be significant for non-stationary processes on the surface, when temperature gradients at the solid wall can be high enough over small spatial scales of ~ 10 nm. These states—with such a high temperature gradient at the surface—cannot last long, so the heat fluxes discussed above are momentary fluxes.

9.3.3 Types of Heat Fluxes

It is possible that some statements from Sect. 9.3 need explanation. Here we discuss the heat flux from another—technical—point of view.

As we remember from Chap. 4, the heat flux in a condensed matter consists of two parts. The first being the usual heat flux, which is determined by the motion of particles:

$$q = \int \frac{mv^2}{2} v f(v) dv. \tag{9.3.4}$$

In an ideal gas the flux (9.3.4) represents the only contribution to the heat flux. However, for a solid dielectric, this flux is approximately zero, because atoms are almost stable in such conditions (for metals, electron heat conductance, another mechanism of heat exchange, must be considered).

The second part of the heat flux is caused by the exchange of potential energy between particles in the medium, see Chap. 4. This type of heat transfer corresponds to the heat conductance.

Thus, in the usual case—for instance, in nucleate boiling—heat is transferred from a solid wall through a liquid by the heat conductance mechanism. When the liquid is seen to be "jumping away" from the surface, the convective term in (9.3.4) switches on. Due to this contribution, the total heat flux increases. In simple words, when heat flux (9.3.4) is present, the heat flux exceeds the normal heat conductance flux, i.e., the stationary heat flux in nucleate boiling is not the theoretical maximum of the heat flux: a jumping liquid provides higher fluxes, however, not for long.

The ability of a liquid to "turn" heat flux (9.3.4) into the total energy flux depends on the condition of a wall surface. Interaction potential between atoms of a liquid and a solid depends, first of all, on what sort of atoms the solid surface consists of. We have two different situations here, i.e., when a liquid contacts a metal surface or an oxide of it. This factor must be taken into account in the eventual comparison with experimental results.

In fine, we see that the maximum heat flux which can exist in the liquid near the solid wall is restricted by the temperature gradient in the liquid. The last quantity depends on the temperature that the liquid can reach near the solid wall. Indeed, if water contacts hot tungsten at 2000 K, does it mean that *liquid water* may obtain a temperature of 2000 K?

9.3.4 The Maximum Contact Temperature

Contact temperature is the measurement which represents the equal temperature of a solid and a liquid at the point where these two phases are in contact. For equilibrium state, this assumption is not in doubt. The initial question addressed in this subsection concerns the maximum value of such a contact temperature.

At the first glance—of course, the first glance may be only from a thermodynamics standpoint—this temperature cannot exceed the temperature on the spinodal curve $T_{\rm sp}$ of the liquid contacted with the solid wall. Actually, this conclusion is based on these two initial postulates:

- At the contact point, the temperatures of the solid and liquid are equal.
- The liquid cannot reach a temperature higher than $T_{\rm sp}$, because otherwise the liquid represents an unstable thermodynamic phase.

Thus, as a summary of these suggestions, we have the overview given above. Moreover, we can continue this logical train of thought. The highest heat fluxes may only be observed for a wall temperature $T < T_{\rm sp}$, because only in such cases do we have contact between a solid and a liquid: otherwise, for the "solid-vapor" contact a much smaller energy flux can be removed from the wall.

As per the final statement, one may conclude that the maximum contact temperature cannot exceed the critical temperature $T_{\rm cr}$, and the heat fluxes at $T_{\rm w} > T_{\rm cr}$ must be lower than the ones at nucleate boiling. Indeed, the main mechanism of heat transfer in boiling is phase transition, thus, how can phase transition be possible in the absence of separate phases?

These inferences look solid. According to them, we cannot observe a contact between the liquid and the wall at $T_{\rm w} > T_{\rm cr}$, cannot obtain high heat fluxes for such temperatures, etc.

However, all of this contains one weak point: it is all about equilibrium. All the conclusions above are based on the hypothesis of stationarity: analogously, this represents the description of a frame of a movie, while the boiling process rather represents the entire movie.

When a cold (comparatively) liquid contacts a solid wall, its temperature at this solid surface rises at the rate that depends on the temperature difference between the liquid and the solid. Simultaneously, heat transfers from the solid wall to the inner layers of the liquid. However, this rate is limited, so there might be a situation when the temperature of the liquid would have an enormous gradient (see above).

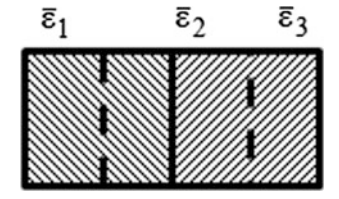
Temperature is determined as being the average kinetic energy of molecules. The temperature gradient means that the kinetic energy of molecules varies with distance from the solid-liquid surface. However, to define temperature as an equilibrium parameter, we have to be sure of the local thermal equilibrium state: between two neighboring points the temperature must differ insignificantly. In the opposite case, when the temperature differs over a scale of ~ 1 nm (i.e., at the scale of the interaction radius) by an order of magnitude, it is impossible to define such a parameter as temperature. One may calculate the average kinetic energy at a given point (i.e., of a small group of molecules), at the next point and at a point between (see Fig. 9.7), and obtain three different values of $\bar{\epsilon}$:

$$\frac{\bar{\varepsilon}_1 - \bar{\varepsilon}_2}{\bar{\varepsilon}_1} \sim \frac{\bar{\varepsilon}_2 - \bar{\varepsilon}_3}{\bar{\varepsilon}_2} \sim 1. \tag{9.3.5}$$

In such a case, as discussed in Chap. 1, the usual correlations (all obtained for a local thermal equilibrium state) become incorrect; all equilibrium conceptions, including "binodal" and "spinodal", lose any sense, etc.

Thus, at high temperatures of a solid wall, at short contact times with a liquid (i.e., almost in a trice), the physical description cannot be provided in our usual,

Fig. 9.7 Energy at neighboring points 1 and 3 and between them at 2 = (1 + 3)/2



equilibrium terms. This would not be a problem, if over such short timescales no "interesting processes" occurred, and we could wait for equilibrium, i.e., we would be able consider this problem over long timescales. Unfortunately, some primary processes, which determine the entire physical picture, may occur on these short timescales. In this situation, we have two options, both of which are bad:

- To use an old equilibrium description, but replace its terms for non-equilibrium analogs; for instance, $T \to \bar{\epsilon}$.
- To construct some new correlations for non-stationary parameters such as $\bar{\epsilon}$.

Here we choose option one. Specifically, we will explain our results in terms of previous subsections. We suppose that it is sufficient to understand the basic physical mechanisms, even when the temperature is not the temperature (but only the mean kinetic energy of molecules at this point), liquid is not a liquid (but only a condensed phase at high temperature $T > T_{\rm cr}$), etc. The second option in the list above appears too complicated for now.

9.3.5 A Sidestep: "An Infinite Rate of Diffusion"

We feel that our assertion about the limited rate of heat transfer process demands explanations.

Possibly, this is one of the most popular tricks that professors perform in front of confused students. For example, the following question would be raised: "We take a very long rod, from here to Mars; then we instantly heat up our end of the rod; at what moment in time do Martians feel the heat?" A variation of this question may involve diffusion: at what instant does the first molecule of a gas sprayed in the opposite corner of a room reach us?

All such questions (specifically, tricks) are based on the infinite rate predicted by the diffusion equation:

$$\frac{\partial n}{\partial t} = D \frac{\partial^2 n}{\partial x^2}. (9.3.6)$$

Thus, from this point of view, the correct answers must contain the word "instantly." However, these answers are wrong (to be fair, the questions are wrong too); Einstein stands in the way of such tricks. Here, we do not mean special relativity, according to which nothing can move faster than light. We mean his work (Einstein 1905) where the diffusion equation was obtained by expansion into series:

$$n(x, t + \tau) = \int_{-\infty}^{\infty} w(\Delta, \tau) n(x + \Delta, t) d\Delta, \qquad (9.3.7)$$

so that:

$$n(x, t + \tau) = n(x, t) + \tau \frac{\partial n}{\partial t}, \qquad (9.3.8)$$

$$n(x + \Delta, t) = n(x, t) + \Delta \frac{\partial n}{\partial x} + \frac{\Delta^2}{2} \frac{\partial^2 n}{\partial x^2}.$$
 (9.3.9)

We will not discuss here all the technical nuances (such as the circumstances at which the second term in (9.3.9) gives zero after substitution in (9.3.7), etc.), but we will mention only the important fact: in this way, we obtain the diffusion equation with the diffusion coefficient $D=\overline{\Delta^2}/2\tau$ for only a small spatial displacement Δ , over short moments of time τ . It is an evident condition for the correctness of expansion (9.3.9). Thus, we cannot expect to find solutions for cases when $\Delta \to \infty$ from our diffusion equation; for such cases, we must hold another number of terms in (9.3.9) and even in (9.3.8).

In simple terms, the diffusion equation can be applied only at reasonable spatial and temporal scales. The rate of disturbance propagation is limited, despite any predictions which follow on from the equation which is indeed incorrect for unlimited scales.

In fine, what we really wanted to explain in this short subsection is that we cannot expect an infinite rate for any process. Not only does physics forbid such constructions—mathematics does too. Now let us return to our evaporation problems.

9.3.6 Stationary Evaporation Versus Explosive Evaporation

The physical process described in the first eight chapters of this book is evaporation: a liquid heated from a solid wall emits atoms from its free surface; possibly, sometimes, even groups of atoms are emitted (see Chap. 6 for so-called hyperevaporation), but common principles stay the same.

However, we may imagine a different mode for the type of the phase transition occurring for a liquid on a solid surface; the physics of this mode is described in Sect. 9.3.2 of this chapter.

Over short timescales, with large gradients of surface temperature, liquid may jump away from a solid wall because of the thermal stresses inside it. After detachment from the wall, the back face of the liquid (facing toward the solid surface) has a high temperature, the liquid evaporates, and due to this evaporation the pressure in the vapor layer between the solid and the liquid rises, continuing to move the liquid away from the wall.

This process may be referred to as explosive boiling, but we prefer here to term this it as "explosive evaporation." Boiling (i.e., the process observed in the corresponding experiments) is a process operating on another timescale (see Chaps. 2–4 for the scales of processes).

9.3.7 Boiling

All non-stationary, unstable types considered in this chapter, describe processes over very short timescales. Usually, in experiments, much larger timescales are investigated. For instance, in numerical simulations we may use an ultimate rate of wall heating, while in experiments this rate may be slower by several orders of magnitude. Consequently, it is harder to obtain enormous rates of heating in experiments: in contrast with numerical simulations, in experiments, the temperature of the liquid varies much less obviously, therefore, it is more difficult to observe temperature gradients in liquids (however, this is not impossible to do).

Another reason: we cannot predict the fate of any liquid which jumps away from the wall. Maybe it returns to the solid surface because of:

- Surface tension (large-scale quantity).
- Instability at the interface (large-scale process).
- Different conditions at a site nearby to the solid wall e.g., a different temperature (large-scale phenomena).

If the liquid returns back to the wall, then we can perform a time-averaging procedure with the heat flux considered in this section. If it does not, then the momentary flux is unlikely to define large-scale and long-timescale boiling processes. However, we have to take into account that explosive evaporation takes place across the whole surface, while the heat flux measured for nucleate boiling represents only an averaged value ...

In fine, we want to refrain from the direct analogy between a steam explosion and the explosive evaporation described in this chapter. Many details must be investigated to define whether this jumping liquid is a steam explosion or not. Thereby, we prefer to consider the results from this section as a pure theoretical description, without direct links to certain experimental conditions.

9.3.8 Numerical Simulation of Explosive Evaporation

In this section, we present the results of molecular dynamics (MD) simulations. Of course, here we consider argon; molecules of argon are bound with a copper surface by a corresponding interaction potential.

Initially in the experiment we brought the "liquid argon + vapor argon" system into a thermal equilibrium state at a temperature $T=100~\rm K$; we remind the reader here that the critical temperature of argon is 150 K.

Next, under this equilibrium system, we spontaneously increased the temperature of the wall, to 200, 225, 250, 300 and 400 K. Depending on the initial conditions (i.e., mainly the temperature itself), one may observe either ordinary evaporation, or an extreme version of it—explosive evaporation. For this set of temperatures, we observed usual evaporation for 200 K, and explosive evaporation

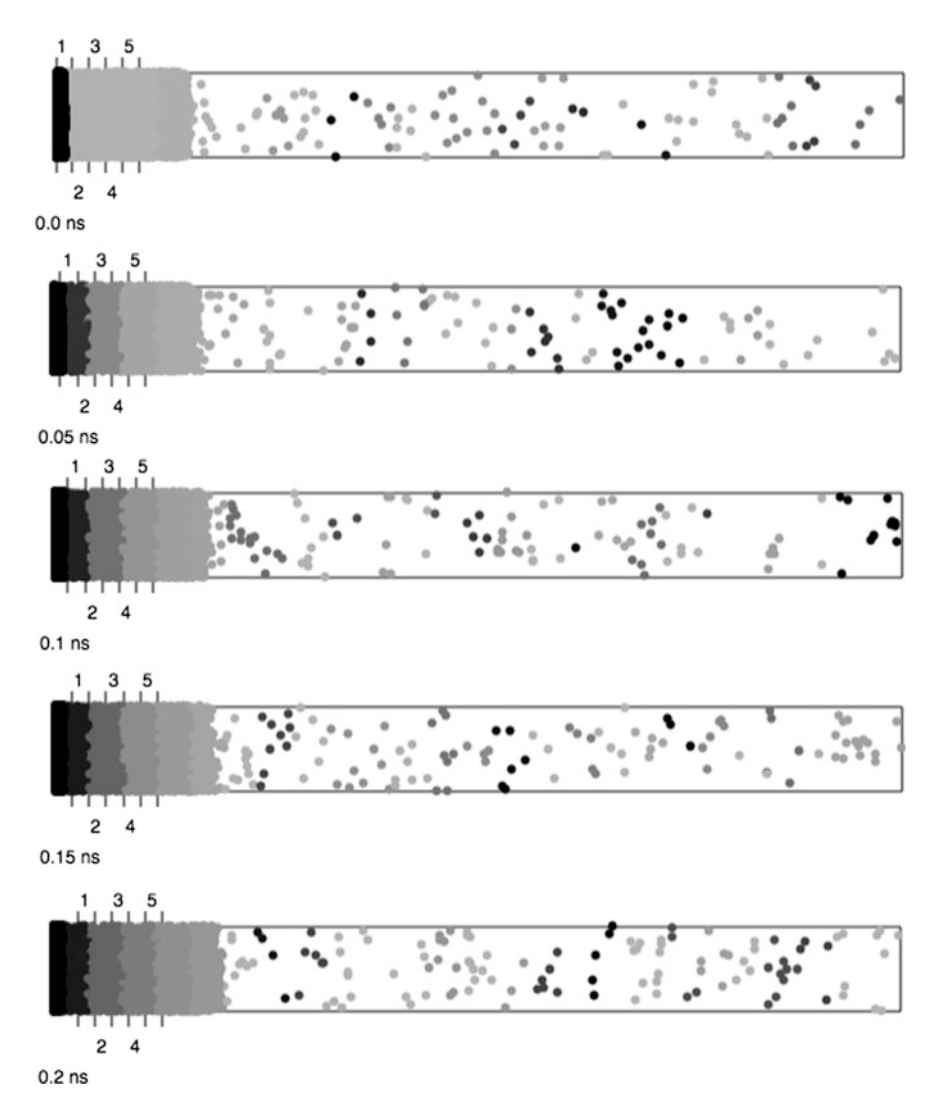


Fig. 9.8 Usual evaporation of argon from a very hot surface (200 K). (Shades of grey represents the value of kinetic energy in the layers, black color corresponds to higher level of energy)

for all other wall temperatures. Consequently, we can establish the lowest limit for explosive evaporation is between 200 and 225 K.

"Usual" evaporation at $T=200~\rm K$ is shown in Fig. 9.8. Despite such a high temperature (note that $T>T_{\rm cr}$), we observe stationary type evaporation. Here the liquid layer "expands" and evaporates (one may see that the width of the liquid layer increases).

The temperature in various liquid layers is shown in Fig. 9.9. We see that the temperature gradient is high, however, it is insufficiently high to throw liquid away

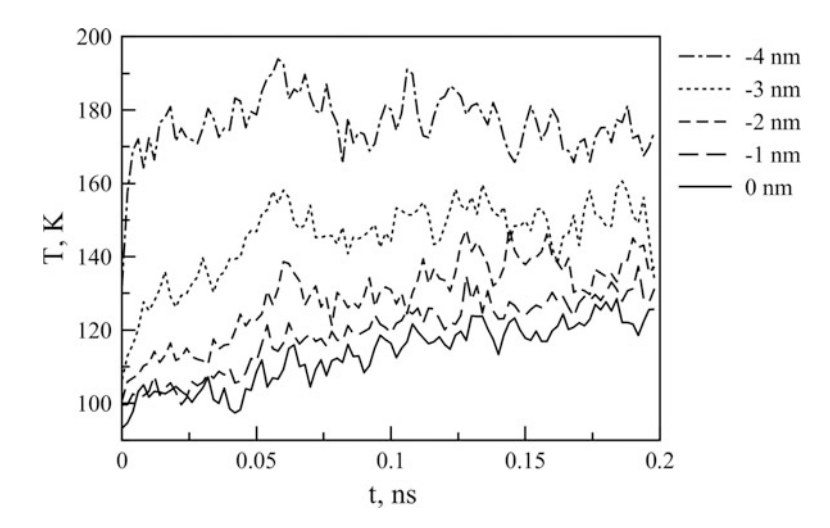


Fig. 9.9 Temperature in layers at various distances from the center of mass of the liquid. Temperature of the solid wall is 200 K. At the wall, temperature of liquid \sim 200 K (layer at z=-4 nm from the center of mass: because axis z is directed out from the solid wall, this coordinate is negative)

from the solid surface. On the whole, the liquid is heated more or less uniformly throughout its depth, especially in comparison to other calculated types.

The example of explosive evaporation is shown in Fig. 9.10. Here we see how the liquid jumps away from the wall with a temperature T = 400 K.

The speed of that departed liquid reaches 120 m/s. The corresponding "temperature" dependences at various layers of the liquid are shown in Fig. 9.11. At such high wall temperatures, the temperature difference between two neighboring layers of liquid (at ~ 1 nm distance) has values of ~ 150 K (from 350 K at the liquid surface to 200 K in the next layer). Of course, this is a "quasi-temperature"—the mean kinetic energy of the particles; this is not a real, equilibrium parameter "temperature"; we hope that the discussion presented earlier explains this sufficiently (Fig. 9.11).

Also, it is worth noting that the "quasi-temperature" of the nearest layer did not reach the 400-K temperature of the wall, the maximum registered value was lower by $\sim\!50$ K. One may suggest that the liquid does not achieve wall temperature, because it has departed the wall; this conclusion may be considered with one important refinement: for a narrower liquid layer the value of "temperature" will be greater, however, this does not make much sense because the scale of the interatom interaction for argon is $\sim\!0.34$ nm.

Thus, we have seen how liquid departs from an overheated surface. It is easy to criticize this approach because of the evident model character of the problem. Yes, we see that the liquid jumped away from the surface when the temperature was increased abruptly from 100 to 400 K. However, this is an idealistic approach; in real life such rates are impossible. For slow heating, one may expect that the liquid will be warmed uniformly, thus, any jump will be impossible.

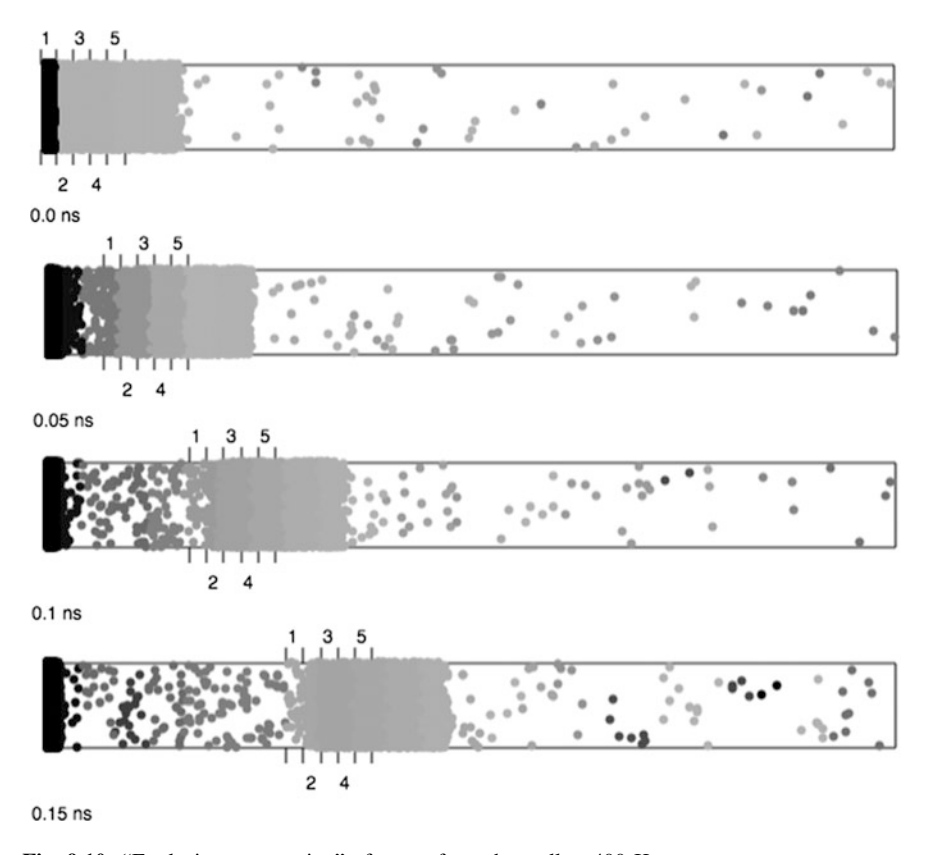
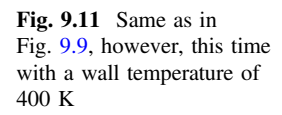
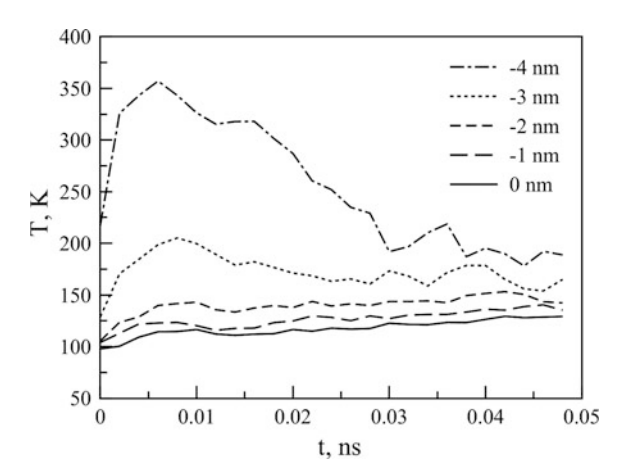


Fig. 9.10 "Explosive evaporation" of argon from the wall at 400 K





We have to consider a more realistic situation for the contact between the liquid and the hot solid wall.

9.3.9 Liquid-Wall Interaction

Here we treat the movement of the liquid to the solid overheated wall. In contrast to the previous consideration, we may expect, first, a more realistic time of contact between the liquid and the overheated solid.

Another question that may be addressed with such numerical modeling is whether this contact between the liquid and the solid is ever possible? In reality, the hot vapor between the liquid and the wall initiates the evaporation of the liquid while it moves toward the hot wall. Evaporated atoms obtain high temperatures (high kinetic energy) from the solid wall, then they provoke additional evaporation, and so on; the final result of this cycle is that one may expect high-pressure vapor to act as a buffer between the liquid and the wall, preventing their contact.

Actually, it is difficult to examine the last matter, because the answer depends on the mass of the oncoming liquid (i.e., on the momentum of the part of the liquid approaching the wall). Moreover, because of technical restrictions we cannot consider a large set of particles in a liquid, i.e., a large liquid mass. However, there is nothing else we can do: we must tackle the task as best we can. If we observe contact of $\sim 10^3$ particles with the wall, we may expect that a larger mass of the liquid would similarly contact the wall.

This process is illustrated in Fig. 9.12. The initial velocity of the liquid was 40 m/s, the initial temperature of argon was 100 K and the temperature of the solid wall remained at 400 K. During motion, the speed of the liquid decreases; however, contact with the solid wall does take place. After contact, the temperature of the liquid increases, and, in common, we obtain the situation described in Sect. 9.3.8.

In Fig. 9.13 the temperature in different liquid layers (relative to the center of mass of the liquid) is presented.

We see that all the conclusions from Sect. 9.3.8 are correct. First, the interaction time is still ~ 0.1 ns, as in the previous problem. One may conclude that during its motion toward the solid surface the liquid stayed "unprepared" for its meeting with the hot wall: its temperature remained at 100 K, as was its initial state. Thus, the temperature gradient remained approximately the same. Probably, the most important result of this numerical calculation is that we may analyze the "liquid-solid" contact in the frame of the previous consideration: with the initial conditions when the liquid was on the solid wall.

The next interesting thing to be observe from this simulation was that during motion toward the wall, a relatively cold liquid ($\sim 100~\rm K$) interacted with vapor which had a temperature (that of the hot solid wall) of $\sim 400~\rm K$. How did this process occur? Why did the hot vapor not heat the liquid mass properly? We will consider these questions in Sect. 9.4.4.

9.4 Cavitation 295

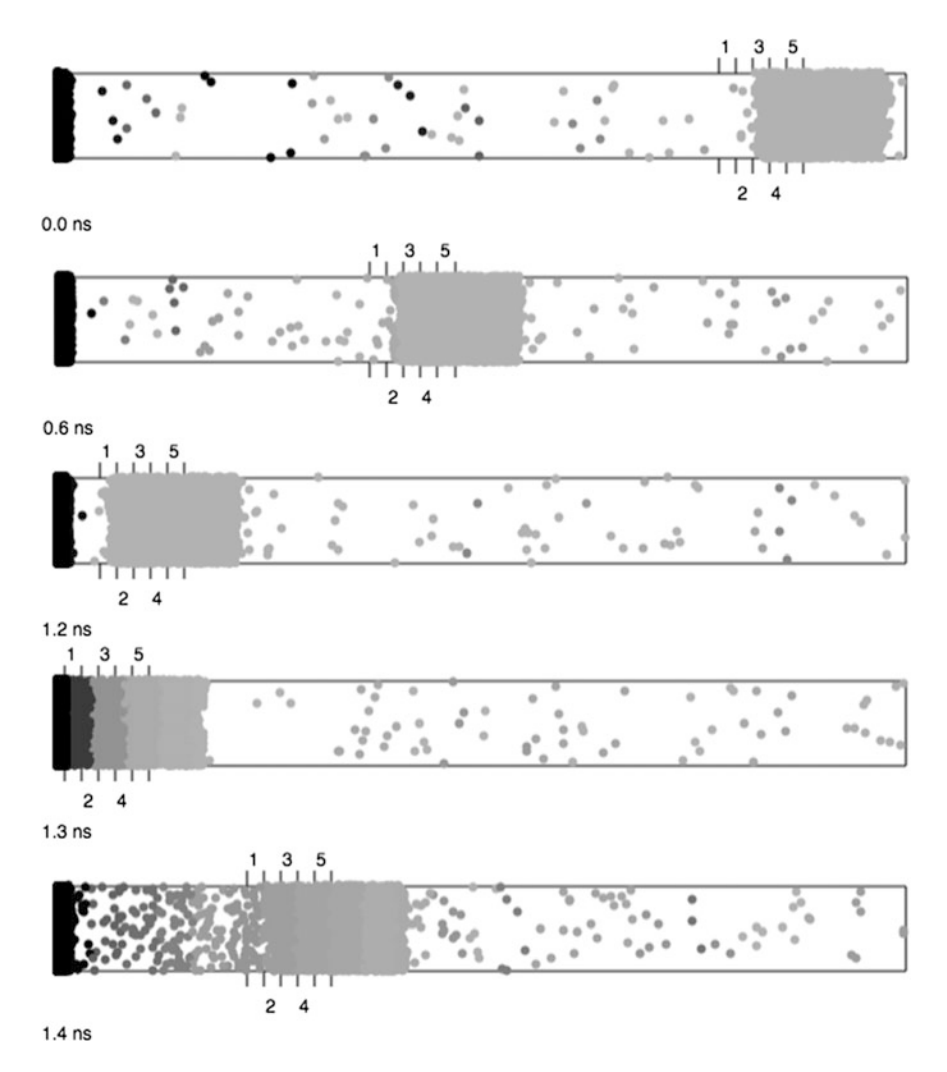
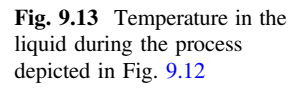


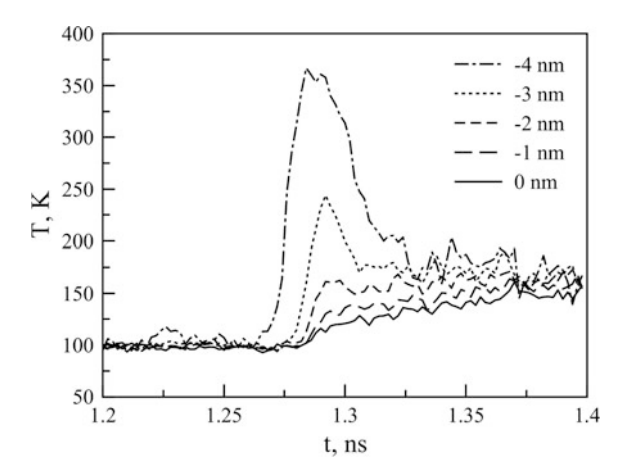
Fig. 9.12 Liquid-wall interaction with a contact time of ~ 0.1 ns

9.4 Cavitation

9.4.1 Cavitation and Sonoluminescence

Cavitation is a close relative to boiling; some aspects of boiling theory can be applied to cavitation, however, its non-thermal nature provides uniqueness to this phenomenon. Besides scientific interest, treatment of cavitation is important for practical reasons.





Cavitation is a non-thermal formation—an extinction of bubbles in a cold liquid due to mechanical effects. At alternating external pressure, a liquid ruptures, creating gaseous space inside it; collapsing, these cavitation bubbles produce an interesting and dangerous processes.

In the bulk of a liquid, cavitation is a very interesting process, which is accompanied in an ultrasonic (sometimes, not only ultrasonic, but normal acoustic) field by one of the most mysterious phenomena—sonoluminescence. It might look strange, but the nature of the light emission during ultrasonic cavitation remained undiscovered for almost a century (sonoluminescence was first reported in 1934); at first glance, such a simple (for observation) phenomenon should not require an overcomplicated explanation. "This is not synchrotron radiation!"—some may exclaim, and they would be right on two fronts: first, sonoluminescence is not synchrotron radiation; second, sonoluminescence is a much more complicated phenomenon than synchrotron radiation (see below). However, the scientific part of the exploration of cavitation has a secondary value: the main reason for the treatment of cavitation is its practical value.

On solid surfaces, cavitation is a very dangerous process, because cavitation on solid (metallic) surfaces leads to their destruction: these small gaseous bubbles determine the lifespan of huge metallic constructions like pumps, stirrer arms, propeller screws, etc.

In Fig. 9.14 we present images of a new metallic (titanium) waveguide and a waveguide after ~ 10 h of work in a jug containing a liquid (glycerol) at ~ 20.5 kHz frequency (see Fig. 9.15).

In these images we can observe dramatic destruction; such damage may be tolerated on laboratory equipment (as on these images), but impairment of technical elements—for example, of propeller screws—is simply dangerous.

The main distinction between cavitation and boiling is the absence of external heating. Thus, without a heat source, one might expect a lack of evaporation, however, this expectation is wrong for two reasons.

9.4 Cavitation 297

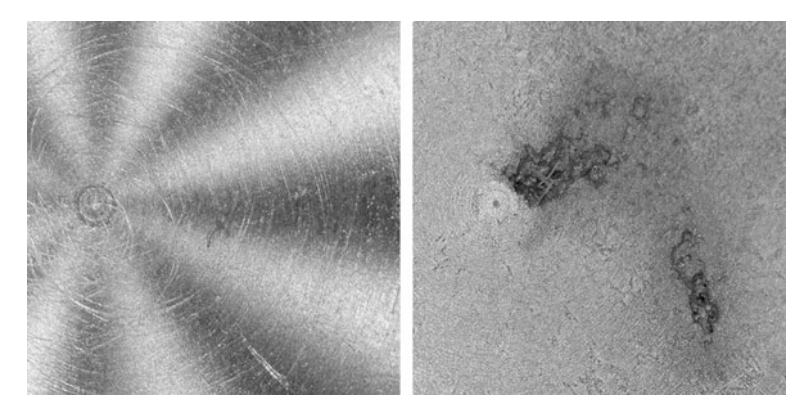


Fig. 9.14 New titanium waveguide (left) and its surface after 10 h of cavitation (right)

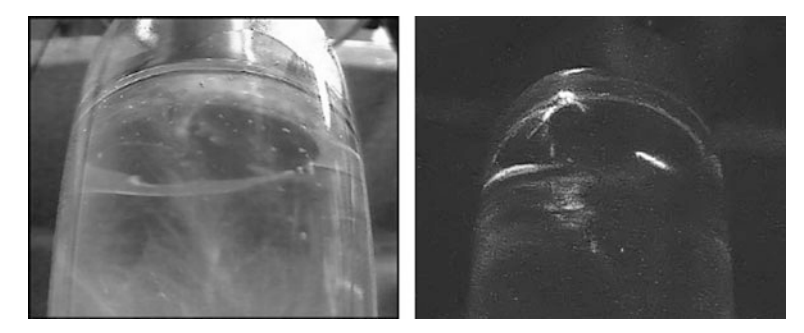


Fig. 9.15 (Left) Cavitation on the titanium waveguide in glycerol (with external light). (Right) Sonoluminescence on the titanium waveguide (no external light)

The first reason is the fact that evaporation always takes place. Slower or faster, counterbalanced by condensation or not (or even dominated by condensation), evaporation is always present. Thereby, many results from this book can be applied to the cavitation process. However, on the whole, we have to admit that this first reason is insufficient to devote a "personal" section to cavitation.

The second reason was already mentioned above: sonoluminescence.

Sonoluminescence is a phenomenon of emission of light by a liquid under the influence of ultrasound. Sonoluminescence has been known since 1934, but until recently the nature of this light has remained a mystery. There are many theories about the physical processes inside a cavitation bubble that could—theoretically—cause this glow, but none of them can explain coherently all the physical mechanisms involved in this strange type of luminescence.

In general, there are two types of sonoluminescence: single-bubble sonoluminescence and multi-bubble. In the last case, there are many forms of glow (see Fig. 9.16). All patterns of luminescence were registered in the same experiment over a period of less than 1 min.

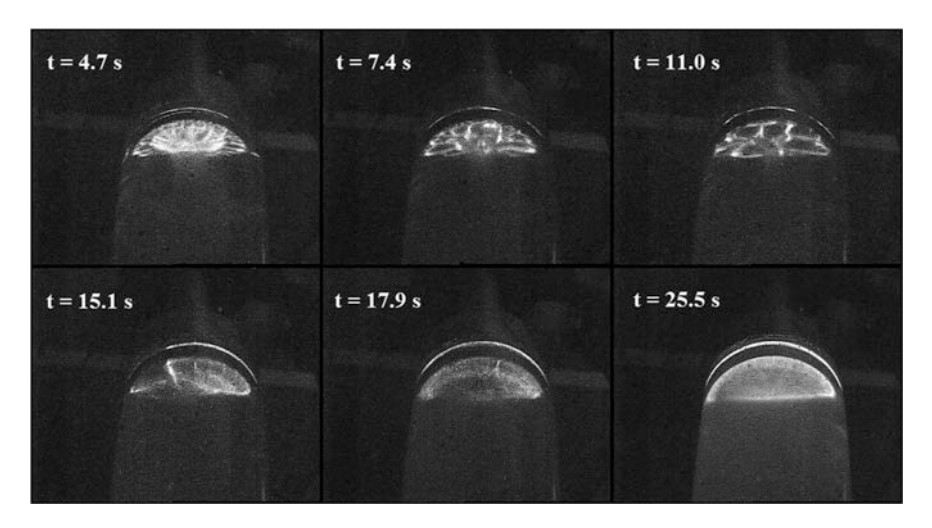


Fig. 9.16 Sonoluminescence on a titanium waveguide in glycerol

It is well established, that sonoluminescence is associated with the cavitation process: cavitation is the necessary precursor of this glow. So, it seems logical to assume that some processes during cavitation are responsible for light emission. Usually, the scheme of explanation of sonoluminescence is described as follows. Let us consider a process X, which—as it is reliably established for other physical objects—leads to some kind of a glow in common conditions (examples of X include electrization and gas discharge, chemical reactions, heating, etc.). Next, one must explain how process X could take place during cavitation. In case of success, X is proposed by the author as an explanation of sonoluminescence; however, this method of deduction has not yet led to a comprehensive theory.

One such explanation is overheating of gas inside a collapsing bubble. Possibly, this is the most popular theory of sonoluminescence to date. Many people think that this is the final answer, however, these people become confused when they find out that this theory has a few issues. According to this theory, the gas compressed in the collapsing bubble achieves temperatures so high that light emission is possible. In addition, the glow of incandescent solids and of plasma are well-known phenomena, thereby sonoluminescence joins this team.

Actually, this explanation in such a form is inadequate. It raises many questions in terms of optical and plasma physics:

- 1. What is the specific mechanism of light emission: recombination, bremsstrahlung or something else?
- 2. What is the spectra of sonoluminescence? In some works it is assumed that these spectra have a Planck shape, but actually they do not.
- 3. How thin an optic layer of plasma can produce an equilibrium "hill-shaped" spectrum?

9.4 Cavitation 299

4. One may expect that at the extension stage of the cavitation bubble, the recombination of plasma, would also lead to a glow, and, generously, the spectrum of this glow must differ from the spectrum at the collapse stage of the bubble oscillations.

This list can be easily extended. It is interesting to discuss any item on this list, however, we can add a more primal question: how can such enormous temperatures be achieved in a collapsing bubble? To produce high internal temperatures, the bubble must collapse to very small sizes. During the compression stage, gas (as a vapor of the liquid, as with other gases like, e.g., air) is heated; thus, we may expect that this hot gas would intensify the evaporation of the liquid surrounding this gaseous space. As a result, the mass of the vapor inside the bubble would increase, so too would pressure, and, consequently, the collapse phase would be stopped because of such high internal pressures. Thus, high compression ratios as well as high temperatures inside the bubble would not be achieved.

The last question deals with evaporation, and fits the scope of this book 100%. In Sect. 9.4.4, we provide an answer to another question: what does a liquid do at the vicinity of a super-overheated gas?

Certainly, despite the fact that this problem is inspired by the phenomenon of sonoluminescence, the application areas of obtained results are not restricted to a collapsing bubble. The neighborhood of overheated vapor and cold liquid is an interesting example of a strongly non-equilibrium system. Thus, we suppose that the results of this section will be interesting on many levels.

However, cavitation is the process that binds all the problems together, and sonoluminescence will be our guideline. First of all, let us see how high temperatures in bubbles can be predicted theoretically.

9.4.2 The Rayleigh Equation and Its Boundary Condition

The main trend in the theoretical description of sonoluminescence involves the Rayleigh equation, which can be obtained as follows.

Let us consider a spherical bubble of radius R in a liquid. Assuming that the liquid is incompressible, we have from the discontinuous equation:

$$\frac{1}{r^2}\frac{\mathrm{d}}{\mathrm{d}r}(r^2v) = 0\tag{9.4.1}$$

where the product $r^2v = \text{const}$, but this constant depends on time. At the interfacial surface, the velocity of the liquid $v(R) = \frac{dR}{dt} = \dot{R}$, thus, at any point inside a liquid:

$$v(r,t) = \dot{R}(t) \frac{R(t)^2}{r^2}.$$
 (9.4.2)

From the Navier-Stokes equation:

$$\frac{\partial v}{\partial t} + v \frac{\partial v}{\partial r} = -\frac{1}{\rho} \frac{\partial p}{\partial r} \tag{9.4.3}$$

(we use partial derivative for p because pressure also depends on time) and with (9.4.2) we have:

$$\frac{1}{r^2}\ddot{R}R^2 + \frac{2}{r^2}\dot{R}^2R - \frac{2}{r^5}\dot{R}^2R^4 = -\frac{1}{\rho}\frac{\partial p}{\partial r}.$$
 (9.4.4)

Integrating (9.4.4) from r = R to $r = \infty$, we get:

$$\ddot{R}R + \frac{3}{2}\dot{R}^2 = \frac{p(R) - p(\infty)}{\rho}.$$
(9.4.5)

This is the Rayleigh equation. We have to insert $\Delta p = p(R) - p(\infty)$ here to obtain the final form of the equation.

To define pressure p(R) in the liquid, we may connect this value to the pressure inside the bubble p. Neglecting all pressure jumps (such as the Laplacian jump) on the interface, we have p(R) = p, and for the pressure inside the bubble of volume $V = 4\pi R^3/3$ we may use the Clapeyron equation p = nT = MT/mV; in turn, in the last formula we need information about the mass of gas inside a bubble M.

Quantity M consists of two parts: the mass of the gas (e.g., air) $M_{\rm g}$ and the mass of the vapor $M_{\rm v}$. Usually, it is assumed that $M_{\rm g}={\rm const}$, while the vapor mass is found from the Hertz-Knudsen relation:

$$\frac{\mathrm{d}M_{\mathrm{v}}}{\mathrm{d}t} = \sqrt{\frac{m}{2\pi}} \left(\frac{p_{\mathrm{l}}}{\sqrt{T_{\mathrm{l}}}} - \frac{p_{\mathrm{v}}}{\sqrt{T_{\mathrm{v}}}} \right) 4\pi R^{2},\tag{9.4.6}$$

where indexes 'l' and 'v' denote liquid and vapor phases correspondingly.

At first glance, we may consider that we have discussed this equation enough in previous chapters; we have mentioned the condensation flux and the overall structure of this correlation in Chap. 7. However, some properties of the evaporation flux from the liquid surface in the vicinity of the vapor were not investigated fully in Chap. 8; these features will be considered here.

To finish the mathematical description of the cavitation bubble, we need the correlation of the temperature inside a bubble. The simplest way is to assume an adiabatic condition, so:

$$pV^{\gamma} = \text{const and } TV^{\gamma-1} = \text{const},$$
 (9.4.7)

where $\gamma = c_p/c_v$ is the specific heat ratio.

It is follows from (9.4.7) that at an unlimited collapse phase, when $V \to 0$ then temperature $T \to \infty$, i.e., this simple theory #1 predicts an infinite growth of temperature.

9.4 Cavitation 301

However, one may suggest another simple theory #2: let the temperature inside the bubble be a constant. Thus, despite the bubble collapse, T = const, anyway. Probably, these models dQ = 0 and T = const look equivalent, however, they are not, of course. The condition of a constant temperature implies a slow process, when the heat transfer may level out the temperature of the gas inside the bubble and the liquid. However, for a fast-collapsing bubble (with a timescale of $\sim 1~\mu s$) or less) this assumption is absolutely wrong; a time such as dQ = 0 represents a much more suitable condition.

Now, one may also propose theory #3, when the temperature of the liquid remains constant, and the evaporation flux is determined with the saturation pressure $p_s(T_l)$. The temperature of the vapor may be calculated through the heat balance on account of the energy loss (or source) on the bubble surface, with the vapor mass inside the bubble still being determined by (9.4.6)

The main part of theory #3 is the assumption that the evaporation flux does not depend on the conditions of the gas (vapor). However, as discussed in Chap. 7, the model of independent evaporation and condensation fluxes is incorrect; mainly, in that chapter we considered the effect of the evaporation flux on the condensation flux. Moreover, in Chap. 8 we considered how the gas may affect the evaporation flux; however, that consideration was framed as a specific problem (the temperature jump in the vicinity of the evaporation surface) of certain experiments; we did not discuss all the physics involved.

Before we consider the interaction of a hot gas and a cold liquid, we must briefly finish our description of sonoluminescence.

9.4.3 The Evolution of the Cavitation Bubble

Here we present the results of bubble dynamics, recalculating the solution of the Rayleigh equation (specifically, its modified version) from Gaitan et al. (1992). We do not discuss all the details of the calculation here, because all that we need is an illustration: whether the temperature inside the cavitation bubble reaches enormous values or not.

The dependence between the bubble radius and the temperature inside the bubble is presented in Fig. 9.17.

As we see, according to these calculations, the temperature inside a cavitation bubble may achieve several thousands of kelvin (note that $T_0 = 300$ K). Thus, all our consideration from previous subsections remains valid: indeed, such temperatures are expected in the bubble.

9.4.4 Evaporation Induced by Condensation

For a normal situation, condensation leads to the increase of a liquid's mass and tends to decease the resulting heat flux from the surface. In an ordinary case when

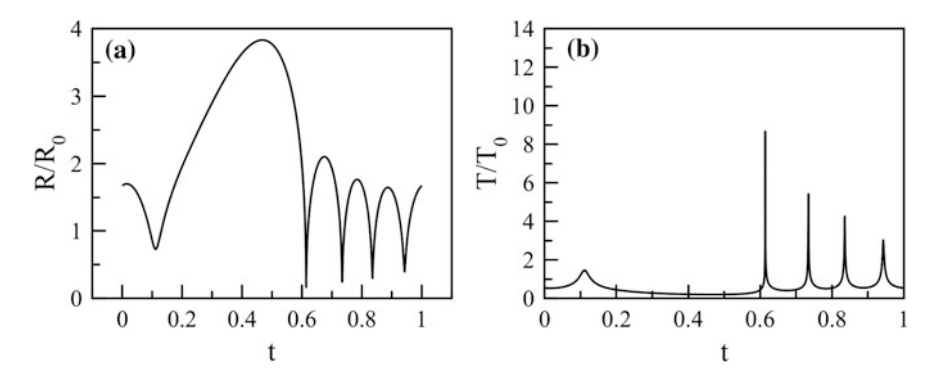


Fig. 9.17 The bubble radius (a) and the temperature inside the vapor bubble (b) during ultrasound cavitation

the temperature of vapor and liquid are approximately same, these statements are correct. However, in the case when cold liquid contacts a (very) hot vapor, the first illation needs to be corrected: when an atom hits a surface, its energy transfers to atoms of a liquid. Due to strong interaction between atoms in a condensed matter, this additional energy distributes among many atoms comprising the surface of the liquid. Thus, a few atoms acquire additional kinetic energy and, consequently, they have an increased probability of evaporating. In other words, when a surface is bombarded by a flux of high-energy atoms from a hot vapor, this surface is locally (at areas where atoms of vapor strike a liquid) overheated and evaporates more intensively.

Strictly speaking, a velocity distribution function (DF) of atoms on the surface of a liquid is distorted and has an increased mean energy. Above, in Sect. 8.3, we assumed that the DF is Maxwellian: only approximately that is, because the real form of the DF is more complicated. However, under this assumption the problem was solved immediately: the local overheated area of the surface has a temperature $\Omega > T$ (T is the temperature of the bulk liquid), the problem being reduced to the previous results. For instance, the probability of evaporation is $\frac{1}{2\sqrt{\pi}}\Gamma(\frac{1}{2},\frac{U}{\Omega})$, etc. Adopting $\Omega = \mu T$ (where coefficient $\mu \geq 1$) and calculating the constant χ from the experimental data (this constant was ~ 1 , see Sect. 8.3), means that we obtained sufficient agreement with the experiment.

However, actually, the interaction of an incoming particle and the liquid surface is more complicated and involves other nuances.

First, when the atom of vapor dives onto the interface, it takes additional energy U due to its acceleration at the field of surface atoms—as a body does due to Earth's gravity. This is the reverse process of the act of detaching an atom from the interface at evaporation. Thus, if an atom has kinetic energy $\bar{\epsilon}$ far from the liquid surface ("at infinity") then it has energy $\bar{\epsilon} + U$ at the surface.

In a specific situation, when the energy of the impacting vapor particle is very high, one may expect that after the impact this incoming particle transfers such high

9.4 Cavitation 303

energy to the atom of the liquid that it leaves the surface immediately. However, it should not be forgotten that:

- The "guest" particle does not give all its energy to a single atom in the liquid in one collision.
- After the impact the atom of the liquid receives a velocity that is directed away
 from the interface into the bulk of the liquid, and redirection of velocity takes a
 comparatively long time and is provided by the loss of energy in further collisions. Several atoms on the liquid surface take their energy from the single
 incoming particle.

The next important question to address is the character of the energy transfer to the interface. We can discuss, generally, two ultimate models of the additional evaporation initiated by the impact of the vapor atom:

- Case A. A group of atoms of gas at the interface have so much non-thermalized energy that they leave the surface immediately if their velocity is directed away from the liquid. The timescale for this process is about the same as the relaxation time τ (see below); the DF of these atoms is non-Maxwellian and this problem cannot be solved by our standard approach with the function of probability (as we did in Sect. 8.3). Fortunately, we can deal with this problem using another approach. Of course, this model can be applied only for the very high energies of an incoming particle.
- Case B. Contrariwise, if the energy of our impacting atom is not so high—i.e., the energy of the atoms at the interface is not being increased so drastically after collisions with this "guest" atom—then the immediate escape of interface atoms is impossible. The impact leads to an increased probability of escape for atoms from the liquid surface, as was considered in Chap. 8. The additional energy of the incoming particle is "thermalized" in the liquid, i.e., atoms at the surface of the liquid obtain an increased temperature Ω (locally). This approach was briefly discussed and used in Sect. 8.3. The timescale of this process is $\sim 10\tau$. The energy then dissipates in the liquid.

Thus, Case B was considered and applied in Chap. 8. In the case where immediate departure of surface atoms in response to an impact is impossible, we may try to describe the evaporation process with the usual Maxwellian distribution function (MDF) of surface atoms, redetermining the local temperature with respect to increased energy (due to the impact of the vapor atom). Of course, this is an assumption, a limiting case, because, strictly, the surface atom may leave the liquid before thermalization of the additional energy. However, we always have to deal with limiting cases, as a rule.

Let us consider Case A—another limiting case—more closely. The first question is: how many particles of vapor hit the interface during the relaxation time? Probably, the consequence of strikes is to heat the surface continuously; in this case the energy of atoms at the liquid surface may reach colossal values.

Relaxation time can be estimated through the energy of interaction φ , spatial scale of this interaction l and the mass of a particle m. We may compose a corresponding correlation which is even based on the arguments of dimension:

$$\tau = l\sqrt{\frac{m}{\varphi}}. (9.4.8)$$

Next, we have to choose characteristic parameters for (9.4.8), i.e., the size of the relaxation area. Because the spatial scale of the interatomic interaction is several angstroms, we may adopt $l \sim 1$ nm. As for the ratio m/φ , we may note that both parameters are proportional to the number of particles N_r in this relaxation area; that is, we may take $m \sim 10^{-26}$ kg and $\varphi \sim 10^{-21}$ J. Thus, we have the relaxation time $\tau \sim 10^{-12}$ s (with a multiplier of ~ 1).

To estimate the number of vapor particles that hits the liquid surface during the relaxation time, we adopt the vapor flux on the surface as:

$$j \sim \frac{p}{T} \bar{v}_T. \tag{9.4.9}$$

We have discussed this correlation for the common case in previous chapters; again, such a correlation can be constructed based on the dimensions of its characteristic variables. The thermal velocity for temperatures of a few hundred (up to $\sim 10^3$) kelvin is $\bar{\nu}_T \sim 10^{2-3}$ m/s. For pressures $p \sim 10^5$ Pa and temperatures $T \sim 10^{2-3}$ K, we get the upper estimation for the flux $j \sim 10^{28}$ m⁻² s⁻¹. If the "effect area" of the strike is about $S \sim 1$ nm², we have an expression for the number of particles that hits the interface during time τ :

$$N \sim j \cdot S \cdot \tau \sim 10^{-2}. \tag{9.4.10}$$

In other words, there are no additional collisions during the relaxation time (at intermediate pressures), hence, there is no additional overheating: for the ultimate case A the total additional energy of the group of atoms at the liquid surface is provided by the energy of a single atom from the vapor phase.

To estimate the maximum number of escaping particles M, we must remember that only a third of the kinetic energy (a generous estimate; corresponding to the normal axis z) can be spent overcoming the potential energy U, while the kinetic energy corresponding to tangential axes x and y stay the same during the evaporation process.

Consequently, if the energy of the vapor atom is $\bar{\epsilon}$ (far from the interface), the energy $(\bar{\epsilon} + U)$ will be distributed between M atoms of the liquid. Remembering that the initial energy of the liquid particle is $\bar{\epsilon}_0$, we have an approximate condition:

$$\frac{\bar{\varepsilon} + U + M \,\bar{\varepsilon}_0}{3M} > U \tag{9.4.11}$$

9.4 Cavitation 305

for the case when M particles of the liquid leave the surface as a response to the single particle of vapor with energy $\bar{\epsilon}$. Probably, it is worth noting that (9.4.11) determines the condition of immediate detachment of M particles, without thermalization of additional energy. Note also, that for this case - when we consider the detachment of several atoms from a single place on the interface at a short time interval—Sect. 6.5, where hyperevaporation was considered, could be referred to. Here we mean that for a number of evaporated particles greater than unity, we may expect the binding energy to decrease relative to the normal situation.

As it follows from (9.4.11), the energy $\bar{\epsilon}$ of the vapor particle must be very high (a well-accepted conclusion, of course). For example, despite the fact that any incoming vapor atom obtains additional energy U, a single atom from the surface cannot accept all this energy in order to leave, because after the first collision (with the impacting vapor atom) this surface atom has a velocity directed toward the bulk of the liquid, and its subsequent collisions (with atoms of a liquid) will be accompanied by an energy loss. Thus, low-energy vapor atoms cannot transfer sufficient energy to the surface atoms for them to depart.

Forgetting for a second all the considerations made about the possibility of an energy transfer to a single atom of a liquid (developed no further than on the previous page), we can find the threshold energy $\bar{\epsilon}$ for M=1:

$$\bar{\varepsilon} = 2U - \bar{\varepsilon}_0, \tag{9.4.12}$$

and, for example, for argon with $U \sim 10^3$ K (slightly less) we see that the threshold energy for such a process is ~ 2000 K (slightly less actually, however, this is an estimation). Thus, if the vapor of argon is heated to thousands of kelvin, then the condensation of this vapor gives rise to evaporation of the liquid: in response to the single vapor particle with energy $\bar{\epsilon}$, the single particle from the liquid flies outward. If the energy of the vapor atom was larger than $\bar{\epsilon}$, we may expect the detachment of a few atoms almost simultaneously. The word "condensation" is not an exact term for such a process, which is more like a sputtering process: in response to a single incoming atom (from vapor to liquid) a few atoms appear (from liquid to vapor).

The last common question concerns the possibility of such a situation in principle: under what conditions would a cold liquid be in contact with an overheated gas? We discussed this in Sect. 9.3.4. It is supposed that during cavitation (at the stage of bubble collapse) the temperature of a gas can reach enormous values (due to adiabatic compression, as is assumed in the simplest models). However, at high temperatures this hot gas (or vapor) induces a very intense evaporation, and the mass of the gaseous phase increases. The increased pressure inside the bubble will stop the collapse and, therefore, will prevent the subsequent increase of temperature.

From this point of view, it is hard to expect that the temperature inside a collapsing bubble could even achieve temperatures of $\sim 10^4$ K. It seems to be that the nature of sonoluminescence does not hide in extremely high temperatures inside a collapsing bubble. However, the nature of sonoluminescence is not the matter of

this chapter, or even of this book. The subject of this section is the possibility of induced evaporation due to a high-energy condensation flux. Here we present only estimations for characteristic parameters of this process; possibly, these evaluations need concrete illustrations. As usual, these results will be obtained with the method of molecular dynamics.

In the next section we are going to present the corresponding results of numerical simulations.

9.4.5 Numerical Simulations

For the purposes of this problem, we will consider a deep layer (~ 10 nm) of cold liquid (argon), placed on a cold solid surface. However, to keep the total number of particles at level of $\sim 10^3$ for the same calculation time, we have to use a narrow column of liquid (see Fig. 9.18).

Next, we bombard the surface of the liquid with separate vapor atoms (the set of which, however, obeys the MDF of velocity with a corresponding temperature of vapor T_v). The 100-K temperature of the liquid is sufficiently low to slow evaporation, and, actually, surface atoms wait for impacts from the vapor atoms in order to detach from the interface.

At temperature $T_{\rm v}=10^3$ K, we have an increased evaporation flux, but this flux is lower than the condensation flux. At temperature $T_{\rm v}=2000$ K we see that $j^{\rm ev}/j^{\rm cond}\sim 1$; for the accuracy of the numerical method, it is difficult to determine exactly whether this ratio is higher or lower than unity.

However, for temperature $T_{\rm v} = 5000$ K the results are clear. In Fig. 9.18 we represent the departure of five surface atoms in response to a single vapor atom.

That is all that we wanted to prove. Indeed, a high-energy vapor particle causes the immediate evaporation of several particles from the liquid surface. The liquid stays cold, because the energy of the vapor atom was spent on emitting evaporated particles.

In addition, as it was considered above, the evaporation flux may exceed the condensation flux. Consequently, the vapor mass must significantly increase at temperatures of $\sim 10^3$ K inside the gaseous phase, even if the temperature of the liquid stays the same.

9.4.6 A Sidestep: The Boiling Chamber

Thus, we have seen that a single incoming atom leads to evaporation of many atoms from the liquid surface. Similar arguments were involved to explain the physical principles of boiling chambers. Gerasimov and Rudavina (2008) propose a mechanism of local overheating with high-energy particles of ionizing radiation.

9.4 Cavitation 307

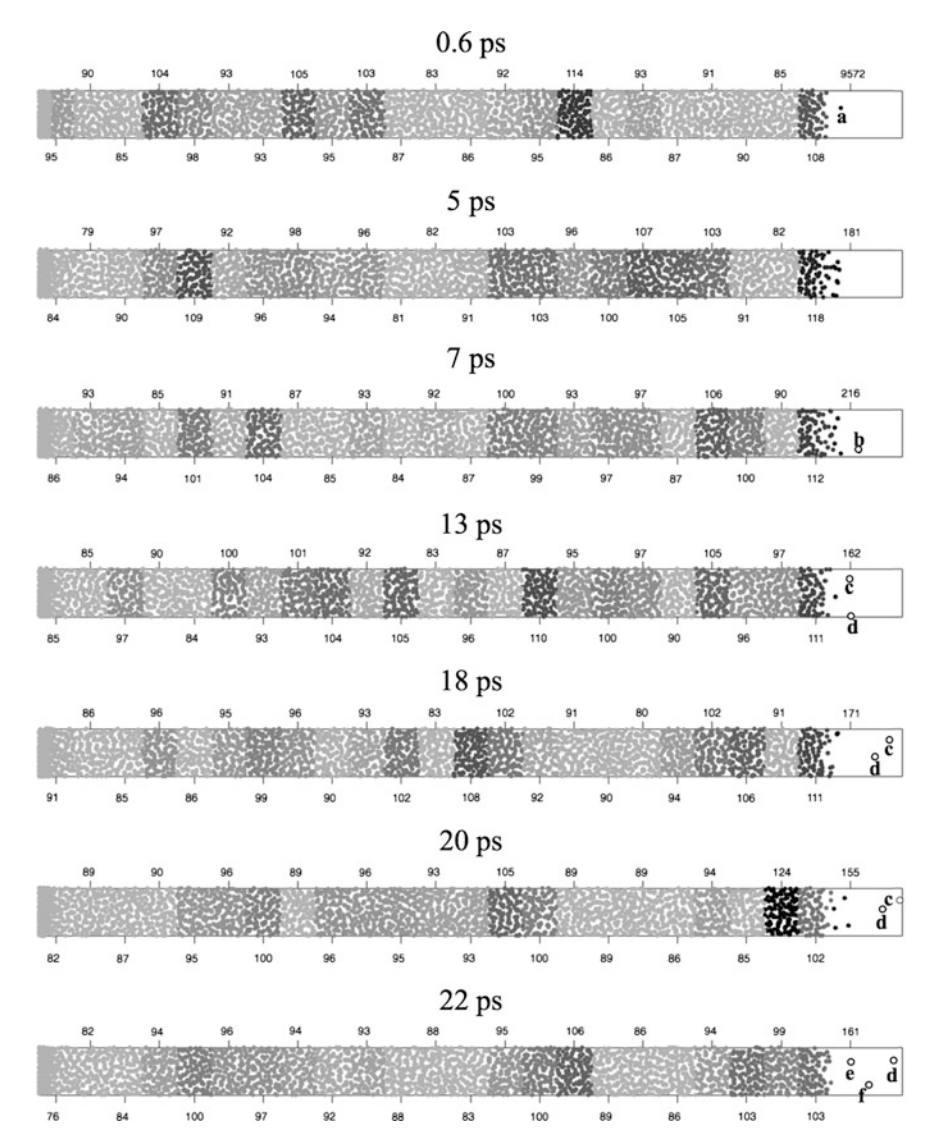


Fig. 9.18 One impacting atom (filled circle, labelled a) forces the evaporation of five atoms from the liquid surface (open circles, labelled b–f). Numbers are the mean kinetic energy in the corresponding layers

The boiling chamber is a kind of a track detector for ionized radiation; like the famous Wilson camera, but with opposite principles of action.

In the Wilson camera the supersaturated vapor (which cannot condense because of the absence of nuclei with critical radiuses) awaits a particle of ionized radiation (for instance, a beta-particle). When such a particle comes into the volume of the

Wilson camera, it ionizes the medium, i.e., vapor. It can be shown via thermodynamical methods (see Chap. 1) that ions produced by ionization processes play the role of centers of condensation, because the critical radius of the nucleus (i.e., of the droplet in the vapor) around the ion is equal to zero. Thereby, each ion appearing in the vapor grows a droplet around it, and we can follow the track of an incoming beta-particle by observing the chain of droplets emerging along its path.

The boiling (or bubble) chamber (invented by Glaser, earning him the Nobel Prize in 1960) uses the contraction principle. Instead of an overcooled vapor, an overheated liquid is used. As in the Wilson camera, this liquid cannot boil without nuclei (in this case—centers of vaporization). As in the Wilson camera, a particle of ionized radiation causes the formation of a new thermodynamic phase (here—vapor), and one can follow the track of ionizing particles using the chain of bubbles in the boiling camera. The advantage of the boiling camera over the Wilson camera is the increased drag property of the vessel with the liquid (in comparison to a jug of vapor).

However, we cannot explain the principal of action of the boiling camera in the same manner as the Wilson camera. Thermodynamics predicts the growth of the charged droplet in a metastable vapor, but the bubble in the liquid is the opposite case (different electrostatic permittivities); thus, the thermodynamic approach cannot explain the formation of a bubble around the ion (we omit here the discussion about the (un)physical forces that hold this ion in the middle of the vapor space, preventing its diffusion into the bubble wall and attachment, which is an obvious process). One may assume that the bubble grows because of many charged particles placed on its wall; however, the charge density in the boiling chamber is quite low.

Thus, it was assumed in Gerasimov and Rudavina (2008), that the kinetic energy of vapor molecules, which increases after collisions with high-energy particles of ionized radiation, is sufficient for the local vaporization of the overheated liquid. This mechanism—when a single particle leads to a macroscopic process—is similar to the problem considered in this chapter.

For the boiling camera, the energy transferred in a single collision between a beta-particle and one vapor molecule, distributed in N particles, leads to the formation of a bubble with a critical size.

9.5 Conclusion

This chapter does not represent any attempt to systematically consider boiling and cavitation. This is a mosaic of separate problems, connected through evaporation.

Two main features of evaporation were discussed in this chapter: explosive evaporation and the sputtering of liquid by hot vapor. Both phenomena are non-equilibrium, short-scale processes which can be investigated, mainly, with numerical simulations.

9.5 Conclusion 309

Explosive evaporation takes place after contact between a cold liquid and a hot solid (at temperatures higher than the critical temperature of the liquid). Actually, the processes occurring in such a system are so intensive that they cannot be described in usual terms, even the definition of "temperature" cannot be applied to the liquid.

It is interesting how such an unusual type of evaporation is connected to processes of non-stationary boiling, especially to transient boiling. Probably, explosive evaporation (the type when a liquid jumps away from a solid surface) may explain some aspects of boiling, but may not explain others, because the timescale of the process is too short. We cannot even directly connect explosive evaporation and steam explosions because of the significantly different spatial scales of the numerical simulation area and real systems.

Despite all the disclaimers, we assume that the processes considered in this chapter may be useful, at least, for understanding of some details of the physics of boiling or cavitation.

One such detail is the interaction between very hot vapor and cold liquid. In some cases, the effect of an overheated vapor on a liquid surface leads to an increased evaporation flux. Specifically, this process takes place in all cases, but the more distinctive results may be observed when the vapor has a temperature of $\sim 10^3~\rm K$. For such a hot gas, the evaporation flux exceeds the condensation flux, i.e., the interaction of the vapor and the gas represents some kind of spraying of the surface atoms: in response to a single incoming atom several atoms are evaporated from the cold liquid. In our opinion, this process limits the compression ratio of the collapsing bubble.

References

Z. Chen, Y. Utaka, Int. J. Heat Mass Transf. 81, 750 (2015)

M.G. Cooper, A.J.P. Lloyd, Int. J. Heat Mass Transf. 12, 895 (1969)

A. Einstein, Ann. Phys. 17, 549 (1905)

D.F. Gaitan et al., J. Acoust. Soc. Am. 91, 3166 (1992)

M. Gao et al., Int. J. Heat Mass Transf. 57, 183 (2012)

D.N. Gerasimov, M.N. Rudavina, High Temp. 46, 136 (2008)

H.-S. Hsu et al., Int. J. Heat Mass Transf. 86, 65 (2015)

D.A. Labuncov, J. Eng. Phys. Thermophys. **6**(4), 33 (1963)

O.A. Sinkevich, Phys. Rev. E 78, 036318 (2008)

V.V. Yagov, A.R. Zabirov, M.A. Lexin, Therm. Eng. 62, 833 (2015)

Recommended Literatures

E.F. Adiutory, The New Heat Transfer (The Ventuno Press, 1974)

V.G. Baidakov, A.M. Kaverin, V.N. Andbaeva, Thermophys. Aeromech. 18, 31 (2011)

V.P. Carey, Exp. Heat Transf. 26, 296 (2013)

L.-H. Chien, C.-H. Cheng, HVAC&R Research 12, 69 (2006)

D.M. Christopher, Lu Zhang, Tsinghua Sci. Technol. 15, 404 (2010)

- M.-C. Chyu, Int. J. Heat Mass Transf. 30, 1531 (1987)
- Y. Dou et al., J. Phys. Chem. A 105, 2748 (2001)
- T. Fu et al., Heat Mass Transf. 52, 1469 (2016)
- V.V. Glazkov, A.N. Kireeva, High Temp. 48, 453 (2010)
- Z. Guo, M.S. El-Genk, Int. J. Heat Mass Transf. 37, 1641 (1994)
- H. Honda, O. Makishi, Int. J. Heat Mass Transf. 79, 829 (2014)
- H.H. Jawurek, Int. J. Heat Mass Transf. 12, 843 (1969)
- J. Kim et al., Int. J. Multiph. Flow 35, 1067 (2009)
- L.D. Koffman, M.S. Plesset, J. Heat Transf. 105, 625 (1983)
- AYu. Kuksin et al., Phys. Rev. B 82, 174101 (2010)
- N. La Foriga, M. Fernandino, C.A. Dorao, Heat Transf. Eng. 35, 440 (2014)
- G.G. Lavalle et al., Am. J. Phys. **60**, 593 (1991)
- V.L. Malyshev et al., High Temp. 53, 406 (2015)
- A. Sanna et al., Int. J. Heat Mass Transf. 76, 45 (2014)
- H.R. Seyf, Y. Zhang, J. Heat Transf. 135, 121503 (2013)
- S.M. Shavik, M.N. Hasan, A.K.M.M. Morshed, J. Electron. Packag. 138, 010904 (2016)
- I. Sher et al., Appl. Therm. Eng. 36, 219 (2012)
- P. Staphan, J. Hammer, Heat Mass Transf. 30, 119 (1994)
- K. Stephan, L.-C. Zhong, P. Stephan, Heat Mass Transf. 30, 467 (1995)
- A. Takamizawa et al., Phys. Chem. Chem. Phys. 5, 888 (2003)
- Y. Utaka, Y. Kashiwabara, M. Ozaki, Int. J. Heat Mass Transf. 57, 222 (2013)
- V.E. Vinogradov, P.A. Pavlov, V.G. Baidakov, J. Chem. Phys. 128, 234508 (2008)
- G.A. Volkov, A.A. Gruzdkov, YuV Petrov, Tech. Phys. 54, 1708 (2009)
- C.M. Voutsinos, R.L. Judd, J. Heat Transf. 97, 88 (1975)
- E. Wagner, P. Stephan, J. Heat Transf. 131, 121008 (2009)
- W. Wang et al., Nanoscale Res. Lett. 10, 158 (2015)
- V.V. Yagov, Heat Mass Transf. 45, 881 (2009)
- V.V. Yagov, Int. J. Heat Mass Transf. 73, 265 (2014)
- S. Zhang et al., Appl. Therm. Eng. 113, 208 (2017)
- A. Zou, D.P. Singh, S.C. Maroo, Langmuir 32, 10808 (2016)

Appendix A Distribution Functions

A.1 Distribution Function

In this book we use the term "distribution function" as a "probability density function." The last variant is more correct, but due to weird reasons the function f(x) that determines the probability from x to x + dx:

$$dp = f(x)dx$$

is referred to as a distribution function (DF), despite the fact that mathematicians understand under that name the function:

$$F(y) = \int_{a}^{y} f(x) \mathrm{d}x,$$

where a is the lowest value of x.

Thus, we put our two cents into incorrect terminology.

A.2 Distribution of a Sum

Let the parameter z be the sum of two random parameters x and y: z = x + y, $x \in [-\infty, \infty]$ and $y \in [-\infty, \infty]$ are independent and DFs f(x) and g(y) are known. The DF of z is:

$$h(z) = \int_{-\infty}^{\infty} f(x)g(z - x)dx.$$

Correspondingly, for z = x - y:

$$h(z) = \int_{-\infty}^{\infty} f(x)g(x-z)dx.$$

A.3 Stable Distribution Functions

The Fourier representation of a stable DF has the form:

$$\hat{f}(t) \sim \exp(-\lambda |t|^{\alpha}), \lambda > 0, 0 < \alpha \le 2.$$

Two of the simplest examples of stable distributions are the Cauchy distribution (for $\alpha = 1$):

$$f(x) = \frac{c}{\pi (c^2(x-a)^2 + 1)},$$

and the Gaussian (for $\alpha = 2$):

$$f(x) = \frac{1}{\sqrt{2\pi\sigma^2}} \exp\left(-\frac{(x-a)^2}{2\sigma^2}\right).$$

Dispersion of any stable DF with $\alpha < 2$ is ∞ .

The main property (for physical applications) of stable DFs is that if two variables x and y are distributed with function f, then the sum of these variables x + y obeys the same distribution f.

The Gaussian satisfies this condition. Let us consider two functions:

$$f_1(x) = \frac{1}{\sqrt{2\pi}\sigma_1} \exp\left(-\frac{(x-a)^2}{2\sigma_1^2}\right), -\infty \le x \le \infty;$$

$$f_2(y) = \frac{1}{\sqrt{2\pi}\sigma_2} \exp\left(-\frac{(y-b)^2}{2\sigma_2^2}\right), -\infty \le y \le \infty.$$

To find a DF for z = x + y, we must integrate for:

$$f_3(z) = \int_{-\infty}^{\infty} f_1(z - y) f_2(y) dy = \frac{1}{2\pi\sigma_1\sigma_2} \int_{-\infty}^{\infty} \exp(-Ay^2 + 2By - C) dy =$$

$$= \frac{1}{2\pi\sigma_1\sigma_2} \sqrt{\frac{\pi}{A}} \exp\left(-\frac{AC - B^2}{A}\right),$$

where:

$$A = \frac{1}{2\sigma_1^2} + \frac{1}{2\sigma_2^2}, B = \frac{(z-a)}{2\sigma_1^2} + \frac{b}{2\sigma_2^2}, C = \frac{(z-a)^2}{2\sigma_1^2} + \frac{b^2}{2\sigma_2^2}.$$

Thus, we have:

$$f_3(z) = \frac{1}{\sqrt{2\pi(\sigma_1^2 + \sigma_2^2)}} \exp\left(-\frac{(z - [a+b])^2}{2(\sigma_1^2 + \sigma_2^2)}\right).$$

Thereby, the final DF also has a Gaussian form with the mean value (a+b) and dispersion $\sigma^2=\sigma_1^2+\sigma_2^2$.

Appendix B Special Functions

B.1 The Gamma Function

The gamma function $\Gamma(z)$ represents a solution of the functional equation:

$$\Gamma(z+1) = z\Gamma(z)$$
.

For integers z = n the gamma function reduces to a factorial function:

$$\Gamma(n) = (n-1)!$$

In the common case:

$$\Gamma(z) = \frac{1}{2\pi i} \int_{-\infty}^{0} e^{t} t^{-z} dt,$$

and in the particular case of Re z > 0:

$$\Gamma(z) = \int_{0}^{\infty} e^{-t} t^{z-1} dt.$$

Below are some formulae:

$$\Gamma(1/2) = \sqrt{\pi},$$

$$\Gamma(z)\Gamma(-z) = -\frac{\pi}{z\sin(\pi z)},$$

$$\Gamma(1+z)\Gamma(1-z) = \frac{\pi z}{\sin(\pi z)},$$

$$\Gamma\left(\frac{1}{2} + z\right)\Gamma\left(\frac{1}{2} - z\right) = \frac{\pi}{\cos(\pi z)},$$

$$\Gamma(z)\Gamma(1-z) = \frac{\pi}{\sin(\pi z)}.$$

Practically, the gamma function can be calculated through:

$$\Gamma(z) = \frac{1}{z} \prod_{n=1}^{\infty} \left(1 + \frac{1}{n} \right)^z \left(1 + \frac{z}{n} \right)^{-1}.$$

B.2 The Incomplete Gamma Function

$$\Gamma(z, a) = \int_{a}^{\infty} e^{-t} t^{z-1} dt,$$

$$\gamma(z, a) = \int_{0}^{a} e^{-t} t^{z-1} dt, \operatorname{Re} a > 0;$$

$$\gamma(z, a) = \Gamma(z) - \Gamma(z, a).$$

Corresponding functional equations for the incomplete gamma function include:

$$\Gamma(z+1,a) = z\Gamma(z,a) + a^{z}e^{-a},$$

$$\gamma(z+1,a) = z\gamma(z,a) - a^{z}e^{-a}.$$

If $a \neq 0, -1, -2, \dots$

$$a^{-z}\gamma(z,a) = \sum_{n=0}^{\infty} \frac{(-1)^n a^n}{n!(z+n)} = e^{-a} \sum_{n=0}^{\infty} \frac{a^n}{z(z+1)\dots(z+n)}.$$

For $-\frac{3\pi}{2} + \varepsilon \le \arg a \le \frac{3\pi}{2} - \varepsilon$, $\varepsilon > 0$ and $|a| \gg 1$:

$$\Gamma(z,a) = a^{z-1} e^{-a} \left(1 + \sum_{n=1}^{\infty} \frac{(z-1)(z-2)...(z-n)}{a^n} \right);$$

$$\gamma(z,a) \approx \Gamma(z) - a^{z-1} e^{-a} \left(1 + \sum_{n=1}^{\infty} \frac{(z-1)(z-2)...(z-n)}{a^n} \right).$$

B.3 The Error Function

$$\operatorname{erf}(z) = \frac{2}{\sqrt{\pi}} \int_{0}^{z} e^{-t^{2}} dt = \frac{1}{\sqrt{t}} \int_{0}^{z^{2}} \frac{e^{-t}}{\sqrt{t}} dt = \frac{1}{\sqrt{\pi}} \gamma \left(\frac{1}{2}, z^{2}\right),$$

$$\operatorname{erfc}(z) = 1 - \operatorname{erf}(z).$$

Series:

$$\operatorname{erf}(z) = \frac{2}{\sqrt{\pi}} e^{-z^2} \sum_{n=0}^{\infty} \frac{2^n}{(2n+1)!!} z^{2n+1}.$$

B.4 The Heaviside Step Function

$$\Theta(x) = \begin{cases} 0, & x < 0, \\ 1, & x \ge 0. \end{cases}$$

Variants of the Heaviside step function are:

$$\Theta(x) = \begin{cases} 0, & x \le 0, \\ 1, & x > 0. \end{cases}$$

$$\Theta(x) = \begin{cases} 0, & x < 0, \\ 1/2, & x = 0, \\ 1, & x > 0. \end{cases}$$

B.5 The Dirac delta function

Generalized function

The delta function $\delta(x)$ can be defined as:

$$\int_{a}^{b} f(x)\delta(x-y)dx = \begin{cases} 0, & x < a \text{ or } y > b, \\ f(y), & a \le y \le b. \end{cases}$$

Variants of the Dirac delta function are:

$$\int_{a}^{b} f(x)\delta(x-y)dx = \begin{cases} 0, & y < a \text{ or } y > b, \\ f(y+0)/2, & y = a, \\ f(y-0)/2, & y = b, \\ (f(y+0)+f(y-0))/2, & a < y < b. \end{cases}$$

Some properties of the Dirac delta function are:

$$\delta(-x) = \delta(x);$$

$$\delta(ax) = \frac{1}{a}\delta(x);$$

$$\delta(x) = \frac{d\Theta(x)}{dx}.$$

Some asymptotic representations of the Dirac delta function are:

$$\delta(x) = \lim_{a \to \infty} \frac{a}{\pi(a^2x^2 + 1)};$$

$$\delta(x) = \lim_{a \to \infty} \frac{a}{\sqrt{\pi}} e^{-a^2x^2}.$$

Index

A

Accommodation coefficient, 203, 210	Critical temperature, 283, 285, 287, 290, 309
Adsorbed particles, 227	Cut-off radius, 112
Attractor, 7, 34, 58, 181, 182	
	D
B	Debye radius, 44, 45, 75
Balance equations, 147, 176, 207, 252, 255,	Diffusion equation, 26, 85, 288, 289
257	Diffusion flux, 208
BBGKY chain, 65, 80	Dirac delta function, 41, 63
Bifurcation, 272, 273	
Block, 52, 113, 114	E
Boiling camera, 308	Electron plasma, 33
Boiling curve, 271, 272	Energy distribution, 69, 148
Boltzmann constant, 2, 3, 258	Entropy, 3, 7, 10, 35, 48–50
Boltzmann distribution, 3, 8, 44, 47, 109	Error function, 26
Boltzmann equation, 62, 65–67, 70, 79, 80, 89,	Evaporation coefficient, 190, 198, 200, 204,
94, 138	206–208, 211–218, 229–231
	Explosive boiling, 289
C	Explosive evaporation, 289–293, 308, 309
Cavitation, 91, 295–302, 305, 308, 309	
Central Processor Unit (CPU), 112, 114–117	\mathbf{F}
Clapeyron-Clausius equation, 16, 189, 190,	Film boiling, 271, 272, 280, 282
207, 209, 240	Fluctuations, 2, 14, 43, 44, 58, 71, 72, 101,
Clapeyron equation, 2, 18, 51, 99, 184, 189,	102, 116, 136, 151, 159, 166, 171, 181,
193, 209, 215, 216, 227, 234, 260, 300	184, 187, 188, 193, 195, 250
Collapsing bubble, 298, 299, 301, 305, 309	Fluctura, 151, 155, 159, 160, 162, 164, 193,
Collision map, 220	194
Compute Unified Device Architecture	Fokker–Planck–Kolmogorov equation, 82
(CUDA), 112, 113, 115	Fourier law, 68, 89
Condensation coefficient, 176, 197–200, 204,	Fourier series, 102
208, 210–213, 219, 220, 222, 224–230,	
236	G
Contacting phase, 233, 241	Gamma-function, 260, 262
Continuity equation, 61, 63, 73	Gaussian, 42, 52, 58, 94, 137, 151, 161

Convective flux, 26, 27

© Springer International Publishing AG, part of Springer Nature 2018 D. N. Gerasimov and E. I. Yurin, *Kinetics of Evaporation*, Springer Series in Surface Sciences 68, https://doi.org/10.1007/978-3-319-96304-4

320 Index

Gibbs-Helmholtz equation, 76	Maxwell Distribution Function (MDF), 51, 52, 56, 58, 59, 150, 163, 165, 175, 178, 183,
Graphic Processor Unit (GPU), 112–116	245, 248, 249
Gravitational–capillary wave, 23	Mean Free Path (MFP), 9, 27, 44, 71, 87–89,
Н	95, 131, 145, 221, 225, 234, 238, 242, 245, 248, 265, 267, 268
Hamilton equation, 35, 51	Molecular Dynamics (MD), 31, 94–96, 100,
Hamiltonian, 38, 47, 75, 76	103, 104, 107, 110, 111, 113, 115, 116,
Heat flux, 24–27, 68, 98, 111, 159, 162, 177,	138, 162, 194
180, 185, 186, 189, 193, 208, 209, 217,	Multiprocessor, 113, 114
218, 237, 240, 242, 244, 251, 257, 259,	
262, 266–268, 271, 274–276, 278–280,	N
283–286, 290, 301	National Institute of Standards and Technology
Heat Transfer Coefficient (HTC), 102, 207	(NIST) database, 18, 19, 218, 261
Hertz formula, 175, 199, 201, 204, 212, 219, 220, 230, 249	Navier–Stokes equation, 21, 22, 27, 28, 234, 299
Hertz-Knudsen equation, 199, 203, 204, 207,	N-body simulation, 113
219	Non-equilibrium process, 4, 16, 29, 233, 248
	Nucleate boiling, 271–273, 275, 279, 280, 283,
I	286, 287, 290
Ideal gas, 1, 21, 44, 52, 56, 89, 99, 193, 199,	Numerical simulations, 38, 57, 59, 68, 88, 98,
285	101, 102, 117, 123, 124, 135, 138, 140,
Interaction parameters, 106, 107	142, 143, 145, 155, 157, 158, 162–166,
Interaction potential, 51, 64, 72, 78, 80, 94, 96, 106, 112, 116, 138, 152, 162, 236, 286,	169, 171, 174–176, 178, 186, 190, 193, 194, 199, 217, 218, 227, 231, 290, 306,
290	308
290	NVIDIA, 113, 116
	11 11 11 11 11 11 11 11 11 11 11 11 11
K	
K Kinetic equation, 28, 29, 61–67, 71–75, 78–85.	P
Kinetic equation, 28, 29, 61–67, 71–75, 78–85,	P Periodic boundary conditions, 95, 103, 109,
	P Periodic boundary conditions, 95, 103, 109, 110, 139
Kinetic equation, 28, 29, 61–67, 71–75, 78–85, 88–90, 93, 94, 100, 101, 127, 138, 176,	Periodic boundary conditions, 95, 103, 109, 110, 139
Kinetic equation, 28, 29, 61–67, 71–75, 78–85, 88–90, 93, 94, 100, 101, 127, 138, 176, 221, 235	Periodic boundary conditions, 95, 103, 109,
Kinetic equation, 28, 29, 61–67, 71–75, 78–85, 88–90, 93, 94, 100, 101, 127, 138, 176, 221, 235 Knudsen effect, 239	Periodic boundary conditions, 95, 103, 109, 110, 139 Phase transition, 2, 4, 11, 16, 17, 19, 21, 24, 25, 29, 89, 155, 271, 283, 284, 287, 289 Poincare-Zermelo theorem, 35
Kinetic equation, 28, 29, 61–67, 71–75, 78–85, 88–90, 93, 94, 100, 101, 127, 138, 176, 221, 235 Knudsen effect, 239 Knudsen layer, 9, 89, 90, 235, 236, 238, 240,	Periodic boundary conditions, 95, 103, 109, 110, 139 Phase transition, 2, 4, 11, 16, 17, 19, 21, 24, 25, 29, 89, 155, 271, 283, 284, 287, 289 Poincare-Zermelo theorem, 35 Poisson equation, 44, 94
Kinetic equation, 28, 29, 61–67, 71–75, 78–85, 88–90, 93, 94, 100, 101, 127, 138, 176, 221, 235 Knudsen effect, 239 Knudsen layer, 9, 89, 90, 235, 236, 238, 240, 247	Periodic boundary conditions, 95, 103, 109, 110, 139 Phase transition, 2, 4, 11, 16, 17, 19, 21, 24, 25, 29, 89, 155, 271, 283, 284, 287, 289 Poincare-Zermelo theorem, 35 Poisson equation, 44, 94 Potential energy distribution function, 29, 46,
Kinetic equation, 28, 29, 61–67, 71–75, 78–85, 88–90, 93, 94, 100, 101, 127, 138, 176, 221, 235 Knudsen effect, 239 Knudsen layer, 9, 89, 90, 235, 236, 238, 240, 247 L Lagrangian, 148–150, 152, 162, 163, 166, 193	Periodic boundary conditions, 95, 103, 109, 110, 139 Phase transition, 2, 4, 11, 16, 17, 19, 21, 24, 25, 29, 89, 155, 271, 283, 284, 287, 289 Poincare-Zermelo theorem, 35 Poisson equation, 44, 94 Potential energy distribution function, 29, 46, 56, 103, 115, 148, 155, 164
Kinetic equation, 28, 29, 61–67, 71–75, 78–85, 88–90, 93, 94, 100, 101, 127, 138, 176, 221, 235 Knudsen effect, 239 Knudsen layer, 9, 89, 90, 235, 236, 238, 240, 247 L Lagrangian, 148–150, 152, 162, 163, 166, 193 Laplace formula, 281	Periodic boundary conditions, 95, 103, 109, 110, 139 Phase transition, 2, 4, 11, 16, 17, 19, 21, 24, 25, 29, 89, 155, 271, 283, 284, 287, 289 Poincare-Zermelo theorem, 35 Poisson equation, 44, 94 Potential energy distribution function, 29, 46, 56, 103, 115, 148, 155, 164 Principle of least action, 31, 193
Kinetic equation, 28, 29, 61–67, 71–75, 78–85, 88–90, 93, 94, 100, 101, 127, 138, 176, 221, 235 Knudsen effect, 239 Knudsen layer, 9, 89, 90, 235, 236, 238, 240, 247 L Lagrangian, 148–150, 152, 162, 163, 166, 193 Laplace formula, 281 Laplace jump, 13, 22, 281	Periodic boundary conditions, 95, 103, 109, 110, 139 Phase transition, 2, 4, 11, 16, 17, 19, 21, 24, 25, 29, 89, 155, 271, 283, 284, 287, 289 Poincare-Zermelo theorem, 35 Poisson equation, 44, 94 Potential energy distribution function, 29, 46, 56, 103, 115, 148, 155, 164 Principle of least action, 31, 193 Principle of maximum entropy, 49
Kinetic equation, 28, 29, 61–67, 71–75, 78–85, 88–90, 93, 94, 100, 101, 127, 138, 176, 221, 235 Knudsen effect, 239 Knudsen layer, 9, 89, 90, 235, 236, 238, 240, 247 L Lagrangian, 148–150, 152, 162, 163, 166, 193 Laplace formula, 281 Laplace jump, 13, 22, 281 Leapfrog integration, 104	Periodic boundary conditions, 95, 103, 109, 110, 139 Phase transition, 2, 4, 11, 16, 17, 19, 21, 24, 25, 29, 89, 155, 271, 283, 284, 287, 289 Poincare-Zermelo theorem, 35 Poisson equation, 44, 94 Potential energy distribution function, 29, 46, 56, 103, 115, 148, 155, 164 Principle of least action, 31, 193 Principle of maximum entropy, 49 Probability density function, 34, 40, 56, 59, 69,
Kinetic equation, 28, 29, 61–67, 71–75, 78–85, 88–90, 93, 94, 100, 101, 127, 138, 176, 221, 235 Knudsen effect, 239 Knudsen layer, 9, 89, 90, 235, 236, 238, 240, 247 L Lagrangian, 148–150, 152, 162, 163, 166, 193 Laplace formula, 281 Laplace jump, 13, 22, 281 Leapfrog integration, 104 Leidenfrost effect, 5, 6	Periodic boundary conditions, 95, 103, 109, 110, 139 Phase transition, 2, 4, 11, 16, 17, 19, 21, 24, 25, 29, 89, 155, 271, 283, 284, 287, 289 Poincare-Zermelo theorem, 35 Poisson equation, 44, 94 Potential energy distribution function, 29, 46, 56, 103, 115, 148, 155, 164 Principle of least action, 31, 193 Principle of maximum entropy, 49
Kinetic equation, 28, 29, 61–67, 71–75, 78–85, 88–90, 93, 94, 100, 101, 127, 138, 176, 221, 235 Knudsen effect, 239 Knudsen layer, 9, 89, 90, 235, 236, 238, 240, 247 L Lagrangian, 148–150, 152, 162, 163, 166, 193 Laplace formula, 281 Laplace jump, 13, 22, 281 Leapfrog integration, 104 Leidenfrost effect, 5, 6 Lennard–Jones potential, 106	Periodic boundary conditions, 95, 103, 109, 110, 139 Phase transition, 2, 4, 11, 16, 17, 19, 21, 24, 25, 29, 89, 155, 271, 283, 284, 287, 289 Poincare-Zermelo theorem, 35 Poisson equation, 44, 94 Potential energy distribution function, 29, 46, 56, 103, 115, 148, 155, 164 Principle of least action, 31, 193 Principle of maximum entropy, 49 Probability density function, 34, 40, 56, 59, 69, 81, 86, 132
Kinetic equation, 28, 29, 61–67, 71–75, 78–85, 88–90, 93, 94, 100, 101, 127, 138, 176, 221, 235 Knudsen effect, 239 Knudsen layer, 9, 89, 90, 235, 236, 238, 240, 247 L Lagrangian, 148–150, 152, 162, 163, 166, 193 Laplace formula, 281 Laplace jump, 13, 22, 281 Leapfrog integration, 104 Leidenfrost effect, 5, 6 Lennard–Jones potential, 106 Liouville theorem, 35, 62	Periodic boundary conditions, 95, 103, 109, 110, 139 Phase transition, 2, 4, 11, 16, 17, 19, 21, 24, 25, 29, 89, 155, 271, 283, 284, 287, 289 Poincare-Zermelo theorem, 35 Poisson equation, 44, 94 Potential energy distribution function, 29, 46, 56, 103, 115, 148, 155, 164 Principle of least action, 31, 193 Principle of maximum entropy, 49 Probability density function, 34, 40, 56, 59, 69, 81, 86, 132
Kinetic equation, 28, 29, 61–67, 71–75, 78–85, 88–90, 93, 94, 100, 101, 127, 138, 176, 221, 235 Knudsen effect, 239 Knudsen layer, 9, 89, 90, 235, 236, 238, 240, 247 L Lagrangian, 148–150, 152, 162, 163, 166, 193 Laplace formula, 281 Laplace jump, 13, 22, 281 Leapfrog integration, 104 Leidenfrost effect, 5, 6 Lennard–Jones potential, 106 Liouville theorem, 35, 62 Liquid layer, 16, 95, 207, 291, 292	Periodic boundary conditions, 95, 103, 109, 110, 139 Phase transition, 2, 4, 11, 16, 17, 19, 21, 24, 25, 29, 89, 155, 271, 283, 284, 287, 289 Poincare-Zermelo theorem, 35 Poisson equation, 44, 94 Potential energy distribution function, 29, 46, 56, 103, 115, 148, 155, 164 Principle of least action, 31, 193 Principle of maximum entropy, 49 Probability density function, 34, 40, 56, 59, 69, 81, 86, 132 R Rayleigh equation, 299–301
Kinetic equation, 28, 29, 61–67, 71–75, 78–85, 88–90, 93, 94, 100, 101, 127, 138, 176, 221, 235 Knudsen effect, 239 Knudsen layer, 9, 89, 90, 235, 236, 238, 240, 247 L Lagrangian, 148–150, 152, 162, 163, 166, 193 Laplace formula, 281 Laplace jump, 13, 22, 281 Leapfrog integration, 104 Leidenfrost effect, 5, 6 Lennard–Jones potential, 106 Liouville theorem, 35, 62	Periodic boundary conditions, 95, 103, 109, 110, 139 Phase transition, 2, 4, 11, 16, 17, 19, 21, 24, 25, 29, 89, 155, 271, 283, 284, 287, 289 Poincare-Zermelo theorem, 35 Poisson equation, 44, 94 Potential energy distribution function, 29, 46, 56, 103, 115, 148, 155, 164 Principle of least action, 31, 193 Principle of maximum entropy, 49 Probability density function, 34, 40, 56, 59, 69, 81, 86, 132 R Rayleigh equation, 299–301 Rayleigh—Taylor instability, 280, 282
Kinetic equation, 28, 29, 61–67, 71–75, 78–85, 88–90, 93, 94, 100, 101, 127, 138, 176, 221, 235 Knudsen effect, 239 Knudsen layer, 9, 89, 90, 235, 236, 238, 240, 247 L Lagrangian, 148–150, 152, 162, 163, 166, 193 Laplace formula, 281 Laplace jump, 13, 22, 281 Leapfrog integration, 104 Leidenfrost effect, 5, 6 Lennard–Jones potential, 106 Liouville theorem, 35, 62 Liquid layer, 16, 95, 207, 291, 292 Lorentz–Berthelote rule, 106	Periodic boundary conditions, 95, 103, 109, 110, 139 Phase transition, 2, 4, 11, 16, 17, 19, 21, 24, 25, 29, 89, 155, 271, 283, 284, 287, 289 Poincare-Zermelo theorem, 35 Poisson equation, 44, 94 Potential energy distribution function, 29, 46, 56, 103, 115, 148, 155, 164 Principle of least action, 31, 193 Principle of maximum entropy, 49 Probability density function, 34, 40, 56, 59, 69, 81, 86, 132 R Rayleigh equation, 299–301 Rayleigh—Taylor instability, 280, 282 Reflection boundary conditions, 109, 110
Kinetic equation, 28, 29, 61–67, 71–75, 78–85, 88–90, 93, 94, 100, 101, 127, 138, 176, 221, 235 Knudsen effect, 239 Knudsen layer, 9, 89, 90, 235, 236, 238, 240, 247 L Lagrangian, 148–150, 152, 162, 163, 166, 193 Laplace formula, 281 Laplace jump, 13, 22, 281 Leapfrog integration, 104 Leidenfrost effect, 5, 6 Lennard–Jones potential, 106 Liouville theorem, 35, 62 Liquid layer, 16, 95, 207, 291, 292 Lorentz–Berthelote rule, 106 M	Periodic boundary conditions, 95, 103, 109, 110, 139 Phase transition, 2, 4, 11, 16, 17, 19, 21, 24, 25, 29, 89, 155, 271, 283, 284, 287, 289 Poincare-Zermelo theorem, 35 Poisson equation, 44, 94 Potential energy distribution function, 29, 46, 56, 103, 115, 148, 155, 164 Principle of least action, 31, 193 Principle of maximum entropy, 49 Probability density function, 34, 40, 56, 59, 69, 81, 86, 132 R Rayleigh equation, 299–301 Rayleigh—Taylor instability, 280, 282 Reflection boundary conditions, 109, 110 Relaxation, 85, 86, 89, 190, 303, 304
Kinetic equation, 28, 29, 61–67, 71–75, 78–85, 88–90, 93, 94, 100, 101, 127, 138, 176, 221, 235 Knudsen effect, 239 Knudsen layer, 9, 89, 90, 235, 236, 238, 240, 247 L Lagrangian, 148–150, 152, 162, 163, 166, 193 Laplace formula, 281 Laplace jump, 13, 22, 281 Leapfrog integration, 104 Leidenfrost effect, 5, 6 Lennard–Jones potential, 106 Liouville theorem, 35, 62 Liquid layer, 16, 95, 207, 291, 292 Lorentz–Berthelote rule, 106	Periodic boundary conditions, 95, 103, 109, 110, 139 Phase transition, 2, 4, 11, 16, 17, 19, 21, 24, 25, 29, 89, 155, 271, 283, 284, 287, 289 Poincare-Zermelo theorem, 35 Poisson equation, 44, 94 Potential energy distribution function, 29, 46, 56, 103, 115, 148, 155, 164 Principle of least action, 31, 193 Principle of maximum entropy, 49 Probability density function, 34, 40, 56, 59, 69, 81, 86, 132 R Rayleigh equation, 299–301 Rayleigh—Taylor instability, 280, 282 Reflection boundary conditions, 109, 110
Kinetic equation, 28, 29, 61–67, 71–75, 78–85, 88–90, 93, 94, 100, 101, 127, 138, 176, 221, 235 Knudsen effect, 239 Knudsen layer, 9, 89, 90, 235, 236, 238, 240, 247 L Lagrangian, 148–150, 152, 162, 163, 166, 193 Laplace formula, 281 Laplace jump, 13, 22, 281 Leapfrog integration, 104 Leidenfrost effect, 5, 6 Lennard–Jones potential, 106 Liouville theorem, 35, 62 Liquid layer, 16, 95, 207, 291, 292 Lorentz–Berthelote rule, 106 M Magic bird, 16–19	Periodic boundary conditions, 95, 103, 109, 110, 139 Phase transition, 2, 4, 11, 16, 17, 19, 21, 24, 25, 29, 89, 155, 271, 283, 284, 287, 289 Poincare-Zermelo theorem, 35 Poisson equation, 44, 94 Potential energy distribution function, 29, 46, 56, 103, 115, 148, 155, 164 Principle of least action, 31, 193 Principle of maximum entropy, 49 Probability density function, 34, 40, 56, 59, 69, 81, 86, 132 R Rayleigh equation, 299–301 Rayleigh—Taylor instability, 280, 282 Reflection boundary conditions, 109, 110 Relaxation, 85, 86, 89, 190, 303, 304
Kinetic equation, 28, 29, 61–67, 71–75, 78–85, 88–90, 93, 94, 100, 101, 127, 138, 176, 221, 235 Knudsen effect, 239 Knudsen layer, 9, 89, 90, 235, 236, 238, 240, 247 L Lagrangian, 148–150, 152, 162, 163, 166, 193 Laplace formula, 281 Laplace jump, 13, 22, 281 Leapfrog integration, 104 Leidenfrost effect, 5, 6 Lennard–Jones potential, 106 Liouville theorem, 35, 62 Liquid layer, 16, 95, 207, 291, 292 Lorentz–Berthelote rule, 106 M Magic bird, 16–19 Mass flux, 22, 25–27, 175, 176, 180, 197–199,	Periodic boundary conditions, 95, 103, 109, 110, 139 Phase transition, 2, 4, 11, 16, 17, 19, 21, 24, 25, 29, 89, 155, 271, 283, 284, 287, 289 Poincare-Zermelo theorem, 35 Poisson equation, 44, 94 Potential energy distribution function, 29, 46, 56, 103, 115, 148, 155, 164 Principle of least action, 31, 193 Principle of maximum entropy, 49 Probability density function, 34, 40, 56, 59, 69, 81, 86, 132 R Rayleigh equation, 299–301 Rayleigh—Taylor instability, 280, 282 Reflection boundary conditions, 109, 110 Relaxation, 85, 86, 89, 190, 303, 304 Reversibility, 38, 39, 59, 94

Index 321

Sticking coefficient, 219, 227–231	V
Stream function, 22	Vapor layer, 242, 280, 289
Striking coefficient, 219	Velocity distribution function (DF), 57, 59,
Surface tension, 6, 12, 24, 281, 282, 290	125, 142, 147, 220, 221, 268
	Verlet method, 104
T	Vlasov equation, 76, 78, 79, 84, 90, 94
Tear of wine effect, 24	
Temperature jump, 90, 200, 237–247, 256,	\mathbf{W}
260, 262, 265–268, 301	Warp, 113, 114
Thermalization, 145, 251, 303, 305	
Thermal radiation, 8, 69, 251, 258, 259, 269	Z
Thermocouple (TC), 15, 16, 187, 188, 241,	Zeebek coefficient, 250
242, 248, 250–252, 254–260, 265,	Zeebek effect, 250
267–269	Zero law of thermodynamic, 6, 69
Thread, 113, 114, 147	
Transient boiling, 272, 283, 309	
Trouton rule, 157, 190	